THE UNIVERSITY *of* EDINBURGH

Prenatal SMN-dependent defects in translation uncover reversible primary cilia phenotypes in a mouse model of spinal muscular atrophy

Federica Genovese

THE UNIVERSITY *of* EDINBURGH

A thesis submitted in fulfilment of the requirements for the degree of Doctor of Philosophy

The University of Edinburgh, August 2025

I declare that this thesis has been composed by myself and that the work has not been submitted for any other degree of professional qualification. The collaborative contributions have been indicated clearly and acknowledged.

Federica Genovese

August 2025

Lay Abstract

Spinal muscular atrophy (SMA) is a rare genetic disease that mostly affects children, and it is characterised by the early loss of motor neurons, which are important for the health of muscles. SMA manifests because of mutations in a gene in our DNA, known as *Survival Motor Neuron 1* or *SMN1*. This causes the body to produce not enough of a protein called SMN, which is very important for our development, especially when we are babies. SMA does not have a definitive cure yet, but there are three treatments available that have greatly improved the life of the patients. However, doctors have been noticing new and unexpected changes in the brain of some young patients that they can't explain.

For this reason, in my thesis I focus my attention on the development of the brain, with the aim of understanding what are the mechanisms that are not functioning properly when the SMN protein is lost. To do this, I used a mouse model that was genetically modified to have the same symptoms as patients with SMA. By studying embryonic development of the brain in these mice, I discovered that, when SMN levels are low, there are problems in translation, which is the mechanism that cells use to build new proteins from the DNA. I also observed that, in turn, these problems cause damage to cellular structures called primary cilia: tiny "antennae" present on almost each cell of our body. In the brain, these antennae help cells to sense signals and communicate to each other to ensure the correct development of the brain. In this study, I found that not only were there fewer primary cilia in the brain of mouse embryos with SMA, but also, I showed that these defects were corrected when the mice were treated with a drug able to restore the levels of the SMN protein before they were born.

Scientific Abstract

Spinal muscular atrophy (SMA) is a rare inherited neuromuscular disease with an incidence of around one in every 10,000 live births. In most patients, SMA is caused by mutations in the survival motor neuron 1 gene *(SMN1)*, resulting in insufficient production of full-length, functional SMN protein. The SMN protein is dynamically regulated during development, where high levels of SMN expression during embryogenesis undergo a significant reduction after birth, suggesting an important role for SMN prenatally. SMN has also been shown to be a ribosome-associated protein that plays a crucial role in translation and ribosome biology. Therefore, when SMN is depleted, widespread perturbations of protein synthesis occur in SMA. Several therapeutic approaches aimed at boosting SMN are now approved for use in human patients, leading to significant improvements in lifespan and symptom severity. However, new and unexpected phenotypes are being reported in treated SMA patients, including significant neurodevelopmental alterations in some individuals, indicative of changes in brain development. In this thesis, I use a mouse model of severe SMA to explore the prenatal development of the central nervous system (CNS). Using a combination of morphological and molecular analyses, I reveal neurodevelopmental defects in SMA embryos and demonstrate that these changes are accompanied by widespread perturbations in translation. Furthermore, by performing network analysis of the genes presenting with alterations in ribosome occupancy, I show the involvement in processes related to primary cilia. Assessments of primary cilia in the CNS *in vivo* and in primary neuronal cultures *in vitro* confirmed the presence of a primary cilia phenotype in SMA. Finally, to demonstrate that this observed novel phenotype is SMN-dependent, and amenable to therapeutic intervention, in this work I show that prenatal transplacental treatment with risdiplam, an approved SMN-restoring drug, can rescue primary cilia defects in SMA mouse embryos. Using these approaches, I unveil that SMN protein is necessary for the normal cellular and molecular development of primary cilia in the CNS, and that prenatal treatment with SMN-restoring therapies can address neurodevelopmental phenotypes in SMA.

Acknowledgements

The first person I would like to thank for guiding me through this PhD is undoubtedly Tom, the supervisor that everyone would be lucky to work with. Thank you for welcoming me into your team as both a person and a scientist, and for always encouraging me to find my own strength and confidence. I will always treasure your advice to find what makes me happy, because, as you once said, “a happy researcher makes good science”.

To Nikky, who has truly made a difference to my PhD journey, inspiring me with her passion and infinite generosity. Thank you for always being there for me every step of the way. Thanks to you and Anna’s guidance through the initial phases of my PhD, I always felt part of something meaningful while finding our place in SMA research.

Thank you to all the members of the Gillingwater lab, both those who have always been there and those whose paths I have briefly crossed, yet who have made a profound impact. To Helena, Kiterie, Hannah, Dinja, Rachel, Kim, Rizwan, Abdullah, Shahd, Bernát and Alaó: thank you for your constant support, inspiration, friendship over the past four years. Every day was a good day with you around. Special mention goes to Hattie and Hannah, my adventure companions. Thank you for being the colleagues, friends and family I needed. It has been an honour to share this journey with you.

I would also like to express my gratitude to the SMABEYOND Consortium. This extraordinary network gave me the opportunity to gain invaluable professional experience while travelling through Europe and most importantly, introduced me to wonderful people with whom I hope to continue collaborating and building friendships. I would like to thank Prof. Gabriella Viero for welcoming me into her lab for four months during my secondment, and for allowing me to discover the fascinating world of protein translation research. Your professionalism and empathy will continue to inspire me throughout my career.

As part of the SMABEYOND family, a heartfelt thank you goes to Ilaria. The months we spent together in Edinburgh are certainly among my favourite memories of my time in Scotland. Thank you for your genuine friendship and unconditional support.

I would also like to sincerely thank my pillar people outside the lab. To Rachel, my gym accomplice, thank you for staying by my side during all those 6am sessions and for our Tuesday evenings together. To Sofia, thank you for the adventures we shared, you brought a ray of sunshine to my days. To Visia, my dancing friend, thank you for bringing me the Italian warmth I needed.

Special thanks go to my lifelong friends back home. Thank you, Iaia, for visiting me whenever you could to experience the Edinburgh life with me. Thank you, Giulia, for our countless hear-to-heart chats, something that never changed despite the distance. Thank you, Gloria, for always empowering me with your inexhaustible strength. Thank you, Giuli and Andri, for all the spontaneous aperitivi we enjoy together whenever I am in Turin. Thank you, Ila, for sparking my ambition to pursue this PhD, your passion has always been an inspiration to me.

To Alberto, who made me feel at home away from home. Thank you for your sincere kindness and love. I will always be grateful for your invaluable support during the writing of this thesis and every day that followed.

Finally, I would like to dedicate this to my family, the solid foundation that has made all my achievements possible. Thank you to my mum, Fulvia; my dad, Calogero; and my brother, Franci. There has not been a single day when I have not felt your love and encouragement. Thanks to my whole family, I am incredibly lucky to have you in my life.

Table of Contents

Chapter 1: **General Introduction**

1.1 Thesis structure and aims

In this thesis, I present the research I have undertaken during the four years of my PhD. The project's primary objective is to investigate the neurodevelopmental manifestations of spinal muscular atrophy (SMA), with a particular focus on the molecular and cellular phenotypes that underpin disease pathogenesis.

The results obtained are divided into four chapters:

- The first chapter describes how I modelled and studied prenatal brain development using an established mouse model of SMA.
- The second results chapter is centred on the study of protein translation in the embryonic stages of SMA. This work, that I performed during a placement in Prof. Gabriella Viero's lab in Italy, revealed a strong correlation between translation dysfunction and primary cilia disruption in the central nervous system (CNS) of SMA mouse embryos.
- In the third chapter, I explore primary cilia biology in the context of embryonic SMA, by studying the mouse hippocampus using *in vivo* and *in vitro* systems.
- Finally, the fourth results chapter concentrates on the implementation of prenatal *in utero* treatment in a mouse model of severe SMA to rescue the hippocampal primary cilia phenotype.

In addition to the four results chapters, this thesis comprises a *materials and methods* section and a final *general discussion*. The aim of this initial introduction is therefore twofold: firstly, to provide the relevant background on the thematic areas that will be discussed in this thesis, and secondly, to contextualise the present study within the existing literature.

1.2 Spinal Muscular Atrophy (SMA)

1.2.1 Overview and historical background

SMA is an inherited neuromuscular disorder characterised by muscle weakness and progressive atrophy associated with loss of spinal motor neurons (Dubowitz, 2009). The first documentation of SMA was reported in 1891 by the Austrian neurologist Guido Werdnig, who described the clinical symptoms observed in two siblings as “early infantile progressive SMA” (Oskoui et al., 2017; Werdnig, 1891). The two patients presented with a progressive loss of muscular strength and atrophy of the pelvic region and lower limbs, as well as loss of tendon reflexes and involvement of respiratory muscles. Their post-mortem examination, respectively at 3 and 6 years of age, revealed atrophy of anterior horn cells, with degeneration of the anterior horn roots. Soon afterwards, Johann Hoffmann, a neurologist from Germany, published further evidence confirming these observations, particularly with regard to the involvement of anterior horn cells of the spinal cord in juvenile cases (Hoffmann, 1893, 1897). However, the severity of clinical manifestations observed in these cases varied.

The idea of distinct clinical subtypes within the disease was solidified following the publication of a case report in 1893 by two physicians from the University of Edinburgh, UK, Thomson and Bruce (Thompson & Bruce, 1893). This report documented the presentation of a paediatric patients with intermediate SMA. Dubowitz’s meticulous description of this milder phenotype led to the subsequent naming of this intermediate SMA form as Dubowitz disease (Dubowitz, 1964). It is an intriguing historical detail that the most severe form of SMA was referred to as Werdnig-Hoffman disease, yet both physicians actually described an intermediate form of SMA. The first documentation of the most severe subtype of the disease was provided by Sylvestre in 1899 and Beevor in 1902, who, alongside the degeneration of anterior horn cells, described severe weakness of the intercostal muscles in patients of six months of age (Beevor, 1902). Almost five decades later, in 1956, Kugelberg and Welander described an additional hereditary form of motor neuron involvement

with less severe phenotypes and compatible with ambulation (Kugelberg, 1956). This description corresponds to one of the mildest forms of the disease described by Werdnig and Hoffman, suggesting that SMA clinical manifestations were broader than the original report.

1.2.2 Genetics

The identification of the location of the responsible gene for SMA in 1990 was fundamental to the understanding that the three different phenotypes described and reported in the previous years were in fact manifestations of the same disease, albeit presenting with a different range of severity (Gilliam et al., 1990; Melki et al., 1990). Thus, five years later this gene was identified as the survival motor neuron (*SMN*) gene located on the long arm of chromosome 5 (Lefebvre et al., 1995). The *SMN* gene region is structurally complex, and it is characterised by a large duplication event, which generates two copies of the gene that are almost identical, with the exception of five nucleotides (Monani et al., 1999). Mutations in the telomeric copy (*SMN1*) are associated with the occurrence of the disease, while the centromeric copy (*SMN2*) does not directly lead to SMA, but can compensate for the loss of the telomeric copy, influencing SMA severity (Lefebvre et al., 1997; Mailman et al., 2002).

In physiological conditions, *SMN1* encodes for full-length transcripts, while *SMN2* produces a truncated version of the same protein. Indeed, the *SMN2* gene is characterised by a C-to-T transition within its sequence, which influence the alternative splicing of the gene, ultimately resulting in the production of mRNA transcripts that are characterised by the absence of the exon 7 (Lorson & Androphy, 2000; Lorson et al., 1999). However, this alteration does not occur in all transcripts, as some transcripts retain exon 7. Therefore, the *SMN2* gene produces 90-95% truncated, non-functional protein and only 5-10% full-length, functional protein **(Figure 1.1)**.

Given that the complete loss of both *SMN1* and *SMN2* is incompatible with life, affected children possess at least one copy of *SMN2* (Oskoui et al., 2017).

Moreover, as the centromeric gene can be present in multiple copies, *SMN2* is considered to be one of the primary genetic modulators of disease severity. In general, the presence of more copies is associated with a milder disease phenotype (Feldkötter et al., 2002). An additional positive phenotypic genetic modifier has been identified in patients, occurring as a single base substitution in the exon 7 of the *SMN2* gene, c.859G>C (Prior et al., 2009). This change has been demonstrated to enhance exon 7 inclusion and, by consequence, the amount of full-length protein produced. This finding serves to demonstrate that not all *SMN2* genes are equivalent, and that their copy number is not always sufficient to accurately predict SMA severity (Oskoui et al., 2017).

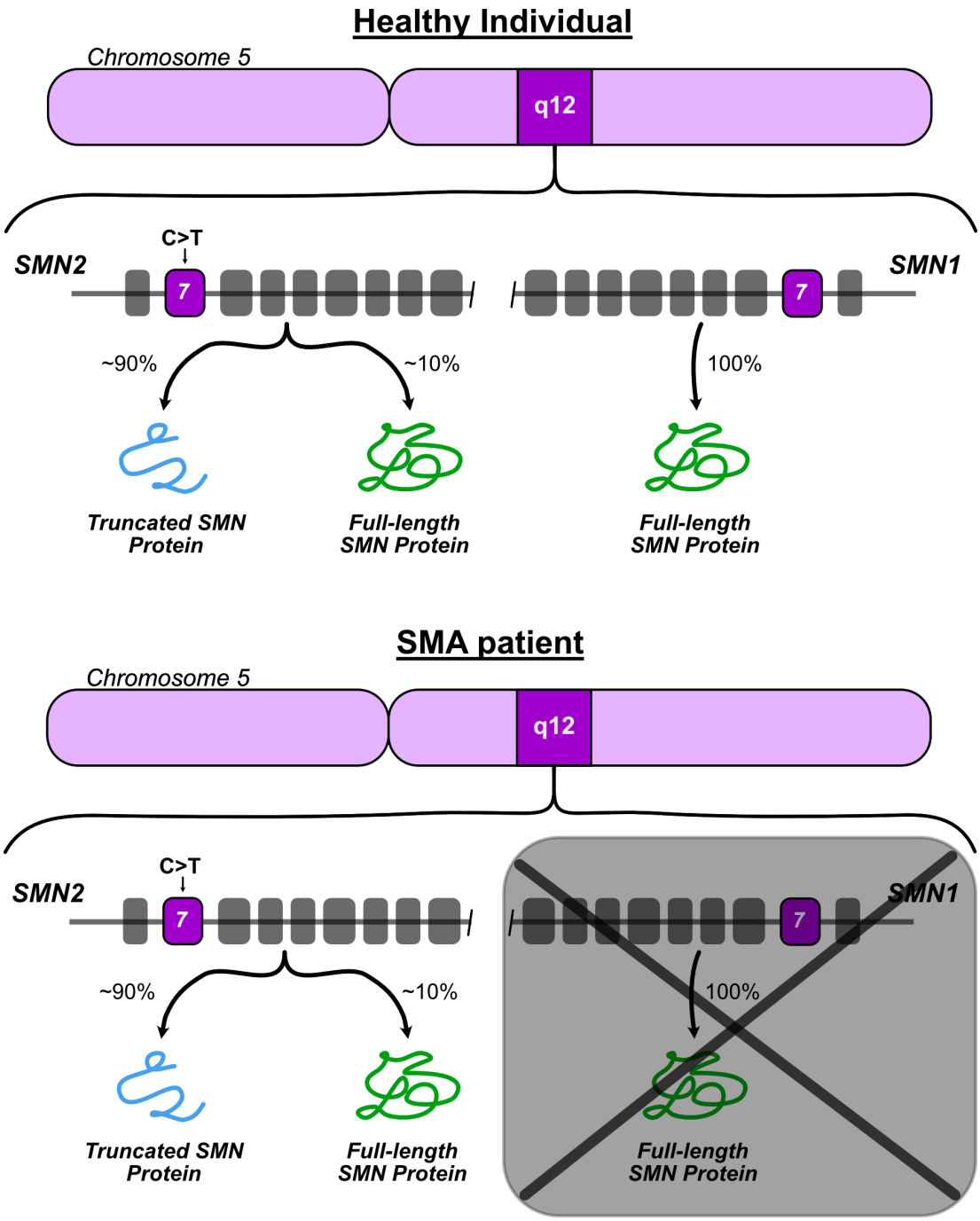

Figure 1.1 Schematic diagram detailing the genetic cause of spinal muscular atrophy. Healthy individuals have a non-mutated copy of the *SMN1* gene and at least one copy of the *SMN2* gene. The *SMN1* gene encodes for a functional, full-length SMN protein, whereas the *SMN2* gene produces only 10% of the full-length SMN protein due to a C-to-T transition in exon 7. As a result, when the *SMN1* gene is deleted or mutated in SMA patients, *SMN2* is unable to produce sufficient levels of the SMN protein.

1.2.3 Clinical subtypes

As introduced above, the phenotypic spectrum of SMA ranges from the manifestation of prenatal symptoms, characterised by the onset of early respiratory insufficiency, to the presentation of mild proximal weakness in adults (Oskoui et al., 2017). This has stimulated considerable ongoing debate concerning the appropriate classification of the various SMA phenotypes. In 1992, the International SMA Consortium established two methods of classifying the SMA clinical spectrum (Munsat & Davies, 1992). The first approach relies on a numerical method that utilises the age of symptom onset and lifespan to categorise cases as Type I, II, or III. The second approach is based on disease severity (severe, intermediate and mild) and on the highest motor milestones achieved (sitting, standing and walking). In view of the considerable variability of these clinical parameters among patients, it was soon evident that patients do not necessarily conform to a single classification (Dubowitz, 1995). Although this limitation is acknowledged, it is important to understand the different disease subtypes, as they are currently widely used in clinical practice.

SMA Type I, also known as *Werdnig-Hoffmann disease*, is the most severe and the most common form of SMA (Arkblad et al., 2009). Affected children present with progressive proximal weakness impacting primarily the lower limbs. Due to their inability to roll or sit independently, they are designated as “nonsitters”. Infants presenting with symptoms within the first week of life are classified as having SMA Type IA (also known as SMA Type 0), which is the most severe subtype and leads to early respiratory failure and death soon after birth (Dubowitz, 1999). Most of these infants have only one copy of the *SMN2* gene (Oskoui et al., 2017). Children who do not reach the ability to sit independently and who present symptoms between one and three months or three and six months of age are classified as SMA Types IB and IC, respectively, with two or three copies of *SMN2* present in the majority of cases.

In the natural history of SMA Type I, children generally do not survive beyond two years without respiratory and nutritional support and/or therapeutic intervention (Oskoui et al., 2007).

Infants with **SMA Type II**, also known as *Dubowitz disease*, have an intermediate form of the disease, and usually present with three copies of the *SMN2* gene. They are classified as 'sitters', as although they cannot walk, they can sit independently. SMA Type II can be subsequently classified into A and B subcategories, based on whether the children affected by this form retain or lose the ability to sit independently over time (Mercuri et al., 2016). The clinical manifestations include hypotonia, absence of reflexes and weakness of the limbs and of the intercostal muscle. This can result in the development of scoliosis, which, in turn, can lead to the onset of restrictive lung disease and the necessity for respiratory support. The natural course of survival in patients with SMA Type II is over two years old, although this can vary due to the heterogeneity of symptoms (Oskoui et al., 2017; Zerres et al., 1997).

SMA Type III is also known as *Kugelberg-Welander disease*. During their development, children affected by this form of SMA learn how to achieve the ability to walk independently, and for this reason are classified as “walkers”, although progressive muscular weakness can lead to loss of ambulation in the most severe cases (Montes et al., 2018). Most of these patients have three or four copies of the *SMN2* gene. Children diagnosed with SMA Type IIIA are those characterised by manifestation of the symptoms prior the age of three; when symptoms occur after 3 years of age, they are classified as Type IIIB. Although these children exhibit proximal muscular weakness, particularly in their lower limbs, their life expectancy is comparable to that of the general population (Oskoui et al., 2017; Piepers et al., 2008).

Finally, the least common and mildest SMA subtype is **Type IV**. In these cases, the onset of symptoms typically occurs in the thirties, manifesting as proximal limb weakness accompanied with a gradual progressive decour that, in some

patients, can result in loss of independent ambulation during life (Clermont et al., 1995). Individuals diagnosed with SMA Type IV typically possess four or five copies of the *SMN2* gene, a factor which enables them to have a normal life expectancy (Oskoui et al., 2017; Wadman et al., 2017).

1.3 Mouse models to study severe SMA

The identification of the precise genetic cause of SMA prompted researchers to initiate exploration of how to mimic and model disease processes in animal models, in order to facilitate a more profound understanding of SMA pathogenesis. Furthermore, the *SMN* gene is characterised by a high degree of evolutionary conservation, and it has been demonstrated that the amino acid sequence of murine *Smn* gene is 82% identical to the coding sequence of the *SMN* gene found in humans (Bergin et al., 1997; Didonato et al., 1997).

Initial evidence published in 1997 showed that homozygous deletion of the *Smn* gene was not compatible with life and resulted in early embryonic lethality in mice (Schrank et al., 1997). This was due to the absence of the *SMN2* gene, which, due to evolutionary reasons, is not generally present in species other than humans (Rochette et al., 2001). Therefore, it soon became clear that the successful development of an animal model able to closely recapitulate SMA phenotypes required the introduction of a human copy of the *SMN2* gene, alongside endogenous *Smn* deletion.

As a result, a number of murine models are currently employed in SMA research, covering the broad spectrum of disease severity. These models range from those replicating the most severe phenotypes, such as the Delta7 and the “Taiwanese” mouse models (Hsieh-Li et al., 2000; Le et al., 2005), which will be discussed in this paragraph, to those that exhibit milder manifestations of disease severity, as evidenced by the 2B mouse model, characterised by motor neuron loss and axonal degeneration, as well as by pancreatic and liver defects (Mélissa Bowerman et al., 2012; Melissa Bowerman et al., 2012; Deguise et al., 2019).

The earliest mouse model generated to study the **severe form of SMA** was reported in 2000 (Monani, 2000). In this murine model, the loss of *Smn* was achieved by the insertion of β-galactosidase gene into exon 2A of the *Smn* gene, generating a mouse *Smn* null allele ($Smn^{2A/2A}$). To demonstrate that *SMN2* could rescue the embryonic lethality observed in a preceding study, this model was characterised by the insertion of two copies of the *SMN2* transgene into the 2A background. This resulted in a mouse model, on a C57BL/6J genetic background, that was able to recapitulate SMA disease, characterised by early loss of motor neurons after 3-5 days of age and a median survival of six days.

In 2005, a new mouse model was developed to study the severe forms of SMA: the **Delta7 (Δ7) mouse model** (Le et al., 2005). Derived from an FVB/N background, this model also relied on the generation of an *Smn* null allele ($Smn^{2A/2A}$), accompanied by the introduction of the *SMN2* transgene. Furthermore, this model involved the introduction of a *SMN* gene lacking exon 7 (*SMNΔ7*). This addition has been shown to result in increased survival up to 11 days and presenting with a phenotype comparable to severe SMA, including manifestations such as muscle weakness, neuromuscular junction pathology and motor neuron loss (Oskoui et al., 2017).

The mouse model employed in this study is the **"Taiwanese" mouse**, a model originally established in 2000 to study severe SMA (Hsieh-Li et al., 2000). The genetic strategy implemented to generate this model differs from the two previously described. Indeed, while still relying on the endogenous *Smn* gene deletion and the human *SMN2* introduction, this model does not involve a null allele. Rather, it consists of a targeted replacement of exon 7 from the *Smn* gene with a hypoxanthine phosphoribosyl-transferase cassette. Furthermore, the *SMN2* transgene (*SMN2* Hung) used in this model contains two tandem copies of the *SMN2* gene per chromosome. This model has been shown to recapitulate the motor neuron disease proper of SMA pathology. However, the severity of the observed phenotype is variable and dependent on the number

of *SMN2* copies inherited. In this regard, alongside the variation of the insertion rate and site of the *SMN2* transgene, the mouse genetic background has also been documented as a major factor influencing disease severity and symptoms presentation (Signoria et al., 2023). In this context, the “Taiwanese” mouse model has been observed to present a less severe phenotype when maintained on a C57BL/6J background compared to an FVB/N background (Buettner et al., 2021). Specifically, “Taiwanese” mice on the FVB/N strain exhibit a lifespan 25% shorter than C57BL/6J mice. Notably, the study did not report any differences in the SMN protein levels between the two strains in this model.

To overcome these limitations, which could potentially compromise the reliability of the model, we use the severe “Taiwanese” mouse model developed using an optimised breeding strategy (Riessland et al., 2010) **(Figure 1.2)**. In this case, the mice were acquired from Jackson Laboratory (JAX), and each of them was characterised by four *SMN2* copies, with two copies per transgene, on an *Smn* null background and a pure FVB/N strain. By carrying four human *SMN2* copies, these homozygous mice ($Smn^{-/-}$, $SMN2^{tg/tg}$) do not manifest the SMA phenotype, however, they exhibit a short tail and can develop necrotic ears. Therefore, upon backcrossing with mice heterozygous for *Smn* deletion ($Smn^{+/-}$), the resultant litters comprise ~50% pups exhibiting SMA disease, characterised by homozygous endogenous *Smn* deletion and two copies of the human *SMN2* gene ($Smn^{-/-}$, $SMN2^{tg/0}$). The remaining ~50% of pups will be control carriers, presenting with a normal survival of approximately 24-30 months and characterised by heterozygous deletion of *Smn* and two copies of *SMN2* ($Smn^{+/-}$, $SMN2^{tg/0}$). This optimised breeding strategy successfully generates a model which recapitulates the severe SMA phenotype, presenting a robust and repeatable genotype and a lifespan of 10 days on average. In addition, this approach allows for a doubling of the number of SMA mice that have a more reliable genetic background for disease characterisation and potential therapeutic intervention.

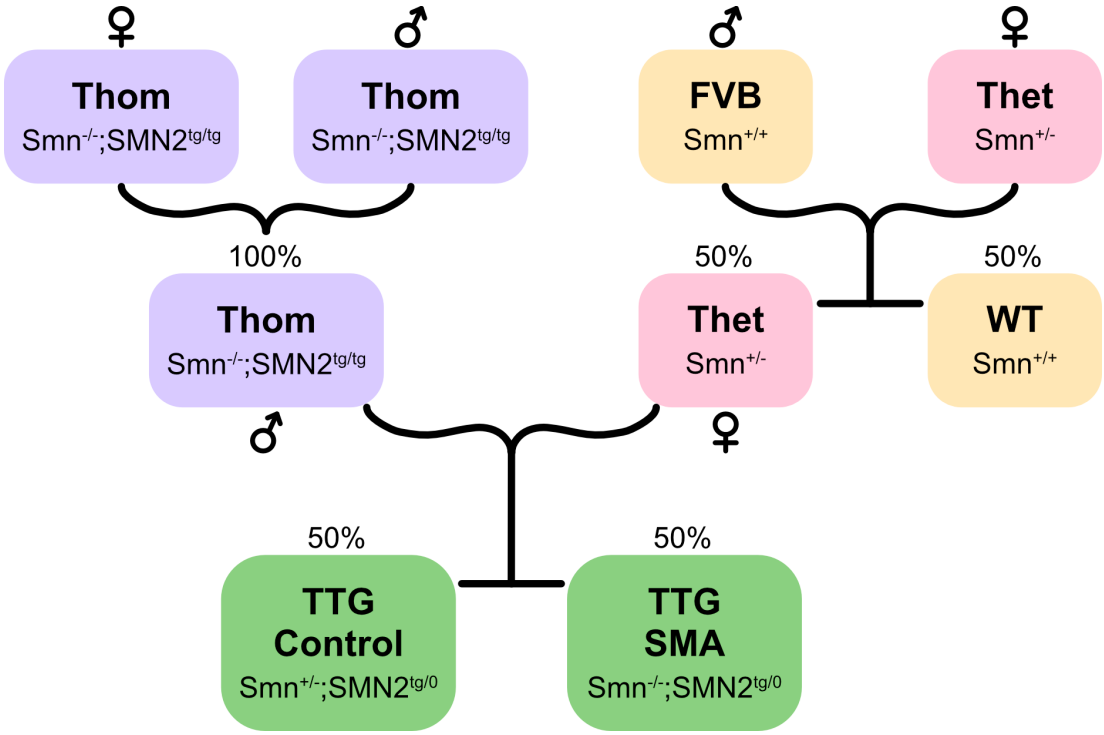

Figure 1.2 Breeding scheme and genetics of the severe SMA Taiwanese mouse model. The breeding protocol involves Thom (transgenic homozygous) mice backcrossed with other Thom mice, followed by a cross with Thet (transgenic heterozygous), which are obtained from the breeding of pure FVB mice to maintain the line. The resultant litter is the TTG (Taiwanese transgenic), comprising 50% of carrier controls and 50% of SMA pups.

1.4 Survival motor neuron (SMN) protein and its role in translation

1.4.1 Overview

The survival motor neuron (SMN) protein is an evolutionarily conserved protein that it is ubiquitously expressed in both the nucleus and the cytoplasm of all cell types (Ewout J. N. Groen et al., 2018). Its structural composition consists of 294 amino acids with a molecular weight of approximately 38 kilodaltons (kDa) and it is encoded by the *SMN* gene (Rochette et al., 2001). Within the cell, SMN localises to the Gemini of Cajal bodies, often also called “gems”, where it is found in conjunction with eight proteins (Gemins 2-8 and Unrip) to form the SMN complex, facilitating the correct splicing of pre-mRNA transcripts (Chaytow et al., 2018; Liu et al., 1997). Furthermore, the SMN protein localises to dendrites, synapses and axons playing a crucial role in the transport of mRNAs (Pagliardini et al., 2000). Alongside these canonical functions, recent research has highlighted a novel role for SMN in the regulation of protein translation (Bernabò et al., 2017; Lauria et al., 2020; Sharma et al., 2024) **(Figure 1.3)**. Importantly, the SMN protein is subjected to a dynamic regulation during the development of the organism (Burlet et al., 1998; Motyl et al., 2020). Its peak of expression occurs during the second and third trimester of gestation, after which it undergoes a significant reduction after birth, suggesting its fundamental role in guiding a correct embryo-foetal development (Ramos et al., 2019).

1.4.2 Canonical functions

Being ubiquitously expressed, SMN is an important protein characterised by several functions involved in numerous nuclear and cytoplasmic RNA-processing processes (Chaytow et al., 2018). The first identified role of the SMN protein is its involvement in the SMN complex, where in conjunction with other proteins, SMN facilitates the biogenesis of small nuclear ribonucleoproteins (snRNPs) (Liu et al., 1997). snRNAs are uridine-rich noncoding RNAs and are essential components of the spliceosome complex, responsible for the correct splicing of pre-mRNA transcripts and therefore for

nuclear post-transcriptional gene expression (Matera & Wang, 2014). The biogenesis of snRNPs begins in the nucleus with the transcription of uridine-rich snRNAs, which are then exported into the cytoplasm. The SMN protein plays a key role in this process by guiding the biogenesis of snRNPs in the cytoplasm and facilitating their subsequent trafficking to the nucleus. Importantly, a decrease in SMN levels results in the disruption of snRNPs assembly in severe SMA, highlighting the correlation between reduced snRNP levels and disease severity (Gabanella et al., 2007). In addition, it has been demonstrated that the SMN protein interacts with telomerase, a large RNP complex responsible for adding repeat sequences to the ends of chromosomes (Zhang et al., 2011). In this process, the SMN protein contributes to telomerase biogenesis by ensuring correct assembly and trafficking (Bachand et al., 2002). Furthermore, it has been shown that a deficiency in the SMN protein can lead to damage to ribosomal DNA (rDNA), resulting in impaired translation and synthesis of ribosomal RNA (rRNA) (Karyka et al., 2022). The rRNA molecules are key components of the ribosomes, the cellular structure where protein synthesis takes place. Impairments to rDNA have previously been linked to other neurodegenerative diseases, such as Huntington's disease, Parkinson's disease, Alzheimer's disease and amyotrophic lateral sclerosis. Therefore, by regulating rRNA synthesis, the SMN protein contributes to the final structure and function of ribosomes (Karyka et al., 2022). Further evidence supporting the interaction between SMN and ribosomes has been found in both *in vivo* and *in vitro* systems, suggesting an important role for SMN in protein translation (Béchade et al., 1999; Sanchez et al., 2013).

1.4.3 Non-canonical functions

The observation of the binding of SMN to ribosomes laid the foundations for further investigations revealing a direct role of SMN protein in translation and its impact on SMA pathology. One pivotal study has in fact demonstrated that reduced levels of SMN across different tissues result in translation and ribosome biology alterations in a SMA mouse model (Bernabò et al., 2017).

Specifically, this study investigated translation efficiency in the brain, spinal cord, kidney and liver of the “Taiwanese” mouse model at different postnatal stages of the disease. To perform translatome analysis, they employed polysome profiling, a technique that enables the isolation of mRNAs that are actively being translated, and that are therefore bound to polysomes (Jin & Xiao, 2018). This approach provides a high-resolution representation of ribosome occupancy and density, which is then examined to investigate the overall efficiency of protein translation. Indeed, by using this methodology, the authors unveiled a systemic but tissue-specific disruption in translation occurring at the early postnatal stages of SMA (Bernabò et al., 2017). In addition, by performing pathway enrichment analysis, the study identified chromatin and ribosomes as the most dysregulated molecular processes affected by translational changes, highlighting the impact of alterations in translation efficiency on ribosome biology.

Furthermore, subsequent research has demonstrated that SMN is a ribosome-associated protein *in vitro* and in postnatal brain and spinal cord of “Taiwanese” mice (Lauria et al., 2020). Notably, the composition of the ribosome is not static, and can be subjected to regulatory processes, including proteins that interact with its structure (Slavov et al., 2015). In their study, Lauria and colleagues revealed that SMN, alongside its canonical role in RNP biogenesis in the cytoplasm, is associated with a distinct population of ribosomes. These SMN-primed ribosomes have been found to be located at the beginning of the coding sequence (CDS) and associated with specific subsets of mRNAs, which have previously been linked to SMA pathogenesis. To obtain these results, the researchers performed ribosome profiling, a recently established technique that allows to determine the position of the ribosomes on the mRNA at a codon-level resolution (Jin & Xiao, 2018). This enables the deep sequencing of actively translating transcripts corresponding to those mRNA fragments protected by the ribosomes. Using this methodology, they revealed that the majority of mRNAs exhibiting significant variations in ribosome occupancy were downregulated in the absence of the SMN protein (Lauria et

al., 2020). Thus, the study demonstrated that SMN associates with ribosomes at the beginning of the CDS, thereby stabilising their conformation, proving a rationale for the translational disruption observed when SMN levels are significantly reduced.

The evidence presented here highlights the importance of the SMN protein in the regulation of translation in the context of SMA. This supports the hypothesis that one of the key consequences of SMN deficiency is the disruption of translation processes already at the early stages of the disease.

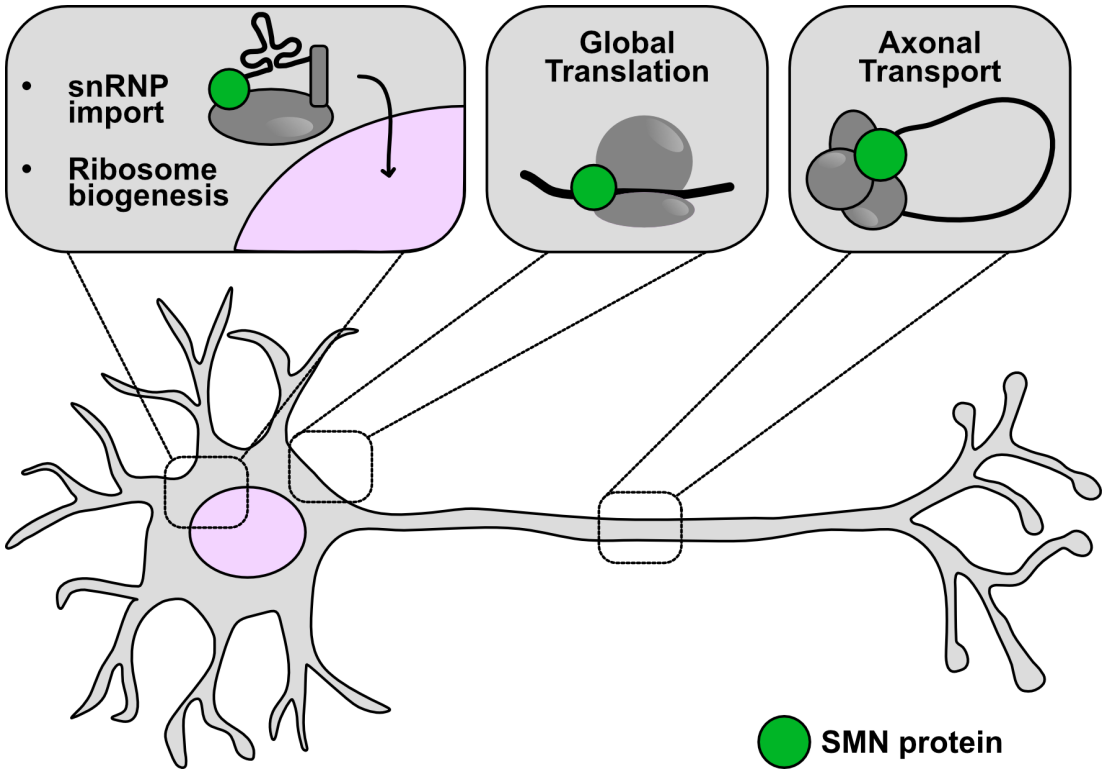

Figure 1.3 Schematic overview (adapted from (Sharma et al., 2024) of the functions of the SMN protein in the neuron. In the nucleus, SMN is responsible of guiding the snRNP biogenesis and its trafficking. Alongside this role, the SMN protein also regulates ribosome and telomerase biogenesis. In the cytoplasm, SMN bins to the ribosomes, stabilising their structure and ensuring a correct global translation. Along the axon, SMN plays a crucial role in mRNA transport, therefore regulating the proper translation of proteins essential for axonal growth and maturation.

1.5 Prenatal manifestations of SMA

Given the early nature of the symptomatology reported in infants presenting with the most severe form of SMA, researchers and clinicians are becoming progressively more interested in exploring whether the disease could manifest even before symptom onset, potentially during embryonic development. This hypothesis is supported by existing clinical observations showing that the highest levels of SMN protein expression occur in the second trimester of gestation, with lower levels after birth (Ramos et al., 2019). In addition, initial studies on SMA preclinical models revealed that a total absence of the SMN protein results in embryonic lethality (Schrank et al., 1997).

One of the earliest reports indicating prenatal SMA manifestations of SMA dates back to 1997, when sonographic and maternal serum screening revealed prenatal abnormalities such as ventriculomegaly and nuchal oedema in two foetuses affected by SMA Type I, manifesting at 11 and 16 weeks of gestation (Rijhsinghani et al., 1997). Furthermore, a case study from 1999 examining five babies with SMA Type I revealed a reduction in foetal movements between weeks 30 and 36 of gestation (MacLeod et al., 1999). Despite their preliminary nature, these observations are in line with subsequent clinical and preclinical studies that reported muscle denervation occurring at the prenatal stages of the disease (Martínez-Hernández et al., 2013; McGovern et al., 2008; Soler-Botija, 2002). Indeed, it has been demonstrated that development of the neuromuscular system during embryogenesis correlates with the occurrence of foetal movements that can be detected by ultrasound from week 8 of gestation (Felsenthal & Zelzer, 2017). For instance, Soler-Botija and colleagues reported the first evidence of progressive loss of motor neurons in the spinal cord of SMA foetuses at 12 weeks of gestation (Soler-Botija, 2002). In accordance with these clinical findings, research performed in the “Taiwanese” mouse model of severe SMA has shown prenatal changes in the innervation of the neuromuscular junctions (NMJ), the fundamental connections between motor neurons and muscle fibres, occurring as early as at embryonic day (E)18.5 (McGovern et al., 2008).

Moreover, quantitative and qualitative examinations on prenatal human samples revealed ultrastructural defects in NMJs in SMA Type I (Martínez-Hernández et al., 2013).

It is important to note, however, that the literature on prenatal manifestation(s) of SMA is limited, with the majority of research focusing on neuromuscular phenotypes. Only a small number of studies have addressed the systemic manifestations of the disease occurring at embryonic stages. Notably, among those, our group examined the systemic developmental components of severe SMA and in a recent publication revealed widespread perturbations in multiple systems and organs in E14.5 “Taiwanese” mouse embryos (Motyl et al., 2020). Specifically, the authors explored morphological and molecular phenotypes occurring in the brain, spinal cord, liver, heart and skeletal muscle at one specific timepoint of embryonic mouse development. Using micro-computed tomography for volumetric measurements and 3D reconstruction, they observed a general decrease in size of SMA mouse embryos compared to control littermates. Furthermore, a significant reduction in the volume of cardiac ventricles was observed in SMA embryos. While the authors did not detect any overt cardiac pathology, their findings are consistent with those reported by previous studies which indicated the presence of heart defects in mouse models of severe SMA at later stages of embryonic development (Shababi et al., 2010). Furthermore, to examine whether the morphological defects observed in SMA mouse embryos were accompanied by molecular differences, Motyl and colleagues performed a proteomic investigation using mass spectrometry on the organs of interest. The analyses revealed a proteome-wide disruption, with differentially expressed proteins detected in all organs, despite minimal overlap. In addition, the generation of a high-resolution proteomic dataset enabled the identification of dysregulated canonical pathways in each organ examined. Notably, organ-specific disruption was observed in some of the pathways known to be essential for development, revealing widespread developmental perturbations in SMA.

While the prenatal developmental nature of SMA is increasingly capturing the attention of the scientific community, the majority of recent research continues to be predominantly focused on motor neuron degeneration (Kataoka et al., 2023; Kong et al., 2021). The central aim of this thesis is therefore to provide a more profound insight into the cellular and molecular mechanisms underlying the observed manifestations of prenatal SMA, with a particular emphasis on the neurodevelopmental aspects of the disease. Moreover, given the recent advancements in the treatment of SMA patients using disease-modifying therapies, this thesis explores the amenability of prenatal defects to therapeutic intervention.

1.6 Disease-modifying therapies

At the time of the initial description of SMA and the subsequent identification of its genetic cause, effective therapeutic measures were not available, and SMA was the primary genetic cause of infant mortality (Moultrie et al., 2025). In the past decades, three disease-modifying therapies (DMTs) have been authorised by the Food and Drug Administration (FDA), in the US, and by the European Medicines Agency (EMA), in Europe, to treat SMA patients by targeting either *SMN1* or *SMN2* to increase SMN full-length protein expression (Chaytow et al., 2021) **(Figure 1.4)**. The three distinct DMTs use different therapeutic approaches. The first one is nusinersen, an antisense oligonucleotide that acts as a *SMN2* splicing modifier (Finkel et al., 2017). The second, onasemnogene abeparvovec, increases SMN protein production through gene therapy, which involves the replacement of the *SMN1* gene (Mendell et al., 2017). The third and most recent is risdiplam, a small molecule that modulates the splicing of the *SMN2* pre-mRNA (Baranello et al., 2021). In terms of their contribution to the SMA field, these therapies have been proven to have a remarkable impact on the clinical management of SMA patients, resulting in improvements in both survival rates and the quality of life (Chaytow et al., 2021).

1.6.1 Nusinersen

The first DMT approved by the Food and Drug Administration (FDA) in 2016 and by the European Medicines Agency (EMA) in 2017 was nusinersen, an antisense oligonucleotide (ASO) (Finkel et al., 2017; Mercuri, Darras, et al., 2018). ASOs are small synthetic single-stranded nucleic acids, ranging from 16 to 21 nucleotides (Collotta et al., 2023). By identifying specific RNAs through complementary base pairing, ASOs are able to bind to a target RNA sequence and modify protein expression. In order to enhance the production of full-length SMN protein, nusinersen was developed to target the intronic splicing silencer N1 (ISS-N1) in intron 7 of *SMN2* (Hua et al., 2008; Singh et al., 2006). The binding of the ASO to ISS-N1 has been demonstrated to inhibit negative splicing factors, thus resulting in increased inclusion of exon 7 consequently enhancing the production of full-length *SMN2* transcripts and protein.

Numerous preclinical studies have demonstrated the efficacy and safety of nusinersen in achieving homogenous distribution within the central nervous system and to increasing SMN expression in a dose-dependent manner following intrathecal infusion (Passini et al., 2011; Rigo et al., 2014). Moreover, clinical evidence has reported improvements in motor functions and the achievement of motor milestones (Finkel et al., 2016). Due to its inability to cross the blood-brain barrier (BBB), the protocol for the administration of nusinersen relies on multiple intrathecal injections (Scoto et al., 2017). Specifically, the first three in injections are delivered at 14-day intervals, the fourth dose is administered after 30 days and then maintenance injections are repeated every four months. While this treatment is available for SMA patients of all ages and subtypes, the requirement of intrathecal injections constitutes a limitation for those patients with severe scoliosis and contractures, as well as for those who have undergone spinal surgery (Xu et al., 2022).

1.6.2 Onasemnogene abeparvovec

In 2019 and 2020, respectively, the FDA and the EMA approved onasemnogene abeparvovec, the first gene replacement therapy to treat SMA (Mendell et al., 2017). The gene-based therapeutic approach has seen a marked increase in interest for the treatment of rare genetic neurodevelopmental disorders (Chaytow et al., 2021). Specifically, it has been demonstrated that the systemic delivery of adeno-associated viral vector serotype 9 (AAV9)-based gene transfer via intravenous injection can successfully cross the blood-brain barrier and efficiently transduce into the CNS (Foust et al., 2009; Meyer et al., 2015). Thus, the monogenic nature of SMA rendered it an optimal ideal candidate for gene therapy development using an AAV9 approach. As a result, onasemnogene abeparvovec, a non-replicating recombinant adeno-associated virus serotype 9 (AAV9) carrying the wild-type *SMN1* gene, was introduced as one-time treatment of paediatric SMA patients under two years of age and carrying a bi-allelic mutations in the *SMN1* gene (Mendell et al., 2017). Clinical evidence has shown significant improvement of motor function and a decrease in the need for respiratory and nutritional support (Day et al., 2021). Alongside these positive effects, it has been demonstrated that high doses of onasemnogene abeparvovec can result in liver dysfunction (Hinderer et al., 2018). Indeed, clinical trial reports have been documented transient elevations in serum aminotransferase levels reported in a number of cases, highlighting what it could be an immune response to the vector capsid. Despite the fact that the underlying mechanism of this dysfunction remains unclear, the administration of an immunomodulatory regimen prior to and following the intravenous injection has now been incorporated into the standard protocol for SMA patients undergoing the treatment (Chand et al., 2021).

1.6.3 Risdiplam

The most recent drug designed to treat SMA is risdiplam, approved by the FDA in 2020 and by the EMA in 2021 (Baranello et al., 2021). Risdiplam is a small-molecule splicing modulator, which acts on *SMN2* pre-mRNA and boosts exon

7 inclusion and full-length SMN protein production (Sivaramakrishnan et al., 2017). The development of this drug began with the RG7800 molecule, a splicer modulator that has been shown to enhance SMN protein expression in healthy adults and SMA patients (Kletzl et al., 2019). However, this molecule was not further advanced due to retinal damage observed in non-human primates (Ratni et al., 2018). Risdiplam is therefore the result of the optimisation of this molecule. The administration protocol of risdiplam relies on a daily oral delivery that allows for systemic distribution in the central nervous system, muscles, blood and other tissues (Poirier et al., 2018). Moreover, recent clinical trial results have indicated increased lifespan and improvement of both motor and respiratory function in SMA patients, with no evidence of retinal toxicity (Poirier et al., 2018; Sergott et al., 2021). A distinguishing characteristic of this drug, in contrast with the two previously described, is its method of administration. Indeed, the administration of risdiplam in the form of an oral solution or tablet facilitates a home-based therapeutic approach with risdiplam, thereby avoiding the necessity for invasive procedures and hospitalisation (Kakazu et al., 2021).

Intriguingly, a recent study suggests that risdiplam could be used for the treatment of Huntington's disease, a rare neurological disorder caused by a CAG trinucleotide expansion in the first exon of the *HTT* gene, which encodes the huntingtin protein. In this disease context, risdiplam acts as a splicing modifier that promotes the inclusion of a pseudoexon in the *HTT* gene's mRNA, introducing a stop signal and reducing the overall amount of the huntingtin protein (McLean et al., 2024). This finding highlights the therapeutic potential of risdiplam for the treatment of diseases beyond SMA and emphasises the importance of delving deeper into its mechanism of action to better understand its applicability and possible off-target sites.

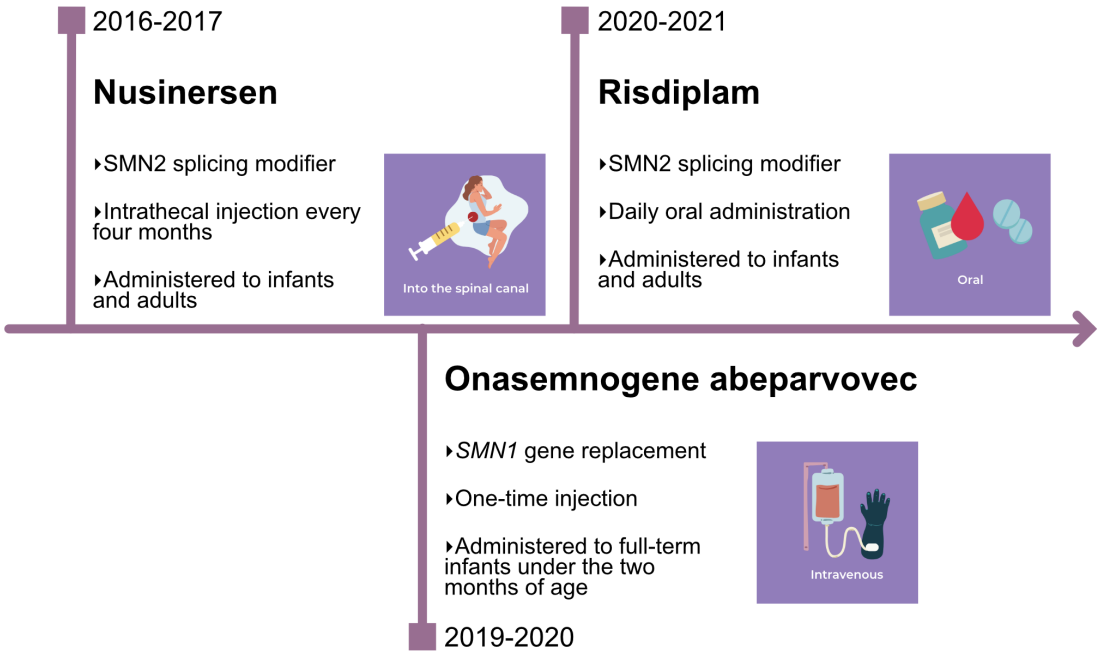

Figure 1.4 Schematic summary of the currently approved disease-modifying therapies (DMTs) to treat SMA. Nusinersen has been the first available DMT and it is a *SMN2* splicing modifier. The route of administration is via multiple intrathecal injections, and its use has been approved for infants and adults. The second DMT to become available was onasemnogene abeparvovec, a gene therapy treatment aimed at replaced the mutate *SMN1* gene. It is administered by a one-time intravenous injection, and it is only approved to full-term infants under the two months of age. Finally, risdiplam is the most recent *SMN2* splicing modifier, delivered daily as an oral solution or tablet. Its administration is available for all SMA patients. (Illustrations are adapted from (Wexler, 2025))

1.6.4 Combinatorial implementation of DMTs

Given the coexistence of three therapeutic approaches that have been demonstrated to be effective in alleviating clinical symptoms in SMA patients, there have been attempts to compare the outcomes in patients who undergo nusinersen, gene therapy or risdiplam treatment (Bitetti et al., 2023; Kokaliaris et al., 2024). However, a direct comparison of the different approaches is challenging due to the heterogeneity of patient symptoms and responses to therapy. Thus, it is not possible to determine whether one DMT is superior to another. Moreover, in recent years DMTs have been used in combinations in trials as well as in clinical practice. Specifically, a second DMT may be administered in the instance where the response to an initial DMT was incomplete or suboptimal (O'Reilly et al., 2025; Oechsel & Cartwright, 2021). Despite the absence of evidence demonstrating the long-term benefits and cumulative effects of this add-on therapy, clinical trials have revealed the safety of nusinersen administration following gene therapy with onasemnogene abeparvovec (Brandsema et al., 2022).

Another combinatorial approach with DMTs to treat SMA that has been implemented in clinical practice is known as bridge therapy (Proud et al., 2023). In this form of therapeutic intervention, nusinersen or risdiplam are administered in patients awaiting gene therapy. The implementation of this approach has the potential to occur in different situations. A relevant scenario could be represented by preterm infants diagnosed with the most severe form of SMA (Trollmann et al., 2024). Due to the significant concerns regarding the administration of immunomodulatory regimen with corticosteroids prior to full-term age, onasemnogene abeparvovec gene therapy has not been approved for administration to babies who have not reached a minimum of 37 weeks of gestation (Lee et al., 2021). Therefore, clinicians have attempted to implement bridge therapy and a number of case reports have highlighted the efficacy and safety of administering either nusinersen or risdiplam while waiting for an appropriate age for gene therapy administration (Bistritzer et al., 2025; Brown et al., 2024; Ferrante et al., 2022; Matesanz et al., 2020; Nigro et al., 2023).

Despite the limited availability of long-term data on combinational therapy with DMTs, it is now clear that, in order to maximise the beneficial therapeutic effects of the existing treatments, SMA must be diagnosed as early as possible (Moultrie et al., 2025). Indeed, it has been demonstrated that, especially in patients presenting with the most severe forms of SMA showing clinical manifestations prenatally and/or at the time of birth, the initiation of an early therapeutic interventions correlates with better outcomes (Goedeker et al., 2024; Sumner & Crawford, 2022). In this regard, several clinical trials including NURTURE, RAINBOWFISH, and SPR1NT, have provided solid evidence of the safety and efficacy of nusinersen, risdiplam, and onasemnogene abeparvovec, respectively, when administered in presymptomatic infants (Crawford et al., 2023; R. S. Finkel et al., 2025; Strauss et al., 2022). Collectively, these three single-arm interventional studies suggest that the early treatment for SMA can boost motor and functional outcomes in babies presenting with two or three copies of *SMN2,* compared to treatment initiated at symptomatic stage (K. Cooper et al., 2024). This emphasises the urgent need to identify babies with SMA before they exhibit any symptoms. A key factor that could facilitate the early diagnosis of SMA is the implementation of a large-scale newborn screening programme (Schwartz et al., 2024). This will allow for the identification of SMA disease in an infant within a few hours of birth.

1.6.5 Newborn screening for SMA

SMA genetic testing is key to identify carriers, confirming diagnosis, and enabling early intervention through newborn and prenatal screening (Wang et al., 2007). The gold standard methods, such as polymerase chain reaction (PCR) and multiple ligation-dependent probe amplification (MLPA), rely on quantitative analysis of *SMN1* and *SMN2* genes (Mercuri, Finkel, et al., 2018). In the event both parents are asymptomatic carriers with a single mutated *SMN1* allele, the risk of foetal SMA is 25%. Thus, prenatal screening can be facilitated through chorionic villous sampling (CVS), amniocentesis and non-invasive prenatal diagnosis (NIPD) (Khaniani et al., 2013; Parks et al., 2017).

However, as these tests are usually offered to mothers who are already known to be carriers of the mutation or who already have a child with a diagnosis of SMA, it cannot be considered a population-wide screening tool (Prior et al., 2010). Therefore, with the advent of disease-modifying therapies to treat SMA, the implementation of newborn screening has emerged as a prominent subject of discussion within the field (Katy Cooper et al., 2024). The fundamental objective of newborn screening is to identify children affected by SMA prior to symptomatic manifestations. This is of particular relevance in the context of SMA, as infants affected by the most severe forms typically manifest symptoms within the initial few months of life and, therefore, treatment administration at an earlier stage within the newborn period would be more beneficial (Strauss et al., 2022). As reported by the *European Alliance for Newborn Screening*, to date, 66% of newborns in Europe are screened for SMA at birth. Unfortunately, despite a general consensus among SMA families and the public, the UK does not yet have a newborn screening programme for SMA (Boardman et al., 2018; Gillingwater et al., 2022).

1.6.6 Limitations of current therapies and unmet needs in SMA

As discussed above, the three available therapies recently approved to treat SMA have shown to provide a broad range of benefits to patients, notably extending lifespan and facilitating the achievement of advanced motor milestones (Chaytow et al., 2021). Furthermore, the exploration of the combinatorial effects of DMTs has been implemented to boost therapeutic responses, and the application of early pre-symptomatic intervention has been found to have a significant impact on the quality of patients' lives (Moultrie et al., 2025; Yeo et al., 2024). Nonetheless, despite the undeniable advancement represented by DMTs, SMA remains a disease without a cure and is accompanied by several unresolved challenges yet to be addressed. Indeed, even with the employment of pre-symptomatic therapeutic intervention, some SMA patients do not fully regain optimal neuromuscular functions, but they continue to exhibit signs of impaired motor functions, respiratory difficulties and limitations in daily activities (Song & Ke, 2025). Moreover, from a logistical

perspective, the financial costs of the treatments, in addition to the individual regional or national regulations on healthcare, prevent inclusive access for SMA patients to therapeutic intervention (Dangouloff et al., 2021; Xiao et al., 2023).

Notably, the advent of newborn screening programmes in multiple countries has facilitated the early diagnosis of SMA in patients presenting with the most severe forms of the disease (Katy Cooper et al., 2024). Consequently, these patients are now receiving treatment at the early stages of the disease, resulting in an increased survival rate to ages that were previously unreported in the natural history of the disorder (Pera et al., 2024). This observation has led to the identification novel developmental symptoms in some SMA patients, including the presence of neurodevelopmental comorbidities (Baranello et al., 2024; Buchignani et al., 2025; Masson et al., 2021).

In consideration of this recent evidence, it is now apparent that SMA remains without a definitive cure, and that further investigation into the emerging clinical manifestations observed in some treated patients is needed. The remarkable milestones achieved in the understanding of SMA, from the initial clinical description of the symptoms to the approval of three disease-modifying therapies **(Figure 1.5)**, highlight the current need to further understand the underlying cellular and molecular mechanisms causing these novel neurodevelopmental phenotypes. This knowledge is therefore key to establish a new gold standard for clinical monitoring and to guide the next generation of therapeutic intervention.

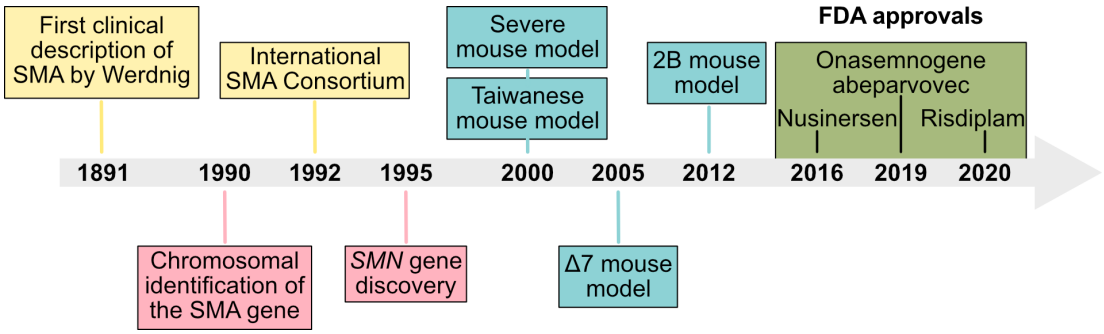

Figure 1.5 Schematic timeline of the key milestones achieved in the understanding and treatment of SMA. The first clinical documentation of SMA was reported in 1891 by the neurologist Guido Werdnig, who described the symptoms of early-onset progressive SMA in infants. Further observations led to the concept of distinct clinical subtypes based on the age of symptoms onset and the motor milestones achieved. This method of classification was introduced at the International SMA Consortium in 1992. Meanwhile, the chromosomal location of the gene responsible for SMA was identified in 1990, leading to the subsequent discovery of the *SMN* gene in 1995. Understanding the genetic cause of SMA enabled researchers to develop animal models that mimic disease processes and phenotypes. As a result, various murine models are now used in SMA preclinical research, including the severe and the "Taiwanese" mouse models, which were established in 2000; the Δ7 mouse model in 2005; and the 2B mouse model, developed in 2012. The advanced and ongoing understanding of SMA, achieved through these animal models, has led to the development of three disease-modifying therapies for the treatment of SMA patients: nusinersen, onasemnogene abeparvovec, and risdiplam.

1.7 Neurodevelopmental comorbidities in SMA

Since the advent of disease-modifying therapies to treat SMA, the most studied outcomes have been motor and respiratory symptoms, with very limited attention to the brain and cognitive development (Dangouloff & Servais, 2019; Giannotta et al., 2024). Notably, however, it has been observed that the SMN protein is highly expressed in the brain and has been hypothesised to play a crucial role in the early stages of brain development (Battaglia et al., 1997; Tizzano et al., 1998). This raised the question of whether reduced levels of SMN could have deleterious effects on the development of the central nervous system (CNS), particularly during the prenatal stages.

1.7.1 The hippocampus in cognitive neuroscience and in SMA pathology

Recent neuropathological studies in both animal models and SMA patients have revealed significant abnormalities in several areas of the CNS, including the hippocampus. In this context, this area of the brain is of particular interest, given its pivotal role in the study of cognitive neuroscience (Rubin et al., 2014). One of the most extensively studied roles of the hippocampus is its involvement in learning and memory. Indeed, as was first documented in a case report published in 1957, which described how a patient, H.M., developed a severe anterograde and retrograde amnesia following a bilateral hippocampal resection, the hippocampus has been linked to the ability to create and retain memories (Scoville & Milner, 1957; Squire, 2009). Furthermore, recent findings have indicated that the presence of hippocampal atrophy has been identified as a hallmark of Alzheimer's disease (Rao et al., 2022).

In addition, since the discovery of the "place cells" in 1971, the hippocampus has also been demonstrated to play a role in spatial navigation (O'Keefe & Dostrovsky, 1971). In this early publication, the authors demonstrated that specific neurons located in the rat hippocampus were indeed responding to the animal's location. In other words, these cells were found to be in an active state when the rat was in a specific place. Subsequent research revealed a

similar finding, where it was demonstrated that total lesions to the hippocampal could result in place-navigational impairments (Morris et al., 1982).

While initial studies on spatial navigation were exclusively limited in terms of physical space, in 1948 Tolman proposed the concept of a “cognitive map” as a representation of the social environment, thereby establishing the foundation for further research focused on the role of the hippocampus in contributing to the navigation of social interactions (Montagrin et al., 2018; Tolman, 1948). In this context, recent studies have explored the potential correlation between the hippocampus and disorders characterised by social and cognitive deficits, including autism spectrum disorder (ASD) (Banker et al., 2021). Despite the challenges in evaluating of such a complex condition, one of the main hallmark features of ASD is the impairment in social functioning, as well as spatial reasoning and episodic memory, suggesting a role for the hippocampus in contributing to the clinical manifestations of the spectrum (Bangerter et al., 2017). Thus, recent studies have reported hippocampal structural alterations, with evidence of altered volume, shape and texture in children diagnosed with ASD compared to healthy controls (Chaddad et al., 2017; Dager et al., 2007; Reinhardt et al., 2020).

Given its key role in regulating memory processes, spatial cognition and social behaviour, as well as its contribution in cognitive disorders, the hippocampus represents a highly relevant structure when explored in the context of SMA. Indeed, it has been demonstrated that the hippocampus is highly vulnerable to low levels of SMN during the early stages of SMA disease. For example, one prior research study showed a significant reduction in cell density and impaired neurogenesis in a severe mouse model of SMA (Wishart et al., 2010). Similarly, a clinical investigation observed substantial neuronal degeneration in the hippocampus of children with SMA Type I (Harding et al., 2015). In addition, these clinical brain manifestations were supported by neuroimaging studies that, by using MRI, revealed hippocampal atrophy and overall brain

macrostructural abnormalities in children with SMA Type I (Groulx-Boivin et al., 2024; Mendonça et al., 2019).

The identification of abnormalities in the hippocampus of both SMA patients and animal models suggests a pivotal role of this structure in the pathogenesis of the disease. In addition, these findings may also provide a biological underpinning contributing to the recent observations of neurodevelopmental comorbidities in some young patients with the most severe cases of the disease.

1.7.2 Cognitive development and functions in SMA patients

A considerable amount of evidence is now suggesting that neurodevelopmental comorbidities are becoming increasingly apparent in SMA patients, particularly in children with the most severe forms of the disease. Furthermore, these observations are highlighted by the increased survival rates of patients who are now able to receive treatment.

Despite the recent growth in interest concerning cognitive functions in SMA, a limited number of clinical case reports had already examined these manifestations as early as 1992. As illustrated in two publications by the neurologist Catherine Billard and her collaborators, the primary focus of their investigation was Duchenne muscular dystrophy (DMD), a X-linked recessive disease characterised by a severe pathology of the skeletal musculature and caused by the absence or disruption of dystrophin (Billard et al., 1998; Billard et al., 1992). To clarify whether DMD patients exhibited cognitive deficits, they compared them with SMA patients, who at the time were not known to present with cognitive impairments. The assessments covered diverse cognitive areas, including language, visuospatial abilities, attention and memory. Despite the absence of appropriate statistical analysis, the tests revealed normal performances by children with SMA, with higher scores compared to the those reported by DMD patients. Despite the preliminary nature of the two studies,

they contributed to the idea, that would last for several years, of optimal cognitive functions in SMA patients, at times even above the normal average.

The first and most differentiated study to focus on intelligence and cognitive functions specifically in SMA patients was published by von Gontard and collaborators in 2002 (von Gontard et al., 2002). The investigation covered vocabulary, memory, executive function, reading and arithmetic. Despite the reported bias in the selection of participants, the patients involved were representing a heterogenous group of children and adolescents presenting with SMA Type I, II or III. While the clinical subtype was not found to have an impact on cognitive performances, the authors hypothesised that the higher intelligence noticed in adolescents compared to the control group may be due to compensatory mechanisms to their difficulties in motor functions. A similar observation was reported in a subsequent study focused on the assessment of spatial language in children with SMA Type II (Rivière et al., 2009). The authors reported that SMA patients exhibited superior performance in producing spatial terms compared to a control cohort.

In contrast to these earlier studies, one of the first case reports to highlight potential cognitive defects in SMA patients was published in 2017 by Polido and colleagues (Polido et al., 2017). In this study, the authors assessed levels of attention, spatial location and executive functions in a cohort of children with SMA Type I. The results of the analyses demonstrated that these children performed below the normal average and had greater difficulties compared to controls when the complexity of the task was increased. Despite the absence of an ophthalmology evaluation prior the cognitive assessment, the study introduced a novel methodology by utilising an eye-tracking device to record the responses of those patients exhibiting severe motor dysfunction.

A retrospective study published in 2021 used a similar approach (Zappa et al., 2021). Here, the clinicians administered tests designed to evaluate cognitive functions, language comprehension and speech, specifically adapted to

enable children affected with the most severe forms of SMA to communicate in a coded way to respond yes or no to the questions. The aim of this study was to provide a baseline of the cognitive profile of SMA Type I patients prior to the therapeutic intervention with DMTs.

One of the first multicentre case reports investigating the possible correlation between cognitive development and motor functions in treated patients with SMA Type II and III was published in 2023 (Buchignani et al., 2023). In this context, only a small proportion of the assessed individuals exhibited intellectual disability, with no significant difference in relation to SMA subtype. Given the highly heterogenous cohort regarding time and type of treatment intervention, DMTs were not considered a variable in the study.

In the same year, a different longitudinal monocentric study explored cognition, expressive language and motor skills in 18 SMA Type I patients that received treatment either pre- or post-symptoms onset (Ngawa et al., 2023). By demonstrating that patients treated post-symptomatically generally exhibited scores below average, this study highlighted the necessity of including intellectual development assessment as one of the treatment outcomes for SMA patients.

Notably, another study included the variable of DMTs to evaluate language, verbal fluency, executive functions, memory and visuospatial functions in adult patients with SMA Type II and III treated with nusinersen (Vidovic et al., 2023). While the authors did not observe any differences in cognition between subtypes, the assessment after treatment revealed an overall improvement in several cognitive domains, although this was not statistically significant.

Subsequent cohort investigations explored cognitive development, expressive language and motor skills in groups of patients who had been diagnosed with SMA through newborn screening and who received treatment in accordance with healthcare regulations (Kölbel et al., 2024; Steffens et al., 2024). In these

studies, a considerable proportion of patients demonstrated subnormal cognitive development. Furthermore, the cognitive scores appeared to be proportionate to the number of *SMN2* gene copies, indicating a more pronounced impairment in children with only two *SMN2* copies. Intriguingly, in both studies female patients were observed to obtain higher scores than males.

Finally, early this year, the multidisciplinary team lead by Professor Baranello and Mercuri published a study aimed at exploring the neurobehavioral profile in children with SMA Type I and young infants diagnosed by newborn screening (Buchignani et al., 2025), all treated with at least one DMT. By assessing neurodevelopmental behaviour, cognition and social communication, the authors demonstrated that, alongside less frequent neurobehavioral difficulties, 10% of SMA patients showed the presence of ASD. Despite the need for a cautious interpretation of the findings, this study provided novel insights into the social and behavioural functioning of children with severe forms of SMA. This was achieved by the administration of comprehensive clinical evaluations and, most importantly, by adapting well-established and standardised tests, such as the ones routinely used to diagnose autism.

The evidence presented here collectively reports the ongoing efforts to enhance our comprehension of the neurodevelopmental comorbidities of SMA pathology, with a particular focus on the patients presenting with the most severe forms of the disease, highlighting the urgent necessity of the development of suitable tools to reliably assess these manifestations.

1.8 Hypothesis and aims of the thesis

The natural history of SMA has been shifted by the advent of the disease-modifying therapies currently available to treat patients (Yeo et al., 2024). Despite the undeniable benefits that these treatments are providing, SMA does not have a definitive cure yet. Indeed, a great amount of evidence has been

revealing novel phenotypes in SMA pathology, including neurodevelopmental comorbidities occurring in some of the treated patients, especially those presenting with the most severe forms of the disease (Baranello et al., 2024; Buchignani et al., 2025; Giannotta et al., 2024). These recent observations have raised the question of whether insufficient levels of SMN protein during the critical period of prenatal brain development could be responsible for these novel neurodevelopmental phenotypes.

Taken together, this evidence indicates the presence of crucial unanswered questions that need to be addressed. As a result, alongside an increased focus on the cognitive aspects in the clinical setting, there is the parallel need for further preclinical research with the aim of deepening the understanding of the early developmental stages of the brain in SMA disease.

Therefore, in this thesis, by using a well-established mouse model of severe SMA, I will explore the prenatal stages of the development of the brain, with a particular focus on protein translation. With this approach, I will test the hypothesis that the presented preclinical model can be reliably employed to study the prenatal manifestations occurring in the central nervous system of SMA embryos and to investigate the underlying molecular defects underpinning SMA pathogenesis, possibly contributing to the neurodevelopmental phenotypes observed in human patients.

Chapter 2: **Materials and Methods**

2.1 Study Design

This study was designed to investigate the prenatal developmental defects of SMA in the “Taiwanese” mouse model, with a particular focus on the role of protein translation. By exploring the development of the embryonic brain throughout the late organogenesis and by performing polysome and ribosome profiling, we unveiled primary cilia as a molecular mechanism underlying embryonic SMA pathogenesis. Sample size was determined by preliminary data and power calculations. All data were quantified and assessed blinded to genotype/treatment.

2.2 Statistical analysis

All statistical results are expressed as mean and SEM from at least five independent samples per group. For each embryo, three consecutive brain sections were analysed and averaged together. Differences between the two genotype groups (CTRL and SMA) were analysed by a one- or two-tailed unpaired parametric t-test. Difference among groups (CTRL, SMA vehicle/untreated and SMA risdiplam treated) were analysed by ordinary one-way ANOVA using Tukey’s correction for multiple comparisons. All statistical analyses were performed using GraphPad Prism 10.

2.3 Animals

2.3.1 Ethics

All animals were bred and handled following the UK Animals (Scientific Procedures) Act, 1986. Procedures were approved by the internal ethics committee at the University of Edinburgh and following UK Home Office regulations. This work was performed under the PPL (Procedure Project Licence) P92BB9F93, and PIL (Personal Licence) I65376428.

2.3.2 Breeding scheme

The “Taiwanese” model of severe SMA was maintained as previously described, and it was originally obtained from Jackson Laboratories (strain 005058) (Hsieh-Li et al., 2000; Riessland et al., 2010). Embryos with the genotype *Smn*$^{+/-}$*; SMN2*$^{tg/0}$ are indicated as healthy controls, while SMA embryos have the following genotype *Smn*$^{-/-}$*; SMN2*$^{tg/0}$. The morning of vaginal plug found was counted as embryonic day 0.5 (E0.5), and the embryos were collected when they reached the age of interest (from E12.5 to E18.5).

2.3.3 Embryo collection and development stage assessment

Pregnant dams were sacrificed at the desired time point and then embryos were collected individually. Each embryo was weighed, and the stage of development was assessed following the Theiler Staging Criteria for Mouse Embryo Development (Richardson et al., 2014). Prior to fixation, embryos’ heads were separated from the bodies. Tail tips were collected during the dissection and used for genotyping. Both genders were included and combined throughout the entire study.

2.3.4 Genotyping

Genotyping was performed following the laboratory’s protocols. DNA was isolated and extracted from tail tips collected during the micro-dissections. TTLB lysis buffer (100 mM Tris pH 8, 200 mM NaCl, 5 mM EDTA pH 8, SDS 0.2%) with proteinase K (50 μg/mL) was used to digest the tissue overnight. The following day, DNA was purified using isopropanol-mediated precipitation and used for PCR with the following programme and primers (Hsieh-Li et al., 2000):

94ºC	**94ºC**	**94ºC**	**58ºC**	**72ºC**	**72ºC**	**12ºC**
2’	2’	30sec	30sec	30sec	5’	∞

36 cycles

Primers:

Hung SMN F: ATAACACCACCACTCTTACTC

Hung SMN R1: GTAGCCGTGATGCCATTGTCA

Hung SMN R2: AGCCTGAAGAACGAGATCAGC

2.3.5 Embryonic sex determination

Embryonic sex determination was performed on tail tips collected during the micro-dissections. Although both genders were used throughout the entire study, sex was not considered as a biological variable. Sex was determined by PCR amplification of X chromosome genes with divergent Y chromosome gametologs. Extracted genomic DNA was then used for PCR with the following programme and primers (Tunster, 2017):

94ºC	**94ºC**	**60ºC**	**72ºC**	**72ºC**	**12ºC**
2'	20sec	20sec	30sec	5'	∞

30 cycles

Primers:

Rbm31 F: CACCTTAAGAACAAGCCAATACA

Rbm31 R: GGCTTGTCCTGAAAACATTTGG

2.3.6 *In utero* SMN replacement treatment with risdiplam

For *in vivo* pharmacological intervention with risdiplam, four pregnant dams were administered the drug at a concentration of 5 mg/kg for five consecutive days by oral gavage (PO). Brain tissues were then micro-dissected and collected at E14.5 or E15.5. Risdiplam was dissolved in 0.5% hydroxypropylmethylcellulose, 0.1% Tween-80 as previously described (Poirier et al., 2018).

2.4 Morphological and primary cilia investigation in the embryonic brain and spinal cord

2.4.1 Microtomy

Whole embryos' heads and bodies were fixed in 4% paraformaldehyde (PFA) overnight at 4°C. On the next day, tissues were rinsed with PBS and stored in 70% ethanol prior paraffin-embedding. Samples were dehydrated using an automated tissue processor and then infiltrated with histological wax. 10µm-thick coronal (heads or brains) and sagittal (bodies) sections using microtome were collected on SuperfrostTMPlus slides and kept overnight at 37°C.

2.4.2 Fluorescence immunohistochemistry

Wax sections were deparaffinised and rehydrated with Xylene and ethanol, respectively. Antigen retrieval was performed by maintaining the slides at a sub-boiling temperature for 20 minutes in Tris-EDTA or sodium citrate buffer depending on the primary antibodies. (10 mM Tris-base and 1mM EDTA solution pH 9.0 for ARL13B and ɣ-tubulin; 10 mM sodium citrate buffer, pH 6 for Ki67). Slides were then left to cool down at room temperature for 30 minutes. The sections were washed two times in 0.1% Triton X-100 in TBS and immersed in corresponding blocking solution at room temperature for one hour (10% donkey serum in TBS for anti-ARL13B and anti-ɣ-tubulin; 1% BSA, 10% donkey serum in TBS for K67). The sections were then incubated with primary antibodies overnight at 4°C (anti-ARL13B and anti-ɣ-tubulin were diluted in 5% donkey serum in TBS; anti-Ki67 was diluted in 1% BSA, 10% donkey serum in TBS). Primary antibodies used in this experiment were: rabbit polyclonal anti-Ki67 antibody (Abcam ab15580, 1:200); rabbit polyclonal anti-ARL13B antibody (ProteIntech 17711-1-AP, 1:200); and mouse monoclonal anti-ɣ-tubulin antibody (Sigma T6557, 1:500). After three washes of 10 minutes each in 0.025% Triton X-100 in TBS, sections were then incubated with secondary antibody at room temperature for two hours (1:400 donkey anti-rabbit Alexa Fluor 488 for Ki67 and ARL13B; 1:400 donkey anti-mouse Alexa Fluor 594 for ɣ-tubulin). After three washes of 10 minutes each in 0.025% Triton X-100 in 1xTBS, slides were counterstained by DAPI and mounted with Mowiol.

2.5 Western blotting for SMN protein quantification

Tissue collection and western blot procedures were performed as previously reported (E. J. N. Groen et al., 2018). Briefly, tissues were snap-frozen in dry ice and stored at -80 °C freezer until use. Tissues were homogenized in radioimmunoprecipitation assay buffer (ThermoFisher Scientific) with Halt™ protease inhibitor (#78429, ThermoFisher Scientific). Protein concentrations were determined using the bicinchoninic acid method. 30 µg of total protein was used in *in utero* SMN replacement experiment. After electrophoresis, proteins were transferred to a polyvinylidene difluoride membrane (iBlot2, ThermoFisher Scientific). Total protein was quantified by RevertTM Total Protein Stain (520nm or 700nm, LI-COR). Membranes were then blocked in Odyssey PBS blocking buffer (LI-COR) or EveryBlot blocking buffer (Bio-Rad), followed by incubation anti-SMN antibody solution (BD Bioscience #610646, 1:1500) overnight at 4°C. The next day, membranes were washed with 1× PBS at RT before and after and secondary antibody incubation (LI-COR). Membrane is dried followed by image acquisition on an LI-COR Scanner Odyssey M.

2.6 Primary hippocampal neuronal cultures and treatment with risdiplam

2.6.1 *Ex vivo* hippocampal neuron preparation

Primary hippocampal cell cultures were prepared as previously described (Brewer et al., 1993). Hippocampal tissues from E17.5 Taiwanese mice embryos were dissociated with papain (Worthington Biochemical PAP2, reconstitute to 10U/mL in PBS) and placed in a 37℃ waterbath for 20 minutes. Supplemented DMEM/F12 (with 5mL penicillin/streptomycin solution and 50mL sterile filtered foetal bovine serum (Life Technologies 21331-020) was then added to the dissociated tissues to a final volume of 5mL followed by centrifuging at 1500rpm for 5 minutes at room temperature. The pellet containing hippocampal cells was resuspended in pre-warmed supplemented Neurobasal (with 10mL B-27 supplement, 1.25mL 0.5mM L-glutamine and

5mL 1% v/v penicillin/streptomycin solution) media. Each embryo's hippocampus was individually dissociated and plated on individual 6-well plates. $6x10^4$ cells per well were plated onto poly-D-lysine coated coverslips in a 6-well plate. The cells were allowed to adhere in a 37℃/5% CO_2 incubator for one hour. Supplemented Neurobasal (2mL) was then added to each well and cells further incubated at 37℃/5% CO_2. Two days later, Cytosine β-D-arabinofuranoside (Ara-C) was added to the culture at a final concentration of 1μM per well to prevent glial proliferation.

2.6.2 Pharmacological treatment with risdiplam

Hippocampal neurons were treated for 72h from day *in vitro* 5 (DIV5). For each 6-well plate, half (3 wells) were treated with risdiplam (Cayman Chemical 29028), while the other half received the same quantity of sterile deionised water as control. Following a protocol previously described by Signoria and colleagues, risdiplam dissolved in deionised water was used at final concentration of 0.5 μM and treatment was refreshed every 24h (Signoria et al., 2024).

2.6.3 SMN expression levels following treatment with risdiplam

Total RNA was extracted from cultured hippocampal cells using a RNeasy Plus Kit (Qiagen). Total RNA (80 ng) was used for first strand cDNA synthesis, using a Maxima First Strand cDNA Synthesis Kit for RT-qPCR (Thermo). Quantitative real-time PCR was performed on CFX Opus Deepwell system (Bio-Rad) using PowerUp™ SYBR™ Green Master Mix for qPCR (Thermo) according to the manufacturer's instruction.

Human-specific full-length *SMN2* primers [133 bp]:

Forward, 5'-ATA CTG GCT ATT ATA TGG GTT TT-3',

Reverse, 5'-TCC AGA TCT GTC TGA TCG TTT C-3';

Human-specific *SMN delta7* primers [125 bp]:

Forward, 5'-TGG ACC ACC AAT AAT TCC CC-3',

Reverse, 5'-ATG CCA GCA TTT CCA TAT AAT AGC C-3';

Mouse-specific *GAPDH* primers [83 bp]:

Forward, 5'-AAT GTG TCC GTC GTG GAT CTG A-3',

Reverse, 5'- GAT GCC TGC TTC ACC ACC TTC T -3'

(Ruggiu et al., 2012; Zhou et al., 2013).

The program includes an activation at 50°C for 2 min, amplification and detection by 40 cycles of 95°C for 10 sec, and 60°C for 30 sec, followed by the melt curve protocol with 5 sec each at 0.5°C increments between 65°C and 95°C. Four biological samples (embryos) for each condition were run in triplicate. The cycle at which the amount of fluorescence was above the threshold (Ct) was detected. Relative full length and delta 7 *SMN* expression for each sample was firstly normalised to its *GAPDH* level then compared to controls.

2.6.4 Fluorescence immunocytochemistry

After 8 days *in vitro* (DIV8), cells were fixed in 4% PFA for 15 minutes. The coverslips were treated in 0.1% Triton X-100 in TBS for permeabilization for 20 minutes and immersed in blocking solution (20% donkey serum in TBS) at room temperature for one hour. The coverslips were then incubated with primary antibodies overnight at 4ºC in 10% donkey serum in TBS (anti-ARL13B 1:500, anti-ɣ-TUBULIN 1:2000, anti-GFAP ThermoFisher 13-0300 1:200, anti-NeuN Merck MAB377 1:100). After three washes of 10 minutes each in 0.025% Triton X-100 in TBS, coverslips were incubated with secondary antibody at room temperature for two hours. After three washes of 10 minutes each in 0.025% Triton X-100 in TBS, the coverslips were counterstained by DAPI then mounted with Mowiol.

2.7 Optical and confocal microscopy

2.7.1 Mouse embryonic development timeline

Immunofluorescent whole brain sections from control embryos stained with the proliferation marker Ki67 were imaged on LI-COR Scanner Odyssey M (LICOR-ODM-0307) using 5 µm resolution and 2.50 mm focus offset.

2.7.2 Hippocampus cell proliferation and ciliated cells

Immunofluorescent sections were imaged on an inverted confocal microscope (Nikon A1R). For Ki67 and DAPI staining, were imaged using a 40x magnification oil-immersion lens and z-stacks were acquired with Galvano scanning at 1 µm step. For ARL13B, ɣ-TUBULIN and DAPI staining used for primary cilia investigation, three consecutive sections per mouse were imaged using a 60x magnification oil-immersion lens. Z-stacks were acquired with Galvano scanning at 0.3 µm step. The precise sections used for the analysis were selected by the identifications of neuroanatomical landmarks illustrated in the Schambra Prenatal Mouse Brain Atlas. Cilia quantification was performed by collapsing five z-stacks in a max intensity z-projection on ImageJ. The field of view was divided in three 60x60 µm squares, randomly distributed around the anatomical region of interest. DAPI and ciliated cells quantification was performed in each of the squares and then averaged.

Immunofluorescent hippocampal cell cultures stained for ARL13B, ɣ-TUBULIN and DAPI were imaged on a Nikon A1R confocal microscope using a 60x magnification oil-immersion lens and z-stacks were acquired with Galvano scanning at 0.3 µm step. Cilia morphological measurements were performed on the entire field of view (208x208 µm) by collapsing all z-stacks in a max intensity z-projection on ImageJ.

2.8 Investigation of protein translation

2.8.1 Polysome profiling

For sucrose gradient preparation, solutions were prepared using a specific buffer composition (10 mM Tris-HCl pH 7.5, 10 mM MgCl2, 10 mM NaCl) with varying sucrose concentrations. Small gradients (4 mL) were prepared by overlaying 1.6 mL of 40% (w/v) sucrose buffer and filling the tube with 10% (w/v) sucrose buffer. The gradient was formed by keeping the tube horizontally for 120 minutes at 4°C. For cytoplasmic lysates preparation mouse-frozen tissues were used following the protocol described in 2017 study (Bernabò et al., 2017). Tissues were pulverized in liquid nitrogen using a pestle and a mortar. After pulverization, tissue polysome lysis buffer (Bernabò et al., 2017)

was added to resuspend the powder. Lysates were kept for 17-20 min on ice for cell lysis. Then samples were centrifuged twice at 12,000 rpm in Eppendorf Centrifuge 5417 for 10 mins and the supernatant was collected. Samples were loaded on 4mL polyallomer ultracentrifuge tubes (Beckman) containing 10%-40% (w/v) linear sucrose gradient and ultracentrifuged for 1 h 30 mins at 40,000 rpm at 4 °C in Beckman Optima XPN-100 Ultracentrifuge in SW41 rotor. Sucrose fractions were collected using Teledyne Isco model 160 gradient analyser equipped with a UA-6 UV/VIS detector to measure the absorbance at 254 nm. Plotting absorbance vs fraction number yields a polysome profile.

2.8.2 Fraction of ribosome in polysomes

The fraction of ribosomes in polysomes (FRP) is measured based on the polysome profiling curve. FRP in percentage is calculated dividing the area under the polysomes by the sum of the areas under the 80S, corresponding to the single ribosome unit, and the area under the polysomes, the result multiplied by 100.

2.8.3 Western blotting for protein co-sedimentation

From each sucrose fractions, proteins were extracted and purified using methanol/chloroform precipitation, as previously described (Bernabò et al., 2017). Briefly, 600 µL of methanol, 150 µL of chloroform, and 450 µL of distilled water were added to each 1 mL fraction. Samples were mixed and centrifuged at 12,000 rpm for 2 min at 4°C. After centrifugation, the aqueous-methanol phase was discarded. To promote protein precipitation, 450 µL of methanol were added to the protein-chloroform phase. Samples were then mixed and centrifuged for 7 minutes at 4°C. The supernatant was removed, and the protein pellet dried under the hood for 45 min to be finally resuspended in 1X electrophoresis sample buffer (Santa Cruz Biotech) for immunoblotting.

Proteins from each fraction were denatured for 10 minutes at 99°C and loaded on polyacrylamide gels and run in a running buffer for 20 minutes at 80 V, followed by 100 V for 20 mins, and finally at 120 V. Proteins were transferred to nitrocellulose membrane in transfer buffer at 200 mA for 90 mins at 4°C.

Membrane was then immerged in blocking solution (3% non-fat milk in TBS-Tween) for 4 hours at room temperature on a shaker. The membrane was incubated overnight at 4°C with the following primary antibodies diluted in the blocking solution: SMN (1:2000, BD Transduction Laboratories #610646); RPL26 (1:2000, Cell Signaling #2217); RPS6 (1:2000, Thermo Scientific #PA5-275451). The following day, after removal of the primary antibody, three washes of 20 minutes each were performed in TBS-Tween. Next, the membrane was hybridized for 1h30 at room temperature with the appropriated secondary antibody: HRP goat anti-mouse (for SMN, 1:2500, Thermo Scientific #31430); HRP goat anti-rabbit (for RPL26 and RPS6, 1:2500, Thermo Scientific #31460). Next, two washes of 15 minutes each were performed with TBS-T, followed by one 20-minute wash with TBS. The acquisition was performed with a ChemiDoc MP imaging system (Bio-Rad). The co-sedimentation profiles of proteins with the translational machinery were calculated and obtained as previously described (Bernabò et al., 2017).

2.8.4 Ribosome profiling and library preparation

Brain and spinal cord were collected from control and SMA embryos at E14.5, snap frozen and then stored at -80℃ until used. Cytoplasmic lysates were prepared as described previously (Bernabò et al., 2017). Briefly, the tissues were pulverised with a sterile pestle and mortar in liquid nitrogen, and then 400-800 µL of tissue was added to ribosome lysis buffer (10mM Tris-HCl pH 7.5, 10mM $MgCl_2$, 10mM NaCl, 1% w/v TritonX-100, 5 U/mL DNAseI, 800 U/mL RiboLock RNAse Inhibitor, 1mM DTT, 200 µg/mL cycloheximide, 1% w/v Na-deoxycholate). To facilitate cell lysis, lysates were incubated on ice for 17-20 mins followed by centrifuging twice at 12,000 rpm for 10 mins at 4°C to remove tissue debris, mitochondria, and nuclei. Supernatants were measured for the 260nm absorbance, the final NaCl salt concentration of the lysate was adjusted to a final salt concentration of 100 mM.

Ribosome purification was achieved by treating lysates with 10 U/Abs RNAse at room temperature for 45 mins followed by addition of 5 µL of SUPERase-In RNase inhibitor (Thermo Fisher Scientific) to halt the reaction. Lysates were

loaded onto 13.2 mL polyallomer ultracentrifuge tubes (Beckman) containing a 10%-40% (w/v) linear sucrose gradient (10mM Tris-HCl ph7.5, 10mM $MgCl_2$, 10mM NaCl). After ultracentrifugation for 90 mins at 40,000 rpm, 4°C in a Beckman Optima XPN-100 ultracentrifuge with an SW41 rotor, the fraction corresponding to the 80S monosomes was collected using a Teledyne ISCO model 160 fractionator equipped with a UA-6 UV/VIS detector. The fraction was then used for RNA purification using the phenol/chloroform protocol. Ribosome-protected fragments (RPFs) measuring 28-32 bps were separated and purified using a 15% Urea-TBE gel. After RNA extraction from the gel, RPFs were then dephosphorylated using 120U T4 polynucleotide kinase (New England Biolabs #M0201S) and 20U of SUPERase-InTM Rnase inhibitor in T4 PNK polynucleotide kinase buffer (New England Biolabs) at 37 °C for 1 hour followed by 10 mins incubation at 70 °C to inactivate the enzymes. After RPFs purification, the libraries were prepared as previously described (Lauria et al., 2020). Experiments were performed in triplicate.

2.8.5 Ribosome profiling data analysis

Libraries from E14.5 brain and spinal cord tissues of Taiwanese mouse embryos were sequenced at the CIBIO NGS facility of the University of Trento, Italy, using an Illumina NovaSeq6000 system.

Reads Clipping and Trimming

Trimming of reads was performed with Cutadapt (v4.1)(Martin, 2011). The first three nucleotides (5' end) were trimmed and the adapter sequence of 15 As was removed (3'end). Reads shorter than 15 nucleotides were discarded. Maximum error rate and minimum overlap parameters were set at 0.15 and 10, respectively.

Reads Alignment

Reads mapping on the collection of *Mus musculus* rRNAs (from the SILVA rRNA database, release 119) and tRNAs (from the Genomic tRNA database: gtrnadb.ucsc.edu/) were removed. The remaining reads were mapped on the

mouse genome (using the Gencode M22 annotations ensembl 97) allowing a maximum of 5 multiple alignments for each read. All alignments were performed with STAR (v2.5.3a) employing default settings. Reads mapping on the same position with respect to transcript coordinates were then removed before proceeding with positional analyses. The identification of reads P-site position on the transcript was performed using riboWaltz (Lauria et al., 2018). Duplicated reads mapping on the same position with respect to transcript coordinates were also removed.

Positional Analysis

After having identified the P-site position of reads on the transcripts, riboWaltz was used to inspect the good quality of the ribosome profiling libraries. The read length distribution of ribosome footprints was computed by averaging replicas of each condition (SMA and controls).

RiboWaltz was used to inspect the trinucleotide periodicity along the coding sequence and investigate potential differences in the localization of the ribosomes between control and SMA mice. Overlaid meta-profiles were computed at single nucleotide resolution, based on P-site position of ribosomes. To compare the meta-profiles, we displayed the frequency of the signal around the translation initiation and translation termination sites, so that the area under each meta-profile (composed by the portion around the start codon and the portion around the stop codon) is equal to one. Meta-profiles were computed on all protein-coding transcripts. Stars are reported on nucleotide positions with significant differences between SMA and control signal, based on pair-end T-test (* P-value < 0.05). Genes with signal lower than a specified threshold were filtered out. This specific threshold value was computed for each replicate as it follows. First, genes with zero counts for all the replicates were removed from the gene count table. We computed fragments per kilobase of transcript per million mapped reads (*fpkm)* with the EdgeR package (Chen et al., 2016; McCarthy et al., 2012; Robinson et al., 2010). We then computed the 80^{th} quantile of the *fpkm* distribution for each replicate and used the resulting values as cut-off in the filtering step. Genes

with *fpkm* values below the threshold values for all the replicates of a condition (control or SMA) were filtered out, resulting in a total amount of 10481 genes. A multidimensional scaling plot was computed using *fpkm* values of genes (n=10,481) to display the differences between the expression values of different replicates in two dimensions. Normalization among replicates was performed with the trimmed mean of M-values normalization method (TMM) implemented in the EdgeR Bioconductor package. Pairwise differential analyses (SMA vs control) were performed independently for each tissue. Significantly differential genes were defined by the following cut-off values: *cpm_thr*=0.05, log_2FC_thr=0.5 and *pval_thr*=0.05.

2.8.6 Ingenuity Pathway Analysis (IPA)

Differentially expressed genes (DEGs) datasets combined from brain and spinal cord were inputted into the IPA application (Ingenuity System, Silicon Valley, CA), applying log_2FC_thr=0.3 and pval_thr=0.05 as cut-off values. To identify affected canonical pathways, IPA assigns input gene IDs to their equivalent entries within the Ingenuity's Knowledge Database, thereby enabling accompanying mapping of each input gene ID against a curated library of accompanying molecular interactions, pathways, and targets reported in the literature. As output, IPA not only calculates the ratio of the number of molecules in the dataset per pathway to the total number of molecules assigned to that pathway, but also through a weighted calculation accounting for pathway size, molecule hierarchy and total number of interactions constituting the pathway, reports upon the likelihood of the entire pathway itself being inhibited or activated. We identified the top 10 most affected canonical pathways represented by our DEGs, including the cilium assembly pathway. We therefore selected the specific molecules IPA ascribed to this pathway (20 genes in total) and we performed a deeper enrichment analysis not restricted to the Ingenuity's Knowledge Database. From this analysis, IPA revealed the top two functional terms showing a strong enrichment in cilia (Formation of cilia pval $5.02E^{-14}$ and Assembly of non-motile cilium pval $1.60E^{-10}$). The directionality of the enrichment was predicted by

applying an overlay of the identified functional terms and the log_2FC and p-value of the genes identified in the canonical pathway.

Chapter 3: **Modelling prenatal brain development in a mouse model of severe SMA**

3.1 Introduction

Understanding the prenatal manifestations of SMA is key to gaining a comprehensive knowledge of how and when the disease begins to emerge, and to identify the underlying causes. The expression of SMN protein is dynamically regulated during development, presenting with higher levels during embryogenesis and a significant reduction after birth, highlighting a potential role of SMN for correct embryonic development (Ramos et al., 2019). As a result, prenatal aspects of SMA have gained increasing attention in the recent years. Post-mortem studies on human prenatal samples have identified deep defects in muscle innervation and motor axon development showing that the degeneration begins in utero and that foetal therapeutic intervention is required to improve axonal function and motor behaviour (Kong et al., 2021; Martínez-Hernández et al., 2013).

To provide additional knowledge on prenatal SMA, a recent study from our lab, using one of the most established mouse models, the “Taiwanese” mouse model for severe SMA (Hsieh-Li et al., 2000; Riessland et al., 2010), revealed that SMN depletion leads to a broad spectrum of morphological and molecular perturbations in the brain, spinal cord, liver, heart and muscle of SMA embryos, long before symptoms appear (Motyl et al., 2020). By focusing on overall morphology, the study showed that at the embryonic age of E14.5 SMA embryos were smaller than littermate controls with internal organs differentially affected, revealing clear embryonic developmental defects.

Taken together, this evidence highlights the prenatal effects of SMN level insufficiency, revealing that the embryonic defects are not limited to motor neurons but extended to different peripheral organs, leading to a widespread systemic developmental delay.

During organogenesis, SMN protein is highly expressed across the central nervous system (CNS) and in particular in the forebrain and hippocampus (Briese et al., 2006). Here, SMN protein contributes to several fundamental biological processes such as cell proliferation, migration and differentiation. Mouse studies on SMA brain during postnatal development revealed selective morphological changes in brain morphology and hippocampal neurogenesis, highlighting the critical role of SMN in brain development, formation, and maintenance (Wishart et al., 2010).

It became, therefore, crucial to deepen the understanding of whether and how SMN deficiency during the prenatal period might contribute to long-term neurological outcomes. Recent clinical observations suggest that some SMA patients, particularly those with severe forms of the disease, may present with delays in cognitive development and difficulties in attention, problem-solving, and memory even after receiving an SMN-restoring therapy (Baranello et al., 2024; Bitetti et al., 2024; Buchignani et al., 2024; Buchignani et al., 2025; Cottam et al., 2023; Kölbel et al., 2024; Masson et al., 2021; Ngawa et al., 2023; Steffens et al., 2024; Tosi et al., 2023; Yang et al., 2023). These emerging developmental phenotypes in SMA are largely unexplored and the reason why they manifest, particularly in patients with SMA type I and II, is still unknown. This is partly due to the lack of a standardised assessment, and partly due to the challenges of accessing human samples (Akodad et al., 2024). Therefore, because of the complexities and ethical challenges of studying cellular and molecular processes directly in the human brain, animal models serve as a critical tool for investigation.

In this chapter, I explored the potential to study prenatal brain development in the “Taiwanese” mouse model for severe SMA, previously shown to have reduced embryonic levels of SMN (Hsieh-Li et al., 2000; Motyl et al., 2020; Riessland et al., 2010).

3.2 Aim

The aim of this chapter was to establish whether it is possible to model and study embryonic brain development using an established mouse model of severe SMA: the “Taiwanese” mouse model (Hsieh-Li et al., 2000; Riessland et al., 2010). I investigated the gross morphology of the healthy mouse (control) brain throughout organogenesis, spanning from embryonic day 12.5 (E12.5) to embryonic day 18.5 (E18.5). At each timepoint I quantified levels of cell proliferation using Ki67 as a marker (Gerdes et al., 1984). For this analysis, I focused on the hippocampus, particularly on the area corresponding to the dentate gyrus. This brain region is known to be affected in the postnatal SMA mouse brain (Wishart et al., 2010), and additionally, it plays a key role in the development of cognitive skills in humans (Rubin et al., 2014).

3.3 Results

3.3.1 Brain late organogenesis in control mouse embryos

To investigate the gross morphology of the embryonic mouse brain, I started with the collection and microdissection of embryos at the timepoints of interest (E12.5, E14.5, E16.5, E18.5). During this process I became confident in understanding the anatomy of the embryonic mouse, how to perform a full-body dissection and the fixation protocol to preserve and study organs. The embryonic development of the mouse is rapid, as gestation lasts about 20 days (Qiu et al., 2024). For this reason, it is important to be precise in selecting the correct timepoint when collecting embryos, especially when considering including more than one litter. To perform a reliable investigation, the stage of development was assessed following the Theiler Staging Criteria for Mouse Embryo Development (Richardson et al., 2014) **(Figure 3.1A)**, and each collected embryo was weighed on a scale **(Figure 3.1B)**. The embryos were then dissected, separating the head from the body, in order to obtain more homogenous penetration of the fixative solution.

To assess the most appropriate approach for tissue sectioning and staining, I performed a series of protocol optimisations. At first, the fixed brains were embedded in a solution of cryo-embedding matrix (OCT) designed for cryostat sectioning. Frozen tissue sections are largely used for immunohistochemistry as they preserve cellular antigens and lipids. However, at the time I performed the experiment, the appropriate tools to collect brain sections were not available in the facility. Because of this technical problem, I switched to a different tissue preparation involving dehydration and infiltration of paraffin. This process allowed me to use different histological equipment: the microtome. Although requiring more intricate tissue preparation, paraffin sections are more physically stable than frozen sections and better at preserving tissue morphology (Qin et al., 2018). Therefore, after paraffin embedding the heads, I collected consequent brain sections of each embryo.

During my training, I experimented with two different sectioning methods: one in the coronal plane and the other in the sagittal plane. After several pilot experiments on sagittal brain sections, I decided to consistently adopt a

coronal sectioning approach. Although both orientations would have allowed me a good visualisation of the hippocampus, I chose to work with coronal brain sections as they provided me with a clearer view for a frontal plane evaluation of bilateral brain structures, such as the hippocampus (Lang et al., 2024).

Having optimised the tissue preparation and sectioning protocols, I drafted a list of possible cellular markers that would have allowed me to investigate embryonic brain development. Among those, I selected Ki67 primary antibody to perform fluorescence immunohistochemistry. Ki67 is widely used in research to study neurogenesis in the developing and adult brain (Mandyam et al., 2007). Notably, Ki67 is a nuclear protein detectable in proliferating cells, as it is expressed during the G1, S, G2 and M phases of the cell cycle but not in the G0 phase (Gerdes et al., 1984).

Due to the exploratory nature of this study, I initially assessed whether this mouse model was suitable for investigating embryonic brain development by focusing exclusively on overall structural changes in the brains of control embryos over time. To achieve this, I used the LI-COR Odyssey M scanner with a resolution of 5 µm and a focus offset of 2.50 mm to image the labelled tissue sections. These imaging parameters were chosen to provide high-resolution visualization of brain architecture across the four selected timepoints of late organogenesis, allowing for detailed observation of structural changes over time **(Figure 3.1C)**. The Ki67 marker revealed several brain regions presenting with a strong proliferative signal in green, including the cortex, the ganglionic eminence and the hippocampus.

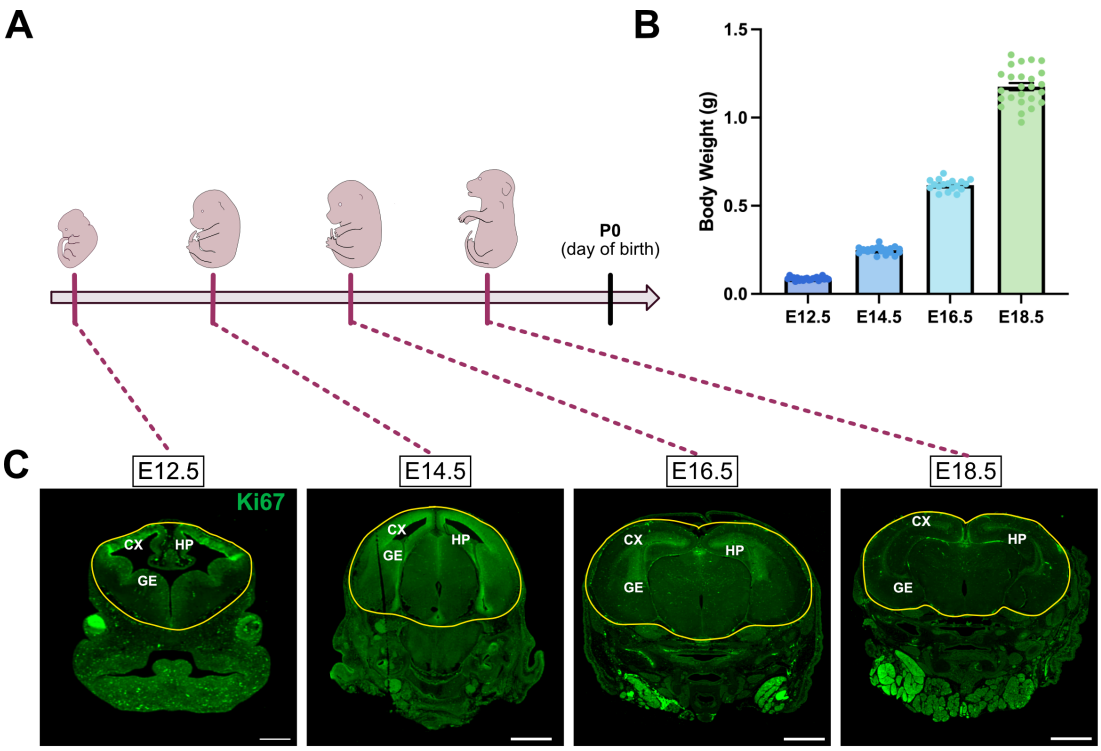

Figure 3.1 Late organogenesis of the brain in control mouse embryos. **(A)** Graphical timeline of mouse embryonic development from E12.5 to E18.5. The dotted lines are linking each timepoint to the corresponding brain section in panel C. **(B)** Body weight from control mouse embryos at timepoints of interest. E12.5 N = 22; E14.5 N = 21; E16.5 N = 18; E18.5 N = 25. Scatter dot plot, mean with SEM. **(C)** Representative coronal paraffin sections from control mouse embryos at E12.5, E14.5, E16.5 and E18.5 to demonstrate whole brain topography in the mouse embryo. The shape of the brain is highlighted by a yellow line. HP = hippocampus; CX = cortex; GE = ganglionic eminence. Scale bar 500 μm (E12.5), 1 mm (E14.5-E18.5). Cells positively labelled by the proliferative marker Ki67 are shown in green.

3.3.2 Hippocampal cell proliferation peaks at E14.5

Cell proliferation is a fundamental biological process with a key role in growth, tissue formation and differentiation, and its disruption can lead to developmental abnormalities (Ciemerych & Sicinski, 2005). In the embryonic brain, cell proliferation is crucial starting from the early stages of its development, and even small changes can have major consequences on its final morphology and function (Cheffer et al., 2013). To investigate cell proliferation in the developing mouse brain, I used the previously mentioned Ki67 maker to label proliferative cells in the brain of Taiwanese mouse embryos, and littermate control animals, from the age of E12.5 to E18.5. With this analysis I was able to evaluate how cell proliferation is modulated during late organogenesis.

I decided to focus on the study of the hippocampus, that during this specific time-window acquires its distinctive anatomical structure and begins to mature (Urban & Guillemot, 2014). The decision of focusing on the hippocampus was guided by two main rationales. First, previous research demonstrated that reduced levels of SMN protein result in abnormal postnatal hippocampal development in a severe SMA mouse model (Wishart et al., 2010). Second, the hippocampus is a critical region with a key role in memory and cognition in humans (Rubin et al., 2014). This focus is particularly relevant in the context of severe SMA, given the emergence of novel neurodevelopmental phenotypes recently identified in patients, highlighting cognitive and mental disorders present in some SMA infants (Akodad et al., 2024; Baranello et al., 2024; Buchignani et al., 2025).

The development of the hippocampus is a highly coordinated process that begins early in embryogenesis and continues into postnatal stages (Urban & Guillemot, 2014). Hippocampal field patterning begins at E10.5 in mice and becomes well-established by E12.5. At this age, the ventricular zone comprises the hippocampal neuroepithelium (HNE), the dentate neuroepithelium (DNE) and the cortical hem (CH), where neural stem cells begin to differentiate into neurons and glia. By E14.5, the DNE starts forming, and dentate precursors begin their migration under the influence of signals

such as WNT and BMP from the CH. At this stage, hippocampal regions like the CA1 and CA3 areas start to emerge. By E17.5, hippocampal neurons organize into layers, and the dentate gyrus (DG) begins to develop, driven by the migration of dentate precursor cells (Urban & Guillemot, 2014). By E18.5, the hippocampal architecture is largely established; although neurogenesis continues postnatally, particularly in the DG, where progenitors from primary, secondary, and tertiary matrices contribute to its formation (Altman & Bayer, 1990) **(Figure 3.2A)**.

Therefore, I started with analysis of proliferating cells in the hippocampus of control embryos at the four timepoints of interest. After normalising the number of Ki67-positive cells to the number of total nuclei stained with DAPI, I was able to observe how cell proliferation is regulated during late organogenesis **(Figure 3.2B)**. Hippocampus proliferation revealed its peak at E14.5, while the number of proliferating cells seemed to be comparable at the other ages **(Figure 3.2C)**. This finding is consistent with previous literature and reports of mouse brain development (Fuentealba et al., 2015; Martynoga et al., 2012), and more importantly, it highlights E14.5 as a crucial timepoint for the prenatal development of mouse hippocampus.

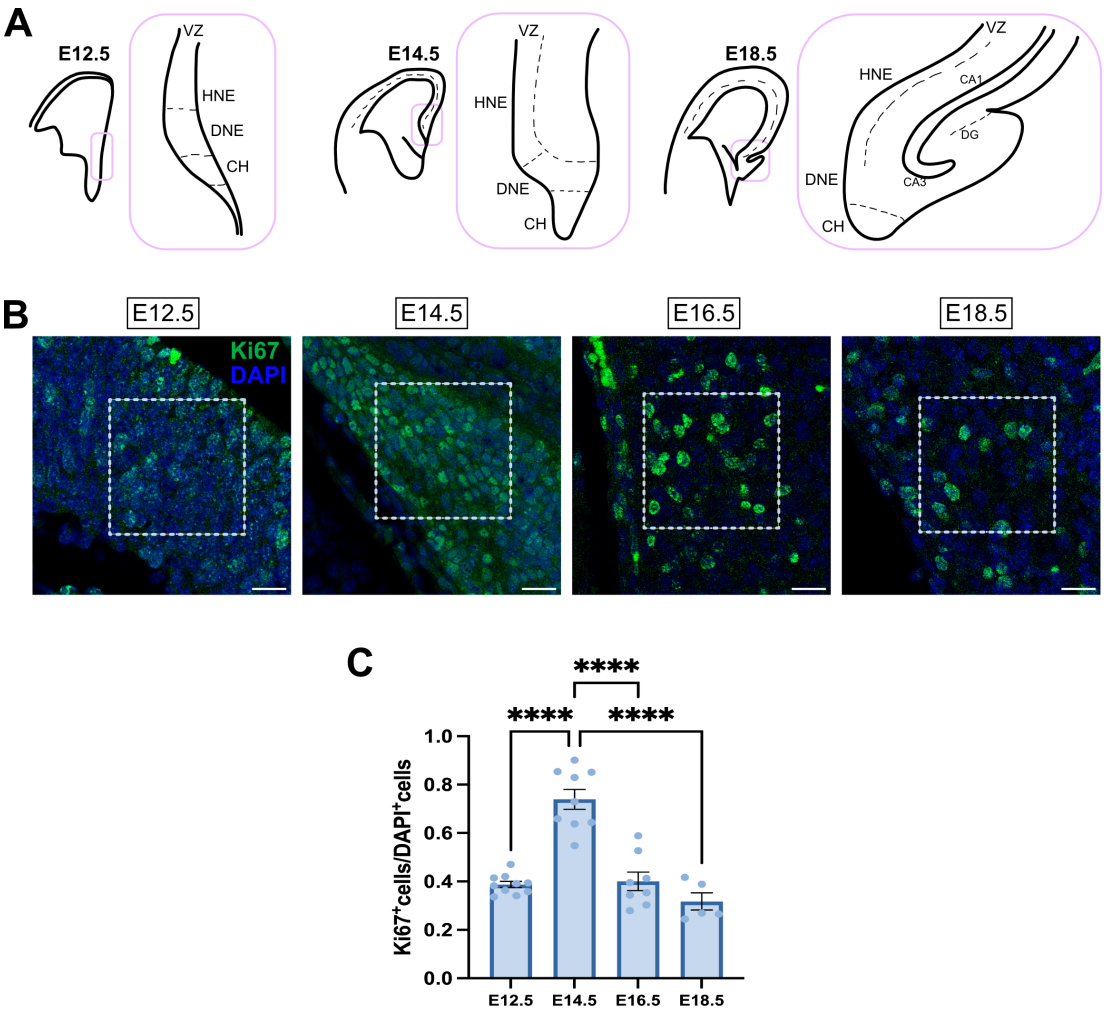

Figure 3.2 Prenatal hippocampus development and cell proliferation peak at E14.5. (A) Schematic representation of the embryonic development of mouse hippocampus, highlighting the morphological changes of the ventricular zone (VZ), including the hippocampal neuroepithelium (HNE), the dentate neuroepithelium (DNE), the cortical hem (CH) and the dentate gyrus (DG). (Adapted from (Urban & Guillemot, 2014)). **(B)** Representative images of cell proliferation in the hippocampus of controls Taiwanese mouse embryos at E12.5, E14.5, E16.5 and E18.5 shown using Ki67 and DAPI labelling. Region of interest corresponding to the dentate gyrus is indicated by the white squares. Scale bar 10 µm. Total and proliferative cells are labelled by DAPI in blue and Ki67 in green, respectively. **(C)** Spike of cell proliferation in E14.5 hippocampus of control mouse embryos. Each datapoint corresponds to one embryo. N = 10 for E12.5; N = 9 for E14.5; N = 8 for E16.5; N = 5 for E18.5. ****p-value ≤ 0.0001, one-way ANOVA with Tukey's correction for multiple comparisons, scatter dot plot, mean with SEM.

3.3.3 Cell proliferation is disrupted in the hippocampus of E14.5 SMA mouse embryos

In this chapter so far, I've demonstrated that it is possible to model and study prenatal brain development in control mouse embryos. Moreover, using well-known cellular markers, Ki67 and DAPI, I identified E14.5 as a critical timepoint in prenatal developmental of the mouse hippocampus.

To bring these findings in the context of embryonic SMA, next I compared the cell proliferation data obtained from controls **(Figure 3.3A)** with those from SMA littermates **(Figure 3.3B)**. Using the same approach and analysis, I calculated the ratio between proliferating cells (labelled with Ki67) and DAPI-positive nuclei in the hippocampus of mouse embryos at different stages of development.

Notably, E14.5 was the only embryonic timepoint at which the quantitative analysis of Ki67 labelling in the hippocampus revealed a statistically significant decrease of cell proliferation in SMA **(Figure 3.4C)**. More specifically, the quantification performed at E12.5, E16.5 and E18.5 showed no difference in cell proliferation rate between the two genotypes, while the analysis performed on E14.5 brain samples revealed an approximate 20% decrease of Ki67 cells in SMA compared to littermate controls.

This finding provides further support for the hypothesis that E14.5 is a key age for brain organogenesis in mice, and shows that defects in cell proliferation defects are already present at this stage of the embryonic development, consistent with previously published data highlighting molecular disruption in the SMA mouse brain (Motyl et al., 2020).

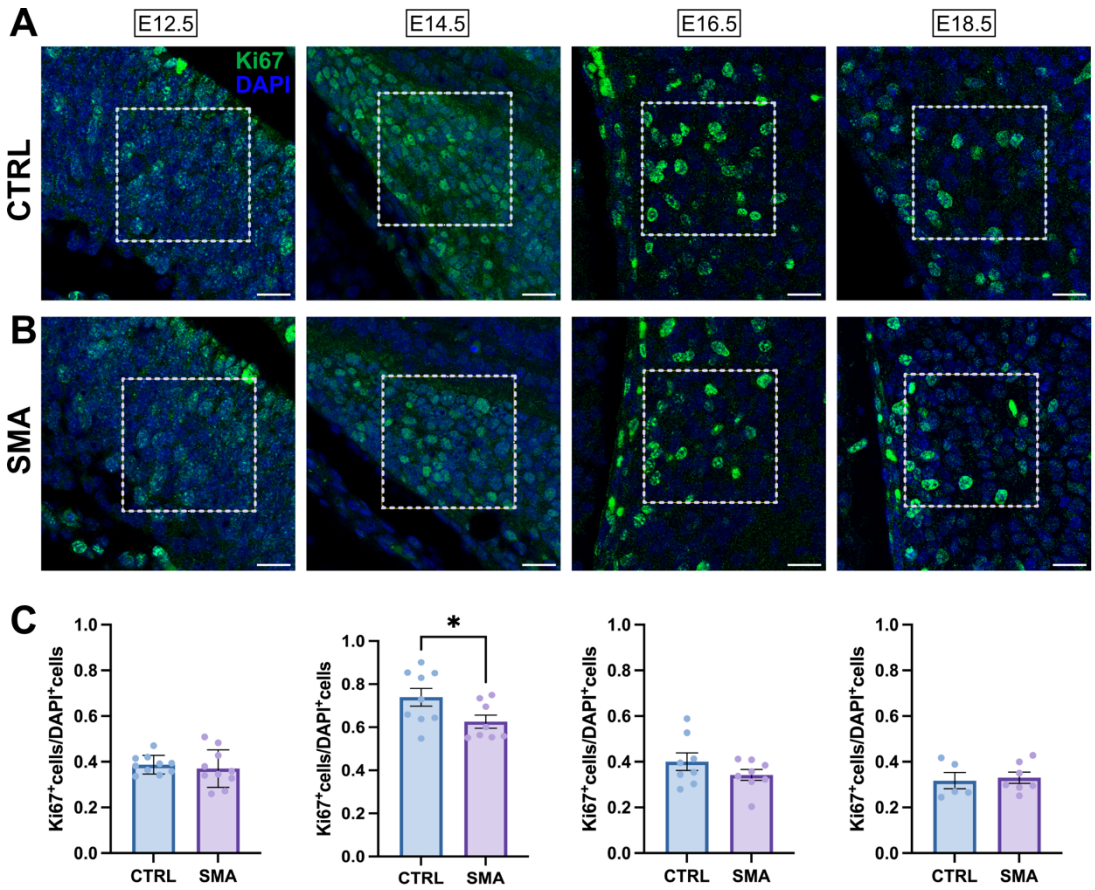

Figure 3.3 Proliferation defects in the SMA mouse hippocampus at E14.5. **(A-B)** Representative images of cell proliferation in the hippocampus of control **(A)** and SMA **(B)** Taiwanese mouse embryos at E12.5, E14.5, E16.5 and E18.5 shown using Ki67 and DAPI labelling. Region of interest corresponding to the dentate gyrus is indicated by the white squares. Scale bar 10 μm. Total and proliferative cells are labelled by DAPI in blue and Ki67 in green, respectively. **(C)** Quantification of cell proliferation in the hippocampus of control (data replotted from Figure 3.2C) and SMA Taiwanese mouse embryos at E12.5, E14.5, E16.5, E18.5, revealing a significant decrease in SMA mice at E14.5. Each datapoint corresponds to the average values from three sections per embryo (10 each for control and SMA at E12.5; 9 for control and 8 for SMA at E14.5; 8 each for control and SMA at E16.5 and 5 for control and 6 for SMA at E18.5). *p-value ≤ 0.05, unpaired t-test, scatter dot plot, mean with SEM.

3.4 Discussion

For several years there has been discussion about SMA being reframed as a developmental disease (Tizzano & Zafeiriou, 2018; Wishart et al., 2010). Despite the more traditional description of SMA as a neurodegenerative, motor neuron disease, the current literature and research is increasingly demonstrating how SMA presents with systemic prenatal defects that may disrupt the correct development of the foetus and contribute to the clinical manifestations observed in children (Kong et al., 2021; Martínez-Hernández et al., 2013; Motyl et al., 2020).

In view of the recent evidence from cohort studies and clinical trials highlighting the presence of cognitive developmental defects in some SMA patients (Baranello et al., 2024; Bitetti et al., 2024; Buchignani et al., 2024; Buchignani et al., 2025; Cottam et al., 2023; Kölbel et al., 2024; Masson et al., 2021; Ngawa et al., 2023; Steffens et al., 2024; Tosi et al., 2023; Yang et al., 2023),
It has become crucial to explore the underlying mechanisms that underpin these phenotypes. A comprehensive understanding of the early developmental stages of the brain in SMA disease is therefore essential.

Given the current practical and ethical challenges to perform this investigation in newborns and to access foetal human samples, it is essential to exploit the animal models available to study SMA. The aim of this chapter was therefore to demonstrate the relevance of studying prenatal brain development in a mouse model of severe SMA, and to provide a valuable foundation for pursuing more complex and mechanistic investigation.
To achieve this, in this project I examined whether the “Taiwanese” mouse model, well-established in the SMA research field (Hsieh-Li et al., 2000; Riessland et al., 2010; Signoria et al., 2023), was a suitable model for this purpose.
The timepoints of interest of this study are E12.5, E14.5, E16.5 and E18.5. The length of this period corresponds to the late stages of mouse organogenesis. The late organogenesis involves a significant amount of progenitor cell

proliferation, migration, and differentiation into various specialized cell types, which in turn lead to the formation of functional adult organs (Chen et al., 2022). Studying late organogenesis in mice, therefore, provides a powerful tool for understanding both normal development and disease. During this period, the brain undergoes a substantial growth characterised by the differentiation of specific neuronal and glial cell types, the establishment of neural circuits, and the maturation of brain structures, including the hippocampus (Cheffer et al., 2013).

Investigating how the brain forms and develops before birth is therefore crucial when studying developmental diseases, as demonstrated by several studies of different developmental and cognitive disorders, such as autism, Down syndrome and Rett syndrome (Bedogni et al., 2016; Chakrabarti et al., 2007; Munz et al., 2023). Therefore, establishing the possibility of investigating embryonic brain development in a severe SMA mouse model represents a novel and significant contribution. This approach will contribute addressing the existing gap in our understanding of brain development during the embryonic stages of the disease.

By studying the hippocampal gross morphology over time and focusing on cell proliferation, I obtain more detailed information on the development of this area of the brain. Here, I confirmed that the peak of neurogenesis occurs at E14.5, as shown in previous studies, highlighting this age as key for a correct embryonic brain development (Fuentealba et al., 2015; Martynoga et al., 2012). Strikingly, when comparing hippocampal cell proliferation in control and SMA embryos, the analysis revealed a significant reduction in proliferation in the hippocampus of E14.5 SMA embryos compared to controls. Since these defects were observed exclusively at E14.5, with no cell proliferation abnormalities detected at earlier (E12.5) or later stages of organogenesis (E16.5, E18.5), more in-depth studies are certainly needed to further investigate and elucidate the potential clinical implications of these findings.

There are several hypotheses may explain what was observed in this study. One potential explanation is that SMN protein expression is significantly higher during prenatal development compared to postnatal stages, as demonstrated by studies showing elevated SMN levels in the foetal brain (Motyl et al., 2020; Ramos et al., 2019). This may reflect the critical role of SMN in early brain development and cell proliferation. Therefore, insufficient SMN levels in SMA could result in impaired proliferative processes during key embryonic stages, as we observed in the hippocampus of “Taiwanese” mouse embryos at E14.5. However, at E12.5, E16.5, and E18.5, compensatory mechanisms may occur, potentially involving changes in the regulation of the cell cycle. At these timepoints, low levels of SMN could impact the expression of key regulators of cell cycle progression, such as cyclins and cyclin-dependent kinases (CDKs), and ultimately disrupt the lengthening of neural progenitor cells division (Hardwick et al., 2015). While these compensatory pathways may allow progenitor cells to maintain an overall proliferative activity at earlier (E12.5) and later (E16.5, E18.5) developmental stages despite reduced levels of SMN, they may be insufficient at E14.5, a crucial stage for embryonic brain development, leading to observable defects. Despite their transient nature, these early disruptions could contribute to postnatal neurodevelopmental phenotypes. Indeed, the dynamic and rapid changes occurring during embryonic brain development suggest that even minor disruptions could lead to severe consequences and phenotypes, as observed in neurodevelopmental disorders, including autism spectrum disorder (ASD) (Stoner et al., 2014; White et al., 2024).

Future evaluations should also focus on cell proliferation in different areas of the brain. Moreover, while this cellular process is critical for the embryonic development of the hippocampus, it represents only one of the several mechanisms contributing to this process (Urban & Guillemot, 2014). For example, in the later stages of the brain, organogenesis, cell differentiation and migration become fundamental. To have a comprehensive understanding of hippocampus and brain development, these cellular mechanisms should be

investigated with additional immunohistochemistry using well-known markers, such as NeuN and NeuroD1 (Duan et al., 2016; Gao et al., 2009).

Ultimately, in this chapter I showed that the severe SMA “Taiwanese” mouse model can be used to investigate the embryonic development of the brain throughout the entire period of late organogenesis. By using this approach, I identified cell proliferation defects in the hippocampus of SMA embryos at one specific timepoint, E14.5, highlighting this age as crucial for correct brain development.

The findings revealed in this study raise the intriguing question of whether the cellular phenotype observed is driven by underlying molecular defects. This hypothesis lay the foundation for the next chapter of this thesis, in which I will deepen the investigation into the potential molecular mechanisms contributing to prenatal SMA pathogenesis.

Chapter 4: **Prenatal disruption of protein translation in the central nervous system of SMA mouse embryos**

4.1 Introduction

As illustrated in the previous chapter, E14.5 represents a key stage in prenatal brain development and, when SMN levels are insufficient, cell proliferation defects occur in the hippocampus of SMA mouse embryos. To deepen the investigation on the impact of SMA on brain development, I next decided to explore the molecular mechanisms driving these SMN-dependent changes. To achieve this, I had the opportunity to organise a placement at the Institute of Biophysics in Trento, Italy, under the supervision of Prof. Gabriella Viero, where we performed a comprehensive study of protein translation in Taiwanese mouse embryos at the age of E14.5.

Thanks to previous studies, it is widely known that SMN plays a role in the biogenesis of ribonucleoprotein complexes and RNA splicing (Fischer et al., 1997; Pellizzoni et al., 2001; Pellizzoni et al., 1998). In addition, increasing evidence shows that SMN interacts with the translational machinery influencing protein synthesis (Bernabò et al., 2017; Lauria et al., 2020; Sanchez et al., 2013). These studies revealed the direct role of SMN in translation and ribosome biology, where SMN establishes a platform within the ribosome regulating the translation of mRNAs functionally linked with neurogenesis, lipid metabolism, ubiquitination, and chromatin regulation; all processes known to be affected in SMA (Lauria et al., 2020; Sharma et al., 2024). Therefore, it is not surprising that proteomic investigations revealed significant changes in global proteomes in both animal models of SMA and patient-derived fibroblasts (Fuller et al., 2016). While most of these studies have focused on postnatal symptomatic stages of the disease, recent research from our lab highlighted proteomic changes even during prenatal stages, well before symptoms onset (Motyl et al., 2020).

Nonetheless, investigations into prenatal SMA have not yet examined whether the observed defects occurring at the proteome level are accompanied by changes in translation. Therefore, with this work I aim at deepening our understanding on the impact of reduced levels of SMN protein on the regulation of translation in different organs of SMA mouse embryos.

4.2 Aim

To explore more detailed processes of protein translation during embryonic development, in collaboration with the Viero lab, I performed polysome and ribosome profiling on prenatal tissues from E14.5 control and SMA “Taiwanese” mouse embryos.

While *polysome profiling* was performed on E14.5 brain, spinal cord and liver to provide a global estimation of the engagement of the ribosomes on total mRNAs present in the tissue, *ribosome profiling* was necessary to gain detailed information on the position of the ribosomes on specific mRNAs, giving precise insights on gene dysregulation. For this second approach we decided to focus our investigation on the central nervous system (CNS), so ribosome profiling was performed on E14.5 whole brain and spinal cord only.

Finally, I used Ingenuity Pathway Analysis (IPA) software to analyse and interpret the datasets obtained from these experiments.

4.3 Results

4.3.1 Experimental design of polysome profiling

As this represents the first study aimed at investigating protein translation in a severe model for SMA during prenatal development, we initially decided to provide insights into the overall efficiency of this molecular process in controls and SMA E14.5 embryos. To achieve this, we performed *polysome profiling*, a technique that allows quantification of variations in ribosome recruitment on mRNAs (Sharma et al., 2024). This method relies on the separation of mRNAs based on the number of ribosomes linked to them by using sucrose density separation centrifugation.

The experimental setting I employed was based on the protocol developed and described in a recent study from the Viero lab (Bernabò et al., 2017). More specifically, I started with the pulverisation of previously dissected embryonic tissues, in this case whole brain, spinal cord and liver, from E14.5 control and SMA embryos. The pulverised tissue was then lysed using a tissue polysome lysis buffer and centrifuged to allow supernatant collection. At this point, samples were loaded on 10%-40% sucrose gradient tubes and ultracentrifuged. This crucial step will separate ribosomes and polysomes along the gradient based on their size and density. As illustrated in the schematics **(Figure 4.1)**, ribonucleoproteins (RNPs) and ribosome subunits (40s and 60s) sediment at the top of the gradient, as they are smaller and less dense, while monosome (80s) and polysomes will travel farther into the gradient. Once all the ribosomal species were separated into the gradient, we collected the different sucrose fractions by using a gradient fractionator connected to an UA-6 UV/VIS detector. This step was performed by carefully removing the centrifuge tubes containing the sucrose gradient from the centrifuge rotor and then mounted on the fractionator collector device. From the top to the bottom of the sucrose gradient, 1 mL fractions were then collected in ~15 tubes. The result of this measurement is a polysome profile showing peaks corresponding to free RNPs, 40S and 60S ribosome subunits, 80S monosomes and polysomes. The isolation of the different translation compartments allows to therefore calculate the fraction of ribosomes in

polysomes (FRP) and to investigate how different proteins of interest sediment within these compartments.

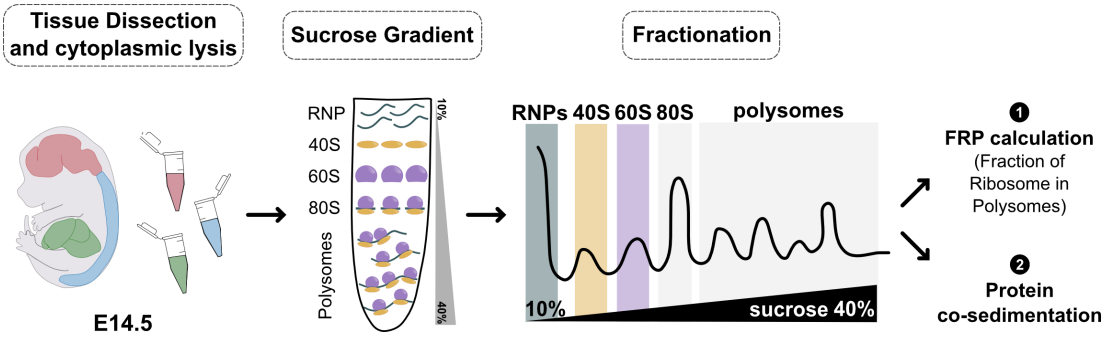

Figure 4.1 Schematic overview of polysome profiling experimental design of E14.5 brain, spinal cord and liver from control and SMA mouse embryos. After tissue dissection and cytoplasmic lysis, samples are loaded onto sucrose gradients. Following ultracentrifugation, the translational machinery compartments separate through the gradient based on their size and density. Ribonucleoproteins (RNPs) and ribosome subunits (40s and 60s) sediment at the top of the gradient, monosome (80s) and polysomes will travel farther into the gradient. While measuring their absorbance, a fractionation will then separate and collect the different compartments. The result of this measurement is a polysome profile showing peaks corresponding to RNPs, 40S, 60S, 80S and polysomes. These samples will then be used for FRP calculations and protein co-sedimentation.

4.3.2 Translation efficiency is tissue-specific in control embryos at E14.5

After performing polysome profiling protocol as described above, we subsequently investigated and compared global translation efficiency in different tissues from control mouse embryos at E14.5. Therefore, we started comparing the profiles obtained from control brain and spinal cord tissues, focusing on the 80S and the polysome peaks. From the initial observation of the structure of the profiles, we noticed a higher 80S peak and less pronounced polysome peak in control brain compared to control spinal cord **(Figure 4.2A)**.

To obtain quantitative information, we then analysed the polysome profiling curve by measuring the fraction of ribosomes in polysomes (FRP). The FRP in percentage is calculated dividing the area under the polysomes by the sum of the areas under the 80S, corresponding to the single ribosome unit, and the area under the polysomes, the result multiplied by 100 (see materials and methods in chapter 2 for details).

The FRP is a key indicator of global translation activity within the tissue of interest. Ribosomes actively synthesising proteins are found within polysomes, while ribosomes that are not currently translating proteins are either free 40S and 60S subunits or monosomes (80S) (Bernabò et al., 2017). As a result, a higher percentage of ribosomes associated in polysomes indicates an overall higher translational activity.

The polysome profiling curves and the quantification of the FRP both revealed significant differences in the translational efficiency between the brain and the spinal cord from healthy embryos **(Figure 4.2B)**. Specifically, the brain was found to be characterised by a lower percentage of ribosomes in polysomes compared to spinal cord, thus suggesting a lower translational activity.

Taken together, these findings indicate that protein translation rate is highly tissue-specific already at embryonic stages.

4.3.3 No changes in the global translation of SMA mouse embryos at E14.5

Having observed differences in the global translation efficacy in controls among different embryonic tissues, we next wanted to investigate whether we could detect any changes when comparing control to SMA embryos. To do this, we performed polysome profiling on brain and spinal cord from E14.5 SMA mouse embryos using the same technique and protocol described above.

Consistently to what was previously observed by Bernabò and colleagues in postnatal pre-symptomatic mice, polysome profiles and FRP quantification in the prenatal brain and spinal cord of SMA embryos did not show a significant difference compared to controls at E14.5 **(Fig.4.2 C and D)**. Specifically, focusing on the polysome profiles obtain form the brain of control and SMA embryos, we can appreciate how the 80S and polysomes peaks are following the same trend **(Figure 4.2C)**. Moreover, when performing quantitative analysis by measuring the FRP, we found no differences between the two genotypes **(Figure 4.2D)**. The same quantitative analysis gave a similar conclusion after analysing polysome profiles from E14.5 control and SMA spinal cord samples **(Figure 4.2D)**.

To further investigate translation efficiency in our prenatal model, I performed the equivalent experiment following the same protocol on one additional organ, the liver. In **Figure 4.2E** can be appreciated how the FRP quantification revealed a different trend in the overall translation in the three organs from control embryos, reinforcing the idea that this cellular process is highly tissue-specific during embryonic development. However, neither of the three organs revealed changes in the global translation levels when the two genotypes were compared.

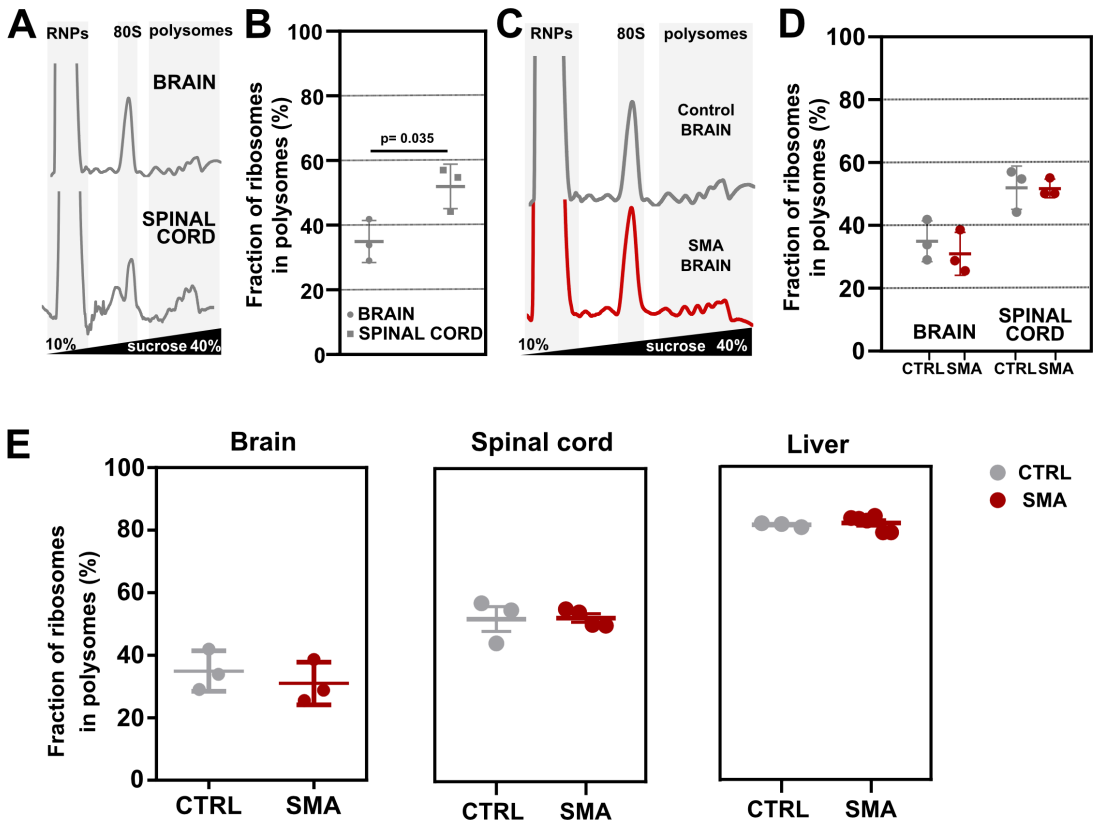

Figure 4.2 Polysome profiling revealed changes in the overall translation efficiency in different organs of E14.5 control embryos, but not between genotypes. (A) Polysomal profiles of E14.5 brain and spinal cord from control mouse embryos. **(B)** Fraction of ribosome in polysome expressed in percentage of E14.5 brain and spinal cord from control mouse embryos. **(C)** Polysomal profiles of E14.5 brain from control and SMA mouse embryos. **(D)** Fraction of ribosome in polysome expressed in percentage of E14.5 brain and spinal cord from control and SMA mouse embryos. **(E)** Fraction of ribosome in polysome expressed in percentage of E14.5 brain, spinal cord and liver from control and SMA mouse embryos. Brain and spinal cord data are replotted from panel (D).

4.3.4 SMN interaction with the translational machinery showed no changes between genotypes in E14.5 embryos

As already mentioned, SMN is a ribosome-associated protein with a direct role in regulating translation, and the loss of this association has already been observed at postnatal ages in the “Taiwanese” mouse model (Bernabò et al., 2017; Lauria et al., 2020). To investigate how SMN associates with the translation machinery prenatally, during my secondment in the Viero lab, I performed western blotting on the sucrose fractions obtained by polysome profiling to study the co-sedimentation of the SMN protein with ribosomes. This experiment was performed by myself on spinal cord and liver samples from E14.5 control and SMA mouse embryos, while brain samples were processed in collaboration with colleagues from the Viero lab. Here, I report data from all three organs to provide an overview of the interaction of SMN protein with the translational machinery at a systemic level, and to facilitate inter-organ comparisons.

After protein purification from the sucrose fractions using methanol/chloroform precipitation (Bernabò et al., 2017), I performed western blotting to quantify SMN, RPL26 and RPS6 protein levels in each fraction from each of the organs of interest. RPL26 and RPS6 are ribosomal proteins used as markers for the large (60S) and small (40S) ribosomal subunits, respectively (Lauria et al., 2020). These proteins were used as sedimentation controls to facilitate the identification of the different sucrose fractions. Consistent with previous observations, the co-sedimentation profiles did not reveal genotype-specific differences in any of the three organs investigated. However, each organ exhibited its own trend **(Figure 4.3)**. More specifically, co-sedimentation profiles and relative quantitative analysis of E14.5 brain showed that SMN co-sediments primarily with RNPs and 40S in both control and SMA **(Figure 4.3 A and B)**. Similarly, E14.5 spinal cord profiles and quantification revealed that SMN is highly present in correspondence to RNPs, 40S and 60S in both genotypes **(Figure 4.3 C and D)**. Furthermore, SMN in the liver of E14.5 control and SMA mouse embryos appears to reach peak co-sedimentation with RNPs and 40S, with no changes between genotypes **(Figure 4.3 E and F)**.

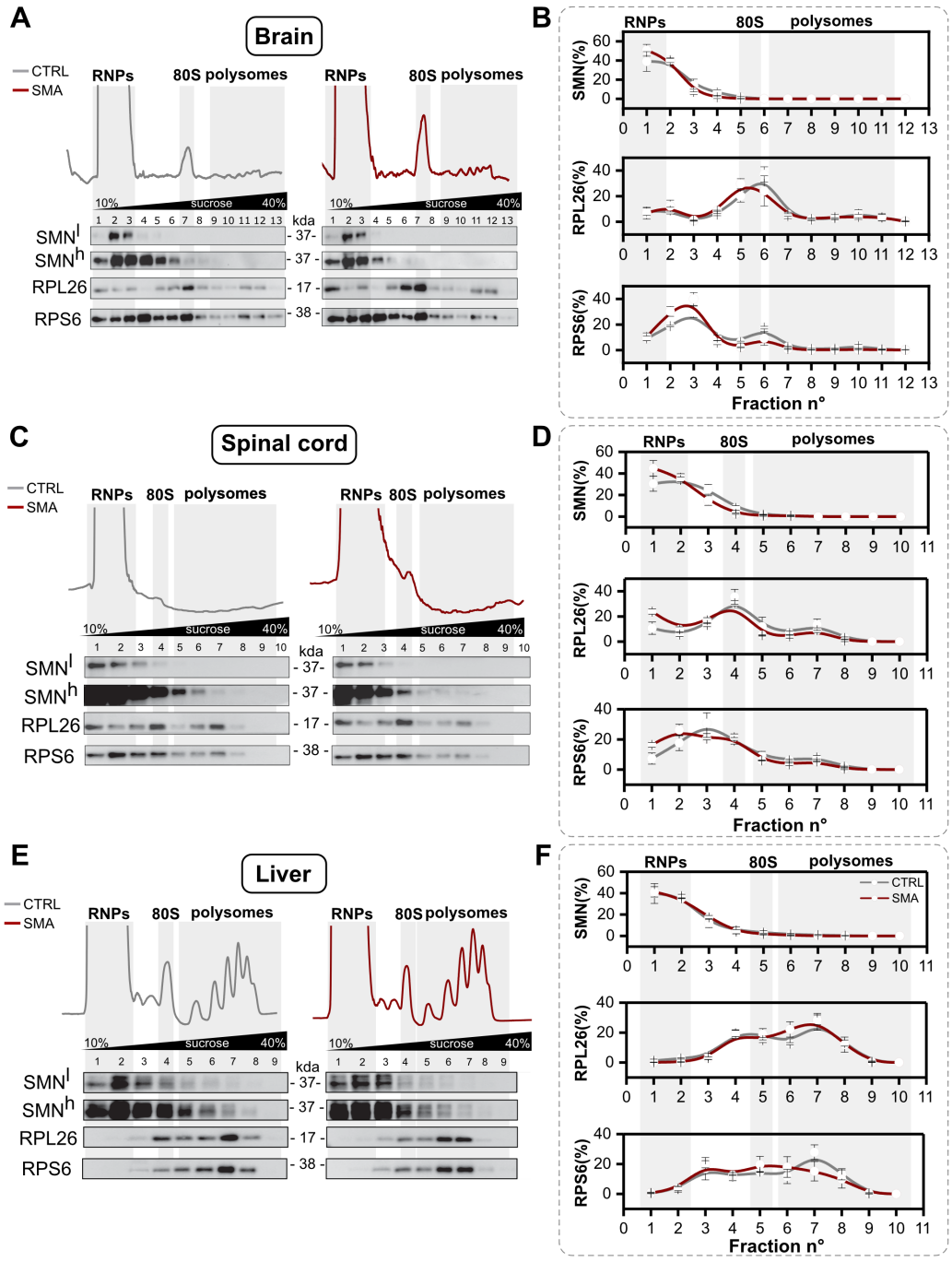

Figure 4.3 SMN protein co-sedimentation with the translation machinery in the brain, spinal cord and liver of E14.5 control and SMA mouse embryos. (A, C, E) Co-sedimentation profiles of SMN from control and SMA brain **(A)**, spinal cord **(C)** and liver **(E)**. **(B, D, F)** Relative distribution of SMN, RPL26 and RPS6 along the profiles of E14.5 brain **(B)**, spinal cord **(D)** and liver **(F)** in control and SMA. SMN^l and SMN^h indicates the immunoblot exposure times during acquisition, auto and high respectively. RPL26 and RPS6 are ribosomal proteins used as markers for the large (60S) and small (40S) ribosomal subunits, respectively. They were used as sedimentation controls to facilitate the identification of the different sucrose fractions.

4.3.5 Experimental design of ribosome profiling

As polysome profiling only provides an indication of the overall translation status in a given tissue at a given timepoint, I therefore decided to deepen our investigation on the effects of prenatal SMN deficiency on translation in the CNS by performing a more sophisticated technique: *ribosome profiling*.

In collaboration with the Viero lab, I performed ribosome profiling on brain and spinal cord samples from controls and SMA mouse embryos at E14.5. We chose these two organs to tailor our experimental question, which focused on determining whether the proliferation defects observed in the brains of E14.5 SMA embryos (illustrated in chapter 3) could be explained by changes at the translational level.

Ribosome profiling is a technique that allowed us to obtain a genome-wide and more detailed measurement of possible alterations in ribosome engagement on mRNAs by specifically isolating ribosome-protected fragments (RPFs), followed by the next generation sequencing, and investigating the differentially translated mRNAs, determining the position of the ribosomes at codon resolution (Ingolia et al., 2009). Ribosome profiling differs from polysome profiling for its specificity and for the type of information it provides (Ingolia, 2014; Jin & Xiao, 2018). Consequently, the experimental protocol also presents a few critical differences and additional steps, illustrated in the reported schematics **(Figure 4.4)**.

As for polysome profiling, after preparing the sucrose gradients, embryonic brain and spinal cord tissues were pulverised with a sterile pestle and mortar in liquid nitrogen, and then ribosome lysis buffer was added followed by centrifuging to remove tissue debris, mitochondria, and nuclei. One of the most crucial steps of the protocol is ribosome purification achieved with RNAse and then followed by a RNase inhibitor to stop the reaction. This action, defined as a limited RNA digestion, is exceptionally sensitive and important while performing ribosome profiling. RNAse are essential to degrade all mRNAs not protected by ribosomes, this includes both free RNAs and mRNAs in between ribosomes. This step will result into the disassembly of all polysomes into

isolated monosomes (80S), each of which remains bound to the corresponding mRNA fragment undergoing translation.

As ribosomes also contain RNA (rRNA), the treatment with RNase inhibitor is necessary to halt the digestion, an excessive RNase activity can cause the degradation of the rRNA within the ribosomes, leading to a compromised structural integrity and loss of the RPFs. Following the ribosome purification step, the lysates are loaded into ultracentrifuge tubes containing a 10%-40% linear sucrose. After ultracentrifugation, the fraction corresponding to the 80S monosomes is collected using a fractionator equipped with a UA-6 UV/VIS detector. The sucrose gradient fractionation process is similar to the one described above for polysome profiling, with the difference that in this case only one tube containing the 80S fraction is collected. Consequently, on the output profile, only one peak corresponding to the 80S monosomes is observed. The collected 80S fraction was then purified from rRNA and then the mRNA was extracted using a phenol/chloroform protocol. At this point, I had to select and extract only the mRNAs corresponding to the RPFs. To do this, I used a 15% Urea-TBE gel to separate and select the bands measuring 28-32bp which were then extracted from the gel. Once obtained the RNA samples, I used the “Takara Kit” protocol for polyadenylation and cDNA synthesis (Lauria et al., 2020). After the amplification and purification, the cDNA libraries were prepared and then sequenced at the CIBIO NGS facility of the University of Trento, Italy, using an Illumina NovaSeq6000 system.

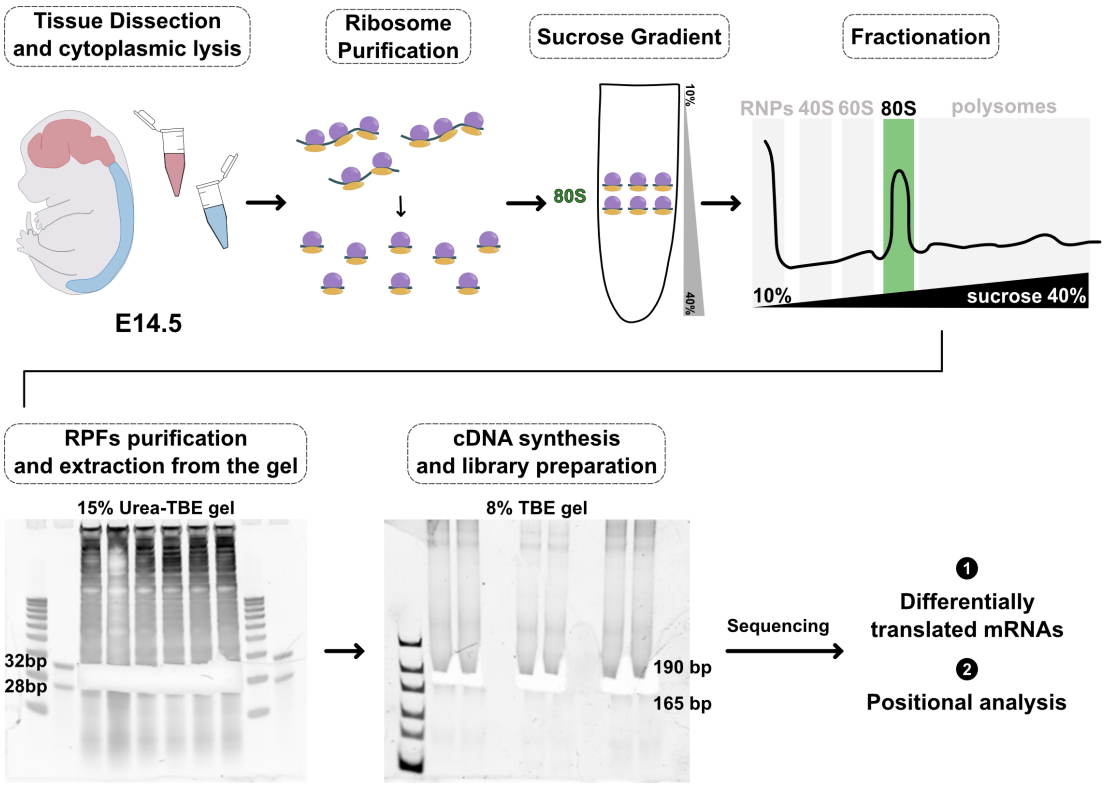

Figure 4.4 Schematic overview of experimental design to facilitate ribosome profiling of E14.5 brain and spinal cord from control and SMA mouse embryos. After tissue preparation and lysis, samples undergo a limited RNAse digestion to purify ribosomes. The 80S monosomes were therefore isolated by sucrose gradient and fractionation. To purify ribosome-protected fragments (RPFs), mRNA was run on a 15% Urea-TBE gel. Only fragments corresponding to 32-28 bp were extracted by incision from the gel and then converted into cDNA, which was amplified and purified using an 8% TBE gel. cDNA libraries were then sequenced and the datasets used to identify differentially translated mRNAs and for positional analysis.

4.3.6 Ribosome profiling: quality assessment

To ensure the optimal quality of the datasets obtained from ribosome profiling and sequencing, we evaluated two important metrics: the distribution of the RPF lengths and the trinucleotide periodicity of ribosomes along the coding sequences **(Figure 4.5 A and B).**

As genuine and non-contaminated RFPs are approximately 28-30 nucleotides long (Ingolia et al., 2009), the analysis of their distribution in the datasets allowed us to validate our experimental design and to assess the good quality of the libraries obtained from brain and spinal cord from both control and SMA embryos **(Figure 4.5A)**.

To ensure that the RFPs analysed were genuinely representing mRNA fragments translated by ribosomes in the correct reading frame, we examined the trinucleotide periodicity by identifying the ribosome's P-site, corresponding to the site holding the t-RNA associated to the growing polypeptide chain during translation (Lauria et al., 2018). As ribosomes translate mRNAs by moving along the transcripts in steps of three nucleotides (one codon), a good quality dataset should be characterised by a strong trinucleotide periodicity pattern, a hallmark of actively translating ribosomes, as observed in **figure 4.5B**. In addition, as the trinucleotide periodicity analysis enables to identify the actively translating open reading frames, we inspected the trinucleotide periodicity along the coding sequence to investigate the potential differences in the localisation of the ribosomes between control and SMA embryos. Notably, SMA mouse embryos showed statistically significant alterations in ribosome positioning at the start and end of the coding sequence of mRNAs when compared to littermate controls in both the brain and spinal cord **(Figure 4.5B)**.

4.3.7 Widespread dysregulation in translation in the prenatal CNS of SMA mouse embryos

As the aim of ribosome profiling and sequencing is to investigate translation at gene-specific level, I collaborated with Dr. Martina Paganin from the Viero lab to perform differential analyses on both datasets obtained from brain and spinal cord of E14.5 controls and SMA embryos to identify specific transcripts with altered ribosome occupancy.

For this analysis, only genes that met both a log2 fold change (log2FC) threshold of ±0.5 and a p-value below 0.05 were considered differentially expressed. In other words, genes were classified as dysregulated if they showed an expression increase of approximately 40% or a decrease of around 30% between the two genotypes.

The analysis revealed numerous differentially expressed genes (DEGs) in both tissues, the majority of which were downregulated **(Figure 4.5 C and D)**. More specifically, in brain, 116 out of with 151 genes with dysregulated translation (DEGs) showed decreased ribosome occupancy **(Figure 4.5C)**. Similarly, in the spinal cord, out of 304 dysregulated genes 231 showed decreased ribosome occupancy **(Figure 4.5D)**. The overwhelming bias towards mRNAs with decreased ribosome occupancy is in line with previous observations from postnatal stages of disease, reinforcing the hypothesis that SMA pathogenesis is caused by a loss of function in translation (Bernabò et al., 2017; Lauria et al., 2020).

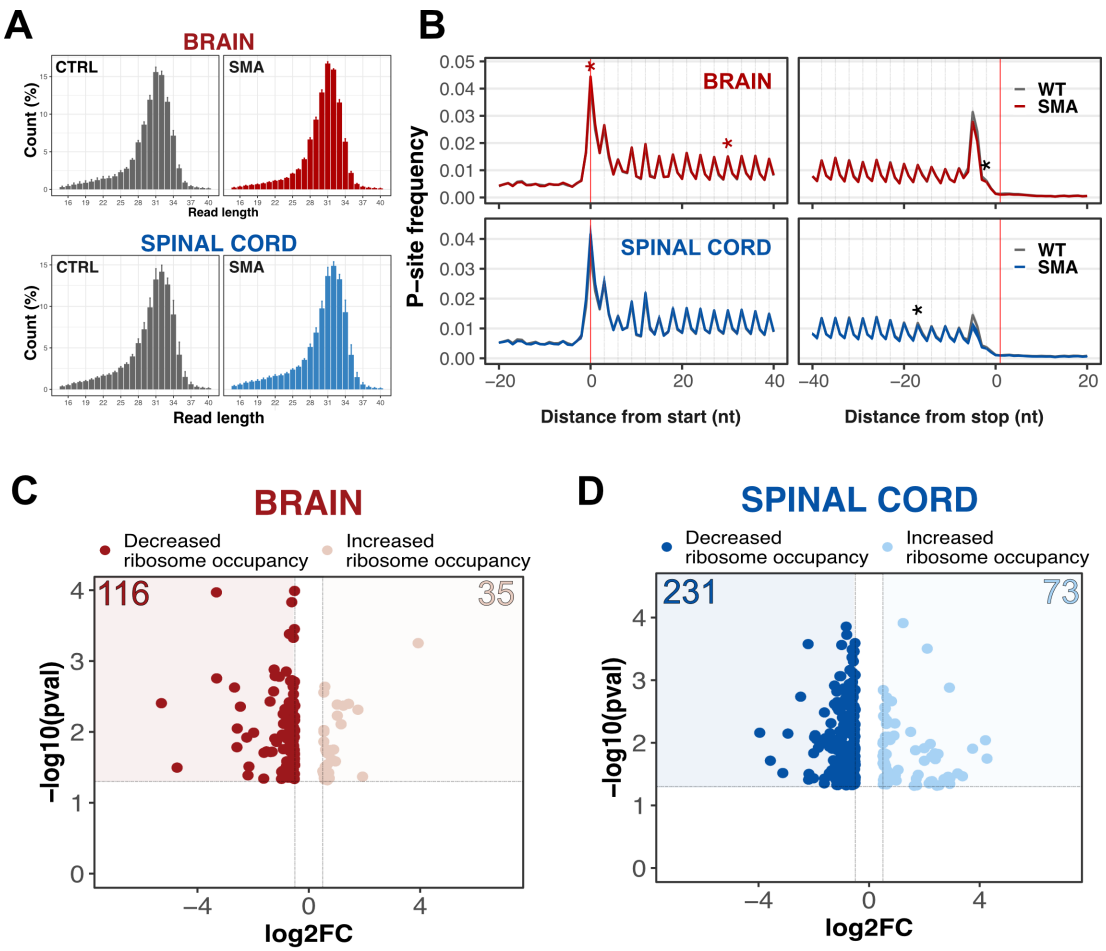

Figure 4.5 Ribosome profiling revealed a widespread disruption in translation throughout the CNS of E14.5 SMA mouse embryos. (A-B) Quality assessment of CNS libraries. **(A)** Distribution analysis of the lengths of ribosome-protected fragments in E14.5 brain and spinal cord from control and SMA samples. **(B)** Trinucleotide periodicity along the coding sequences in E14.5 brain and spinal cord from control and SMA samples. Asterisks indicate nucleotide positions with significant differences between SMA and control signal, based on pair-end t-test. *p-value < 0.05. **(C-D)** Volcano plots showing the variations in ribosome occupancy of genes identified in brain **(C)** and spinal cord **(D)** of E14.5 controls and SMA mouse embryos. In brain, dark red dots represent DEGs with decreased ribosome occupancy, while pink dots with increased ribosome occupancy. In spinal cord, blue dots represent DEGs with decreased ribosome occupancy, while light-blue dots with increased ribosome occupancy. Significantly differential genes were defined by the following cut-off values: log2FC_thr=0.5 and pval_thr=0.05. DEG: differentially expressed genes. N = 3 embryos each for control and SMA.

4.3.8 IPA analysis of ribosome profiling datasets identifies novel affected biological pathways in SMA mouse embryos

The differential analysis performed in collaboration with Dr. Paganin revealed that both SMA brain and spinal cord present with a widespread disruption in translation during the prenatal stages of the disease. This novel finding laid the foundation for a more in-depth investigation to identify the specific genes and biological pathways affected in the CNS of SMA mouse embryos.

To achieve this, I analysed the combined DEGs datasets obtained from brain and spinal cord using Ingenuity Pathway Analysis (IPA) software. IPA is a widely used bioinformatics tool developed by QIAGEN used to analyse and interpret gene expression data. By exploiting a manually curated knowledge base derived from peer-reviewed literature, the Ingenuity's Knowledge Database, IPA can map input datasets to identify significantly enriched canonical pathways, upstream regulators, and disease-associated processes (Krämer et al., 2014). Thus, using IPA I performed an enrichment analysis to identify the biological pathways that were significantly associated with the differentially expressed genes provided by the input dataset. This analysis revealed a widespread disruption in several biological pathways already known to be involved in the postnatal pathogenesis of SMA, including cell cycle regulation (Sheng et al., 2018), cytoskeleton signalling pathway (Bowerman et al., 2009; Bowerman et al., 2007; Hensel et al., 2014) and p53 signalling (Courtney et al., 2019; Simon et al., 2017) **(Figure 4.6A)**.

While there is extensive literature describing these SMA-linked pathways, these results provided valuable insights, highlighting that these molecular defects can be explained by translational dysfunctions, and, more importantly, that they are already present prenatally.

Surprisingly, in addition to these well-characterised pathways, IPA identified changes in the translation of genes of a biologically interesting pathway not previously associated with SMA: the cilium assembly pathway (highlighted in purple in **Figure 4.6A**). Based on the IPA scoring, this canonical pathway is highly significantly enriched with a p-value of 3.5×10^{-5} and a z-score of -1.789. As the z-score value indicates the direction of the pathway regulation, IPA

predicted that the cilium assembly pathway is inhibited in the CNS of SMA mouse embryos. Accordingly, the investigation of the individual genes ascribed to this pathway revealed changes in 20 genes involved in the structure and function of primary cilia, the majority of them being downregulated **(Figure 4.6B)**.

As primary cilia have a critical role in coordinating key signalling pathways to ensure a correct embryonic development, tissue homeostasis and organ function (Anvarian et al., 2019), I decided to pursue the investigation of these important cellular organelles further, with the hypothesis that their dysfunction, due to translational defects, could represent one of the molecular causes underlying CNS prenatal defects in SMA.

A

Ingenuity Canonical Pathways	*-log(p-value)*	*z-score*
Cell Cycle Checkpoints	21.4	-6.223
Nuclear Cytoskeleton Signaling Pathway	13.9	-3.333
SUMOylation of DNA damage response and repair proteins	12	-4.472
Metabolism of non-coding RNA	10.4	-4
Major pathway of rRNA processing in the nucleolus and cytosol	6.18	-0.426
Kinesins	5.95	-1.155
Cilium Assembly	4.45	-1.789
p53 Signaling	4.43	0
Sirtuin Signaling Pathway	4.43	-1.414
Glucose metabolism	3.98	-3.317

B

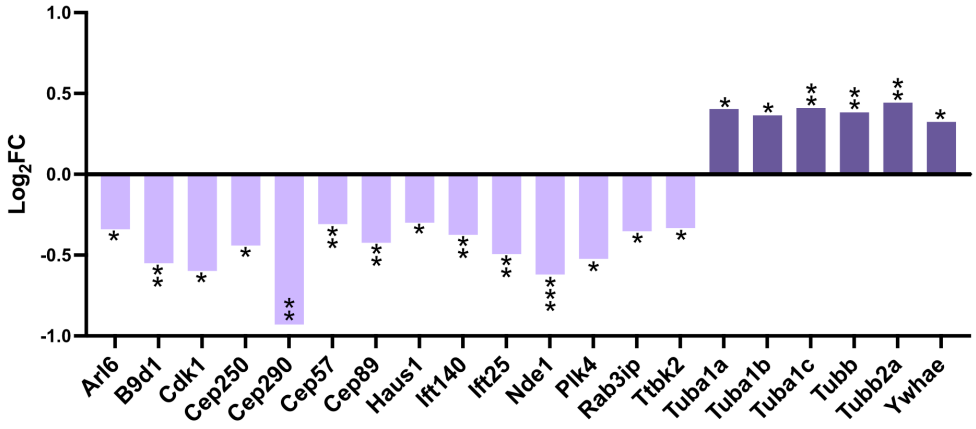

Figure 4.6 Translational defects of genes involved in the cilium assembly pathway in the CNS of SMA mouse embryos. (A) Top ten canonical pathways identified by IPA as being dysregulated in the CNS of E14.5 SMA mouse embryos compared to controls. **(B)** Bar chart showing the dysregulated genes associated to the "cilium assembly" canonical pathway identified by IPA. Light purple bars represent downregulated DEGs; dark purple bars represent upregulated DEGs. Statistical significance was defined using the following cut-off values: log_2FC_thr=0.3 and *pval_thr*=0.05. *p-value ≤ 0.05, **p-value ≤ 0.01, ***p-value ≤ 0.001.

4.3.9 IPA analysis predicts primary cilia dysfunction in the CNS of SMA mouse embryos

Primary cilia are non-motile sensory organelles extending from the cell membrane, containing a microtubule-based axoneme originating from the basal body (Fry et al., 2014). The cilia cytoplasm is isolated from the cell by a specialised structure, the transition zone, which acts as a ciliary gate filtering the passage of molecules into or out of the cilium (Wang et al., 2022). The molecules that pass the transition zone are carried along the axoneme by two intraflagellar transport complexes (IFT A and B) (Jensen & Leroux, 2017) **(Figure 4.7A)**.

As previously mentioned, primary cilia play a vital role in coordinating the fundamental signaling pathways that promote proper embryonic development (Anvarian et al., 2019). Dysfunction in these subcellular organelles leads to multisystemic disorders known as ciliopathies and several studies have demonstrated a crucial role for primary cilia in brain development and neurodevelopmental disease, often accompanied by cognitive impairment (Andreu-Cervera et al., 2021; Karalis et al., 2022; Ma et al., 2022; Mill et al., 2023; Park et al., 2019).

Interestingly, several dysregulated genes identified in our dataset have been extensively described in the literature and associated with well-known ciliopathies. *ARL6* and *CEP290* are two of the most frequently mutated genes in Bardet-Biedl syndrome, a multisystem primary ciliopathy characterised by heterogenous clinical manifestations, including cognitive impairment and developmental delay (Florea et al., 2021). Moreover, *CEP290* has also been linked to Joubert Syndrome, a primary ciliopathy presenting with a distinctive midbrain-hindbrain malformation, leading to motor and cognitive impairments that manifest in early life (Aksu Uzunhan et al., 2023; Brancati et al., 2010). Notably, mutations in *B9D1* gene are implicated in Meckel syndrome, a severe ciliopathy that is perinatally lethal due to polydactyly, kidney disease, liver fibrosis and central nervous system defects (Dowdle et al., 2011).

By selecting the 20 specific genes IPA ascribed to the cilium assembly canonical pathway described above, I performed an additional analysis consisting of a deeper pathway enrichment not restricted to Ingenuity's Knowledge Database. This more specific IPA function allowed me to identify a strong correlation between the identified ciliary genes and the top two independent functional terms with a strong enrichment in cilia. Specifically, these two terms were "formation of cilia" and "assembly of non-motile cilium" with a p-values of 5.02×10^{-14} and 1.60×10^{-10}, respectively **(Figure 4.7B)**.

To appreciate the directionality of the changes predicted by IPA, I applied an overlay of the identified functional terms with the $\log_2$FC and p-value of the genes identified in the canonical pathway. Importantly, this *in silico* analysis revealed a predicted inhibition of these two pathways, thereby indicating primary cilia dysfunction in the CNS of SMA mouse embryos **(Figure 4.7B)**.

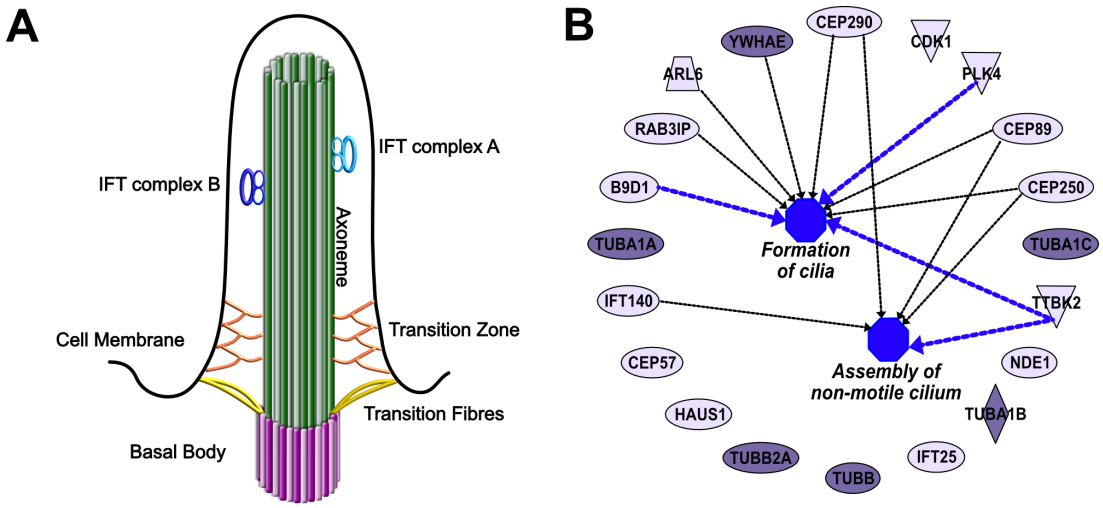

Figure 4.7 IPA enrichment analysis revealed inhibition of primary cilia-related functional terms. (A) Schematic of a primary cilium highlighting the main structural components: Intraflagellar Transport Proteins (IFT) complex A and B, transition zone and fibres, basal body and cell membrane. **(B)** Functional enrichment analysis network of cilium assembly DEGs. Downregulated molecules in light purple; upregulated molecules in dark purple. Different shapes indicate molecules with distinct biological functions. Dotted black arrows show the enrichment of individual molecules to the functional terms “Formation of cilia” and “Assembly of non-motile cilium”. Blue arrows indicate a predicted inhibition state on the specific functional term. Both functional terms are highlighted in blue, indicating an overall inhibition.

4.4 Discussion

Recent findings have provided further insights into the role of SMN protein in both translation and ribosome biology, contributing to a more advanced understanding of SMA pathology (Bernabò et al., 2017; Lauria et al., 2020; Sanchez et al., 2013; Thelen et al., 2020). Among others, the research group led by Prof. Gabriella Viero have provided substantial evidence demonstrating the function of SMN as a ribosome-associated protein, thereby playing a direct role in translation (Bernabò et al., 2017; Lauria et al., 2020; Sharma et al., 2024).

Given the pivotal role of the Viero's lab into investigating mRNA translation and its role in SMA, during the second year of my PhD I had the invaluable opportunity to embark on a four-month secondment at the Institute of Biophysics in Trento, Italy, under the supervision of Prof. Gabriella Viero. This collaborative study allowed me to deepen the understanding of the consequences at the molecular level of SMN protein insufficiency during the prenatal stages of SMA. To achieve this, I learned how to perform two challenging molecular techniques: *polysome* and *ribosome profiling*.
Polysome profiling allows the investigation of the overall translation level in a tissue by quantifying the percentage of ribosomes engaged in polysomes, and therefore actively translating. Nevertheless, this technique does not provide ribosome positional information and does not allow the identification of differentially expressed genes. The acquisition of such detailed information is possible through the implementation of ribosome profiling, a technique that enables the specific isolation and sequencing of mRNA fragments protected by ribosomes.

To date, and to the best of my knowledge, no studies have examined translation defects in prenatal SMA. Therefore, in this chapter I illustrated how I first used polysome profiling to obtain an overview of the translation activity in three main organs from Taiwanese mouse embryos at E14.5, and secondly, how I used ribosome profiling to specifically identify the dysregulated

transcripts in the mouse embryonic brain and spinal cord. Ultimately, I performed IPA enrichment analyses on the omics datasets generated to investigate the biological causes of SMA-related brain development defects.

Polysome profiling of E14.5 brain, spinal cord and liver revealed that translation is a process with tissue-specific characteristics. Specifically, the fraction of ribosomes in polysomes (FRPs), aimed at studying how active translation is, showed that each organ from control embryos presents with a unique trend, with the liver profile being strikingly different from those of the brain and spinal cord. The higher levels of translation activity in the liver could be justified by the intense protein synthesis occurring in this organ during embryonic development. Although a direct correlation would have to be established by further studies, the foetal liver has a high metabolic activity, and it is the predominant site of haematopoiesis and other essential factors required for systemic growth (Zhao & Duncan, 2005). By contrast, the reason why the embryonic brain and spinal cord present with a lower translation activity could be due to their specific and more tailored protein synthesis allowing neural development and signalling (Holt et al., 2019).

While we were able to appreciate tissue-specific changes in translation between different organs from control embryos, polysome profiling did not show any differences in the overall translation activity when comparing control with SMA. However, while polysome profiling represents a powerful technique to obtain a direct measurement of the translational activity, it lacks high-resolution and ribosome positional information (Jin & Xiao, 2018). For this reason, I therefore performed ribosome profiling. This time the focus was on E14.5 brain and spinal cord only, as the main aim of this study and thesis is to investigate the morphological and molecular causes of CNS development defects in SMA embryos. Ribosome profiling allowed us to identify several genes presenting with a dysregulated ribosome occupancy in both brain and spinal cord from SMA mouse embryos at E14.5.

As mentioned in this chapter, these sophisticated techniques were performed using whole embryonic tissue rather than isolated regions, such as the hippocampus or specific tracts of the spinal cord. The reason of this experimental design lies in the technical challenges involved. Despite the high level of sensitivity of these methods, a substantial amount of input material is necessary to guarantee reliable functionality and outcomes (Tomuro & Iwasaki, 2025). In this regard, the prenatal organs that were dissected from mouse embryos at E14.5 and used in this study are relatively small. Therefore, obtaining sufficient material from specific subregions would have been technically challenging, potentially compromising the quality and reproducibility of the data. Nevertheless, this methodological approach may have limitations. It is well documented that brain and spinal cord are highly heterogenous tissues, and for this reason translational changes occurring in specific regions may not be detected when using lysates obtained from whole tissues (Sultana et al., 2024; Zhu et al., 2025). Consequently, the results presented in this chapter should be interpreted as an assessment of the translational activity across the entire organ, rather than effects limited to a specific area.

Taken together, the results I obtained during my secondment by performing polysome and ribosome profiling reveal that SMN is essential to ensure normal translation activity throughout the brain and spinal cord during embryonic development, with tissue/organ-specific translational defects observed in SMA mice. To further expand on the biological significance of these findings, I employed IPA to identify the canonical signalling pathways enriched with the differentially expressed genes revealed by ribosome profiling. This analysis provided some unexpected insights. Among the well-characterised pathways that are already linked to postnatal SMA, I also noticed the relevance of a key biological pathway that has never before been analysed in the context of SMA: cilium assembly. Given the fundamental role of primary cilia to guide and ensure the correct course of prenatal development (Anvarian et al., 2019), I

decided to further study and focus on this subcellular organelle to uncover their role in the CNS of SMA embryos.

Primary cilia are sensory organelles that capture extracellular signals and transduce them into intracellular responses (Mill et al., 2023). To undertake their role, they are characterised by a specialised structure in which each component is essential for their correct functioning. One of the most relevant element of primary cilia architecture is the transition zone (TZ), which plays a crucial role in controlling the entry and exit of cargo proteins essential for cilia assembly and signalling (Wang et al., 2022). Thanks to ribosome profiling and IPA enrichment analyses, here I found that several genes that encode for proteins that form the TZ, such as *ARL6*, *B9D1* and *CEP290*, have decreased ribosome occupancy in the CNS of SMA mouse embryos at E14.5.
Alongside the TZ, the Intraflagellar Transport (IFT) proteins are also essential for the correct assembly and maintenance of cilia. These proteins are indeed responsible of the bidirectional transport of structural and signalling molecules along the microtubular axoneme (Ma et al., 2023). Interestingly, two genes that encode for crucial components of the IFT system, *IFT140* and *IFT25*, were also found in our dataset as downregulated in the CNS of SMA mouse embryos. Importantly, IFT25 ensure the correct anterograde transport to the tip of the cilium of SMO and GLI, two well-known proteins essential for the activation of Sonic Hedgehog (Shh) signalling pathways, a key modulator of embryonic development and tissue homeostasis (Andreu-Cervera et al., 2021; Brian et al., 2012; Eguether et al., 2018).

As previously mentioned, primary cilia dysfunction can lead to ciliopathies, a spectrum of severe prenatal and developmental diseases often characterised, among other symptoms, by brain malformations and cognitive defects (Karalis et al., 2022; Ma et al., 2022; Mill et al., 2023; Park et al., 2019). Therefore, the study of primary cilia biology in the context of embryonic SMA could provide novel insights and advance our understanding of the underlying causes of

CNS prenatal defects and neurodevelopmental phenotypes observed in some SMA patients.

The following chapter of this thesis will thus concentrate on primary cilia. By employing *in vivo* and *in vitro* models of prenatal SMA, I will explore primary cilia phenotypes in the embryonic CNS, highlighting the effects of insufficient SMN protein levels on these organelles and exploring how these can be rescued by therapeutic intervention.

Chapter 5: **SMN-dependent primary cilia defects in the central nervous system of SMA mouse embryos**

5.1 Introduction

Historical evidence attributes the first observation of cilia to Antony van Leewenhoek in 1677. who, in a letter to the Royal Society of London, described the observation of protozoa provided with “thin little feet” (Bloodgood, 2009; Van Leewenhoeck, 1677). While the term “cilium” to refer to these cellular structures was later introduced by Otto Friedrich Muller in 1786 (Muller, 1786), it was only in 1898 when the scientist Karl Wilhelm Zimmermann, working at the Institute of Anatomy of the University of Bern, in Switzerland, first recognised primary cilia in mammals and correctly predicted their sensory function (Zimmermann, 1898). This discovery established the foundation for a research field that would continue for many years. As a result of these preliminary observations, it has now been established primary cilia are conserved non-motile cellular organelles present on nearly all nucleated eukaryotic cells (Fry et al., 2014).

As a solitary extension protruding in continuity with the plasma membrane, the cilium structure consists of a microtubule core composed of nine microtubule doublets, called axoneme, that extend from a specialised centriole, the basal body, into the extracellular space (Hoey et al., 2012). Despite their small size (~200–300 nm in diameter and ~1–10 μm long), primary cilia have a crucial role in sensing extracellular stimuli and converting them into intracellular signalling responses (Ko, 2012). Current evidence highlights the multitude of signalling pathways regulated by primary cilia, including Sonic Hedgehog (Shh), WNT and mTOR to control developmental processes, tissue plasticity and organ function (Anvarian et al., 2019). Specifically, in the brain, the Shh signalling is essential for the spatial patterning of the developing

neuroepithelium, for the correct cellular identity in the CNS, for axonal guidance and neuronal activity. As the proteins involved in Shh signalling are localised within the cilium, it has been demonstrated that defects in primary cilia lead to Shh signalling dysfunction resulting in compromised brain development in mice, causing defects in neural patterning, cerebellar hypoplasia, and impaired hippocampal neurogenesis (Ferent & Traiffort, 2015; Park et al., 2019). The correct functioning of primary cilia is closely linked to another key developmental signalling pathway: WNT signalling. In this regard, several studies have reported abnormal WNT signalling accompanied by impaired neuronal migration and defects in synapse formation in the hippocampus when neuronal ciliogenesis is compromised (Kumamoto et al., 2012; Park et al., 2018). In addition, mTOR signalling pathway has also been shown to be involved in several cellular processes essential for the correct development of the brain (Park et al., 2019). Studies have revealed that impaired cilia increase mTOR signalling, resulting in the formation of enlarged brain ventricles (Foerster et al., 2017). Furthermore, mTOR signalling disruption linked to impaired neuronal ciliogenesis has been described in patients with focal malformations of cortical development (FMDC) (Park et al., 2018).

As a result, acting as signaling hubs, primary cilia play a key role during embryogenesis and development by coordinating fundamental biological processes as cell cycle progression and cell proliferation (Gopalakrishnan et al., 2023; Mill et al., 2023).

Dysfunctions in primary cilia gives rise to ciliopathies, a heterogeneous group of diseases and multisystemic disorders (Hildebrandt et al., 2011; Waters & Beales, 2011). Ciliopathies can affect nearly every major organ in the body, causing brain malformations, cardiac defects, renal malformations, liver disease and musculoskeletal abnormalities, as described in well-characterised ciliopathies such as Joubert, Meckel-Gruber and Bardet Biedl Syndromes (Elawad et al., 2022; Hartill et al., 2017; Parisi, 2009). Furthermore, in addition to these severe clinical manifestations, defects in primary cilia have been

associated with neurodevelopmental phenotypes, including intellectual disabilities (Bennouna-Greene et al., 2011; Berbari et al., 2014; Ma et al., 2022; Mill et al., 2023; Rhee et al., 2016).

As in the previous chapter of this thesis I have identified prenatal translational disruption in genes involved in primary cilia biology and, in addition, primary cilia dysfunction has never been investigated in the context SMA pathology, here I explore whether the observed embryonic defects could be explained by changes in primary cilia occurring in the CNS of Taiwanese SMA mouse embryos.

5.2 Aim

The primary aim of this chapter is to investigate primary cilia biology in the CNS of SMA mouse embryos using *in vivo* and *in vitro* approaches.

An *in vivo* primary cilia study was performed to identify and quantify primary cilia density in the embryonic hippocampus and spinal cord at two different timepoints of prenatal development (E14.5 and E18.5). This was carried out via fluorescence immunohistochemistry using two well-established ciliary markers: ARL13B, labelling the axoneme, and ɣ-tubulin, labelling the basal body.

An *in vitro* model was established to permit more detailed examination of the morphology of primary cilia. In collaboration with Prof. Mike Cousin (UoE), I generated primary hippocampal cell cultures from control and SMA Taiwanese mouse embryos at E17.5, a developmental age selected for the technical practicality of hippocampal dissection. This *in vitro* system also allowed me to investigate whether primary cilia defects were amenable to therapeutic intervention using an SMN-restoring treatment.

5.3 Results

5.3.1 *In vivo* primary cilia biology investigation in the CNS

5.3.1.1 Visualisation of primary cilia in the embryonic hippocampus

To be able to study primary cilia biology in prenatal SMA, I first had to design and optimise an immunohistochemistry protocol to be able to visualise their structure. My experimental plan consisted of using two different antibody markers to label primary cilia. This was to allow me a more precise visualisation of their unique structure and to increase confidence for their accurate identification. For this reason, the first primary antibodies I decided to select and test to stain primary cilia were anti-ARL13B and anti-Pttg1, whose encoding genes were not translationally dysregulated in our DEGs datasets. Specifically, ALR13B is a small GTPase holding diverse cellular functions, including the regulation of Shh signalling and intraflagellar transport (IFT) (Caspary et al., 2007). *ARL13B* is considered a ciliopathy gene, as its mutation has been found in Joubert syndrome patients (Cantagrel et al., 2008). As ARL13B localises along the cilium (Larkins et al., 2011), in this study I used it as a marker of the axoneme. Pttg1, also known as Securin, is encoded by the pituitary tumour transforming gene 1 (*PTTG1*) and has been linked to several biological functions, including cell cycle control, DNA repair and gene regulation (Moreno-Mateos et al., 2011). Moreover, Pttg1 plays a role in microtubule dynamics and has been shown to localise at the base of primary cilia in the brain (Mecklenburg et al., 2021).

Following the manufacturer recommendations, I therefore proceeded to perform immunohistochemistry on paraffin brain sections previously collected from E14.5 control mouse embryos. Unfortunately, the first trial using ARL13B and Pttg1 markers was unsuccessful as neither of the two antibodies gave me satisfactory results **(Figure 5.1 A and B)**. Consequently, I refined the staining protocol by implementing a multistep optimisation process. Specifically, I increased the concentration of primary antibodies to enhance antigen binding, I extended the incubation time of secondary antibodies to compensate for a potential low-affinity interaction with the primary antibody, and most

importantly, I changed the antigen retrieval protocol. Antigen retrieval is a crucial step when performing immunohistochemistry, especially on formalin-fixed, paraffin-embedded tissues (Shi et al., 2011). As the fixation and embedding processes may mask the epitope recognised by primary antibodies, antigen retrieval is necessary to expose the antigen, thereby enhancing the primary antibody's to bind to it (Shi et al., 2011). For this optimisation, instead of using sodium citrate buffer at pH 6 for heat-induced epitope retrieval, I decided to use Tris-EDTA at pH 9. This buffer is better suited to antigens that are more difficult to detect, as the alkaline pH is more effective at revealing the epitopes (Ramos-Vara & Miller, 2014).

To make my primary cilia study more time-efficient, I decided to expand the list of antibodies I wanted to test by adding ɣ-tubulin marker. This protein plays a crucial role in the nucleation of microtubules, and it localises to the basal body of primary cilia (Breunig et al., 2008; Oakley et al., 2015), and it therefore represents a reliable marker for the identification of these organelles. Unfortunately, this second attempt was not entirely satisfactory either. While the anti-ARL13B antibody worked efficiently, both anti-Pttg1 and anti-ɣ-tubulin antibodies resulted in a non-specific signal **(Figure 5.1 C and D)**.

As the anti-Pttg1 primary antibody was ineffective for the second time, I decided to focus solely on the ARL13 and ɣ-tubulin markers, in attempting to achieve clear visualisation of the axoneme and basal body of the primary cilia. For this third trial, I tested the affinity between the primary and secondary antibodies. Initially, I used Alexa Fluor 488 (green) for ɣ-tubulin and Alexa Fluor 594 (here in magenta) for Arl13b **(Figure 5.2 A and B)**. Using this antibody combination, only Arl13b could be detected and visualised. Therefore, I exchanged the fluorophores. In combination with Alexa Fluor 594, γ-tubulin produced a stronger, more specific signal. This allowed me to successfully label two fundamental components of the primary cilia structure: the axoneme, labelled with ARL13B, and the basal body, labelled with γ-tubulin **(Figure 5.2 C and D)**.

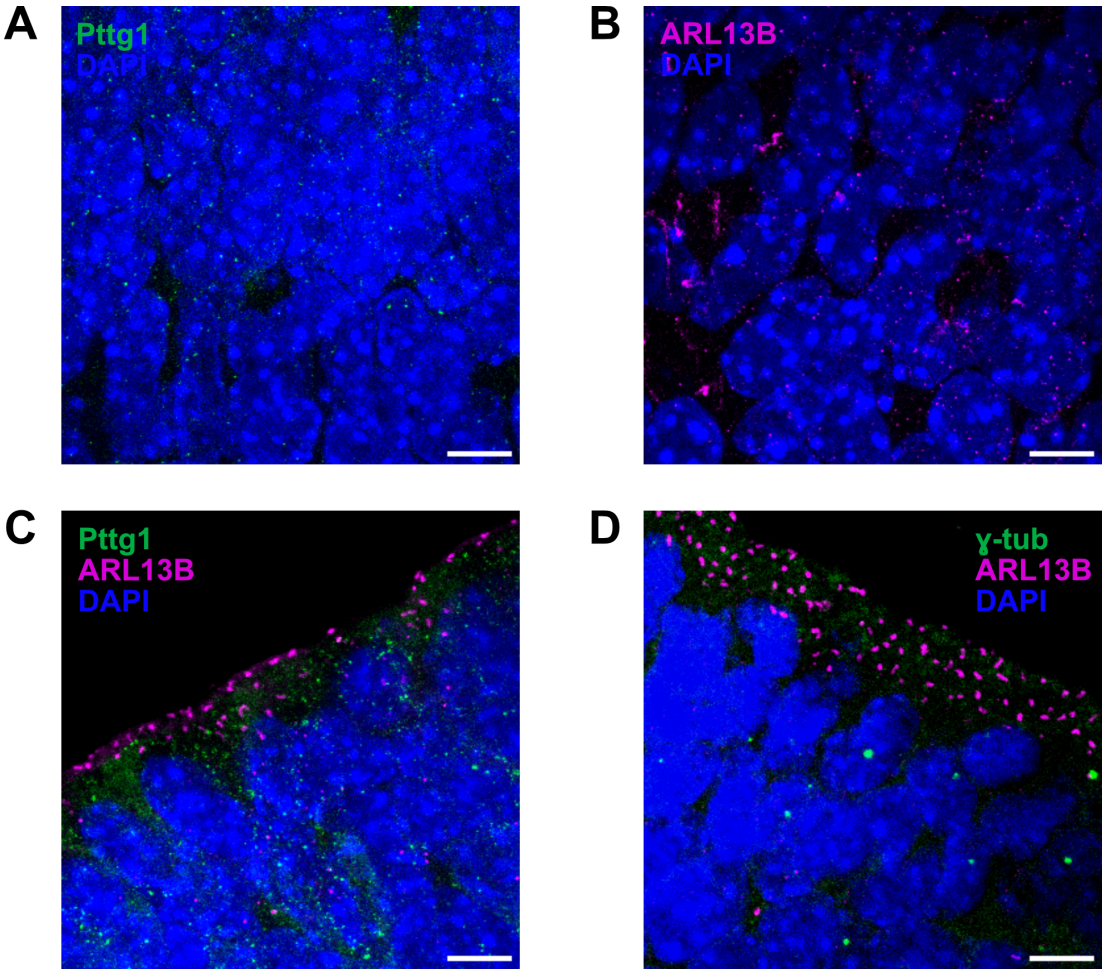

Figure 5.1 Initial immunohistochemistry optimisations to visualise primary cilia in the brain of E14.5 embryos. (A) Unsuccessful Pttg1 staining on paraffin brain section. **(B)** The preliminary application of the anti-ARL13B primary antibody produced a non-specific signal on a paraffin-embedded brain section. **(C)** Subsequent staining trial on paraffin brain section provided positive results for the labelling of the primary cilia axoneme labelled with ARL13B (magenta), while the anti-Pttg1 antibody produced a non-specific signal. **(D)** The ARL13B antibody consistently recognised the axoneme of primary cilia axoneme (magenta), whereas the anti-ɣ-tubulin antibody failed to label the basal body of primary cilia. Scale bar 10 μm. Coronal paraffin sections obtained from control mouse embryos at E14.5, 10 μm thickness.

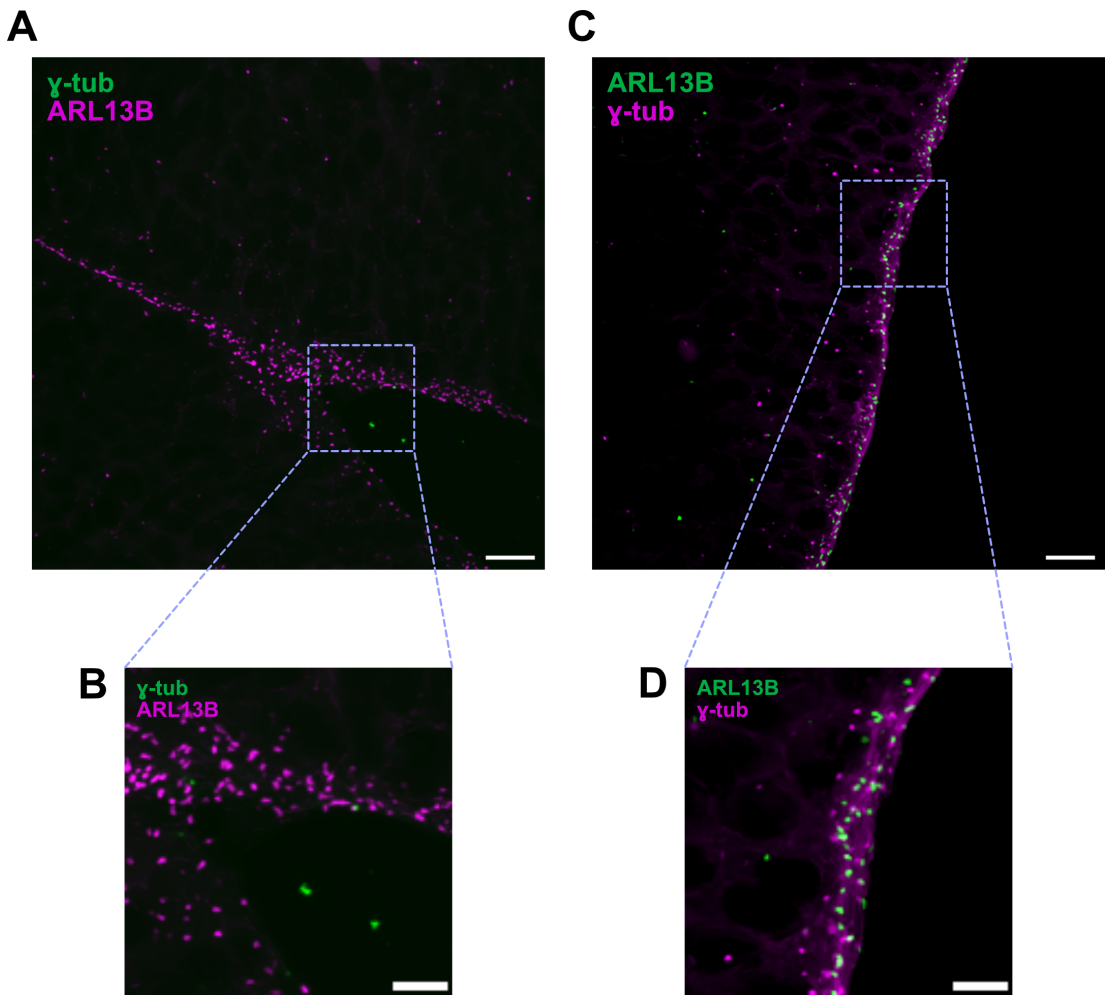

Figure 5.2 Primary and secondary antibodies affinity tests to successfully label axoneme and basal body of primary cilia in the brain of E14.5 mouse embryos. (A and B) The anti-ARL13B primary antibody was compatible with the Alexa Fluor 594 secondary antibody (here in magenta). In contrast, the anti-ɣ-tubulin primary antibody was ineffective when used in combination with Alexa Fluor 488 secondary antibody (green). This resulted in labelling the axoneme, but not basal body of the primary cilium. **(C and D)** Switching the fluorophores revealed that the anti-ɣ-tubulin antibody had higher affinity for Alexa Fluor 594, resulting in successfully labelling and visualisation of the primary cilia basal body (showed in magenta). The anti-ARL13B antibody was effective even when combined with Alexa Fluor 488 secondary antibody (green). Scale bar 20 μm, zoom 10 μm. Coronal paraffin sections obtained from control mouse embryos at E14.4, 10 μm thickness.

5.3.1.2 Preliminary analysis of primary cilia in the ventricular zone of the dorsal telencephalon and the hippocampus

After designing an optimised immunohistochemistry protocol to visualise primary cilia in the embryonic mouse brain, I proceeded with a preliminary analysis to investigate whether there were any changes in primary cilia phenotype in SMA embryos when compared to control littermates.

To achieve this, I first identified the anatomical brain regions I wanted to focus the analysis on. Primary cilia are present on nearly all cell type in the developing brain, but they are particularly enriched towards the ventricles (Tong et al., 2014). To enable a first-stage analysis of primary cilia phenotypes, I decided to focus on the lateral ventricles of mouse embryos at E14.5. More specifically, I focused on the ventricular zone of the dorsal telencephalon (DT) and of the hippocampus (HPC) **(Figure 5.3 and Figure 5.4)**. For both these regions I measured the area and the thickness of the cellular layer presenting with cilia. Subsequently, I counted the number of cilia within this layer.

After identifying the DT in the E14.5 brain **(Figure 5.3A)**, I used confocal microscopy to acquire and analyse images of the primary cilia layer in both control and SMA Taiwanese mouse embryos **(Figure 5.3B)**. As can be seen in the representative images, I used Fiji/ImageJ to manually trace the perimeter of the cilia layer and measure its area and thickness. Neither measurement revealed a difference between genotypes **(Figure 5.3 C and D)**. Additionally, I manually counted the number of primary cilia in the restricted area to measure their density. This analysis also showed no changes in SMA compared to control littermates **(Figure 5.3E)**.

In parallel, I applied the same approach of investigation to the ventricular zone in correspondence of the HPC **(Figure 5.4A)**. Defining the ciliated region of interest **(Figure 5.4B)**, I subsequently quantified the area and the thickness of the layer. Similarly to what observed in the DT, these analyses did not show any differences between control and SMA (Figure **5.4 C and D)**. Finally, I calculated the density of primary cilia in the area. However, the measurement revealed no primary cilia phenotype in the SMA mouse brain when compared to the control **(Figure 5.4E)**.

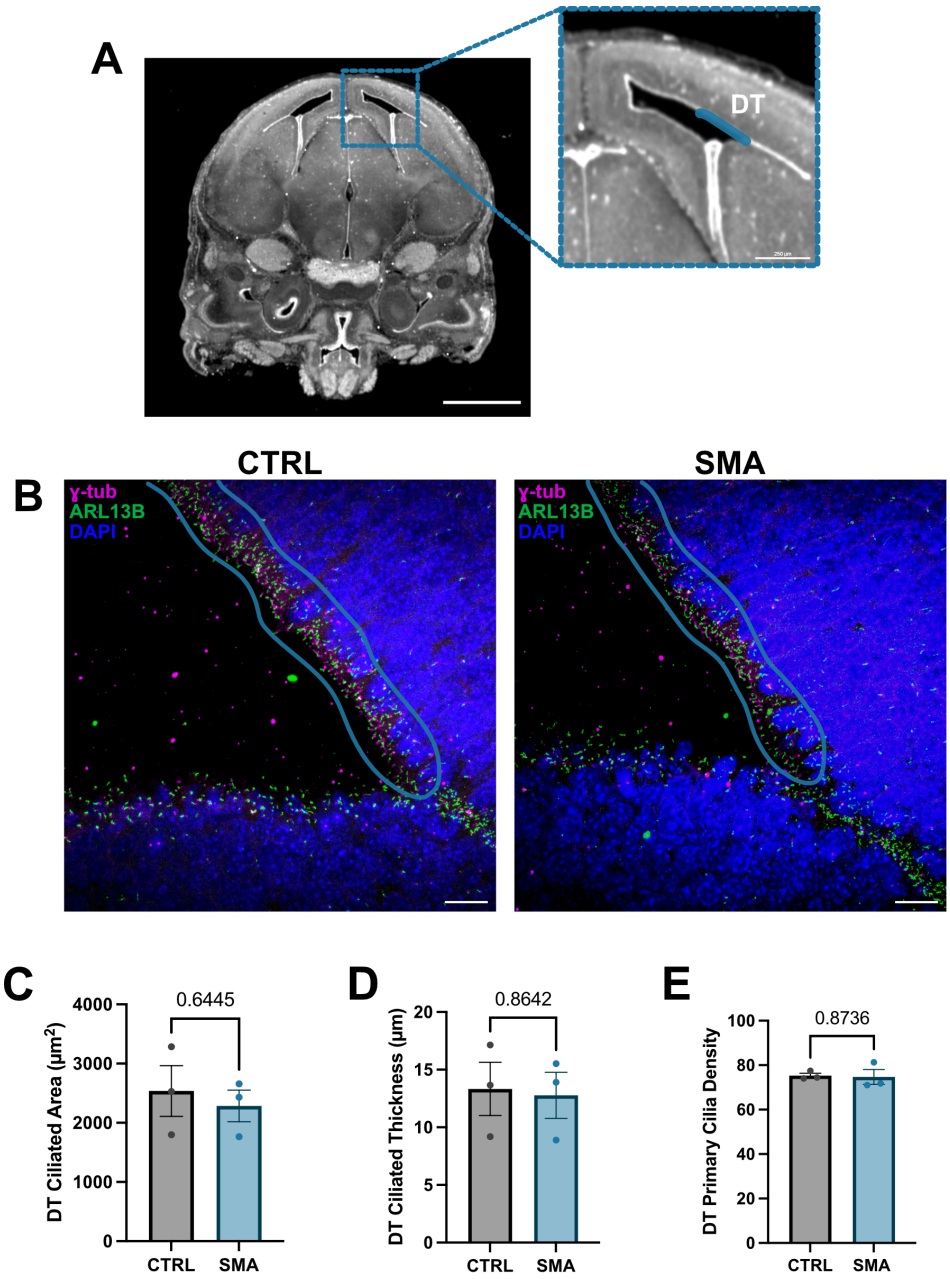

Figure 5.3 Preliminary primary cilia investigation in the ventricular zone of the dorsal telencephalon of E14.5 mouse embryos. (A) Representative coronal paraffin section from control mouse embryo at E14.5 to demonstrate whole brain topography. The blue square indicates the relative position of the dorsal telencephalon (DT). Scale bar 1 mm, zoom 250 µm. **(B)** Primary cilia staining in the ventricular zone of the DT of control and SMA mouse embryos at E14.5. Blue lines indicate the specific area where the quantitative analysis was performed. Scale bar 20 µm. **(C-D)** Measurements of the area **(C)** and thickness **(D)** of the ciliated layer of the DT in control and SMA mouse embryos. **(E)** Primary cilia density quantification in the ventricular zone of the DT of control and SMA mouse embryos at E14.5. Unpaired t-test, scatter dot plot, mean with SEM. One datapoint corresponds to the average values from three sections per embryo. N = 3 embryos for control and 3 for SMA.

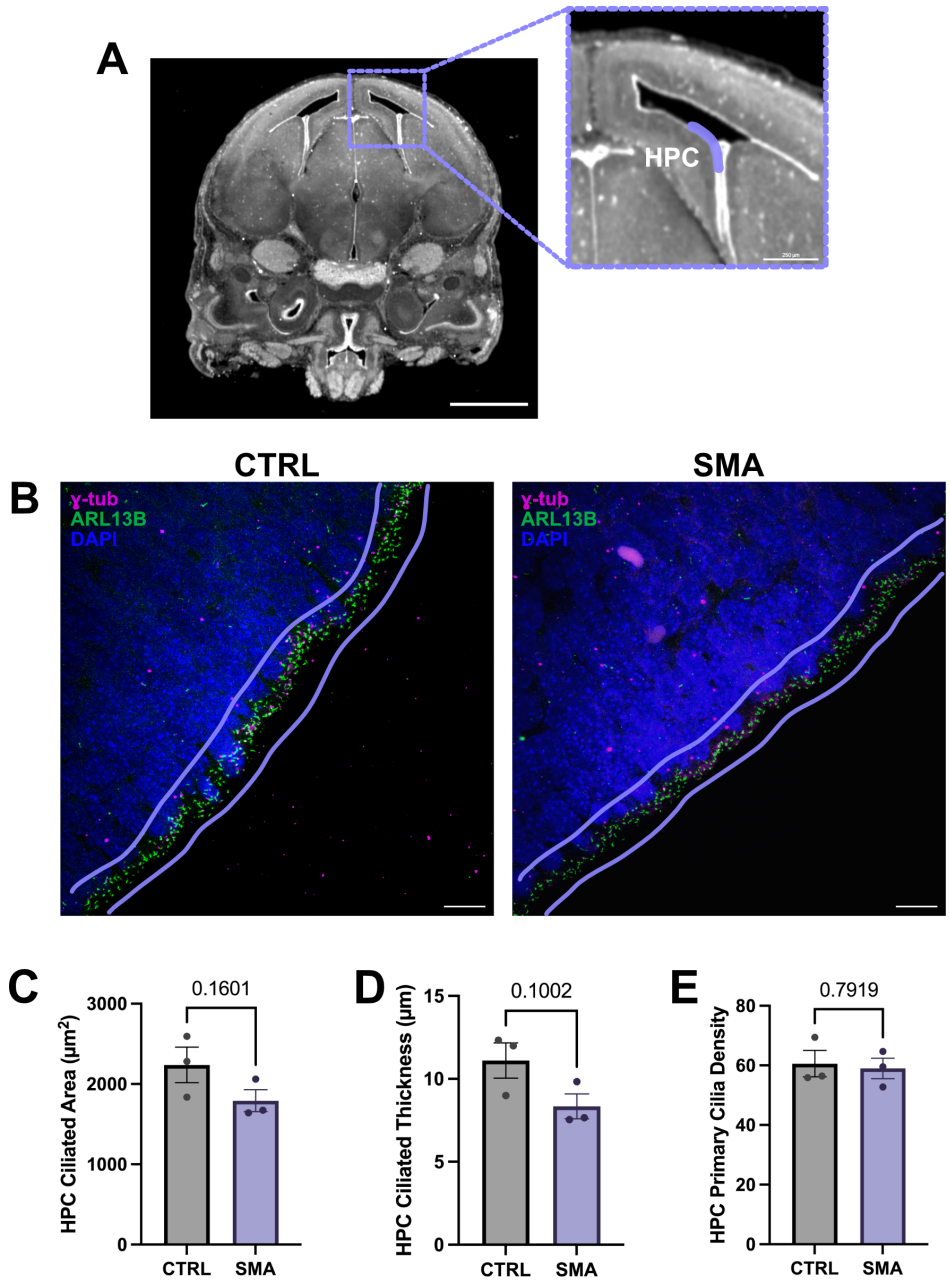

Figure 5.4 Preliminary primary cilia investigation in the ventricular zone of the hippocampus of E14.5 mouse embryos. (A) Representative coronal paraffin section from control mouse embryo at E14.5 to demonstrate whole brain topography. The violet square indicates the relative position of the hippocampus (HPC). Scale bar 1 mm, zoom 250 µm. **(B)** Primary cilia staining in the ventricular zone of the HPC of control and SMA mouse embryos at E14.5. Violet lines indicate the specific area where the quantitative analysis was performed. Scale bar 20 µm. **(C-D)** Measurements of the area **(C)** and thickness **(D)** of the ciliated layer of the HPC in control and SMA mouse embryos. **(E)** Primary cilia density quantification in the ventricular zone of the HPC of control and SMA mouse embryos at E14.5. Unpaired t-test, scatter dot plot, mean with SEM. One datapoint corresponds to the average values from three sections per embryo. N = 3 embryos for control and 3 for SMA.

5.3.1.3 Reduced primary cilia density in the hippocampus of E14.5 SMA mouse embryos

Despite the preliminary analysis performed on primary cilia in the embryonic brain did not unveil any specific changes occurring in SMA, it is essential to remember that the brain, especially during its prenatal stages, is highly heterogenous, where different regions exhibit unique characteristics (Stiles & Jernigan, 2010). This leads to the hypothesis that the same investigation performed on a different anatomical area could lead to different results and interpretations. Furthermore, although primary cilia are highly present in the ventricular zone during embryonic brain development, they also undergo a dynamic and developmental transformation there (Mirzadeh et al., 2010). Radial glial cells are neural stem cells in the developing nervous system, and, with their soma lying into the ventricular zone, are characterised by the presence of a primary cilium, allowing the correct morphogenesis of the ventricles (Foerster et al., 2017). During prenatal development, from the age of E14, radial glial cells initiate their maturation and differentiation giving rise to different cell populations, including ependymal cells (Miranda-Negrón & García-Arrarás, 2022; Spassky et al., 2005). Ependymal cells are essential components of the CNS and present with multiple motile cilia (Deng et al., 2022; Ringers et al., 2020). Primary and motile cilia differ in their microtubular structure and function. While primary cilia are solitary organelles present in different cell types and have a sensory function to regulate fundamental processes and development (Mill et al., 2023), motile cilia are restricted to epithelial cells, usually organised in clusters, where they function as motor machinery to facilitate fluid transport (Jain et al., 2010). As during embryogenesis, the primary cilia on radial glial cells in the ventricular zone are replaced by motile cilia on ependymal cells, and the focus of this study is solely on primary and not motile cilia, the results of the preliminary analysis I performed could be misleading and not in line with the objective.

I therefore decided to move my investigation to focus on neuron-rich areas of the hippocampus, specifically the dentate gyrus. As already mentioned, the

hippocampus plays a key role in memory and cognition in humans (Rubin et al., 2014), and with this study, I previously revealed hippocampal cell proliferations defects in E14.5 SMA mouse embryos. In addition, several previous studies showed a correlation between primary cilia depletion and hippocampal-dependent learning and memory deficits (Berbari et al., 2014; Rhee et al., 2016), as well as hippocampal dysgenesis and volume loss in ciliopathy patients, highlighting the impact of primary cilia in hippocampus development and in cognition (Baker et al., 2011; Bennouna-Greene et al., 2011).

Thus, I proceeded by performing immunohistochemistry on E14.5 hippocampus from both control and SMA Taiwanese mouse embryos. Following the protocol described above, I used anti-ARL13B and anti-ɣ-tubulin primary antibodies to label the primary cilia axoneme and basal body, respectively. After identifying the anatomical region of the dentate gyrus in the brain of at E14.5 (**Figure 5.5A**), I used confocal microscopy to systematically acquire high-magnification images representing the same area of the hippocampus, allowing for a consistent analysis. In **Figure 5.5B** it can be appreciated the presence of primary cilia with an intact structure complete of axoneme and basal body in both SMA and littermate controls. As in the region of interest primary cilia are not organised in layers, here I decided to focus on the quantification of their density. To achieve this, I counted the total number of primary cilia and normalised it to the total number of DAPI-positive cells. The result of this analysis revealed a statistically significant decrease in the percentage of ciliated cells in SMA mouse hippocampus compared to control littermates at E14.5 **(Figure 5.5C)**.

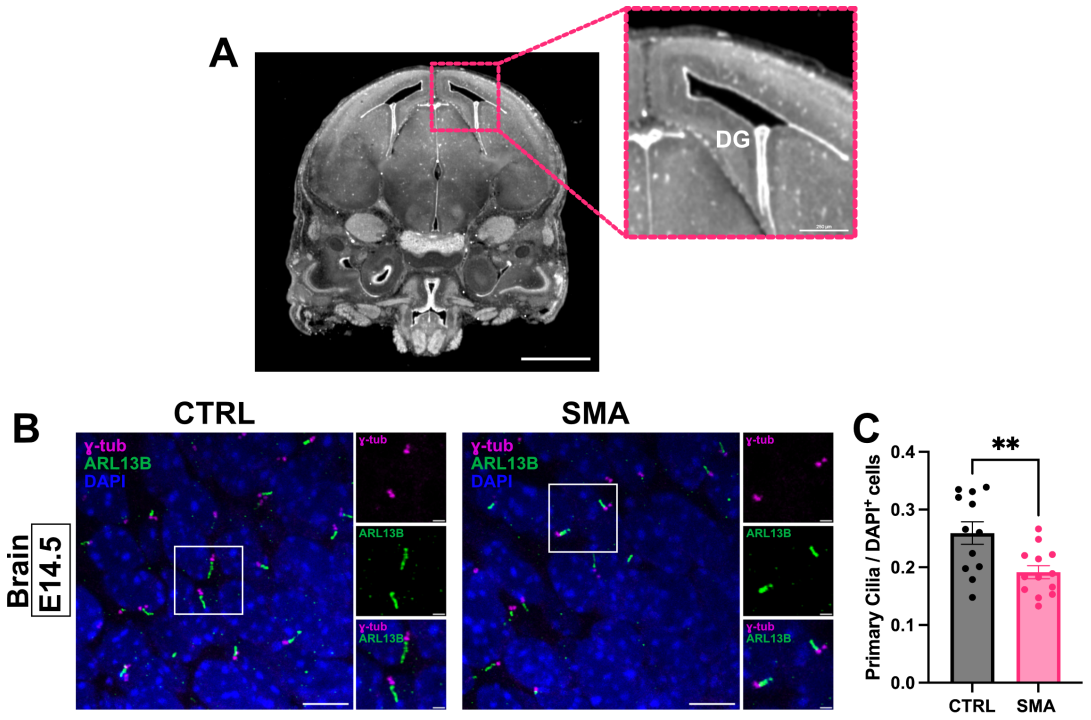

Figure 5.5 Reduced density of primary cilia in the SMA mouse embryonic hippocampus at E14.5 (A) Representative coronal paraffin section from control mouse embryo at E14.5 to demonstrate whole brain topography. The pink square indicates the relative position of the dentate gyrus (DG), where the analysis was performed. Scale bar 1 mm, zoom 250 µm. **(B)** Primary cilia visualisation using ciliary markers ARL13B (axoneme, in green) and ɣ-tubulin (basal body, in magenta) in the hippocampus of E14.5 control and SMA embryos. **(C)** Primary cilia density quantification reveals reduced primary cilia number in SMA compared to littermate controls. Coronal paraffin sections, 10 µm thickness, scale bar 10 µm, zoom 2 µm. N = 12 embryos for control and 13 for SMA at E14.5. **p-value ≤ 0.01, unpaired t-test, scatter dot plot, mean with SEM. One datapoint corresponds to the average values from three sections per embryo.

5.3.1.4 Defects in primary cilia defects are consistently present in the hippocampus of SMA mouse embryos at E18.5

To assess whether the SMA-related cilial defects observed in the hippocampus at E14.5 persisted into later stages of prenatal brain development, I repeated the analysis in mouse embryos at the age of E18.5. This is one of the latest phases of murine gestation prior to birth, and it represents a pivotal transition period in which the brain is almost fully formed but continues to undergo a process of refinement and maturation (Chen et al., 2017).

The study of primary cilia in the anatomical region corresponding to the dentate gyrus was conducted by performing immunohistochemistry in accordance with the protocol I used to investigate cilia biology at early stages of development, thereby ensuring a consistent approach **(Figure 5.6A)**. As previously observed at a younger age, both control and SMA presented with intact primary cilia labelled by ARL13B to identify the axoneme and ɣ-tubulin to visualise the basal body **(Figure 5.6B)**. Excitingly, primary cilia quantitative analysis exhibited a statistically significant decrease in cilia density in SMA mice compared to littermate controls **(Figure 5.6C)**.

Taken together, these results suggest that primary cilia are impaired in the hippocampus of SMA mouse embryos and that these defects are preserved throughout prenatal development.

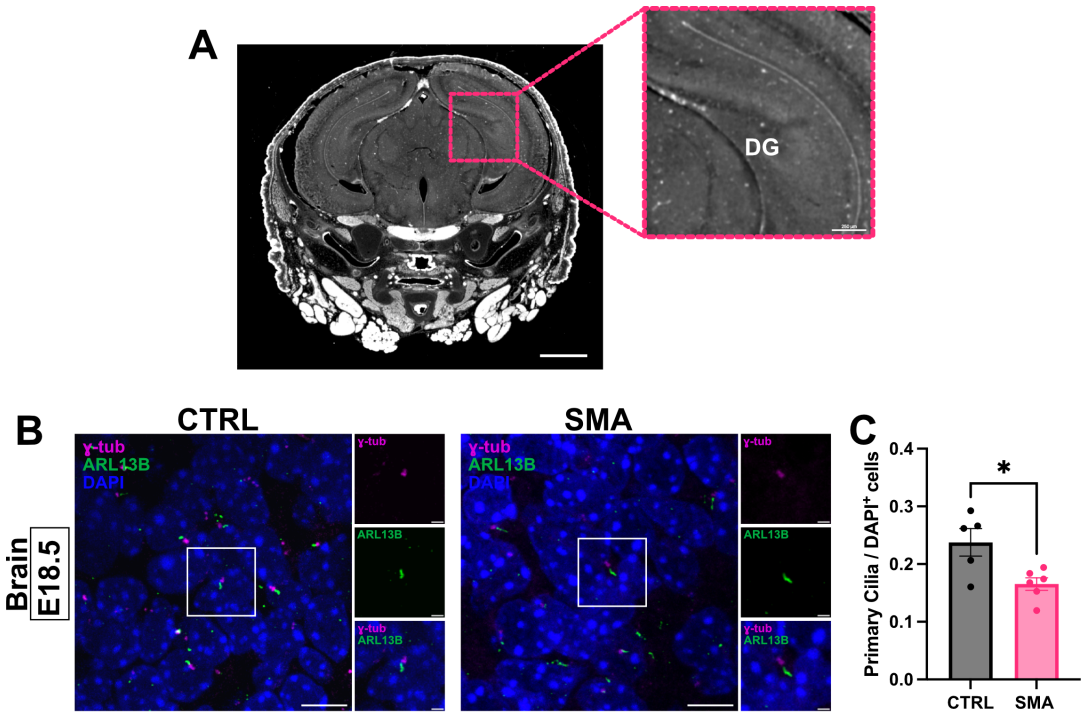

Figure 5.6 Reduced density of primary cilia in the SMA mouse embryonic hippocampus at E18.5 (A) Representative coronal paraffin section from control mouse embryo at E18.5 to demonstrate whole brain topography. The pink square indicates the relative position of the dentate gyrus (DG), where the analysis was performed. Scale bar 1 mm, zoom 250 µm. **(B)** Primary cilia visualisation using ciliary markers ARL13B (axoneme, in green) and ɣ-tubulin (basal body, in magenta) in the hippocampus of E18.5 control and SMA embryos. **(C)** Primary cilia density quantification reveals reduced primary cilia number in SMA compared to littermate controls. Coronal paraffin sections, 10 µm thickness, scale bar 10 µm, zoom 2 µm. N = 5 embryos for control and 6 for SMA at E14.5. *p-value ≤ 0.05, unpaired t-test, scatter dot plot, mean with SEM. One datapoint corresponds to the average values from three sections per embryo.

5.3.1.5 Primary cilia defects do not persist in the hippocampus of postnatal SMA mice

As I observed primary cilia disruption in the hippocampus of SMA embryos at two key timepoints of prenatal development, I decided to further investigate whether these defects were still present at postnatal stages of the disease. To achieve this, I explored two postnatal timepoints of postnatal (P) day 2 and P10, representing the pre- and late-symptomatic stages respectively in the Taiwanese mouse model.

While the anatomical architecture of the postnatal brain differs from that seen so far in this thesis, I consistently focused the investigation of primary cilia on the hippocampal region corresponding to the dentate gyrus **(Figure 5.7 A and B)**. An initial qualitative observation revealed that primary cilia are present in both control and SMA postnatal hippocampus, and that at both timepoints they can be visualised by using ALR13B and ɣ-tubulin markers, labelling the cilium axoneme (in green) and the basal body (in magenta), respectively **(Figure 5.7 C and E)**. However, in contrast to what observed in the prenatal hippocampus, primary cilia density quantification did not show any differences between SMA mice and littermate controls **(Figure 5.7 D and F)**.

Thus, these results suggest that primary cilia disruption is a largely prenatal phenotype occurring in the SMA brain during embryonic development, correlating with the higher levels of SMN protein observed in both mice and humans at these stages (Ramos et al., 2019).

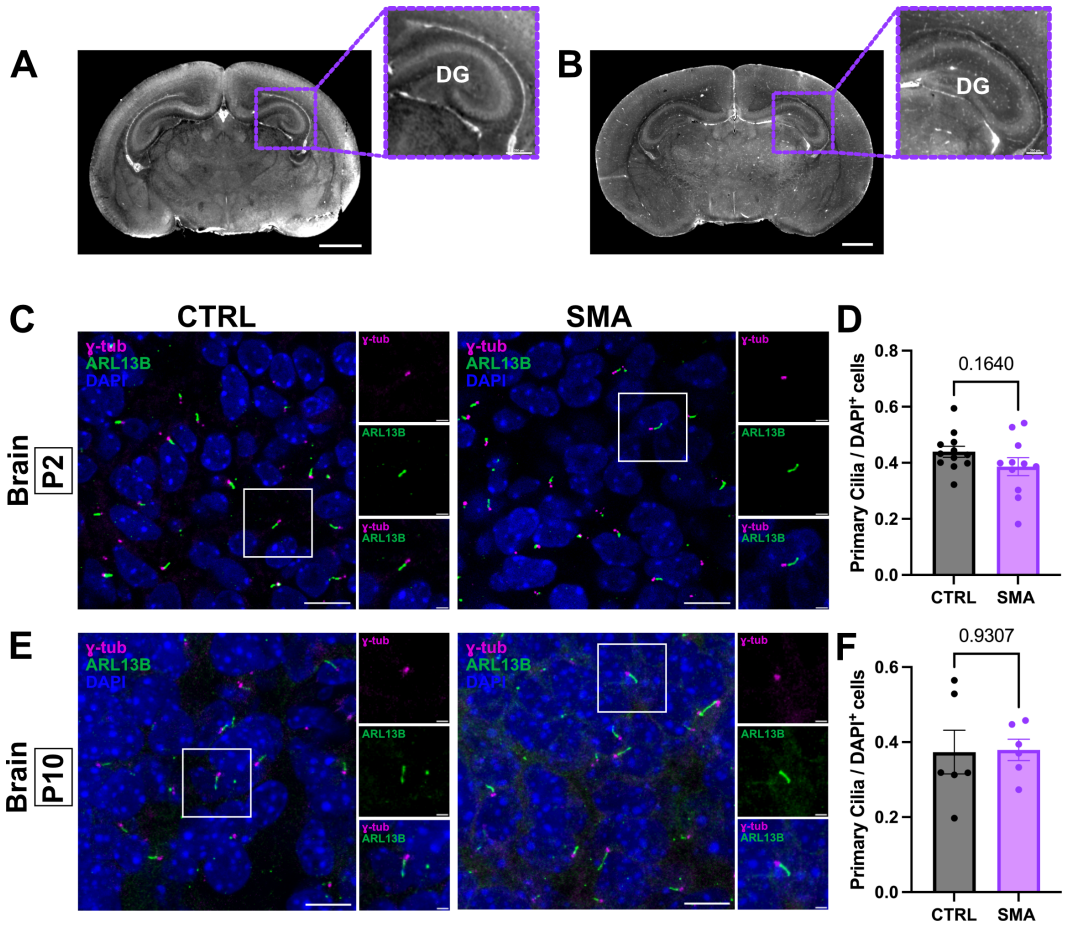

Figure 5.7 No difference in primary cilia density in the hippocampus of P2 and P10 control and SMA mice. (A-B) Representative coronal paraffin sections from control mouse embryo at P2 **(A)** and P10 **(B)** to demonstrate whole brain topography. The violet squares indicate the relative position of the dentate gyrus (DG), where the analysis was performed. Scale bar 1 mm, zoom 250 µm. **(C-D)** Representative confocal images and quantification of primary cilia density in the brain of P2 **(C)** and P10 **(D)** control and SMA mice. Quantification at both timepoints did not reveal any differences between genotypes. Coronal paraffin sections, 10 µm thickness, scale bar 10 µm, zoom 2 µm. N= 12 mice for control and 11 for SMA at P2; N= 6 for control and 6 for SMA at p10. Unpaired t-test, scatter dot plot, mean with SEM. One datapoint corresponds to the average values from three sections per mouse.

5.3.1.6 Primary cilia phenotypes extend into other regions of the CNS

In chapter four of this thesis, I illustrated how ribosome profiling revealed dysregulated ribosome occupancy of genes involved with primary cilia in the brain and spinal cord of SMA mouse embryos at E14.5. Therefore, after the investigation of primary cilia phenotype in the brain, specifically in the hippocampus, of SMA embryos at different timepoints, here, I next explored *in vivo* primary cilia defects in the spinal cord of E14.5 and E18.5 Taiwanese mouse embryos.

After the collection of embryos at the ages of interest, the head was separated from the body, and both parts were fixed in paraformaldehyde (PFA) and embedded in paraffin separately. Embryonic bodies from both E14.5 and E18.5 were sectioned in sagittal plane, allowing me to identify and visualise the anatomical disposition of the major organs simultaneously. **Figure 5.8 A and B** show a representative image of a sagittal section of the embryonic body at E14.5 **(A)** and at E18.5 **(B)** from control embryos. While immunohistochemistry was performed on the entire section, the analysis focused on the lumbar region of the spinal cord. This region of the spinal cord is indeed one of the primary sites of motor neuron degeneration in infantile spinal muscular atrophy, as the motor neurons in this area control the muscles of the lower limbs, which can be severely affected in SMA (Chen et al., 2017; Kong et al., 2021).
Here, I quantified primary cilia density by counting the number of cilia, identified using ARL13B and ɣ-tubulin markers, and normalising to the total number of nuclei, labelled with DAPI staining. The analysis performed on E14.5 spinal cord revealed a significant decrease in cilia density, indicating that primary cilia phenotypes are conserved throughout the CNS at this crucial stage of prenatal development **(Figure 5.8C)**. However, the same quantification conducted on E18.5 spinal cord showed that reductions in primary cilia density did not persist to later prenatal timepoints **(Figure 5.8D)**.

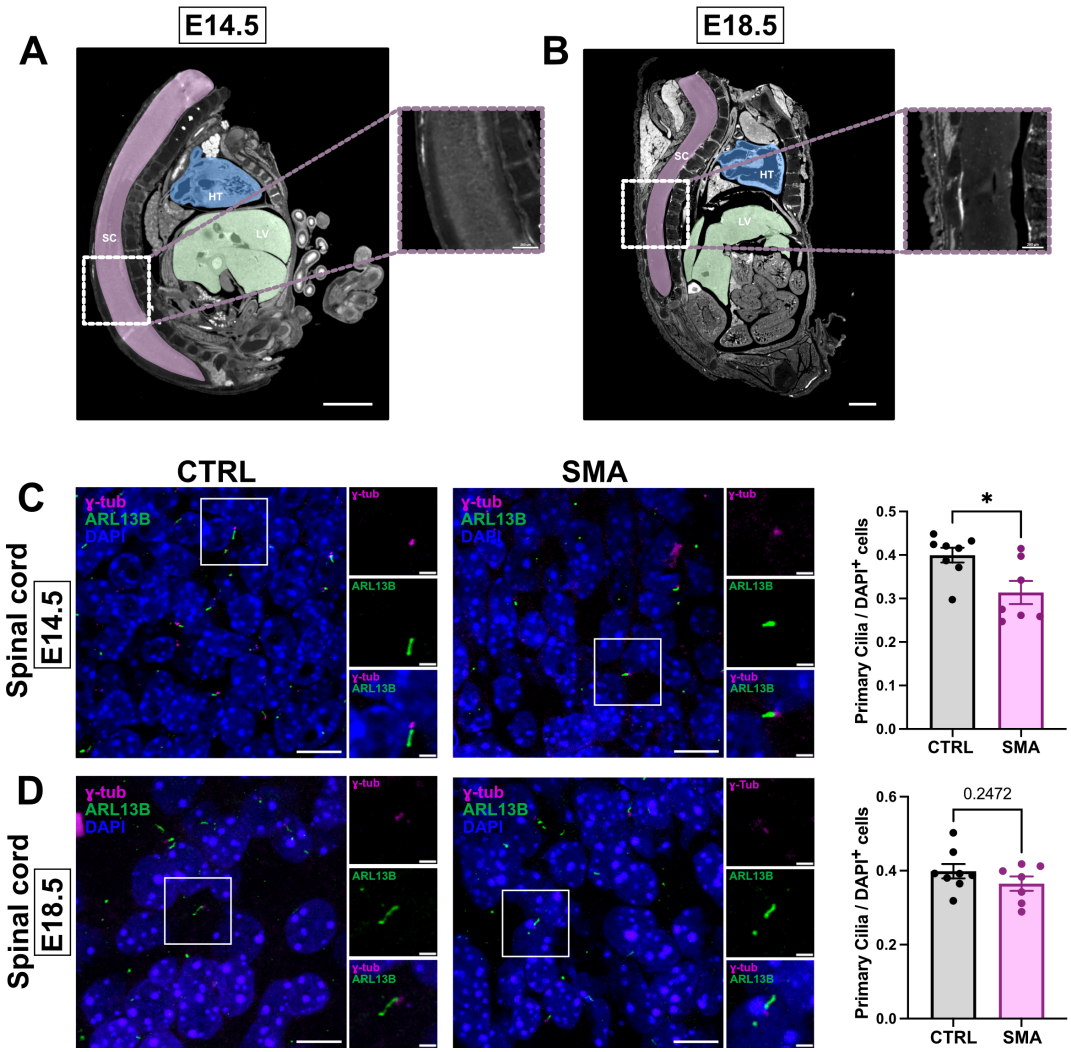

Figure 5.8 Reduced density of primary cilia in the SMA mouse embryonic spinal cord at E14.5, but not at E18.5. (A-B) Representative sagittal paraffin sections of E14.5 **(A)** and E18.5 **(B)** bodies of control embryos. The spinal cord (SC) is highlighted in pink, the heart (HT) in blue, and the liver (LV) in green. The white square indicates the region where primary cilia quantification was performed. Scale bar 1 mm, zoom 250 µm. **(C)** Primary cilia density quantification in the spinal cord of E14.5 identifies reduced primary cilia number in SMA compared to littermate controls. **(D)** No difference between genotypes observed in primary cilia density in E18.5 spinal cord. Sagittal paraffin sections, 10 µm thickness, scale bar 10 µm, zoom 2 µm. N = 8 embryos for control and 7 for SMA at E14.5 and E18.5. *p-value ≤ 0.05, unpaired t-test, scatter dot plot, mean with SEM. One datapoint corresponds to the average values from three sections per embryo.

5.3.2 *In vitro* primary cilia morphology investigation and therapeutic rescue

5.3.2.1 Establishing primary hippocampal cell cultures from Taiwanese mouse embryos

In the sections above I described how we identified reduced density of primary cilia in the CNS of SMA mice during prenatal development. As primary cilia are characterised by a specialised structure which is directly connected to their ability to function properly (Hoey et al., 2012), I decided to investigate primary cilia morphology to broaden understanding of their role in SMA pathogenesis. Therefore, to address primary cilia morphological features I established an *in vitro* model system. This system was chosen because it is more suitable for quantitative morphometric analysis than brain slice preparations. The rationale behind this can be attributed to the compacted tridimensional organisation of cells in brain tissues, which significantly complicates the reliable isolation of individual cilia. As in our lab we did not have the necessary equipment to develop the desired in vitro system, we started a collaboration with Prof. Mike Cousin's lab (UoE). This allowed us to establish primary cultures of hippocampal cells harvested from Taiwanese mouse embryos.

The protocol used to prepare primary hippocampal cell cultures was in accordance with the method previously described by Brewer et al. (Brewer et al., 1993), which is currently employed as the gold-standard in the Cousin lab **(Figure 5.9)**. In brief, we collected mouse embryos at E17.5 from pregnant dams and microdissected their hippocampi. Harvesting the hippocampus from embryos at this age allows for smooth dissection, as its anatomical structure is well-defined and easy to locate and isolate at this stage of development (Tomassoni-Ardori et al., 2020; Urban & Guillemot, 2014). The dissected hippocampi were then processed individually using papain, a widely used proteolytic enzyme derived from *Carica papaya* latex, allowing the dissociation of the tissue into single cells while preserving their integrity and viability. The obtained cells were placed in a tube containing cell culture medium and centrifuged to form a pellet containing the hippocampal cells. This was then resuspended in a specialised medium called supplemented neurobasal, which

is specifically designed for the growth and maintenance of neuronal cells. At this stage, the cells were ready to be plated onto coverslips. To achieve the desired cell density, which in this case was $6x10^4$ cells per well, a small sample of the cell suspension was added to a haemacytometer for cell counting. Thus, each embryo's hippocampus was individually plated onto poly-D-lysine coated coverslips in individual 6-well plates. After two days in an incubator at 37 °C and 5% CO_2, cytosine β-D-arabinofuranoside (Ara-C) was added to the culture to prevent glial proliferation. The primary hippocampal cultures were then kept in the incubator at 37 °C and 5% CO_2 until *day in vitro* 8 (DIV8), after which cells were fixed, and immunocytochemistry was performed for primary cilia investigation.

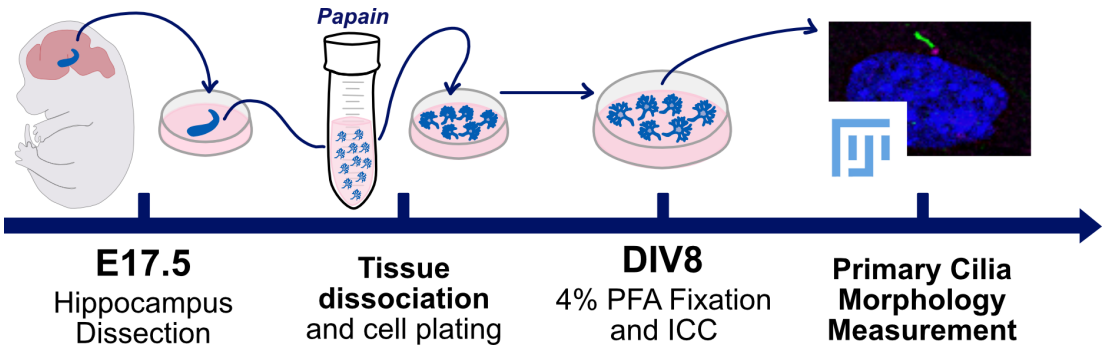

Figure 5.9 Establishment of primary hippocampal cell culture. Schematic illustrating the experimental design for primary hippocampal cell culture experiments. The hippocampus was dissected from control and SMA embryos collected at the age of E17.5. The individual hippocampi were then individually dissociated in cells using papain and plated on 6-well plates. After 8 days *in vitro*, cells were fixed using PFA at 4% and immunocytochemistry to visualise primary cilia was performed. Fiji/ImageJ software was then used to investigate primary cilia morphology.

5.3.2.2 Optimisation of protocol to quantify primary cilia morphology *in vitro*

Following the aforementioned protocol, we succeeded in establishing primary hippocampal cell cultures from Taiwanese mouse embryos. The aim of this result section is therefore to illustrate the optimisations steps I followed to be able to stain and visualise primary cilia in this new *in vitro* system.
As several prior studies have already demonstrated that hippocampal neurons possess primary cilia in culture and that they are visible starting from day *in vitro* 5 (DIV5) (Bansal et al., 2019; Berbari et al., 2007), I decided to grow the cell cultures until day *in vitro* 8 (DIV8) and then fix them with paraformaldehyde (PFA) at 4% prior to staining.

To start, I performed immunocytochemistry using the same protocol I optimised and used to label primary cilia *in vivo*. This involved an antigen retrieval step with the Tris-EDTA at pH 9 and anti-ARL13B and anti-ɣ-tubulin primary antibodies to stain primary cilia's axoneme and basal body, respectively. While I was able to visualise both structures, the axoneme appeared to be fragmented and not intact **(Figure 5.10A)**. As previously mentioned, antigen retrieval is essential for ensuring epitope exposure, and it proved to be advantageous when using the anti-ARL13B and anti-ɣ-tubulin primary antibodies *in vivo*. However, this technique may compromise cellular integrity (Ramos-Vara & Miller, 2014). To adopt a less aggressive approach, I decided to perform a second attempt at antigen retrieval by using a sodium citrate buffer at pH 6, a less alkaline solution. However, even with these conditions, the heat-induced epitope retrieval proved to be destructive, resulting in the axoneme structure being clearly compromised. **(Figure 5.10B)**.

Furthermore, to exclude the possibility that the disruption of the structure of the cilium was due to under- or over- fixation of the hippocampal cells, I applied PFA at 4% for 10 and 15 minutes and then proceeded with the immunocytochemistry protocol without performing antigen retrieval. The results of these two trials are illustrated in **figure 5.10 C and D**, which show

that the axoneme of the primary cilia is intact in both conditions. This suggests that the heat-induced antigen retrieval was damaging the cilia structure, not the fixation. Nevertheless, while skipping the antigen retrieval step was preserving the axoneme architecture, the basal body labelling was lost due to the low affinity of anti-ɣ-tubulin primary antibody with its antigen. In order to improve the chances for the correct binding of the antibody, I performed cell fixation with PFA at 4% for 15 minutes and increased the time of the blocking step from 1 hour to 2 hours. Blocking in immunocytochemistry reduces non-specific antibody bindings, enhancing the ability of the primary antibody to bind more accurately to its target antigen (Ramos-Vara & Miller, 2014). Unfortunately, this modification in the protocol was not sufficient to provide a clear and detectable signal of the basal body staining **(Figure 5.10E)**.

As the final aim was to explore primary cilia morphology, obtaining a good visualisation of both the axoneme and the basal body was necessary. Therefore, alongside with the increasing of the anti-ɣ-tubulin primary antibody concentration, I also lengthened the duration of the permeabilisation step. Permeabilisation is indeed pivotal in increasing cell membrane permeability, thus enabling the entry of the antibodies and their subsequent binding to intracellular antigens (Jamur & Oliver, 2010). As described in chapter 2 “Materials and Methods”, for this protocol I therefore employed a solution of 0.1% Triton X-100 in TBS and treated the cells for 20 minutes, instead of 5 minutes as done in previous trials. This adjustment, together with the concentration increase of the primary antibody, resulted in a successful immunocytochemistry where both the axoneme and the basal body were visible and detectable **(Figure 5.10F)**.

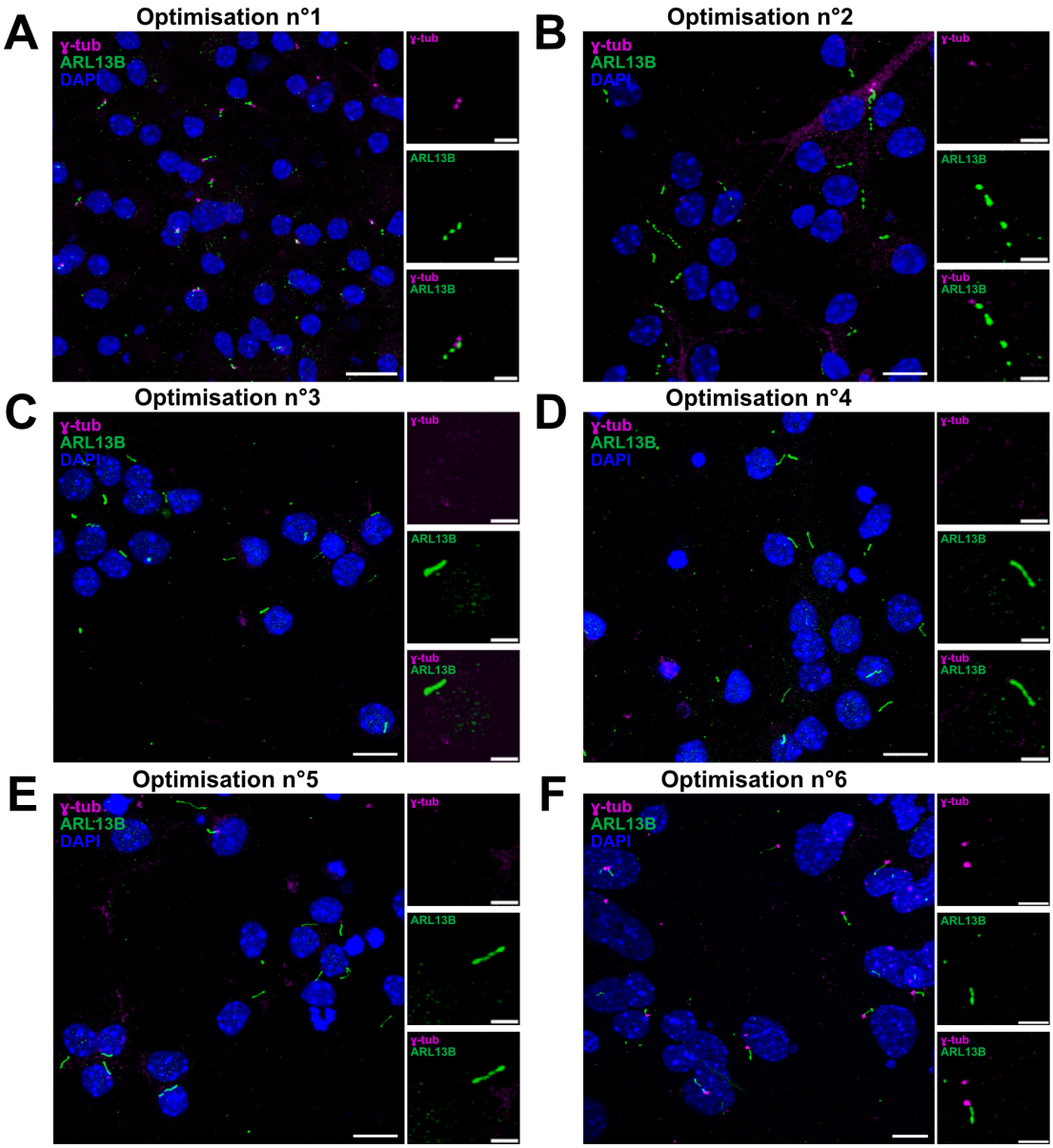

Figure 5.10 Immunocytochemistry optimisations to visualise primary cilia in primary hippocampal cell culture. (A-B) Fragmented axoneme labelled with ARL13B marker (green) due to heat-induced antigen retrieval using Tris-EDTA at pH 9 **(A)** and sodium citrate at pH 6 **(B)** buffers. Primary cilia basal body was labelled with anti-ɣ-tubulin primary antibody (magenta). **(C-D)** Fixation time optimisations using PFA at 4% for 10 **(C)** and 15 minutes **(D)**. Primary cilia axoneme is visible and labelled with ARL13B marker (green), while the basal body staining with anti-ɣ-tubulin primary antibody was unsuccessful. **(E)** Lengthening of the blocking step with donkey serum is not enough to successfully label the basal body with anti-ɣ-tubulin primary antibody. **(F)** After increasing anti-ɣ-tubulin primary antibody concentration and permeabilisation step time, both axoneme and basal body signals are detected using ARL13B (green) and ɣ-tubulin (magenta) markers.

5.3.2.3 Primary cilia length is reduced in SMA hippocampal cell culture

Optimising the immunocytochemistry protocol was key to observe the whole architecture of primary cilia expressed by hippocampal cells at DIV8. Specifically, I was able to properly visualise the axoneme and the basal body, labelled with anti-ARL13B and anti-ɣ-tubulin primary antibodies, respectively.

Using confocal microscopy at high magnification, I acquired a minimum of two images for each of the stained coverslips obtained from control and SMA embryos. As previously observed *in vivo*, an initial qualitative assessment revealed that hippocampal cells from both control and SMA embryos possessed a clear cilium structure defined by basal body and axoneme. However, many primary cilia in SMA preparations appeared to be shorter and more truncated than those from controls **(Figure 5.11 A and B)**. Using the Fiji/ImageJ software I therefore performed a quantitative morphological measurement of the axoneme length, spanning from the basal body to the tip of the cilium, of individual cilia.

To allow an accurate axoneme length measurement, I analysed a total of 863 primary cilia from 22 controls and 728 primary cilia from 19 SMA hippocampal culture preparations. This quantification showed a clear difference between the two genotypes: SMA hippocampal cells presented with primary cilia with a shorter axoneme compared to controls. To be precise, an average cilium length of 3.53 µm was observed in control cultures, while SMA cells demonstrated an average cilium length of 3.03 µm. **(Figure 5.11C)**. Consequently, I averaged the obtained values for each embryo, and this analysis revealed a significantly reduced cilium length in SMA hippocampal cell culture compared to littermate controls **(Figure 5.11D)**.

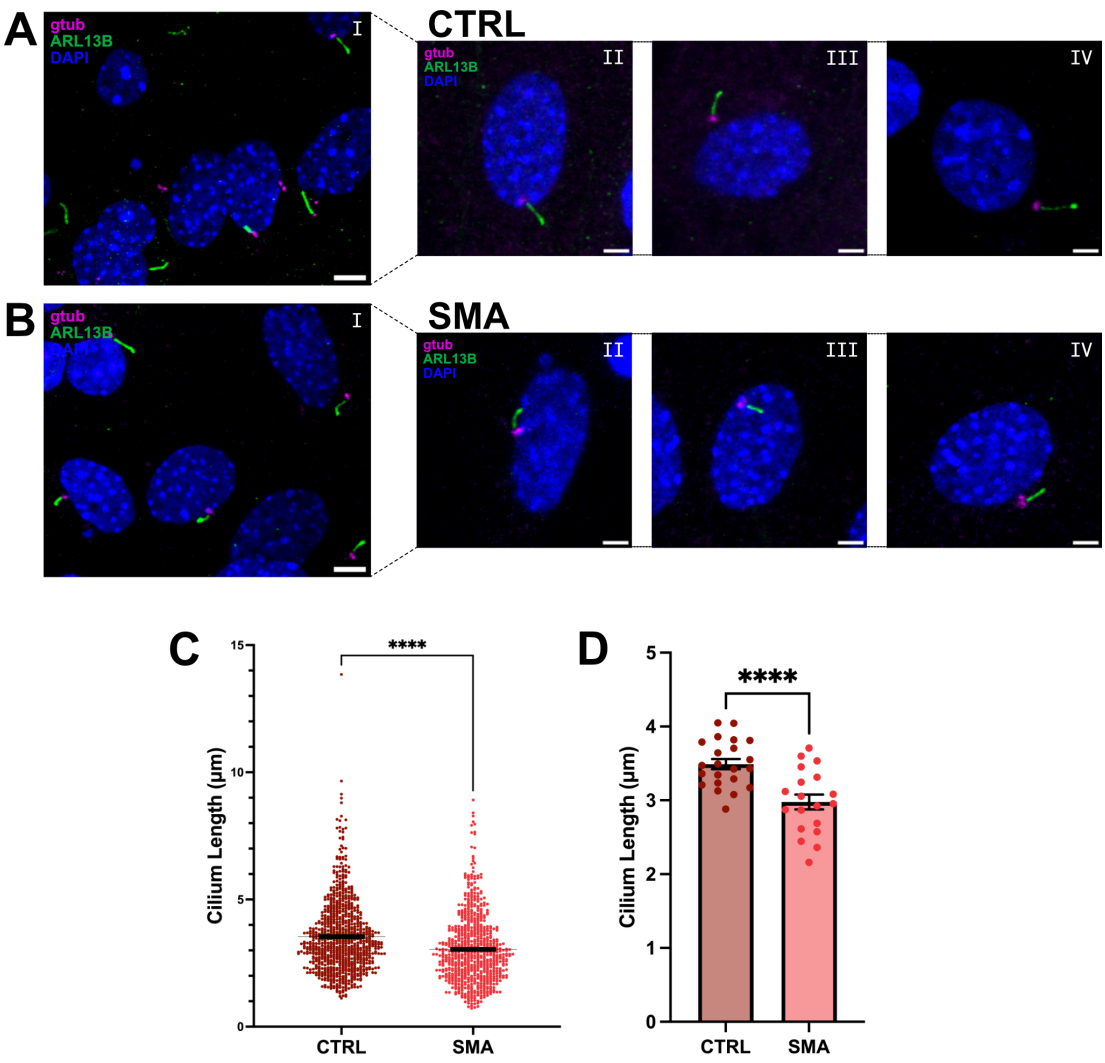

Figure 5.11 Primary length is reduced in SMA hippocampal cel culture. **(A-B)** Representative confocal images showing primary cilia length in hippocampal cell culture from **(A)** control and **(B)** SMA. Primary cilia were labelled with the ciliary markers ARL13B (axoneme, in green) and gamma tubulin (basal body, in magenta). **(C)** Primary cilia length individual measurement in hippocampal cell culture from control and SMA preparations. **(D)** Primary cilia length measurements averaged per embryo in hippocampal cell culture from control and SMA preparations. Scale bar lower magnification representative images (I) 5 µm. Scale bar micrographs (II, III, IV) 2 µm. ****p-value ≤ 0.001, unpaired t-test, scatter dot plot, mean with SEM. In panel (C), one datapoint corresponds to one individual cilium. In panel (D), one datapoint corresponds to one embryo. N= 22 embryos for control and N= 19 embryos for SMA.

5.3.2.4 Primary cilia morphological defects affect multiple cell types in SMA primary hippocampal cell culture

Considering the primary cilia phenotype observed in the *in vitro* system, I decided to assess whether cilia defects were specific to a particular cell type. To achieve this, using coverslip preparations remaining from control and SMA embryos, I performed an additional experiment of immunocytochemistry co-staining for NeuN, a neuron-specific nuclear protein, and GFAP, the glial fibrillary acidic protein found in astrocytes. This allowed me to representatively describe and compare different cell types present in our cultures. As expected based on the protocol followed for the culture preparation, the majority of cells were neurons, as evidenced by their positive reaction to the NeuN staining. However, the presence of astrocytes was also observed, although at a lower percentage **(Figure 5.12A)**.

Subsequently, to obtain an estimation of whether the observed primary cilia phenotype was cell-type specific, I performed the same quantification explained above, to measure the length of the axoneme from individual cilia. The investigation of ciliary length on both neurons and astrocytes revealed similar phenotypes, with shorter primary cilia axoneme in both cell types from SMA mice **(Figure 5.12 B and C)**. Although I acknowledge the limitation due to the small sample size, this descriptive result suggests that primary cilia dysregulation is likely to be impacting different cell types in the CNS in SMA.

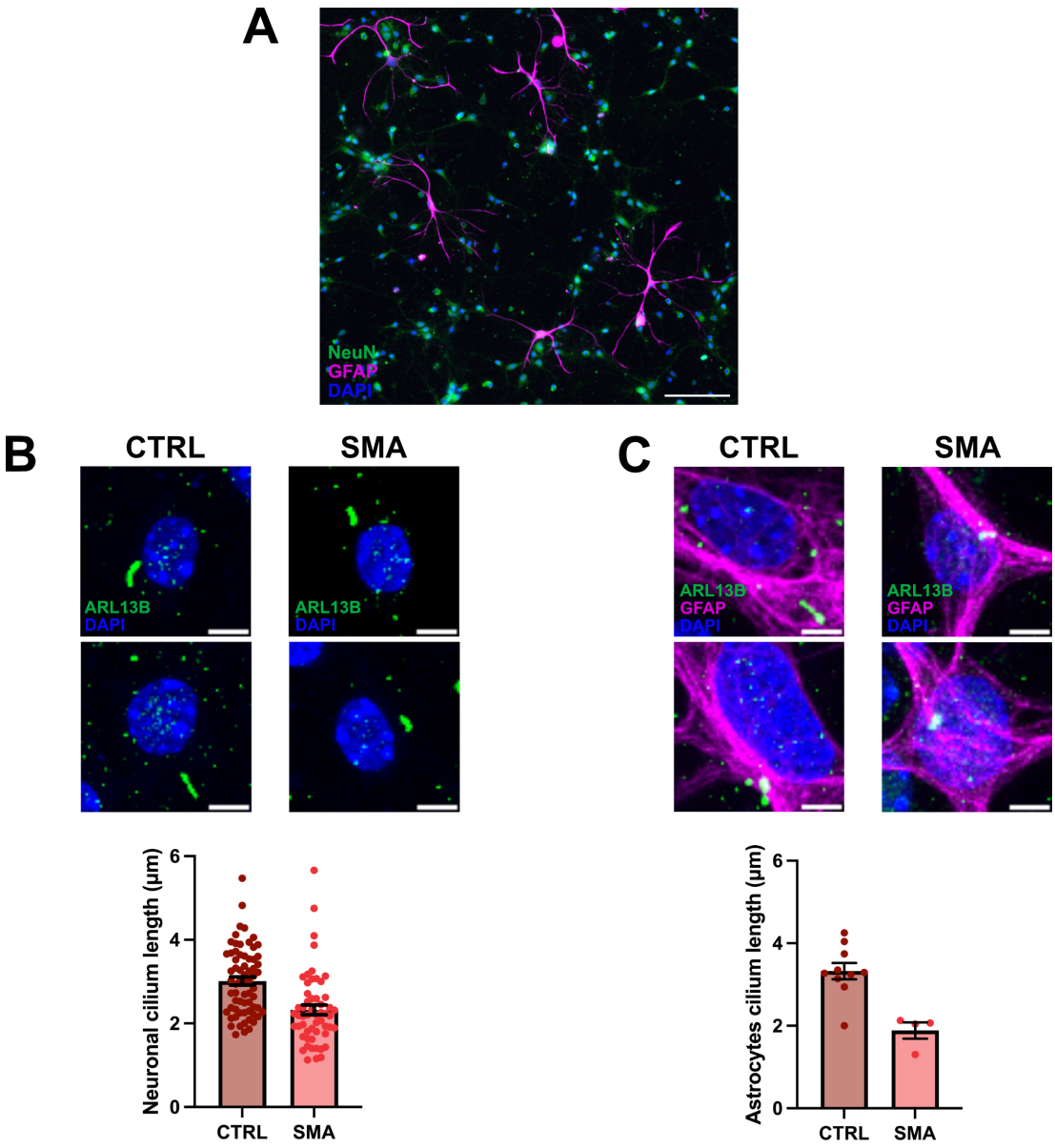

Figure 5.12 Hippocampal cell culture contains neurons and astrocytes, both expressing primary cilia. (A) Immunocytochemistry on hippocampal cell culture shows the presence of neurons, labelled with NeuN (green), and a smaller number of astrocytes, labelled with GFAP (magenta). Representative image at 20x magnification from a control sample. Scale bar 100 µm. **(B-C)** Confocal micrographs of primary cilia, labelled with ARL13B (green) expressed in **(B)** neurons (labelled with NeuN) and **(C)** astrocytes (labelled with GFAP), in control and SMA cell cultures. Length of primary cilia in neurons and astrocytes show the same trend where the axoneme is shorter in SMA than in controls, suggesting that the observed primary cilia phenotype is not cell-type specific. Scale bar = 5 µm. Each datapoint represents a single cilium (1 control and 1 SMA coverslip).

5.3.2.5 Risdiplam treatment in hippocampal cell cultures

So far in this chapter, I revealed primary cilia phenotypes in the CNS of SMA embryos. Given that *in vitro* systems are experimentally accessible with regards to applying drug treatments and testing therapeutic approaches (Seliger et al., 2022), I next wanted to establish whether the morphological defects observed in primary cilia in SMA were amenable to therapeutic intervention by restoring SMN levels. To achieve this, I used risdiplam, one of the three SMN-restoring therapies approved for use in human SMA patients (Baranello et al., 2021). Risdiplam is an orally bioavailable molecule which distributes systemically. Its mechanism of action targets the splicing of *SMN2* pre-mRNA, which under physiological conditions produces low levels of functional SMN protein, not enough to compensate for the loss of the *SMN1* gene (Ratni et al., 2018). Risdiplam acts as an *SMN2* splicing modifier, facilitating the inclusion of exon 7 in the mature transcript and enabling the production of sufficient functional (full-length) SMN protein (Ratni et al., 2021). To investigate whether risdiplam treatment could rescue the morphology primary cilia phenotype observed *in vitro*, I treated hippocampal cells for 72h starting from day *in vitro* 5 (DIV5) following a methodology previously reported as successful in SMA patient-derived fibroblasts (Signoria et al., 2024) **(Figure 5.13A)**. More specifically, after the hippocampal dissection from SMA and control Taiwanese mouse embryos and the cell culture preparation described above, three wells of each 6-well plate (from single embryo) were treated with risdiplam, while the remaining three wells received an equivalent quantity of sterile deionised water as a control **(Figure 5.13B)**. To maintain a standardised approach and obtain consistent results, at DIV8 I performed immunocytochemistry to investigate primary cilia. In addition, to analyse and verify SMN expression levels I collected the total RNA from the available preparations.

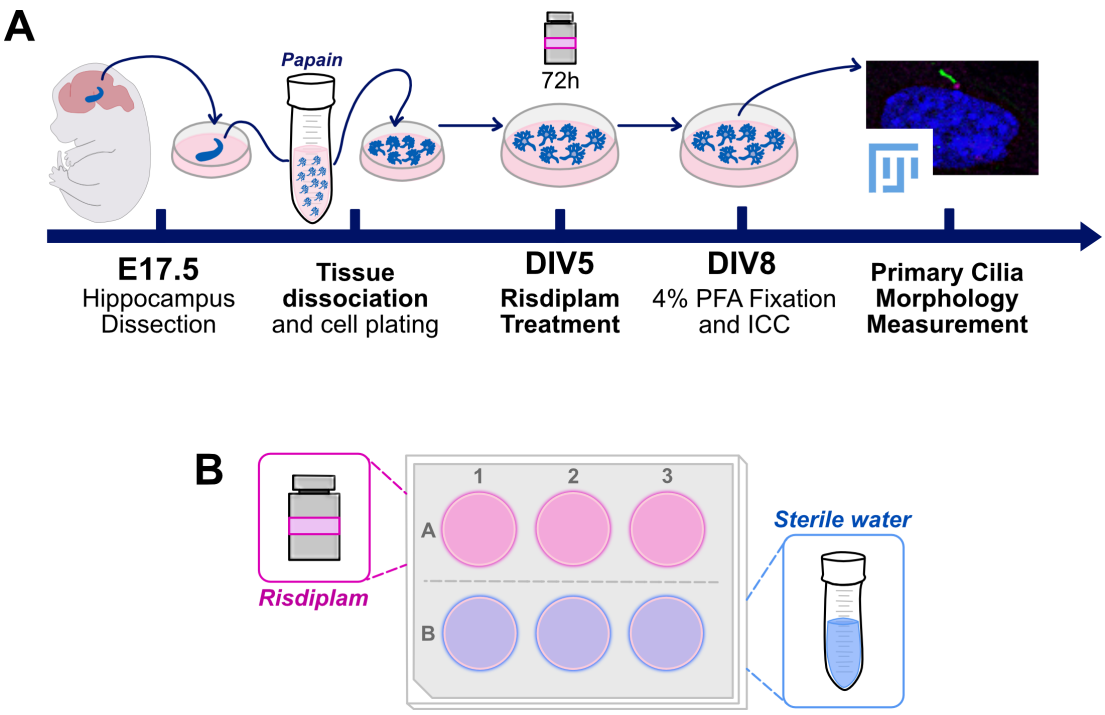

Figure 5.13 Therapeutic treatment of hippocampal cells *in vitro* using risdiplam. (A) Schematic illustrating the experimental design for therapeutic intervention on primary hippocampal cell culture. The hippocampus was dissected from control and SMA embryos collected at the age of E17.5. The individual hippocampi were then individually dissociated in cells using papain and plated on 6-well plates. Starting from day *in vitro* 5 (DIV5), cells were treated with 0.5 µM risdiplam for 72 hours until DIV8, when cells were fixed using PFA at 4% and immunocytochemistry to visualise primary cilia was performed. Fiji/ImageJ software was then used to investigate primary cilia morphology. **(B)** Schematic overview to facilitate *in vitro* risdiplam treatment methodology. For each 6-well plate, wells A1, A2 and A3 were daily treated with risdiplam; while wells B1, B2 and B3 were given an equivalent quantity of sterile deionised water to serve as a control.

5.3.2.6 Risdiplam treatment rescues SMN-dependent morphological defects in primary cilia in hippocampal cell culture

After revealing that the axoneme of primary cilia is shorter in SMA hippocampal neurons, here I wanted to assess whether these defects were amenable by increasing SMN protein levels through risdiplam treatment. To achieve this, I added the risdiplam drug to the cell media daily for three days, and then performed immunocytochemistry, using ARL13B and ɣ-tubulin markers to label the primary cilia axoneme and basal body, respectively.

To exclude the possibility that risdiplam had any effect on control hippocampal neurons, I first conducted a preliminary pilot study in which the analysis of primary cilia length in untreated and treated control cells revealed no difference. Consequently, to investigate the effect of risdiplam on the cilia phenotype in SMA, I proceeded with the measurement of the length of the axoneme of 373 primary cilia from 12 SMA-Risdiplam treated cell preparations and I compared the results obtained with the ones observed from controls and SMA untreated (or vehicle) samples previously reported in this chapter **(Figure 5.14 A, B and C)**. Strikingly, risdiplam treatment rescued primary cilia defects in the SMA cells, restoring cilia length to be indistinguishable from those observed in healthy controls **(Figure 5.14D)**.

Furthermore, to assess whether this rescue depended on an increase in SMN levels as a result of risdiplam being effective in modifying *SMN2* splicing by enhancing exon 7 inclusion, we designed quantitative real-time PCR primers specifically to quantify SMN transcripts lacking exon 7 (delta7-SMN) and full-length SMN transcripts (Zhou et al., 2013). As expected, Risdiplam treatment reduced *delta7-SMN* levels and restored full-length *SMN* levels compared to vehicle-treated SMA preparations **(Figure 5.14 E and F)**.

Taken together, these results revealed that restoring SMN levels *in vitro* is sufficient to reverse SMA-driven primary cilia defects and therefore confirms a critical role for SMN in regulating primary cilia during development.

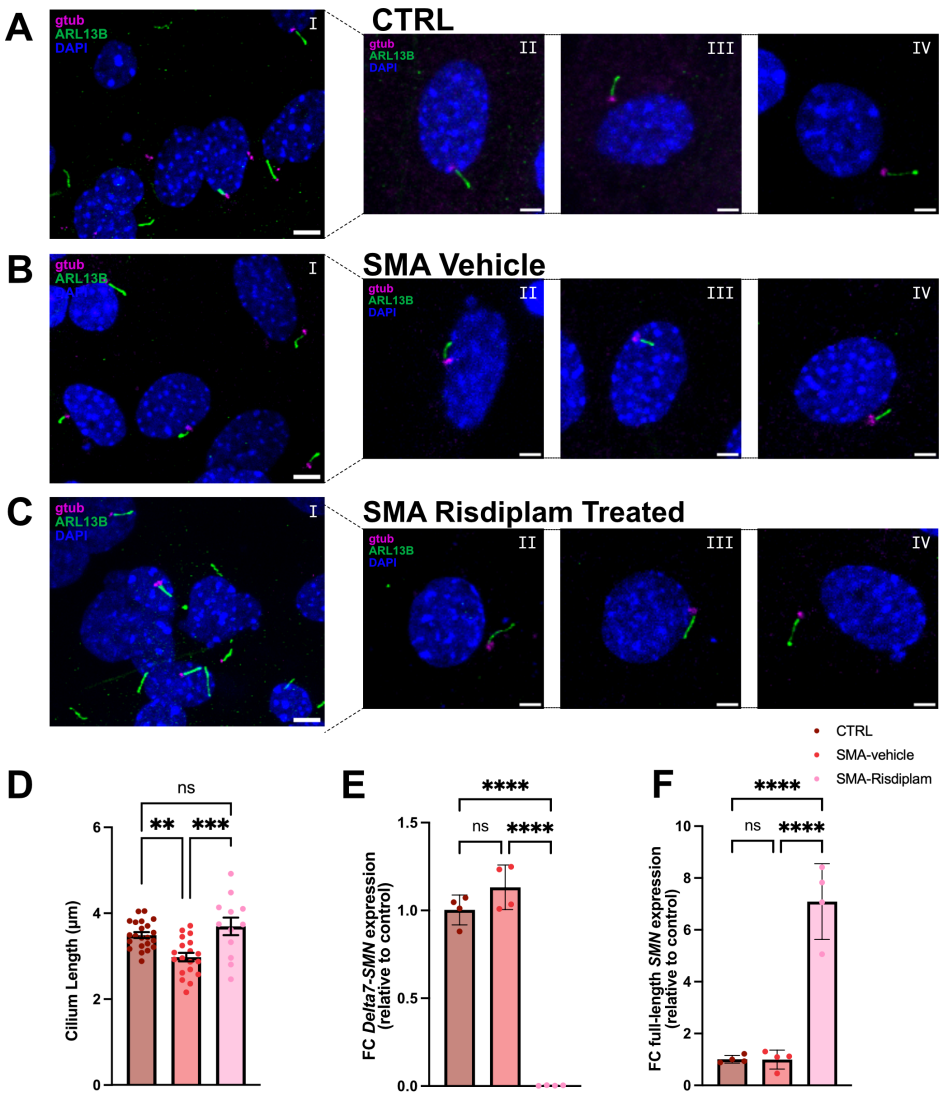

Figure 5.14 Reduced primary cilia length in SMA is restored following Risdiplam treatment in primary hippocampal neurons. (A-C) Representative confocal images showing primary cilia length in hippocampal cell culture from control **(A)**, SMA vehicle-treated **(B)** and SMA Risdiplam-treated **(C)** preparations. Primary cilia were labelled with the ciliary markers ARL13B (axoneme, in green) and ɣ-tubulin (basal body, in magenta). Scale bar of lower magnification representative images (I) 5 µm. Scale bar micrographs (II, III, IV) 2 µm. **(D)** Primary cilia length measurement and quantification in hippocampal cell culture from control, SMA vehicle-treated and SMA Risdiplam-treated preparations. **p-value ≤ 0.01, ***p-value ≤ 0.001, one-way ANOVA, scatter dot plot, mean with SEM. One datapoint corresponds to one embryo. N= 22 embryos for control, 19 for SMA vehicle-treated and 12 for SMA Risdiplam-treated. Values from control and SMA-vehicle were replotted from figure 5.10D. **(E-F)** Full-length and delta7human-SMN levels were quantified using real-time PCR. Bar charts show full-length SMN was increased, corresponding with decreased delta 7 SMN, in SMA hippocampal neurons treated with Risdiplam. ****p-value < 0.0001, one-way ANOVA, scatter dot plot, mean with SD. One datapoint corresponds to one embryo. N= 4 embryos for each group. FC= fold change.

5.4 Discussion

In this chapter, I focused on the investigation of primary cilia biology and morphology in the CNS of Taiwanese SMA mouse embryos. Using both *in vivo* and *in vitro* systems, I showed a widespread disruption of these important sensory cellular organelles potentially revealing neurodevelopmental defects in SMA.

Primary cilia are small cellular organelles that play a major role in ensuring the correct development of our entire organism and, remarkably, extensive evidence highlight their key implication in neurodevelopmental disorders (Mill et al., 2023; Serpieri et al., 2025; Youn & Han, 2018). Here, I demonstrated that primary cilia are significantly reduced in number in both the hippocampus and the spinal cord of SMA mouse embryos during embryonic development. However, primary cilia defects were not conserved in the postnatal brain. Similarly, I observed defects in the density of ciliated cells in the spinal cord only at E14.5, but not at later stages of development. Although it could be speculated that primary cilia are more vulnerable to low SMN levels in the brain than in the spinal cord, this difference may also be explained by the distinct developmental timelines of these two structures. Hippocampal field patterning begins early in embryogenesis, as early as E10.5, but the neurogenesis that leads to its complete maturation extends postnatally (Grove, 1999; Urban & Guillemot, 2014). In contrast, the regional patterning and cell identity in the spinal cord is established by E9.5, and the transition from neural progenitor cells to postmitotic neurons largely complete embryonically (Alaynick et al., 2011; Chen et al., 2017).

An additional observation that emerges from these data is the distinct proportion of ciliated cells in the two tissues throughout development. Specifically, the percentage of ciliated cells in the hippocampus of control embryos is approximately 25% of the total number of cells, whereas in the postnatal hippocampus this proportion increases to nearly 40%. These results are consistent with previous reports in the literature demonstrating that primary cilia maturation peaks during the postnatal development in mice (around P14-

P30) (Ishii et al., 2021; Lee et al., 2020). Moreover, prior research has shown that primary cilia are retained on most postmitotic neuronal cells at all postnatal stages, where they continue to coordinate neuromodulatory functions throughout lifespan (Tereshko et al., 2022). Similarly, the data presented in this chapter reveal that approximately 40% of cells in the spinal cord region of interest from control embryos are ciliated, a percentage that is higher compared to what observed in the embryonic hippocampus of control mice. Overall, these findings are in line with previous studies demonstrating that the presence of primary cilia varies across different regions of the CNS (Zhai et al., 2025).

Furthermore, with this study I explored the correlation between primary cilia function and structure. To reliably investigate primary cilia morphology, I established *in vitro* system of embryonic hippocampal cells and revealed structural defects in the axoneme of primary cilia in SMA embryos. This observation is in line to what has been reported in many ciliopathies and neurodevelopmental disorders, where primary cilia are often found to be fewer in number and shorter in length, as observed in some patients suffering from Bardet–Biedl and Joubert syndromes (Hardee et al., 2017; Hernandez-Hernandez et al., 2013).

Most importantly, I demonstrated that primary cilia phenotypes are driven directly by SMN deficiency, being amenable to rescue following therapeutic intervention *in vitro* using risdiplam to restore SMN levels. Risdiplam is a small-molecule drug that was approved in 2021 for treating SMA patients. It works by targeting the splicing of the centromeric *SMN2* gene to increase overall levels of the functional SMN protein (Ratni et al., 2021). Excitingly, risdiplam was successful in increasing SMN levels in hippocampal cell culture leading to a significant rescue of primary cilia morphology back to control levels. This result highlights the correlation between SMN deficiency and primary cilia defects, highlighting the importance of studying primary cilia in the context of SMA pathogenesis.

In light of this, the current findings propose a new approach to the study of the developmental manifestations of SMA, focusing on the disruption of primary cilia in the prenatal CNS and its impact on social behaviour and cognition. Numerous recent patient-based studies have reported deficits in attention, memory and language, as well as autism-like symptoms such as difficulties in social communication and interaction, in SMA patients (Baranello et al., 2024; Masson et al., 2021). In addition, postnatal investigations in both SMA mouse models and human patients have already described hippocampus disruptions, characterised by reduced neurogenesis and structural abnormalities (Mugisha et al., 2023; Wishart et al., 2010).

Primary cilia play a key role in the early stages of brain development, particularly in the formation of the hippocampus, regulating the proliferation, migration and signalling of neural progenitor cells. (Amador-Arjona et al., 2011). Consequently, patients with ciliopathies, where primary cilia disruption occurs in the brain, have been reported to have hippocampal dysgenesis and volume loss alongside learning and memory deficits (Baker et al., 2011; Bennouna-Greene et al., 2011; Berbari et al., 2014; Rhee et al., 2016). Thus, as the neurodevelopmental symptoms recently reported in some SMA patients resemble those observed in ciliopathies, this study proposes that primary cilia defects in the CNS during prenatal development may be a novel cellular phenotype contributing to these symptoms.

To further address this hypothesis, the next chapter of this thesis will explore the biological consequences of risdiplam treatment on hippocampal primary cilia *in vivo*. This will enable me to investigate the impact of prenatal therapeutic intervention on SMA, as well as its subsequent effects on the primary cilia phenotype observed in CNS of Taiwanese mouse embryos.

Chapter 6: **In utero SMN-replacement therapy increases SMN protein levels in the brain of SMA mouse embryos and rescues primary cilia phenotypes**

6.1 Introduction

Before the introduction of therapeutic interventions, SMA patients were mostly supported by palliative care, in the most severe cases, or by pulmonary and nutritional support and physical therapy for patients with milder symptoms (McPheron & Felker, 2024). Since 2016, three gene-targeted disease modifying therapies have been approved to treat SMA patients, each of them with a different mechanism of action, but all designed to enhance full-length SMN protein production (Chaytow et al., 2021).

The therapy employed and discussed in this thesis is the one that was approved most recently: risdiplam, or Evrysdi in its commercial name. Risdiplam is a small molecule that acts as a splicing modulator directly binding to the *SMN2* pre-mRNA promoting exon 7 inclusion and thus, full-length SMN protein production (Sivaramakrishnan et al., 2017). Thanks to a daily oral administration, either as oral solution or tablet, risdiplam allows for systemic treatment, efficiently distributing to the CNS and peripheral organs (Poirier et al., 2018). Originally approved for administration to SMA patients aged over two months and presenting with one to four copies of *SMN2*, the use of risdiplam has now been extended for the treatment of presymptomatic babies under two months old (Kakazu et al., 2021; Roche, 2022).

Regardless of the undeniable benefits that these treatments are providing to SMA patients, it has become clear that they do not yet offer a cure. Specifically, it is now widely accepted within the scientific community that there may be a specific time window during which administering the treatment could lead to significant benefits, and that this time window corresponds with the very early

stages of the disease (Chaytow et al., 2024). Specifically, it has been demonstrated that in physiological conditions SMN protein levels are higher prenatally, in particular in the second and third trimester of gestation, and then undergo a rapid decrease after birth (Motyl et al., 2020; Ramos et al., 2019). For this reason, more and more preclinical and clinical studies have recently been exploring a prenatal therapeutic approach to treating the most severe forms of SMA (Borges et al., 2025; Richard S. Finkel et al., 2025; Kong et al., 2021).

As with this work I unveiled a primary ciliopathy phenotype manifesting in the SMA central nervous system during the embryonic stages of the disease, I wanted to explore whether the prenatal delivery of risdiplam could intervene and correct these developmental perturbations. Thanks to a close collaboration with Dr. Yu-Ting Huang (UoE), I was able to perform an *in utero* transplacental treatment on Taiwanese mice embryos and demonstrate that our approach can restore SMN protein levels and rescue primary cilia defects in the prenatal brain of SMA mice treated with risdiplam.

6.2 Aim

The aim of this chapter is to explore the impact of prenatal therapeutic intervention on the primary cilia phenotype observed in the brain of SMA mouse embryos. To achieve this, we established and validated an *in utero* transplacental treatment approach using an existing SMN-restoring therapy, risdiplam. First, this allowed us to investigate the efficacy of our method in restoring SMN protein levels in the brain SMA mouse embryos. Second, it enabled us to examine the subsequent impact on prenatal primary cilia phenotypes.

6.3 Results

6.3.1 Efficacy and safety of *in utero* risdiplam treatment approach

Given the prenatal nature of the primary cilia defects observed in the hippocampus of Taiwanese mouse embryos, and the rescue outcomes of risdiplam on hippocampal cell cultures, we decided to explore the effects the SMN-restoring therapy in our *in vivo* model when administered *in utero*.

Similarly to what previously described in cell culture experiments, for the *in vivo* treatment we used risdiplam, purchased from Cayman Chemical company (Ratni et al., 2018). For the correct establishment of the therapeutic protocol, we performed an initial series of pilot experiments, where we treated one pregnant dam with risdiplam during early gestation. To determine the most effective dosage, we followed the approach previously published by Ratni *et al.*, who tested a series drug concentration from 0.3 - 10 mg/kg for oral therapeutic intervention in mouse models of SMA, and defined that both methodologies were safe, as well as efficient in distributing risdiplam to the CNS and peripheral organs (Poirier et al., 2018; Ratni et al., 2018). Moreover, previous work in the lab performed by Dr. Yu-Ting Huang demonstrated that a four-day course oral treatment with 10 mg/kg of risdiplam was effective in restoring SMN protein levels in the spinal cord of SMA Taiwanese mouse embryos. Based on this evidence, we designed an optimised therapeutic approach that would enable us to administer a lower dose of the drug while still ensuring its safety and efficacy.

Thus, in our pilot experimental design, the pregnant dam was treated with 5 mg/kg of risdiplam given by oral gavage (PO) for five consecutive days, starting from E10.5. To then assess the transplacental passage efficacy of risdiplam, we collected the embryos at E15.5, when brains were microdissected to allow quantification of SMN protein levels using western blot, following the method previously established in our lab (E. J. N. Groen et al., 2018) **(Figure 6.1A)**.

In total, we analysed SMN protein levels from three untreated controls and SMA embryos and one control and four SMA embryos treated with risdiplam **(Figure 6.1B)**. After normalising each value to the total protein quantity for

each sample obtained from the total protein stain, the quantification revealed that the treatment approach was sufficient to generate a 1.9-fold increase in SMN levels in the brain of treated SMA embryos compared to SMA embryos that did not undergo any therapeutic intervention **(Figure 6.1C)**.

Importantly, we observed that the oral treatment with risdiplam was well tolerated by the pregnant dam, as well as the embryos, with no adverse events or phenotypes.

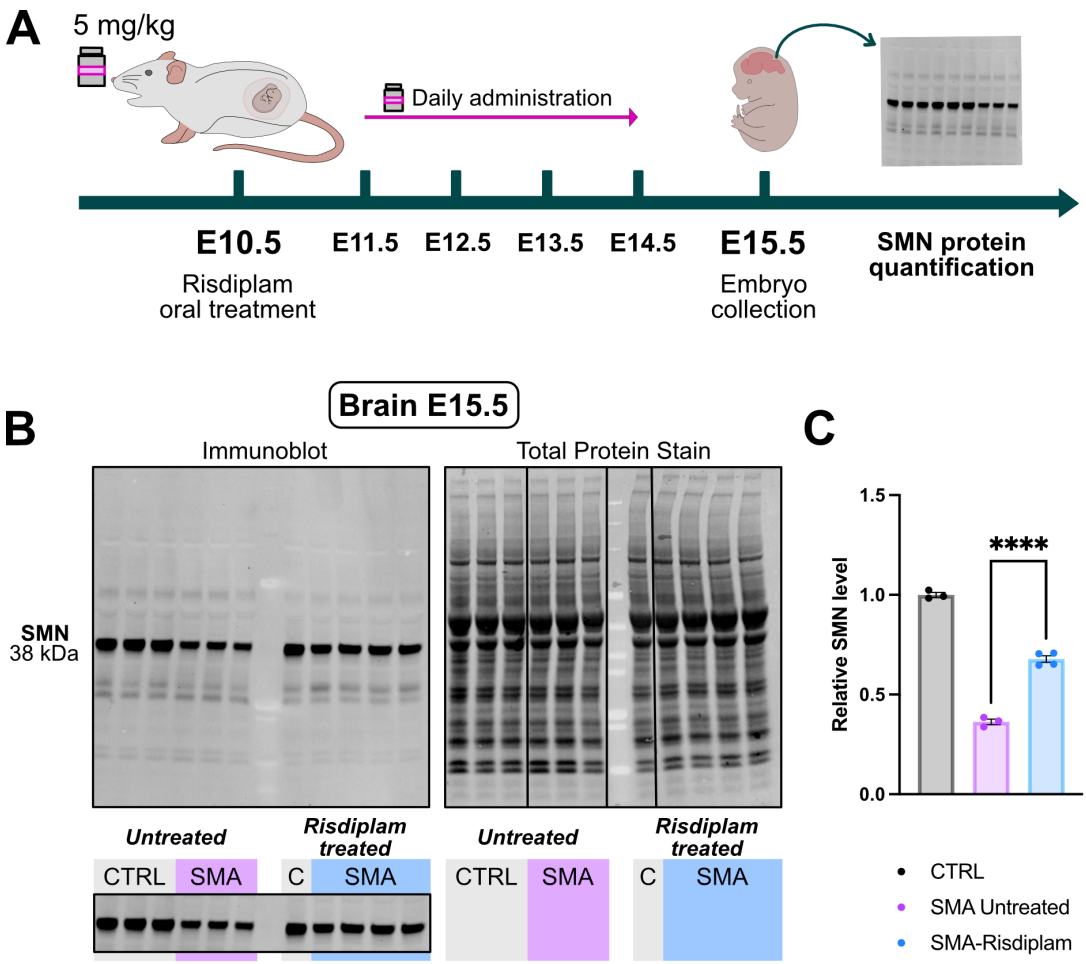

Figure 6.1 *In utero* risdiplam administration to the pregnant dam increases SMN protein levels in SMA embryos. (A) Schematic showing experimental design for short duration, in utero SMN replacement therapy via oral administration to the pregnant dam at 5 mg/kg dose. After five consecutive days of oral gavage, the embryos were collected at E15.5 and SMN protein levels were assessed in the brain using western blot. **(B)** Full immunoblot from E15.5 brain tissues and total protein stain used to normalise total quantity of the protein for each sample. Each lane represents one embryo. N=3 for untreated control and SMA, and N=1 and 4 for risdiplam-treated control and SMA, respectively. **(C)** Quantification of relative SMN levels from (B). SMN protein quantification values for the untreated control sample were not included in the statistical analysis as N=1. Scatter dot plot with mean with SEM. **p-value ≤ 0.01, one-way ANOVA. One datapoint corresponds to one embryo. N=3 embryos for control and SMA, N=4 embryos for risdiplam-treated SMA.

6.3.2 *In utero* risdiplam treatment administered in early gestation

The success of the pilot transplacental experiments confirmed the safety and efficacy of our *in utero* transplacental treatment approach. Therefore, we proceeded to perform a full set of experiments to be able to assess impacts of treatment on primary cilia defects at the key developmental stage of interest: E14.5. To achieve this, we treated three pregnant dams with risdiplam 5 mg/kg for five consecutive days via oral delivery, this time starting from gestational day E9.5 **(Figure 6.2A)**. Following the therapeutic approach described above, we collected embryos at E14.5 after daily pharmacological administration and microdissected the brain tissue. Half of the tissue was fixed and prepared for immunohistochemistry, while the rest was frozen and prepared for protein extraction.

Prior to primary cilia investigation, we wanted to re-confirm that risdiplam administration had increased SMN protein levels, even when administration started at an earlier stage of gestation. We therefore performed western blot for SMN protein quantification in the E14.5 brain from three untreated controls and SMA, and six SMA embryos treated with risdiplam *in utero* **(Figure 6.2B)**. After total protein quantity normalisation, the western blot analysis confirmed a significant increase in the levels of SMN protein in the brain of treated SMA embryos compared to untreated embryos **(Figure 6.2C)**. This result was in accordance and comparable to the increase effect of SMN protein observed in the pilot experiment described above. Notably, as the pilot data indicated that transplacental treatment with risdiplam does not affect SMN protein levels in untreated control embryos, this group was not included in subsequent experimental design.

It is worth mentioning that the early therapeutic approach adopted at E9.5 was well tolerated by both the pregnant dams and the embryos, and no harmful events or abnormalities were reported. As we established the transplacental efficacy of risdiplam in restoring SMN protein levels in the embryonic SMA brain when administered in the early stages of gestation, we can now proceed to evaluate the biological consequences of this increase.

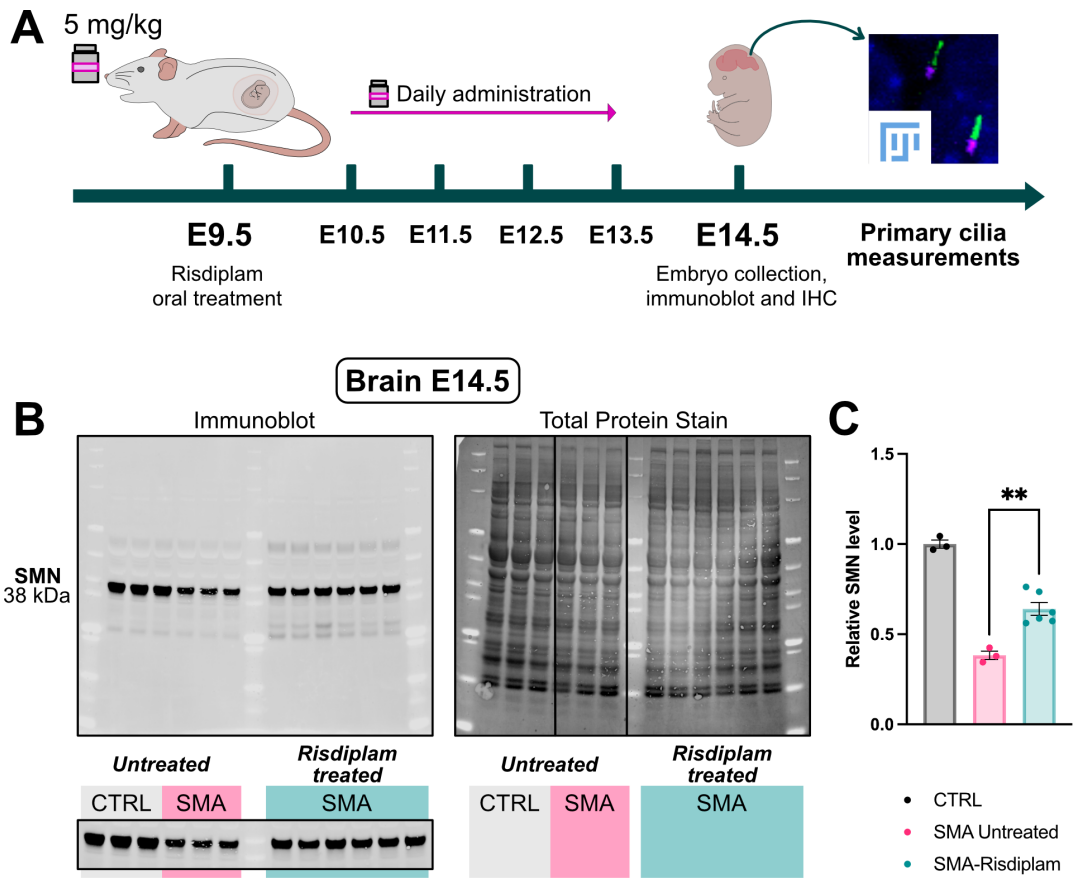

Figure 6.2 Early gestation *in utero* risdiplam administration increases SMN protein levels in SMA embryos. (A) Schematic showing experimental design optimised for early gestation *in utero* SMN replacement therapy via oral administration to the pregnant dam at 5 mg/kg dose. After five consecutive days of oral gavage, the embryos were collected at E14.5 and the brain tissue were microdissected to allow primary cilia investigation and SMN protein quantification. **(B)** Immunoblot and total protein stain of SMN levels from brain tissues from control, SMA and risdiplam-treated SMA embryos at E14.5. Each lane represents one embryo. **(C)** Quantification of relative SMN protein levels analysed from (B). Scatter dot plot with mean with SEM. **p-value ≤ 0.01, one-way ANOVA. One datapoint corresponds to one embryo. N=3 for untreated control and SMA, and N=6 for Risdiplam-treated SMA.

6.3.3 Primary cilia defects are rescued in the embryonic SMA brain following risdiplam prenatal transplacental delivery

In the previous chapter of this thesis, I revealed SMN-dependent defects of primary cilia occurring in the hippocampus of SMA mouse embryos at E14.5. As we designed a safe *in utero* therapeutic approach able to efficiently restore SMN protein levels prenatally, here I investigate whether primary cilia disruption could be rescued by early gestation delivery of risdiplam.

After treating pregnant dams with risdiplam via oral delivery for five consecutive days starting from E9.5, I collected the embryos once reached the developmental stage of interest (E14.5). At this point, I microdissected the brain tissue, fixed with paraformaldehyde at 4% and embedded in paraffin for microtome sectioning. In order to obtain data from SMA samples treated with risdiplam that were directly comparable with that obtained from untreated samples, as described in chapter 5, I adopted a consistent approach throughout the experiment, from tissue preparation and sectioning to immunohistochemistry and image analysis. Briefly, the wax blocks containing the dissected brains from E14.5 SMA embryos treated with risdiplam were sectioned at 10 μm thickness in coronal plane using a microtome, to clearly visualise the hippocampus. The sections obtained were subsequently stained using the previously described immunohistochemistry protocol, which involved ARL13 and ɣ-tubulin markers to label the axoneme and the basal body of primary cilia, respectively. After the acquisition of three consecutive sections from each embryo using a confocal microscope at high magnification, I performed primary cilia density quantification in the area of interest, the hippocampus, specifically in the region corresponding to the dentate gyrus.

The presence of primary cilia in the embryonic brain from controls, SMA untreated and SMA treated with risdiplam is shown in **figure 6.3 A**, **B** and **C**, identifiable by the axoneme, in green, and the basal body, in magenta. Strikingly, after the normalisation of the total number of cilia to the total number of nuclei labelled with DAPI, the quantitative analysis of cilia density showed a

two-fold increase in primary cilia number in the hippocampus of SMA embryos treated *in utero* with risdiplam compared to untreated SMA embryos, restoring them to levels observed in littermate controls **(Figure 6.3D)**.

Taken together, these results revealed that the prenatal transplacental delivery of SMN-restoring therapeutics was sufficient to rescue primary ciliopathy phenotypes in SMA mice *in vivo*.

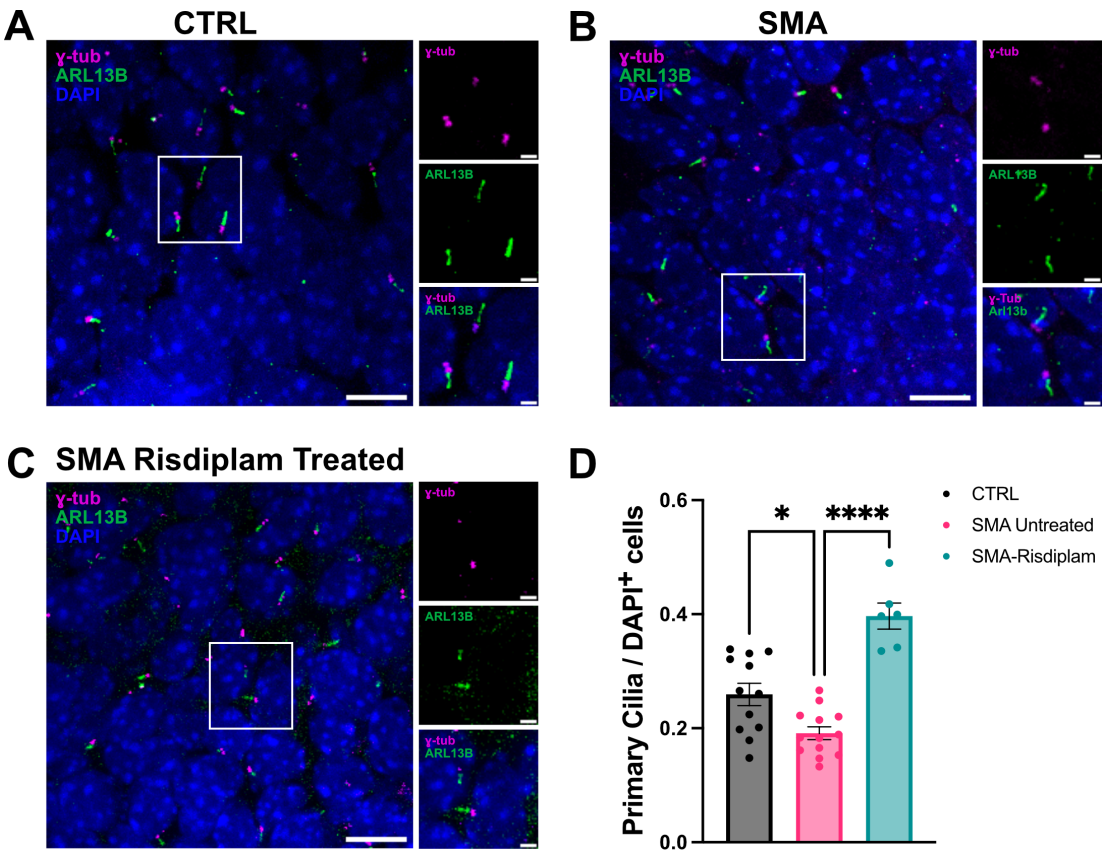

Figure 6.3 Primary cilia density is rescued in the hippocampus of SMA mouse embryos following *in utero* risdiplam treatment. (A-C) Representative confocal micrographs showing primary cilia in the hippocampus of E14.5 from control **(A)**, SMA untreated **(B)** and SMA risdiplam-treated **(C)** embryos. Primary cilia were labelled with the ciliary markers ARL13B (axoneme, in green) and ɣ-TUBULIN (basal body, in magenta). Scale bar 10 µm, zoom 2 µm. Coronal paraffin sections, 10 µm thickness. **(D)** Quantification bar chart of primary cilia density in the hippocampus of control, SMA untreated and SMA risdiplam-treated embryos. Scatter dot plot with mean with SEM. One datapoint corresponds to one embryo. N = 12 embryos for control, 13 for SMA untreated and 6 for SMA risdiplam-treated. Data for control and untreated SMA are replotted from data presented in chapter 5 of this thesis (Figure 5.5C). *p-value ≤ 0.05, ****p-value ≤ 0.0001, one-way ANOVA.

6.4 Discussion

In utero therapeutic intervention to treat SMA is a topic that has been the focus of considerable discussion among researchers and clinicians in recent months (Borges et al., 2025; Richard S. Finkel et al., 2025; Tizzano et al., 2025).
In this study, I have demonstrated the safety and the efficacy of prenatal transplacental delivery of risdiplam in restoring SMN protein levels in the brain of SMA embryos and consequently, in rescuing the primary ciliopathy phenotype.

To date, a number of studies have explored *in utero* SMN replacement using antisense oligonucleotides, viral vectors or small molecules in preclinical mouse models of SMA (Borges et al., 2025; Butchbach et al., 2010; Chaytow et al., 2024; Hua et al., 2010; Kong et al., 2021; Rashnonejad et al., 2019). While the aforementioned studies concentrated on the neuromuscular aspects of the disease, the results I presented in this chapter not only reinforce the notion that an early therapeutic approach may be significantly beneficial for SMA patients but also expand upon the prenatal phenotypes that can be rescued by *in utero* SMN replacement intervention. Indeed, here I revealed that primary cilia disruption occurring throughout the embryonic development of the hippocampus, the region of the brain with a key role in memory and cognition, can be rescued by prenatal treatment.
As recent findings from cohort studies have indicated the presence of neurodevelopmental and mental disorders in children diagnosed with severe forms of SMA, the results illustrated here suggest the hypothesis that *in utero* intervention targeting the changes occurring in the embryonic CNS could prove effective in addressing the recently described neurodevelopmental comorbidities in SMA.

Notably, the first documented case of prenatal therapy for SMA in human subjects was published in February 2025 (Richard S. Finkel et al., 2025). In this single-patient investigation, risdiplam was administered orally during the last six weeks of gestation to a healthy mother pregnant with a foetus

diagnosed with SMA type I, demonstrating the efficacy of transplacental drug delivery and potential early intervention benefits. Despite the significant contribution of this single-case study to our understanding of the advantages of prenatal SMA treatment, further research is essential to address unresolved issues. For instance, despite undergoing treatment during gestation, the infant girl born with SMA exhibited motor development delays and abnormal brain development, suggesting the presence of SMA features not entirely resolved by administering risdiplam prenatally. One potential explanation for the incomplete rescue of symptoms may be attributed to the delayed initiation of treatment. It has indeed been established that the expression of the SMN protein reaches its peak during the second trimester of pregnancy, and that this is essential for the normal prenatal development (Kong et al., 2021; Motyl et al., 2020; Ramos et al., 2019). While a direct comparison between human and murine gestation is challenging, the key difference between the clinical case and our study lies in the timing of intervention. While in the pregnant mum, the treatment was initiated from 32 weeks of gestation, in our study risdiplam administration began at E9.5, allowing for earlier targeting of embryonic processes. Notably, our study also revealed that the short dosing regimen we employed (a maximum of five days out of a total gestation period of twenty days in mice) was sufficient to have a significant impact on the prenatal primary cilia phenotype.

Finally, one consideration is worth mentioning is that, to date, no prenatal therapeutic interventions have been specifically designed to target primary cilia defects during embryonic development. Despite researchers actively focusing on developing gene therapy approaches and small-molecule combinatorial therapeutic strategies, the current management of ciliopathies remains largely limited to postnatal care and the alleviation of symptoms (Kim & Kim, 2019). While the significant challenge in implementing a gold-standard therapeutic approach is likely due to the high genetic heterogeneity of ciliopathies, this study provides with novel insights on prenatal primary cilia biology and

treatment, which may encourage cross-disciplinary efforts into the development of novel potential therapeutic strategies in these disorders.

Chapter 7: **General Discussion**

7.1 Summary

The overall aim of this thesis was to demonstrate the validity and relevance of exploring prenatal manifestations of SMA occurring in the embryonic central nervous system. This investigation led me to the identification of a novel cellular phenotype involving primary cilia, which I demonstrated to be amenable to *in utero* therapeutic intervention using a SMN-restoring treatment. To achieve this, I employed the widely accepted “Taiwanese” mouse model of severe SMA to study the morphological and molecular processes underpinning prenatal disease pathogenesis.

To demonstrate the reliability of the chosen preclinical model, in the first results chapter of this thesis I illustrated how the prenatal development of mouse brain can be staged and monitored to allow investigation of fundamental cellular processes, such as cell proliferation. The employment of the Ki67 proliferation marker enabled me to identify reduced cell proliferation occurring in the hippocampus of SMA mouse embryos at E14.5. Given the proven reliability of the “Taiwanese” mouse model to study embryonic development of the brain in SMA disease, these findings allowed me to proceed with more in-depth cellular and molecular investigations.

Therefore, to explore whether the cellular proliferation phenotype observed could be due to defects occurring at the molecular level, the second result chapter of this thesis was centred on the study of protein translation in “Taiwanese” mouse embryos at E14.5. While I observed no overt changes in the overall levels of translation, ribosome profiling highlighted defects in the translation of genes involved in a cellular organelle never previously associated with SMA: the primary cilium.

Given the critical relevance of the role of primary cilia in guiding embryonic development of the brain, in the third chapter of this thesis I explored the

biology of primary cilia in the context of prenatal SMA. *In vivo*, I revealed a significant decrease in the number of primary cilia in both the hippocampus and the spinal cord of “Taiwanese” mouse embryos. *In vitro*, I showed that the length of the axoneme of primary cilia was shortened in SMA hippocampal cell culture, and that this phenotype was rescued by the SMN-restoring treatment risdiplam.

Finally, in the last result chapter of this thesis I demonstrated that the implementation of *in utero* transplacental treatment with risdiplam is able to restore SMN protein levels and rescue primary cilia density in the hippocampus of “Taiwanese” mouse embryos.

7.2 Prenatal developmental brain defects in SMA: where preclinical research meets clinical observations

By providing novel insights into the molecular and cellular processes underpinning prenatal stages of SMA disease, this study has highlighted the feasibility and the relevance of studying embryonic brain development using preclinical models. This aspect is particularly important when put in the context of the neurodevelopmental comorbidities recently observed by physicians in some SMA patients, and more specifically in those presenting with the most severe forms of the disease (Masson et al., 2021). Indeed, to be able to gain a comprehensive understanding of the developmental causes underpinning these phenotypes, a close collaboration between clinical and preclinical realities has never been so urgently required.

It is evident that clinical observations are vital components of a patient’s assessment, as they provide invaluable insights into the natural progression of symptoms and the efficacy of real-life treatment approaches. In this scenario, preclinical research represents a complementary asset, as it is essential to unveil novel in-depth mechanistic insights underlying the symptoms observed, to test new potential therapies and to identify the most effective timing for intervention (Signoria et al., 2023; Yeo et al., 2024).

Consequently, within the context of prenatal neurodevelopment in SMA and of the cognitive impairments observed in patients, this study introduces novel insights concerning cellular defects occurring in the hippocampus, a region of the brain that is critical for cognition and social behaviour (Bird & Burgess, 2008; Fortin et al., 2002; Rubin et al., 2014). Based on these findings, physicians may consider targeting this area and functions for further observation and assessment in SMA patients.

Similarly, this study has revealed primary cilia impairments in the prenatal hippocampus of SMA mouse embryos. To date, and to the best of my knowledge, this is the first evidence of a primary ciliopathy in the context of SMA pathology. It may represent, therefore, a novel translational opportunity where clinicians may integrate insights from exiting ciliopathy disorders into the assessment and interpretation of SMA disease.

Finally, this study has also demonstrated the safety and efficacy of *in utero* transplacental treatment with risdiplam to rescue the primary cilia phenotype in the central nervous system of SMA mice. In light of the increasing emphasis on prenatal care for SMA in clinical settings (Tizzano et al., 2025), it is crucial to explore potential consequences of this approach in prenatal preclinical models. Therefore, this study could contribute to the advancement of this therapeutic approach and facilitate the identification of the optimal conditions for establishing a safe and effective prenatal therapeutic intervention in SMA patients.

7.3 *In utero* therapeutic intervention: the emerging consensus

As mentioned above, the identification of prenatal primary cilia defects in SMA and their amenability to SMN-restoring therapy delivered during the embryonic stages of development, provides novel mechanistic insights that reinforce the idea of the efficacy of early therapeutic strategies. A recently published case study by Finkel and colleagues described the first preliminary results of a single

case of prenatal treatment delivered to a foetus diagnosed with SMA Type I by orally administering risdiplam to the mother (Richard S. Finkel et al., 2025). Notably, at the 18-month follow-up, the infant presented with a partially mitigated SMA phenotype. Importantly, however, developmental delays and brain abnormalities were evident. While this single case is highly encouraging with regards to the application of DMTs to foetuses with SMA, it also serves to highlight the necessity for a re-definition of the methodology of SMA prenatal therapeutic intervention.

In light of this evidence, the SMA clinical and preclinical field is actively exploring new approaches and applications to make *in utero* treatments more effective. To cite one of the latest preclinical efforts into exploring prenatal intervention in SMA, earlier this year, Borges *et al.* demonstrated the feasibility of antisense oligonucleotide (ASO) intra-amniotic treatment in mouse embryos and foetal sheep (Borges et al., 2025). Notably, they described this approach as minimally invasive and able to enhance SMN protein expression in multiple tissues, hereby ameliorating SMA phenotypes.

Furthermore, given the monogenic nature of the disease, SMA is an excellent candidate for *in utero* gene replacement therapy (Haque & Yokota, 2024). In this regard, in 2019 Rashnonejad and colleagues described the first use of *in utero* gene therapy in an SMA mouse model (Rashnonejad et al., 2019). The study explored the optimal administration route of the AAV9, demonstrating a rescue of the muscle atrophy phenotype. However, the medial survival remained below control levels, and most significantly, low survival to full gestation was observed, suggesting a potential inflammatory response and safety issues.

The evidence discussed here, together with the findings described in this thesis, offers an overview of the current direction of clinical and preclinical research. The overall aim is therefore to have a more comprehensive

understanding of SMA prenatal manifestations and to design the most effective and safe therapeutic intervention to address them *in utero.*

7.4 Can we consider SMA as a ciliopathy?

The definition of ciliopathies used and recognised today was firstly adopted by Badano *et al.* to indicate the varied phenotypes caused by mutations that disrupt cilia structure and functions (Badano et al., 2006). The term ciliopathy has also been more broadly used to described disorders characterised by cilia defects and dysfunctions (O'Toole et al., 2010). As a result, a recent survey of the Human Phenotype Ontology database estimated that more than 300 additional human disorders, not classified as a ciliopathy, present with a phenotypic spectrum that involves defects in cilia (Lovera & Lüders, 2021; Mill et al., 2023). In this regard, while the causative gene of SMA does not directly encode for a ciliary protein, in this study I have unveiled that the insufficient levels of the SMN protein, caused by deletions on the *Smn1* gene, cause widespread defects in the translation of proteins involved in primary cilia in "Taiwanese" mice.

As primary cilia are known to play crucial roles in coordinating essential signalling pathways involved in the control of the development and homeostasis of tissues and organs (Mill et al., 2023), it is not surprising that the clinical manifestations of ciliopathies affect multiple organs, including brain, liver and kidney and skeleton (Waters & Beales, 2011). Notably, these organs have been reported to be affected also in SMA disease (Allardyce et al., 2020; Hamilton & Gillingwater, 2013; Motyl et al., 2020; Yeo & Darras, 2020).

Primary cilia are key organelles for the correct development of the CNS (Mill et al., 2023). As a result, many well-known ciliopathies, such as Joubert syndrome and Meckel syndrome, exhibit common neurological malformations accompanied by intellectual disability (Park et al., 2019). In this study I have focused my investigation on the hippocampus, revealing neuronal primary cilia defects in SMA. Notably, several studies have also reported hippocampal

abnormalities in some patients with ciliopathies (Baker et al., 2011; Bennouna-Greene et al., 2011; Berbari et al., 2014; Rhee et al., 2016). These observations not only demonstrated the presence of hippocampal dysgenesis but also provided a correlation between hippocampal primary cilia loss and learning and memory deficits. Consequently, the observations presented in this thesis may contribute a novel perspective on the neurodevelopmental comorbidities observed in some SMA patients.

In the first result chapter of this thesis, I also showed the occurrence of cell proliferation defects in the hippocampus of SMA mouse embryos. This could be speculated to be one of the functional consequences of primary cilia impairment. Indeed, it has been demonstrated that the assembly and disassembly of primary cilia are dependent on and impact cell cycle progression (Wang & Dynlacht, 2018) . Specifically, under physiological conditions, cilium assembly occurs during the non-proliferative G0 phase, and it disassembles during the proliferative G1/S phase of the cell cycle. Notably, primary cilia function as specialised signalling hubs coordinating key developmental pathways, such as Sonic Hedgehog and WNT, that regulate essential cellular processes including cell proliferation and differentiation (Mill et al., 2023). Consequently, the loss of primary cilia prevents the proper transduction of these signals, which in turn may lead to impaired cell proliferation and tissue development.

In conclusion, as this study focused on the investigation of primary cilia exclusively in the CNS of mouse embryos, it may be premature to strictly re-define SMA as a ciliopathy. Nevertheless, it is hoped that the findings described in this thesis and the evidence discussed may provide a solid foundation to stimulate the SMA field to deepen the primary cilia study in multisystem preclinical models and in clinical settings, to evaluate the presence of ciliopathy manifestations in SMA patients.

7.5 Future perspectives

This study has contributed to the enrichment of understanding regarding the neurodevelopmental manifestations occurring in SMA and has uncovered novel molecular and cellular insights which potentially contribute to the disease pathogenesis. Nonetheless, further research is required to expand upon these findings and establish their clinical relevance.

Alongside the investigation of prenatal manifestations in different organs, the exploration of the early stages of brain development has becoming increasingly crucial to understand the novel neurocognitive phenotypes observed in SMA patients (Baranello et al., 2024; Buchignani et al., 2025). For this reason, as this study solely focused on the hippocampus, the assessment of other anatomical areas is imperative. One innovative approach with the potential to provide significant insights into this extensive investigation could rely on the implementation of whole-brain optical imaging (Ding et al., 2022; Jiang et al., 2023). This technique has been recently established for the study of the brain in rodent animal models and has been proven to be a functional tool in the study of neurodevelopmental disorders (Craigie et al., 2025). Given the complexity of the structural organisation of the brain, this technique could facilitate the simultaneous mapping of multiple developmental markers across all areas of the brain. While potentially holding limitations, the integration of this technique could provide a comprehensive overview of the early stages of the development of the brain in preclinical models of SMA disease.

Further work could also be conducted with the aim of exploring early developmental defects in the different mouse models currently available in preclinical research to study SMA. Although the “Taiwanese” mouse model employed in this study reliably recapitulates key genetic and phenotypic features of the disease, additional SMA mouse models have been developed using alternative genetic strategies. For instance, the 2B mouse model carries a mutation affecting the splicing of the endogenous *Smn* gene, presenting with a milder phenotype compared to “Taiwanese” mice and allowing the

investigation of the disease mechanisms at later stages (Mélissa Bowerman et al., 2012). Consequently, validating the findings presented in this thesis using additional models with different genetic modifications and disease severities would strengthen the robustness and translational relevance of the results.

An additional relevant contribution to the SMA field could be represented by an expanded investigation of the prenatal translational defects. Indeed, the primary cilia defects observed in this study have been identified thanks to the analysis of DEGs datasets obtained from ribosome profiling. As demonstrated in the present study, primary cilia phenotypes in the hippocampus of SMA mouse embryos were rescued by delivering an SMN-restoring therapy *in utero*. As a result, it would be of significant interest to perform ribosome profiling on tissues harvested from mouse embryos treated prenatally with risdiplam, with the objecting of investigating whether the disruption in protein translational can be rescued by prenatal therapeutic intervention.

Finally, in this study I have demonstrated that the “Taiwanese” mouse is a powerful and reliable model that can be used to study neurodevelopment and the molecular and cellular defects occurring in the prenatal brain. However, given the novel and often serious neurodevelopmental comorbidities, including cognitive defects and autism spectrum disorder, observed in some SMA patients, is it evident that there is the need for an ideal preclinical model for studying cognition and neurodevelopmental behaviours (Baranello et al., 2024; Buchignani et al., 2025). To overcome this lack of an appropriate tool, a significant enhancement for the field could be the generation of a rat model for SMA, which would allow the evaluation of neurobehavioral aspects as well as responses to therapeutic intervention. Compared to mice, rats are characterised by a more complex social behaviour and cognitive capacities and therefore would represent a perfect preclinical model for assessing learning, memory, attention and social interaction (Ellenbroek & Youn, 2016; Parker et al., 2014). In this regard, several behavioural tests exist to investigate

neurodevelopmental phenotypes in newborn rats: the ultrasonic vocalisation test can be used to assess emotional behaviour and communication (Boulanger-Bertolus & Mouly, 2021), the huddling test to study social behaviour (Alberts, 2007), and the maternal odour preference test to investigate learning and memory (Sreng et al., 2016). As a result, the integration of the neurobehavioral data obtained from this preclinical model into clinical practice could facilitate the development of a standardised cognitive assessment for SMA patients.

7.6 Final remarks

Alongside presenting and discussing the scientific findings collected during my PhD, this thesis has retraced the major milestones achieved in the understanding SMA disease, from the identification of the *SMN1* gene over a century ago, to the development and implementation of treatments, and the clinical observation of unexpected clinical manifestations. As a researcher dedicated to the study of SMA, I believe that this present time represents one of the most exciting and challenging chapter in the history of the disease. The advances made are remarkable, yet they represent not an endpoint but rather the foundation for a new era. As the natural history of SMA has been reshaped by disease-modifying therapies, it becomes essential the ongoing monitoring of patient symptoms, the refinement of therapeutic approaches, and the identification of the most beneficial strategies to provide patients with care and support.

References

Akodad, S., De Smedt, D., Baijot, S., Stevens, H., & Deconinck, N. (2024). Cognition and communication in patients with spinal muscular atrophy: A systematic review. *Heliyon*, *10*(13), e33677. https://doi.org/10.1016/j.heliyon.2024.e33677

Aksu Uzunhan, T., Erturk, B., Aydin, K., Ayaz, A., Altunoglu, U., Yarar, M. H., Gezdirici, A., Icagasioglu, D. F., Gokpinar Ili, E., Uyanik, B., Eser, M., Kutbay, Y. B., Topcu, Y., Kilic, B., Bektas, G., Arduc Akcay, A., Ekici, B., Chousein, A., Avci, S., . . . Kayserili, H. (2023). Clinical and genetic spectrum from a prototype of ciliopathy: Joubert syndrome. *Clin Neurol Neurosurg*, *224*, 107560. https://doi.org/10.1016/j.clineuro.2022.107560

Alaynick, W. A., Jessell, T. M., & Pfaff, S. L. (2011). SnapShot: spinal cord development. *Cell*, *146*(1), 178-178 e171. https://doi.org/10.1016/j.cell.2011.06.038

Alberts, J. R. (2007). Huddling by rat pups: Ontogeny of individual and group behavior. *Developmental Psychobiology*, *49*(1), 22-32. https://doi.org/10.1002/dev.20190

Allardyce, H., Kuhn, D., Hernandez-Gerez, E., Hensel, N., Huang, Y. T., Faller, K., Gillingwater, T. H., Quondamatteo, F., Claus, P., & Parson, S. H. (2020). Renal pathology in a mouse model of severe Spinal Muscular Atrophy is associated with downregulation of Glial Cell-Line Derived Neurotrophic Factor (GDNF). *Hum Mol Genet*, *29*(14), 2365-2378. https://doi.org/10.1093/hmg/ddaa126

Altman, J., & Bayer, S. A. (1990). Mosaic organization of the hippocampal neuroepithelium and the multiple germinal sources of dentate granule cells. *The Journal of Comparative Neurology*, *301*(3), 325-342. https://doi.org/10.1002/cne.903010302

Amador-Arjona, A., Elliott, J., Miller, A., Ginbey, A., Pazour, G. J., Enikolopov, G., Roberts, A. J., & Terskikh, A. V. (2011). Primary Cilia Regulate Proliferation of Amplifying Progenitors in Adult Hippocampus: Implications for Learning and Memory. *Journal of Neuroscience*, *31*(27), 9933-9944. https://doi.org/10.1523/jneurosci.1062-11.2011

Andreu-Cervera, A., Catala, M., & Schneider-Maunoury, S. (2021). Cilia, ciliopathies and hedgehog-related forebrain developmental disorders. *Neurobiol Dis*, *150*, 105236. https://doi.org/10.1016/j.nbd.2020.105236

Anvarian, Z., Mykytyn, K., Mukhopadhyay, S., Pedersen, L. B., & Christensen, S. T. (2019). Cellular signalling by primary cilia in development, organ function and disease. *Nature Reviews Nephrology*, *15*(4), 199-219. https://doi.org/10.1038/s41581-019-0116-9

Arkblad, E., Tulinius, M., Kroksmark, A. K., Henricsson, M., & Darin, N. (2009). A population-based study of genotypic and phenotypic variability in children with spinal muscular atrophy. *Acta Paediatrica*, *98*(5), 865-872. https://doi.org/10.1111/j.1651-2227.2008.01201.x

Bachand, F., Boisvert, F.-M., Côté, J., Richard, S., & Autexier, C. (2002). The Product of the Survival of Motor Neuron(SMN) Gene is a Human Telomerase-associated Protein. *Molecular Biology of the Cell*, *13*(9), 3192-3202. https://doi.org/10.1091/mbc.e02-04-0216

Badano, J. L., Mitsuma, N., Beales, P. L., & Katsanis, N. (2006). The ciliopathies: an emerging class of human genetic disorders. *Annu. Rev. Genomics Hum. Genet.*, *7*(1), 125-148.

Baker, K., Northam, G. B., Chong, W. K., Banks, T., Beales, P., & Baldeweg, T. (2011). Neocortical and hippocampal volume loss in a human ciliopathy: A quantitative MRI study in Bardet-Biedl syndrome. *Am J Med Genet A*, *155A*(1), 1-8. https://doi.org/10.1002/ajmg.a.33773

Bangerter, A., Ness, S., Aman, M. G., Esbensen, A. J., Goodwin, M. S., Dawson, G., Hendren, R., Leventhal, B., Khan, A., Opler, M., Harris, A., & Pandina, G. (2017). Autism Behavior Inventory: A Novel Tool for Assessing Core and Associated Symptoms of Autism Spectrum Disorder. *Journal of Child and Adolescent Psychopharmacology*, *27*(9), 814-822. https://doi.org/10.1089/cap.2017.0018

Banker, S. M., Gu, X., Schiller, D., & Foss-Feig, J. H. (2021). Hippocampal contributions to social and cognitive deficits in autism spectrum disorder. *Trends Neurosci*, *44*(10), 793-807. https://doi.org/10.1016/j.tins.2021.08.005

Bansal, R., Engle, S. E., Antonellis, P. J., Whitehouse, L. S., Baucum, A. J., Cummins, T. R., Reiter, J. F., & Berbari, N. F. (2019). Hedgehog Pathway Activation Alters Ciliary Signaling in Primary Hypothalamic Cultures. *Frontiers in Cellular Neuroscience*, *13*. https://doi.org/10.3389/fncel.2019.00266

Baranello, G., Darras, B. T., Day, J. W., Deconinck, N., Klein, A., Masson, R., Mercuri, E., Rose, K., El-Khairi, M., Gerber, M., Gorni, K., Khwaja, O., Kletzl, H., Scalco, R. S., Seabrook, T., Fontoura, P., & Servais, L. (2021). Risdiplam in Type 1 Spinal Muscular Atrophy. *New England Journal of Medicine*, *384*(10), 915-923. https://doi.org/10.1056/nejmoa2009965

Baranello, G., Roy, S. Q., Servais, L., Munell, F., Molinero, M. A., Natera De Benito, D., Nascimento, A., Gomez-Andres, D., Comellas, L. C., Exposito, J., Tizzano, E. F., Cuppen, I., Van Der Pol, L., Aleman, A., Lochmuller, H., McMillan, H., Kirschner, J., Müller, C., Oskoui, M., . . . Muntoni, F. (2024). The emerging spectrum of neurodevelopmental

comorbidities in early-onset Spinal Muscular Atrophy. *European Journal of Paediatric Neurology*, *48*, 67-68. https://doi.org/10.1016/j.ejpn.2023.11.006

Battaglia, G., Princivalle, A., Forti, F., Lizier, C., & Zeviani, M. (1997). Expression of the SMN Gene, the Spinal Muscular Atrophy Determining Gene, in the Mammalian Central Nervous System. *Human Molecular Genetics*, *6*(11), 1961-1971. https://doi.org/10.1093/hmg/6.11.1961

Béchade, C., Rostaing, P., Cisterni, C., Kalisch, R., Bella, V. L., Pettmann, B., & Triller, A. (1999). Subcellular distribution of survival motor neuron (SMN) protein: possible involvement in nucleocytoplasmic and dendritic transport. *European Journal of Neuroscience*, *11*(1), 293-304. https://doi.org/10.1046/j.1460-9568.1999.00428.x

Bedogni, F., Cobolli Gigli, C., Pozzi, D., Rossi, R. L., Scaramuzza, L., Rossetti, G., Pagani, M., Kilstrup-Nielsen, C., Matteoli, M., & Landsberger, N. (2016). Defects DuringMecp2Null Embryonic Cortex Development Precede the Onset of Overt Neurological Symptoms. *Cerebral Cortex*, *26*(6), 2517-2529. https://doi.org/10.1093/cercor/bhv078

Beevor, C. E. (1902). A CASE OF CONGENITAL SPINAL MUSCULAR ATROPHY (FAMILY TYPE), AND A CASE OF HÆMORRHAGE INTO THE SPINAL CORD AT BIRTH, GIVING SIMILAR SYMPTOMS. *Brain*, *25*(1), 85-108. https://doi.org/10.1093/brain/25.1.85

Bennouna-Greene, V., Kremer, S., Stoetzel, C., Christmann, D., Schuster, C., Durand, M., Verloes, A., Sigaudy, S., Holder-Espinasse, M., Godet, J., Brandt, C., Marion, V., Danion, A., Dietemann, J. L., & Dollfus, H. (2011). Hippocampal dysgenesis and variable neuropsychiatric phenotypes in patients with Bardet-Biedl syndrome underline complex CNS impact of primary cilia. *Clinical Genetics*, *80*(6), 523-531. https://doi.org/10.1111/j.1399-0004.2011.01688.x

Berbari, N. F., Bishop, G. A., Askwith, C. C., Lewis, J. S., & Mykytyn, K. (2007). Hippocampal neurons possess primary cilia in culture. *Journal of Neuroscience Research*, *85*(5), 1095-1100. https://doi.org/10.1002/jnr.21209

Berbari, N. F., Malarkey, E. B., Yazdi, S. M., McNair, A. D., Kippe, J. M., Croyle, M. J., Kraft, T. W., & Yoder, B. K. (2014). Hippocampal and cortical primary cilia are required for aversive memory in mice. *PLoS One*, *9*(9), e106576. https://doi.org/10.1371/journal.pone.0106576

Bergin, A., Kim, G., Price, D. L., Sisodia, S. S., Lee, M. K., & Rabin, B. A. (1997). Identification and characterization of a mouse homologue of the spinal muscular atrophy-determining gene, survival motor neuron. *Gene*, *204*(1-2), 47-53. https://doi.org/10.1016/s0378-1119(97)00510-6

Bernabò, P., Tebaldi, T., Groen, E. J. N., Lane, F. M., Perenthaler, E., Mattedi, F., Newbery, H. J., Zhou, H., Zuccotti, P., Potrich, V., Shorrock, H. K., Muntoni, F., Quattrone, A., Gillingwater, T. H., & Viero, G. (2017). In Vivo Translatome Profiling in Spinal Muscular Atrophy Reveals a Role for SMN Protein in Ribosome Biology. *Cell Reports*, *21*(4), 953-965. https://doi.org/10.1016/j.celrep.2017.10.010

Billard, C., Gillet, P., Barthez, M. A., Hommet, C., & Bertrand, P. (1998). Reading ability and processing in Duchenne muscular dystrophy and spinal muscular atrophy. *Developmental Medicine & Child Neurology*, *40*(1), 12-20. https://doi.org/10.1111/j.1469-8749.1998.tb15351.x

Billard, C., Gillet, P., Signoret, J. L., Uicaut, E., Bertrand, P., Fardeau, M., Barthez-Carpentier, M. A., & Santini, J. J. (1992). Cognitive functions in Duchenne muscular dystrophy: a reappraisal and comparison with spinal muscular atrophy. *Neuromuscul Disord*, *2*(5-6), 371-378. https://doi.org/10.1016/s0960-8966(06)80008-8

Bird, C. M., & Burgess, N. (2008). The hippocampus and memory: insights from spatial processing. *Nature Reviews Neuroscience*, *9*(3), 182-194. https://doi.org/10.1038/nrn2335

Bistritzer, J., Avital, D., Golan-Tripto, I., Abramsky, R., & Noyman, I. (2025). Early Treatment in Preterm Twins With Spinal Muscular Atrophy. *Journal of Child Neurology*, *40*(5), 371-373. https://doi.org/10.1177/08830738251322224

Bitetti, I., Manna, M. R., Stella, R., & Varone, A. (2023). Sequential treatment with nusinersen, Zolgensma® and risdiplam in a paediatric patient with spinal muscular atrophytype 1: a case report [Article]. *Acta Myologica*, *42*(2-3), 82-85. https://doi.org/10.36185/2532-1900-356

Bitetti, I., Manna, M. R., Stella, R., & Varone, A. (2024). Motor and neurocognitive profiles of children with symptomatic spinal muscular atrophy type 1 with two copies of SMN2 before and after treatment: a longitudinal observational study. *Frontiers in Neurology*, *15*. https://doi.org/10.3389/fneur.2024.1326528

Bloodgood, R. A. (2009). Chapter 1 - From Central to Rudimentary to Primary: The History of an Underappreciated Organelle Whose Time Has Come.The Primary Cilium. In R. D. Sloboda (Ed.), *Methods in Cell Biology* (Vol. 94, pp. 2-52). Academic Press. https://doi.org/https://doi.org/10.1016/S0091-679X(08)94001-2

Boardman, F. K., Sadler, C., & Young, P. J. (2018). Newborn genetic screening for spinal muscular atrophy in the <scp>UK</scp>: The views of the general population. *Molecular Genetics & Genomic Medicine*, *6*(1), 99-108. https://doi.org/10.1002/mgg3.353

Borges, B., Brown, S. M., Chen, W. J., Clarke, M. T., Herzeg, A., Park, J. H., Ross, J., Kong, L., Denton, M., Smith, A. K., Lum, T., Zada, F. M., Cordero, M., Gupta, N., Cook, S. E., Murray, H., Matson, J., Klein, S., Bennett, C. F., . . . Sumner, C. J. (2025). Intra-amniotic antisense oligonucleotide treatment improves phenotypes in preclinical models of spinal muscular atrophy. *Sci Transl Med*, *17*(798), eadv4656. https://doi.org/10.1126/scitranslmed.adv4656

Boulanger-Bertolus, J., & Mouly, A.-M. (2021). Ultrasonic Vocalizations Emission across Development in Rats: Coordination with Respiration and Impact on Brain Neural Dynamics. *Brain Sciences*, *11*(5), 616. https://doi.org/10.3390/brainsci11050616

Bowerman, M., Anderson, C. L., Beauvais, A., Boyl, P. P., Witke, W., & Kothary, R. (2009). SMN, profilin IIa and plastin 3: a link between the deregulation of actin dynamics and SMA pathogenesis. *Mol Cell Neurosci*, *42*(1), 66-74. https://doi.org/10.1016/j.mcn.2009.05.009

Bowerman, M., Murray, L. M., Beauvais, A., Pinheiro, B., & Kothary, R. (2012). A critical smn threshold in mice dictates onset of an intermediate spinal muscular atrophy phenotype associated with a distinct neuromuscular junction pathology. *Neuromuscular Disorders*, *22*(3), 263-276. https://doi.org/https://doi.org/10.1016/j.nmd.2011.09.007

Bowerman, M., Shafey, D., & Kothary, R. (2007). Smn depletion alters profilin II expression and leads to upregulation of the RhoA/ROCK pathway and defects in neuronal integrity. *J Mol Neurosci*, *32*(2), 120-131. https://doi.org/10.1007/s12031-007-0024-5

Bowerman, M., Swoboda, K. J., Michalski, J. P., Wang, G. S., Reeks, C., Beauvais, A., Murphy, K., Woulfe, J., Screaton, R. A., Scott, F. W., & Kothary, R. (2012). Glucose metabolism and pancreatic defects in spinal muscular atrophy. *Annals of Neurology*, *72*(2), 256-268. https://doi.org/10.1002/ana.23582

Brancati, F., Dallapiccola, B., & Valente, E. M. (2010). Joubert Syndrome and related disorders. *Orphanet Journal of Rare Diseases*, *5*(1), 20. https://doi.org/10.1186/1750-1172-5-20

Brandsema, J., Parsons, J., Proud, C., Finkel, R., Swoboda, K., Masson, R., Liu, Y., Makepeace, C., Paradis, A., & Berger, Z. (2022). Baseline characteristics and initial safety results in RESPOND: a Phase 4 study of nusinersen in children with spinal muscular atrophy (SMA) who received onasemnogene abeparvovec (P18-5.003). *Neurology*, *98*(18_supplement), 1698.

Breunig, J. J., Sarkisian, M. R., Arellano, J. I., Morozov, Y. M., Ayoub, A. E., Sojitra, S., Wang, B., Flavell, R. A., Rakic, P., & Town, T. (2008). Primary cilia regulate hippocampal neurogenesis by mediating sonic hedgehog

signaling. *Proceedings of the National Academy of Sciences*, *105*(35), 13127-13132. https://doi.org/10.1073/pnas.0804558105

Brewer, G. J., Torricelli, J. R., Evege, E. K., & Price, P. J. (1993). Optimized survival of hippocampal neurons in B27-supplemented Neurobasal, a new serum-free medium combination. *J Neurosci Res*, *35*(5), 567-576. https://doi.org/10.1002/jnr.490350513

Brian, Samtani, R., Tobita, K., Tsuchya, M., Jovenal, John, Julie, Subramanian, R., Cecilia, & Gregory. (2012). IFT25 Links the Signal-Dependent Movement of Hedgehog Components to Intraflagellar Transport. *Developmental Cell*, *22*(5), 940-951. https://doi.org/10.1016/j.devcel.2012.04.009

Briese, M., Richter, D.-U., Sattelle, D. B., & Ulfig, N. (2006). SMN, the product of the spinal muscular atrophy-determining gene, is expressed widely but selectively in the developing human forebrain. *The Journal of Comparative Neurology*, *497*(5), 808-816. https://doi.org/10.1002/cne.21010

Brown, S. M., Ajjarapu, A. S., Ramachandra, D., Blasco-Pérez, L., Costa-Roger, M., Tizzano, E. F., Sumner, C. J., & Mathews, K. D. (2024). Onasemnogene-abeparvovec administration to premature infants with spinal muscular atrophy. *Annals of Clinical and Translational Neurology*. https://doi.org/10.1002/acn3.52213

Buchignani, B., Cicala, G., Cumbo, F., Ricci, M., Capasso, A., Ticci, C., Mazzanti, S., Brolatti, N., Tosi, M., Dosi, C., Antonaci, L., Coratti, G., Pera, M. C., Leone, D., Palermo, C., Berti, B., Frongia, A. L., Sacchini, M., Bruno, C., . . . Mercuri, E. (2024). Communicative development inventory in type 1 and presymptomatic infants with spinal muscular atrophy: a cohort study. *Archives of Disease in Childhood*, archdischild-20. https://doi.org/10.1136/archdischild-2023-326613

Buchignani, B., Cicala, G., Moriconi, F., Ricci, M., Capasso, A., Coratti, G., Casiraghi, J., Albamonte, E., Cristofani, P., Cutrona, C., Pera, M. C., Antonaci, L., Roncoroni, C., Chieffo, D., Sansone, V. A., Battini, R., Pane, M., & Mercuri, E. (2023). Profile of cognitive abilities in spinal muscular atrophy type II and III: what is the role of motor impairment? *Neuromuscul Disord*, *33*(10), 711-717. https://doi.org/10.1016/j.nmd.2023.08.005

Buchignani, B., Coratti, G., Cutrì, C., Scattoni, M. L., Pane, M., Palermo, C., Leone, D., De Sanctis, R., Stanca, G., Antonaci, L., Cutrona, C., Pera, M. C., Brogna, C., Cristofani, P., Fulceri, F., Baranello, G., & Mercuri, E. (2025). Neurodevelopmental and mental disorders in children with type I and presymptomatic spinal muscular atrophy. *Scientific Reports*, *15*(1). https://doi.org/10.1038/s41598-025-12484-8

Buettner, J. M., Sime Longang, J. K., Gerstner, F., Apel, K. S., Blanco-Redondo, B., Sowoidnich, L., Janzen, E., Langenhan, T., Wirth, B., & Simon, C. M. (2021). Central synaptopathy is the most conserved feature of motor circuit pathology across spinal muscular atrophy mouse models. *iScience*, *24*(11), 103376. https://doi.org/https://doi.org/10.1016/j.isci.2021.103376

Burlet, P., Huber, C., Bertrandy, S., Ludosky, M. A., Zwaenepoel, I., Clermont, O., Roume, J., Delezoide, A. L., Cartaud, J., Munnich, A., & Lefebvre, S. (1998). The distribution of SMN protein complex in human fetal tissues and its alteration in spinal muscular atrophy. *Hum Mol Genet*, *7*(12), 1927-1933. https://doi.org/10.1093/hmg/7.12.1927

Butchbach, M. E. R., Singh, J., Þorsteinsdóttir, M., Saieva, L., Slominski, E., Thurmond, J., Andrésson, T., Zhang, J., Edwards, J. D., Simard, L. R., Pellizzoni, L., Jarecki, J., Burghes, A. H. M., & Gurney, M. E. (2010). Effects of 2,4-diaminoquinazoline derivatives on SMN expression and phenotype in a mouse model for spinal muscular atrophy. *Human Molecular Genetics*, *19*(3), 454-467. https://doi.org/10.1093/hmg/ddp510

Cantagrel, V., Silhavy, J. L., Bielas, S. L., Swistun, D., Marsh, S. E., Bertrand, J. Y., Audollent, S., Attié-Bitach, T., Holden, K. R., Dobyns, W. B., Traver, D., Al-Gazali, L., Ali, B. R., Lindner, T. H., Caspary, T., Otto, E. A., Hildebrandt, F., Glass, I. A., Logan, C. V., . . . Gleeson, J. G. (2008). Mutations in the Cilia Gene ARL13B Lead to the Classical Form of Joubert Syndrome. *The American Journal of Human Genetics*, *83*(2), 170-179. https://doi.org/10.1016/j.ajhg.2008.06.023

Caspary, T., Larkins, C. E., & Anderson, K. V. (2007). The Graded Response to Sonic Hedgehog Depends on Cilia Architecture. *Developmental Cell*, *12*(5), 767-778. https://doi.org/10.1016/j.devcel.2007.03.004

Chaddad, A., Desrosiers, C., Hassan, L., & Tanougast, C. (2017). Hippocampus and amygdala radiomic biomarkers for the study of autism spectrum disorder. *BMC Neuroscience*, *18*(1). https://doi.org/10.1186/s12868-017-0373-0

Chakrabarti, L., Galdzicki, Z., & Haydar, T. F. (2007). Defects in Embryonic Neurogenesis and Initial Synapse Formation in the Forebrain of the Ts65Dn Mouse Model of Down Syndrome. *The Journal of Neuroscience*, *27*(43), 11483-11495. https://doi.org/10.1523/jneurosci.3406-07.2007

Chand, D., Mohr, F., McMillan, H., Tukov, F. F., Montgomery, K., Kleyn, A., Sun, R., Tauscher-Wisniewski, S., Kaufmann, P., & Kullak-Ublick, G. (2021). Hepatotoxicity following administration of onasemnogene abeparvovec (AVXS-101) for the treatment of spinal muscular atrophy. *Journal of*

Hepatology, *74*(3), 560-566. https://doi.org/https://doi.org/10.1016/j.jhep.2020.11.001

Chaytow, H., Faller, K. M. E., Huang, Y. T., & Gillingwater, T. H. (2021). Spinal muscular atrophy: From approved therapies to future therapeutic targets for personalized medicine. *Cell Rep Med*, *2*(7), 100346. https://doi.org/10.1016/j.xcrm.2021.100346

Chaytow, H., Huang, Y.-T., Gillingwater, T. H., & Faller, K. M. E. (2018). The role of survival motor neuron protein (SMN) in protein homeostasis. *Cellular and Molecular Life Sciences*, *75*(21), 3877-3894. https://doi.org/10.1007/s00018-018-2849-1

Chaytow, H., Motyl, A. A. L., Huang, Y.-T., Wong, C., Currie, G. L., Bahor, Z., Sena, E., & Gillingwater, T. H. (2024). Timing of SMN replacement therapies in mouse models of spinal muscular atrophy: a systematic review and meta-analysis. *Brain Communications*. https://doi.org/10.1093/braincomms/fcae267

Cheffer, A., Tárnok, A., & Ulrich, H. (2013). Cell Cycle Regulation During Neurogenesis in the Embryonic and Adult Brain. *Stem Cell Reviews and Reports*, *9*(6), 794-805. https://doi.org/10.1007/s12015-013-9460-5

Chen, A., Liao, S., Cheng, M., Ma, K., Wu, L., Lai, Y., Qiu, X., Yang, J., Xu, J., Hao, S., Wang, X., Lu, H., Chen, X., Liu, X., Huang, X., Li, Z., Hong, Y., Jiang, Y., Peng, J., . . . Wang, J. (2022). Spatiotemporal transcriptomic atlas of mouse organogenesis using DNA nanoball-patterned arrays. *Cell*, *185*(10), 1777-1792.e1721. https://doi.org/10.1016/j.cell.2022.04.003

Chen, V. S., Morrison, J. P., Southwell, M. F., Foley, J. F., Bolon, B., & Elmore, S. A. (2017). Histology Atlas of the Developing Prenatal and Postnatal Mouse Central Nervous System, with Emphasis on Prenatal Days E7.5 to E18.5. *Toxicol Pathol*, *45*(6), 705-744. https://doi.org/10.1177/0192623317728134

Chen, Y., Lun, A. T. L., & Smyth, G. K. (2016). From reads to genes to pathways: differential expression analysis of RNA-Seq experiments using Rsubread and the edgeR quasi-likelihood pipeline. *F1000Research*, *5*, 1438. https://doi.org/10.12688/f1000research.8987.2

Ciemerych, M. A., & Sicinski, P. (2005). Cell cycle in mouse development. *Oncogene*, *24*(17), 2877-2898. https://doi.org/10.1038/sj.onc.1208608

Clermont, O., Burlet, P., Lefebvre, S., Bürglen, L., Munnich, A., & Melki, J. (1995). SMN gene deletions in adult-onset spinal muscular atrophy. *Lancet*, *346*(8991-8992), 1712-1713. https://doi.org/10.1016/s0140-6736(95)92881-2

Collotta, D., Bertocchi, I., Chiapello, E., & Collino, M. (2023). Antisense oligonucleotides: a novel Frontier in pharmacological strategy. *Front Pharmacol*, *14*, 1304342. https://doi.org/10.3389/fphar.2023.1304342

Cooper, K., Nalbant, G., Sutton, A., Harnan, S., Thokala, P., Chilcott, J., McNeill, A., & Bessey, A. (2024). Systematic Review of Newborn Screening Programmes for Spinal Muscular Atrophy. *International Journal of Neonatal Screening*, *10*(3), 49. https://doi.org/10.3390/ijns10030049

Cooper, K., Nalbant, G., Sutton, A., Harnan, S., Thokala, P., Chilcott, J., McNeill, A., & Bessey, A. (2024). Systematic Review of Presymptomatic Treatment for Spinal Muscular Atrophy. *Int J Neonatal Screen*, *10*(3). https://doi.org/10.3390/ijns10030056

Cottam, N. C., Bamfo, T., Harrington, M. A., Charvet, C. J., Hekmatyar, K., Tulin, N., & Sun, J. (2023). Cerebellar structural, astrocytic, and neuronal abnormalities in the <scp>SMNΔ7</scp> mouse model of spinal muscular atrophy. *Brain Pathology*, *33*(5). https://doi.org/10.1111/bpa.13162

Courtney, N. L., Mole, A. J., Thomson, A. K., & Murray, L. M. (2019). Reduced P53 levels ameliorate neuromuscular junction loss without affecting motor neuron pathology in a mouse model of spinal muscular atrophy. *Cell Death & Disease*, *10*(7). https://doi.org/10.1038/s41419-019-1727-6

Craigie, K. J., Till, S., Van De Gevel, B., Vandrey, B., Strangward, P., Sieger, D., Gonzalez-Sulser, A., Kind, P., Rochefort, N., Duguid, I., & Martinez-Gonzalez, C. (2025). *RatDISCO, a tissue clearing and immunolabelling protocol for large rat brains*. Cold Spring Harbor Laboratory. https://dx.doi.org/10.1101/2025.08.17.670723

Crawford, T. O., Swoboda, K. J., De Vivo, D. C., Bertini, E., Hwu, W. L., Finkel, R. S., Kirschner, J., Kuntz, N. L., Nazario, A. N., Parsons, J. A., Pechmann, A., Ryan, M. M., Butterfield, R. J., Topaloglu, H., Ben-Omran, T., Sansone, V. A., Jong, Y. J., Shu, F., Zhu, C., . . . Berger, Z. (2023). Continued benefit of nusinersen initiated in the presymptomatic stage of spinal muscular atrophy: 5-year update of the<scp>NURTURE</scp>study. *Muscle & Nerve*, *68*(2), 157-170. https://doi.org/10.1002/mus.27853

Dager, S. R., Wang, L., Friedman, S. D., Shaw, D. W., Constantino, J. N., Artru, A. A., Dawson, G., & Csernansky, J. G. (2007). Shape mapping of the hippocampus in young children with autism spectrum disorder. *AJNR Am J Neuroradiol*, *28*(4), 672-677. https://www.ncbi.nlm.nih.gov/pubmed/17416819

Dangouloff, T., Botty, C., Beaudart, C., Servais, L., & Hiligsmann, M. (2021). Systematic literature review of the economic burden of spinal muscular atrophy and economic evaluations of treatments. *Orphanet Journal of Rare Diseases*, *16*(1). https://doi.org/10.1186/s13023-021-01695-7

Dangouloff, T., & Servais, L. (2019). Clinical Evidence Supporting Early Treatment Of Patients With Spinal Muscular Atrophy: Current Perspectives. *Therapeutics and Clinical Risk Management*, *Volume 15*, 1153-1161. https://doi.org/10.2147/tcrm.s172291

Day, J. W., Finkel, R. S., Chiriboga, C. A., Connolly, A. M., Crawford, T. O., Darras, B. T., Iannaccone, S. T., Kuntz, N. L., Peña, L. D. M., Shieh, P. B., Smith, E. C., Kwon, J. M., Zaidman, C. M., Schultz, M., Feltner, D. E., Tauscher-Wisniewski, S., Ouyang, H., Chand, D. H., Sproule, D. M., . . . Mendell, J. R. (2021). Onasemnogene abeparvovec gene therapy for symptomatic infantile-onset spinal muscular atrophy in patients with two copies of SMN2 (STR1VE): an open-label, single-arm, multicentre, phase 3 trial. *The Lancet Neurology*, *20*(4), 284-293. https://doi.org/https://doi.org/10.1016/S1474-4422(21)00001-6

Deguise, M. O., Baranello, G., Mastella, C., Beauvais, A., Michaud, J., Leone, A., De Amicis, R., Battezzati, A., Dunham, C., Selby, K., Warman Chardon, J., McMillan, H. J., Huang, Y. T., Courtney, N. L., Mole, A. J., Kubinski, S., Claus, P., Murray, L. M., Bowerman, M., . . . Kothary, R. (2019). Abnormal fatty acid metabolism is a core component of spinal muscular atrophy. *Annals of Clinical and Translational Neurology*, *6*(8), 1519-1532. https://doi.org/10.1002/acn3.50855

Deng, S., Gan, L., Liu, C., Xu, T., Zhou, S., Guo, Y., Zhang, Z., Yang, G.-Y., Tian, H., & Tang*, Y. (2022). Roles of Ependymal Cells in the Physiology and Pathology of the Central Nervous System. *Aging and disease*, 0. https://doi.org/10.14336/ad.2022.0826-1

Didonato, C. J., Chen, X.-N., Noya, D., Korenberg, J. R., Nadeau, J. H., & Simard, L. R. (1997). Cloning, Characterization, and Copy Number of the Murine Survival Motor Neuron Gene: Homolog of the Spinal Muscular Atrophy-Determining Gene. *Genome Research*, *7*(4), 339-352. https://doi.org/10.1101/gr.7.4.339

Ding, Z., Zhao, J., Luo, T., Lu, B., Zhang, X., Chen, S., Li, A., Jia, X., Zhang, J., Chen, W., Chen, J., Sun, Q., Li, X., Gong, H., & Yuan, J. (2022). Multicolor high-resolution whole-brain imaging for acquiring and comparing the brain-wide distributions of type-specific and projection-specific neurons with anatomical annotation in the same brain. *Frontiers in Neuroscience*, *16*. https://doi.org/10.3389/fnins.2022.1033880

Dowdle, W. E., Robinson, J. F., Kneist, A., Sirerol-Piquer, M. S., Frints, S. G., Corbit, K. C., Zaghloul, N. A., van Lijnschoten, G., Mulders, L., Verver, D. E., Zerres, K., Reed, R. R., Attie-Bitach, T., Johnson, C. A., Garcia-

Verdugo, J. M., Katsanis, N., Bergmann, C., & Reiter, J. F. (2011). Disruption of a ciliary B9 protein complex causes Meckel syndrome. *Am J Hum Genet*, *89*(1), 94-110. https://doi.org/10.1016/j.ajhg.2011.06.003

Duan, W., Zhang, Y.-P., Hou, Z., Huang, C., Zhu, H., Zhang, C.-Q., & Yin, Q. (2016). Novel Insights into NeuN: from Neuronal Marker to Splicing Regulator. *Molecular Neurobiology*, *53*(3), 1637-1647. https://doi.org/10.1007/s12035-015-9122-5

Dubowitz, V. (1964). INFANTILE MUSCULAR ATROPHY A PROSPECTIVE STUDY WITH PARTICULAR REFERENCE TO A SLOWLY PROGRESSIVE VARIETY. *Brain*, *87*(4), 707-718. https://doi.org/10.1093/brain/87.4.707

Dubowitz, V. (1995). Chaos in the classification of SMA: a possible resolution. *Neuromuscul Disord*, *5*(1), 3-5. https://doi.org/10.1016/0960-8966(94)00075-k

Dubowitz, V. (1999). Very severe spinal muscular atrophy (SMA type 0): an expanding clinical phenotype. *Eur J Paediatr Neurol*, *3*(2), 49-51. https://doi.org/10.1053/ejpn.1999.0181

Dubowitz, V. (2009). Ramblings in the history of spinal muscular atrophy. *Neuromuscul Disord*, *19*(1), 69-73. https://doi.org/10.1016/j.nmd.2008.10.004

Eguether, T., Cordelieres, F. P., & Pazour, G. J. (2018). Intraflagellar transport is deeply integrated in hedgehog signaling. *Molecular Biology of the Cell*, *29*(10), 1178-1189. https://doi.org/10.1091/mbc.e17-10-0600

Elawad, O. A. M. A., Dafallah, M. A., Ahmed, M. M. M., Albashir, A. A. D., Abdalla, S. M. A., Yousif, H. H. M., Daw Elbait, A. A. E., Mohammed, M. E., Ali, H. I. H., Ahmed, M. M. M., Mohammed, N. F. N., Osman, F. H. M., Mohammed, M. A. Y., & Abu Shama, E. A. E. (2022). Bardet–Biedl syndrome: a case series. *Journal of Medical Case Reports*, *16*(1). https://doi.org/10.1186/s13256-022-03396-6

Ellenbroek, B., & Youn, J. (2016). Rodent models in neuroscience research: is it a rat race? *Disease Models & Mechanisms*, *9*(10), 1079-1087. https://doi.org/10.1242/dmm.026120

Feldkötter, M., Schwarzer, V., Wirth, R., Wienker, T. F., & Wirth, B. (2002). Quantitative Analyses of SMN1 and SMN2 Based on Real-Time LightCycler PCR: Fast and Highly Reliable Carrier Testing and Prediction of Severity of Spinal Muscular Atrophy. *The American Journal of Human Genetics*, *70*(2), 358-368. https://doi.org/10.1086/338627

Felsenthal, N., & Zelzer, E. (2017). Mechanical regulation of musculoskeletal system development. *Development*, *144*(23), 4271-4283. https://doi.org/10.1242/dev.151266

Ferent, J., & Traiffort, E. (2015). Hedgehog: Multiple Paths for Multiple Roles in Shaping the Brain and Spinal Cord. *Neuroscientist*, *21*(4), 356-371. https://doi.org/10.1177/1073858414531457

Ferrante, L., Melendez-Zaidi, A., Lindsey, W., & Lotze, T. (2022). Novel use of nusinersen as a therapeutic bridge to onasemnogene abeparvovec-xioi in a premature neonate with type 1 spinal muscular atrophy [Letter]. *Muscle and Nerve*, *66*(2), E8-E10. https://doi.org/10.1002/mus.27648

Finkel, R. S., Chiriboga, C. A., Vajsar, J., Day, J. W., Montes, J., De Vivo, D. C., Yamashita, M., Rigo, F., Hung, G., Schneider, E., Norris, D. A., Xia, S., Bennett, C. F., & Bishop, K. M. (2016). Treatment of infantile-onset spinal muscular atrophy with nusinersen: a phase 2, open-label, dose-escalation study. *The Lancet*, *388*(10063), 3017-3026. https://doi.org/https://doi.org/10.1016/S0140-6736(16)31408-8

Finkel, R. S., Hughes, S. H., Parker, J., Civitello, M., Lavado, A., Mefford, H. C., Mueller, L., & Kletzl, H. (2025). Risdiplam for Prenatal Therapy of Spinal Muscular Atrophy. *New England Journal of Medicine*. https://doi.org/10.1056/nejmc2300802

Finkel, R. S., Mercuri, E., Darras, B. T., Connolly, A. M., Kuntz, N. L., Kirschner, J., Chiriboga, C. A., Saito, K., Servais, L., Tizzano, E., Topaloglu, H., Tulinius, M., Montes, J., Glanzman, A. M., Bishop, K., Zhong, Z. J., Gheuens, S., Bennett, C. F., Schneider, E., . . . De Vivo, D. C. (2017). Nusinersen versus Sham Control in Infantile-Onset Spinal Muscular Atrophy. *New England Journal of Medicine*, *377*(18), 1723-1732. https://doi.org/10.1056/nejmoa1702752

Finkel, R. S., Servais, L., Vlodavets, D., Zanoteli, E., Mazurkiewicz-Beldzinska, M., Jong, Y. J., Navas-Nazario, A., Al-Muhaizea, M., Araujo, A., Nelson, L., Wang, Y., Jaber, B., Gorni, K., Kletzl, H., Palfreeman, L., Rabbia, M., Summers, D., Gaki, E., Wagner, K. R., . . . Group, R. S. (2025). Risdiplam in Presymptomatic Spinal Muscular Atrophy. *N Engl J Med*, *393*(7), 671-682. https://doi.org/10.1056/NEJMoa2410120

Fischer, U., Liu, Q., & Dreyfuss, G. (1997). The SMN–SIP1 Complex Has an Essential Role in Spliceosomal snRNP Biogenesis. *Cell*, *90*(6), 1023-1029. https://doi.org/10.1016/s0092-8674(00)80368-2

Florea, L., Caba, L., & Gorduza, E. V. (2021). Bardet–Biedl Syndrome—Multiple Kaleidoscope Images: Insight into Mechanisms of Genotype–Phenotype Correlations. *Genes*, *12*(9), 1353. https://doi.org/10.3390/genes12091353

Foerster, P., Daclin, M., Asm, S., Faucourt, M., Boletta, A., Genovesio, A., & Spassky, N. (2017). mTORC1 signaling and primary cilia are required for brain ventricle morphogenesis. *Development*, *144*(2), 201-210. https://doi.org/10.1242/dev.138271

Fortin, N. J., Agster, K. L., & Eichenbaum, H. B. (2002). Critical role of the hippocampus in memory for sequences of events. *Nature Neuroscience*, *5*(5), 458-462. https://doi.org/10.1038/nn834

Foust, K. D., Nurre, E., Montgomery, C. L., Hernandez, A., Chan, C. M., & Kaspar, B. K. (2009). Intravascular AAV9 preferentially targets neonatal neurons and adult astrocytes. *Nature Biotechnology*, *27*(1), 59-65. https://doi.org/10.1038/nbt.1515

Fry, A. M., Leaper, M. J., & Bayliss, R. (2014). The primary cilium. *Organogenesis*, *10*(1), 62-68. https://doi.org/10.4161/org.28910

Fuentealba, L. C., Rompani, S. B., Parraguez, J. I., Obernier, K., Romero, R., Cepko, C. L., & Alvarez-Buylla, A. (2015). Embryonic Origin of Postnatal Neural Stem Cells. *Cell*, *161*(7), 1644-1655. https://doi.org/10.1016/j.cell.2015.05.041

Fuller, H. R., Gillingwater, T. H., & Wishart, T. M. (2016). Commonality amid diversity: Multi-study proteomic identification of conserved disease mechanisms in spinal muscular atrophy. *Neuromuscular Disorders*, *26*(9), 560-569. https://doi.org/10.1016/j.nmd.2016.06.004

Gabanella, F., Butchbach, M. E. R., Saieva, L., Carissimi, C., Burghes, A. H. M., & Pellizzoni, L. (2007). Ribonucleoprotein Assembly Defects Correlate with Spinal Muscular Atrophy Severity and Preferentially Affect a Subset of Spliceosomal snRNPs. *PLoS One*, *2*(9), e921. https://doi.org/10.1371/journal.pone.0000921

Gao, Z., Ure, K., Ables, J. L., Lagace, D. C., Nave, K.-A., Goebbels, S., Eisch, A. J., & Hsieh, J. (2009). Neurod1 is essential for the survival and maturation of adult-born neurons. *Nature Neuroscience*, *12*(9), 1090-1092. https://doi.org/10.1038/nn.2385

Gerdes, J., Lemke, H., Baisch, H., Wacker, H. H., Schwab, U., & Stein, H. (1984). Cell cycle analysis of a cell proliferation-associated human nuclear antigen defined by the monoclonal antibody Ki-67. *J Immunol*, *133*(4), 1710-1715. https://www.ncbi.nlm.nih.gov/pubmed/6206131

Giannotta, G., Ruggiero, M., De Rinaldis, M., & Trabacca, A. (2024). Exploring variability in cognitive functioning in patients with spinal muscular atrophy: a scoping review. *Neurological Sciences*, *45*(8), 3699-3710. https://doi.org/10.1007/s10072-024-07503-x

Gilliam, T. C., Brzustowicz, L. M., Castilla, L. H., Lehner, T., Penchaszadeh, G. K., Daniels, R. J., Byth, B. C., Knowles, J., Hislop, J. E., Shapira, Y., Dubowitz, V., Munsat, T. L., Ott, J., & Davies, K. E. (1990). Genetic homogeneity between acute and chronic forms of spinal muscular atrophy. *Nature*, *345*(6278), 823-825. https://doi.org/10.1038/345823a0

Gillingwater, T. H., McWilliam, C., Horrocks, I., McWilliam, K., Hamilton, M., Fletcher, E., Williams, N., Smith, S., & Parson, S. H. (2022). A call to introduce newborn screening for spinal muscular atrophy (SMA) in Scotland. *Scott Med J*, *67*(1), 46-47. https://doi.org/10.1177/00369330221078994

Goedeker, N. L., Rogers, A., Fisher, M., Arya, K., Brandsema, J. F., Farah, H., Farrar, M. A., Felker, M. V., Gibbons, M., Hamid, O. A., Harmelink, M., Herbert, K., Kichula, E., King, K., Lakhotia, A., Lee, B. H., Kuntz, N. L., Parsons, J., Rehborg, R., . . . Zaidman, C. M. (2024). Outcomes of early-treated infants with spinal muscular atrophy: A multicenter, retrospective cohort study. *Muscle Nerve*, *70*(6), 1247-1256. https://doi.org/10.1002/mus.28267

Gopalakrishnan, J., Feistel, K., Friedrich, B. M., Grapin-Botton, A., Jurisch-Yaksi, N., Mass, E., Mick, D. U., Müller, R. U., May-Simera, H., Schermer, B., Schmidts, M., Walentek, P., & Wachten, D. (2023). Emerging principles of primary cilia dynamics in controlling tissue organization and function. *The EMBO Journal*, *42*(21). https://doi.org/10.15252/embj.2023113891

Groen, E. J. N., Perenthaler, E., Courtney, N. L., Jordan, C. Y., Shorrock, H. K., van der Hoorn, D., Huang, Y. T., Murray, L. M., Viero, G., & Gillingwater, T. H. (2018). Temporal and tissue-specific variability of SMN protein levels in mouse models of spinal muscular atrophy. *Hum Mol Genet*, *27*(16), 2851-2862. https://doi.org/10.1093/hmg/ddy195

Groen, E. J. N., Talbot, K., & Gillingwater, T. H. (2018). Advances in therapy for spinal muscular atrophy: promises and challenges. *Nature Reviews Neurology*, *14*(4), 214-224. https://doi.org/10.1038/nrneurol.2018.4

Groulx-Boivin, E., Oliveira-Carneiro, A., Carlson, H., Floer, A., Kirton, A., Mah, J., Saint-Martin, C., La Piana, R., & Oskoui, M. (2024). Macrostructural Brain Abnormalities in Spinal Muscular Atrophy: A Case-Control Study. *Neurol Genet*, *10*(5), e200193. https://doi.org/10.1212/NXG.0000000000200193

Grove, E. A. (1999). Patterning Events and Specification Signals in the Developing Hippocampus. *Cerebral Cortex*, *9*(6), 551-561. https://doi.org/10.1093/cercor/9.6.551

Hamilton, G., & Gillingwater, T. H. (2013). Spinal muscular atrophy: going beyond the motor neuron. *Trends Mol Med*, *19*(1), 40-50. https://doi.org/10.1016/j.molmed.2012.11.002

Haque, U. S., & Yokota, T. (2024). Recent Progress in Gene-Targeting Therapies for Spinal Muscular Atrophy: Promises and Challenges. *Genes*, *15*(8), 999. https://doi.org/10.3390/genes15080999

Hardee, I., Soldatos, A., Davids, M., Vilboux, T., Toro, C., David, K. L., Ferreira, C. R., Nehrebecky, M., Snow, J., Thurm, A., Heller, T., Macnamara, E. F., Gunay-Aygun, M., Zein, W. M., Gahl, W. A., & Malicdan, M. C. V. (2017). Defective ciliogenesis in INPP5E-related Joubert syndrome. *American Journal of Medical Genetics Part A*, *173*(12), 3231-3237. https://doi.org/10.1002/ajmg.a.38376

Harding, B. N., Kariya, S., Monani, U. R., Chung, W. K., Benton, M., Yum, S. W., Tennekoon, G., & Finkel, R. S. (2015). Spectrum of Neuropathophysiology in Spinal Muscular Atrophy Type I. *Journal of Neuropathology & Experimental Neurology*, *74*(1), 15-24. https://doi.org/10.1097/nen.0000000000000144

Hardwick, L. J. A., Ali, F. R., Azzarelli, R., & Philpott, A. (2015). Cell cycle regulation of proliferation versus differentiation in the central nervous system. *Cell and Tissue Research*, *359*(1), 187-200. https://doi.org/10.1007/s00441-014-1895-8

Hartill, V., Szymanska, K., Sharif, S. M., Wheway, G., & Johnson, C. A. (2017). Meckel–Gruber Syndrome: An Update on Diagnosis, Clinical Management, and Research Advances. *Frontiers in Pediatrics*, *5*. https://doi.org/10.3389/fped.2017.00244

Hensel, N., Stockbrugger, I., Rademacher, S., Broughton, N., Brinkmann, H., Grothe, C., & Claus, P. (2014). Bilateral crosstalk of rho- and extracellular-signal-regulated-kinase (ERK) pathways is confined to an unidirectional mode in spinal muscular atrophy (SMA). *Cell Signal*, *26*(3), 540-548. https://doi.org/10.1016/j.cellsig.2013.11.027

Hernandez-Hernandez, V., Pravincumar, P., Diaz-Font, A., May-Simera, H., Jenkins, D., Knight, M., & Beales, P. L. (2013). Bardet–Biedl syndrome proteins control the cilia length through regulation of actin polymerization. *Human Molecular Genetics*, *22*(19), 3858-3868. https://doi.org/10.1093/hmg/ddt241

Hildebrandt, F., Benzing, T., & Katsanis, N. (2011). Ciliopathies. *New England Journal of Medicine*, *364*(16), 1533-1543. https://doi.org/10.1056/nejmra1010172

Hinderer, C., Katz, N., Buza, E. L., Dyer, C., Goode, T., Bell, P., Richman, L. K., & Wilson, J. M. (2018). Severe Toxicity in Nonhuman Primates and

Piglets Following High-Dose Intravenous Administration of an Adeno-Associated Virus Vector Expressing Human SMN [Article]. *Human Gene Therapy*, *29*(3), 285-298. https://doi.org/10.1089/hum.2018.015

Hoey, D. A., Downs, M. E., & Jacobs, C. R. (2012). The mechanics of the primary cilium: An intricate structure with complex function. *Journal of Biomechanics*, *45*(1), 17-26. https://doi.org/10.1016/j.jbiomech.2011.08.008

Hoffmann, J. (1893). Ueber chronische spinale Muskelatrophie im Kindesalter, auf familiärer Basis. *Deutsche Zeitschrift für Nervenheilkunde*, *3*(6), 427-470. https://doi.org/10.1007/bf01668496

Hoffmann, J. (1897). Weiterer Beitrag zur Lehre von der hereditären progressiven spinalen Muskelatrophie im Kindesalter. *Deutsche Zeitschrift für Nervenheilkunde*, *10*(3-4), 292-320. https://doi.org/10.1007/bf01668174

Holt, C. E., Martin, K. C., & Schuman, E. M. (2019). Local translation in neurons: visualization and function. *Nature Structural & Molecular Biology*, *26*(7), 557-566. https://doi.org/10.1038/s41594-019-0263-5

Hsieh-Li, H. M., Chang, J.-G., Jong, Y.-J., Wu, M.-H., Wang, N. M., Tsai, C. H., & Li, H. (2000). A mouse model for spinal muscular atrophy. *Nature Genetics*, *24*(1), 66-70. https://doi.org/10.1038/71709

Hua, Y., Sahashi, K., Hung, G., Rigo, F., Passini, M. A., Bennett, C. F., & Krainer, A. R. (2010). Antisense correction of SMN2 splicing in the CNS rescues necrosis in a type III SMA mouse model. *Genes & Development*, *24*(15), 1634-1644. https://doi.org/10.1101/gad.1941310

Hua, Y., Vickers, T. A., Okunola, H. L., Bennett, C. F., & Krainer, A. R. (2008). Antisense Masking of an hnRNP A1/A2 Intronic Splicing Silencer Corrects SMN2 Splicing in Transgenic Mice. *The American Journal of Human Genetics*, *82*(4), 834-848. https://doi.org/10.1016/j.ajhg.2008.01.014

Ingolia, N. T. (2014). Ribosome profiling: new views of translation, from single codons to genome scale. *Nature Reviews Genetics*, *15*(3), 205-213. https://doi.org/10.1038/nrg3645

Ingolia, N. T., Ghaemmaghami, S., Newman, J. R. S., & Weissman, J. S. (2009). Genome-Wide Analysis in Vivo of Translation with Nucleotide Resolution Using Ribosome Profiling. *Science*, *324*(5924), 218-223. https://doi.org/10.1126/science.1168978

Ishii, S., Sasaki, T., Mohammad, S., Hwang, H., Tomy, E., Somaa, F., Ishibashi, N., Okano, H., Rakic, P., Hashimoto-Torii, K., & Torii, M. (2021). Primary cilia safeguard cortical neurons in neonatal mouse forebrain from

environmental stress-induced dendritic degeneration. *Proc Natl Acad Sci U S A*, *118*(1). https://doi.org/10.1073/pnas.2012482118

Jain, R., Pan, J., Driscoll, J. A., Wisner, J. W., Huang, T., Gunsten, S. P., You, Y., & Brody, S. L. (2010). Temporal Relationship between Primary and Motile Ciliogenesis in Airway Epithelial Cells. *American Journal of Respiratory Cell and Molecular Biology*, *43*(6), 731-739. https://doi.org/10.1165/rcmb.2009-0328oc

Jamur, M. C., & Oliver, C. (2010). Permeabilization of Cell Membranes. In (pp. 63-66). Humana Press. https://doi.org/10.1007/978-1-59745-324-0_9

Jensen, V. L., & Leroux, M. R. (2017). Gates for soluble and membrane proteins, and two trafficking systems (IFT and LIFT), establish a dynamic ciliary signaling compartment. *Curr Opin Cell Biol*, *47*, 83-91. https://doi.org/10.1016/j.ceb.2017.03.012

Jiang, T., Gong, H., & Yuan, J. (2023). Whole-brain Optical Imaging: A Powerful Tool for Precise Brain Mapping at the Mesoscopic Level. *Neuroscience Bulletin*, *39*(12), 1840-1858. https://doi.org/10.1007/s12264-023-01112-y

Jin, H. Y., & Xiao, C. (2018). An Integrated Polysome Profiling and Ribosome Profiling Method to Investigate In Vivo Translatome. In (pp. 1-18). Springer New York. https://doi.org/10.1007/978-1-4939-7514-3_1

Kakazu, J., Walker, N. L., Babin, K. C., Trettin, K. A., Lee, C., Sutker, P. B., Kaye, A. M., & Kaye, A. D. (2021). Risdiplam for the Use of Spinal Muscular Atrophy. *Orthopedic Reviews*, *13*(2). https://doi.org/10.52965/001c.25579

Karalis, V., Donovan, K. E., & Sahin, M. (2022). Primary Cilia Dysfunction in Neurodevelopmental Disorders beyond Ciliopathies. *J Dev Biol*, *10*(4). https://doi.org/10.3390/jdb10040054

Karyka, E., Berrueta Ramirez, N., Webster, C. P., Marchi, P. M., Graves, E. J., Godena, V. K., Marrone, L., Bhargava, A., Ray, S., Ning, K., Crane, H., Hautbergue, G. M., El-Khamisy, S. F., & Azzouz, M. (2022). SMN-deficient cells exhibit increased ribosomal DNA damage. *Life Science Alliance*, *5*(8), e202101145. https://doi.org/10.26508/lsa.202101145

Kataoka, M., Sahashi, K., Tsujikawa, K., Takeda, J. I., Hirunagi, T., Iida, M., & Katsuno, M. (2023). Dysregulation of Aldh1a2 underlies motor neuron degeneration in spinal muscular atrophy. *Neurosci Res*, *194*, 58-65. https://doi.org/10.1016/j.neures.2023.04.007

Khaniani, M. S., Derakhshan, S. M., & Abasalizadeh, S. (2013). Prenatal diagnosis of spinal muscular atrophy: clinical experience and molecular genetics of SMN gene analysis in 36 cases. *J Prenat Med*, *7*(3), 32-34.

Kim, Y. J., & Kim, J. (2019). Therapeutic perspectives for structural and functional abnormalities of cilia. *Cellular and Molecular Life Sciences*, *76*(19), 3695-3709. https://doi.org/10.1007/s00018-019-03158-6

Kletzl, H., Marquet, A., Günther, A., Tang, W., Heuberger, J., Groeneveld, G. J., Birkhoff, W., Mercuri, E., Lochmüller, H., Wood, C., Fischer, D., Gerlach, I., Heinig, K., Bugawan, T., Dziadek, S., Kinch, R., Czech, C., & Khwaja, O. (2019). The oral splicing modifier RG7800 increases full length survival of motor neuron 2 mRNA and survival of motor neuron protein: Results from trials in healthy adults and patients with spinal muscular atrophy. *Neuromuscular Disorders*, *29*(1), 21-29. https://doi.org/https://doi.org/10.1016/j.nmd.2018.10.001

Ko, H.-W. (2012). The primary cilium as a multiple cellular signaling scaffold in development and disease. *BMB Reports*, *45*(8), 427-432. https://doi.org/10.5483/bmbrep.2012.45.8.167

Kokaliaris, C., Evans, R., Hawkins, N., Mahajan, A., Scott, D. A., Sutherland, C. S., Nam, J., & Sajeev, G. (2024). Long-Term Comparative Efficacy and Safety of Risdiplam and Nusinersen in Children with Type 1 Spinal Muscular Atrophy. *Advances in Therapy*, *41*(6), 2414-2434. https://doi.org/10.1007/s12325-024-02845-6

Kölbel, H., Kopka, M., Modler, L., Blaschek, A., Schara-Schmidt, U., Vill, K., Schwartz, O., & Müller-Felber, W. (2024). Impaired Neurodevelopment in Children with 5q-SMA - 2 Years After Newborn Screening. *Journal of Neuromuscular Diseases*, *11*(1), 143-151. https://doi.org/10.3233/jnd-230136

Kong, L., Valdivia, D. O., Simon, C. M., Hassinan, C. W., Delestree, N., Ramos, D. M., Park, J. H., Pilato, C. M., Xu, X., Crowder, M., Grzyb, C. C., King, Z. A., Petrillo, M., Swoboda, K. J., Davis, C., Lutz, C. M., Stephan, A. H., Zhao, X., Weetall, M., . . . Sumner, C. J. (2021). Impaired prenatal motor axon development necessitates early therapeutic intervention in severe SMA. *Sci Transl Med*, *13*(578). https://doi.org/10.1126/scitranslmed.abb6871

Krämer, A., Green, J., Pollard, J., & Tugendreich, S. (2014). Causal analysis approaches in Ingenuity Pathway Analysis. *Bioinformatics*, *30*(4), 523-530. https://doi.org/10.1093/bioinformatics/btt703

Kugelberg, E. (1956). Heredofamilial Juvenile muscular Atrophy Simulating muscular Dystrophy. *Archives of Neurology And Psychiatry*, *75*(5), 500. https://doi.org/10.1001/archneurpsyc.1956.02330230050005

Kumamoto, N., Gu, Y., Wang, J., Janoschka, S., Takemaru, K., Levine, J., & Ge, S. (2012). A role for primary cilia in glutamatergic synaptic integration of adult-born neurons. *Nat Neurosci*, *15*(3), 399-405, S391. https://doi.org/10.1038/nn.3042

Lang, M., Colby, S., Ashby-Padial, C., Bapna, M., Jaimes, C., Rincon, S. P., & Buch, K. (2024). An imaging review of the hippocampus and its common pathologies. *Journal of Neuroimaging*, *34*(1), 5-25. https://doi.org/10.1111/jon.13165

Larkins, C. E., Aviles, G. D. G., East, M. P., Kahn, R. A., & Caspary, T. (2011). Arl13b regulates ciliogenesis and the dynamic localization of Shh signaling proteins. *Molecular Biology of the Cell*, *22*(23), 4694-4703. https://doi.org/10.1091/mbc.e10-12-0994

Lauria, F., Bernabò, P., Tebaldi, T., Groen, E. J. N., Perenthaler, E., Maniscalco, F., Rossi, A., Donzel, D., Clamer, M., Marchioretto, M., Omersa, N., Orri, J., Dalla Serra, M., Anderluh, G., Quattrone, A., Inga, A., Gillingwater, T. H., & Viero, G. (2020). SMN-primed ribosomes modulate the translation of transcripts related to spinal muscular atrophy. *Nature Cell Biology*, *22*(10), 1239-1251. https://doi.org/10.1038/s41556-020-00577-7

Lauria, F., Tebaldi, T., Bernabò, P., Groen, E. J. N., Gillingwater, T. H., & Viero, G. (2018). riboWaltz: Optimization of ribosome P-site positioning in ribosome profiling data. *PLOS Computational Biology*, *14*(8), e1006169. https://doi.org/10.1371/journal.pcbi.1006169

Le, T. T., Pham, L. T., Butchbach, M. E., Zhang, H. L., Monani, U. R., Coovert, D. D., Gavrilina, T. O., Xing, L., Bassell, G. J., & Burghes, A. H. (2005). SMNDelta7, the major product of the centromeric survival motor neuron (SMN2) gene, extends survival in mice with spinal muscular atrophy and associates with full-length SMN. *Hum Mol Genet*, *14*(6), 845-857. https://doi.org/10.1093/hmg/ddi078

Lee, B., Panda, S., & Lee, H. Y. (2020). Primary Ciliary Deficits in the Dentate Gyrus of Fragile X Syndrome. *Stem Cell Reports*, *15*(2), 454-466. https://doi.org/10.1016/j.stemcr.2020.07.001

Lee, B. H., Waldrop, M. A., Connolly, A. M., & Ciafaloni, E. (2021). Time is muscle: A recommendation for early treatment for preterm infants with spinal muscular atrophy. *Muscle & Nerve*, *64*(2), 153-155. https://doi.org/10.1002/mus.27261

Lefebvre, S., Burglen, L., Reboullet, S., Clermont, O., Burlet, P., Viollet, L., Benichou, B., Cruaud, C., Millasseau, P., Zeviani, M., & et al. (1995). Identification and characterization of a spinal muscular atrophy-determining gene. *Cell*, *80*(1), 155-165. https://doi.org/10.1016/0092-8674(95)90460-3

Lefebvre, S., Burlet, P., Liu, Q., Bertrandy, S., Clermont, O., Munnich, A., Dreyfuss, G., & Melki, J. (1997). Correlation between severity and SMN protein level in spinal muscular atrophy. *Nature Genetics*, *16*(3), 265-269. https://doi.org/10.1038/ng0797-265

Liu, Q., Fischer, U., Wang, F., & Dreyfuss, G. (1997). The Spinal Muscular Atrophy Disease Gene Product, SMN, and Its Associated Protein SIP1 Are in a Complex with Spliceosomal snRNP Proteins. *Cell*, *90*(6), 1013-1021. https://doi.org/10.1016/s0092-8674(00)80367-0

Lorson, C. L., & Androphy, E. J. (2000). An exonic enhancer is required for inclusion of an essential exon in the SMA-determining gene SMN. *Hum Mol Genet*, *9*(2), 259-265. https://doi.org/10.1093/hmg/9.2.259

Lorson, C. L., Hahnen, E., Androphy, E. J., & Wirth, B. (1999). A single nucleotide in the SMN gene regulates splicing and is responsible for spinal muscular atrophy. *Proceedings of the National Academy of Sciences*, *96*(11), 6307-6311. https://doi.org/10.1073/pnas.96.11.6307

Lovera, M., & Lüders, J. (2021). The ciliary impact of nonciliary gene mutations. *Trends in Cell Biology*, *31*(11), 876-887. https://doi.org/10.1016/j.tcb.2021.06.001

Ma, R., Kutchy, N. A., Chen, L., Meigs, D. D., & Hu, G. (2022). Primary cilia and ciliary signaling pathways in aging and age-related brain disorders. *Neurobiol Dis*, *163*, 105607. https://doi.org/10.1016/j.nbd.2021.105607

Ma, Y., He, J., Li, S., Yao, D., Huang, C., Wu, J., & Lei, M. (2023). Structural insight into the intraflagellar transport complex IFT-A and its assembly in the anterograde IFT train. *Nature Communications*, *14*(1). https://doi.org/10.1038/s41467-023-37208-2

MacLeod, M. J., Taylor, J. E., Lunt, P. W., Mathew, C. G., & Robb, S. A. (1999). Prenatal onset spinal muscular atrophy. *Eur J Paediatr Neurol*, *3*(2), 65-72. https://doi.org/10.1053/ejpn.1999.0184

Mailman, M. D., Heinz, J. W., Papp, A. C., Snyder, P. J., Sedra, M. S., Wirth, B., Burghes, A. H. M., & Prior, T. W. (2002). Molecular analysis of spinal muscular atrophy and modification of the phenotype by SMN2. *Genetics in Medicine*, *4*(1), 20-26. https://doi.org/10.1097/00125817-200201000-00004

Mandyam, C. D., Harburg, G. C., & Eisch, A. J. (2007). Determination of key aspects of precursor cell proliferation, cell cycle length and kinetics in the adult mouse subgranular zone. *Neuroscience*, *146*(1), 108-122. https://doi.org/10.1016/j.neuroscience.2006.12.064

Martin, M. (2011). Cutadapt removes adapter sequences from high-throughput sequencing reads [next generation sequencing; small RNA; microRNA; adapter removal]. *2011*, *17*(1), 3. https://doi.org/10.14806/ej.17.1.200

Martínez-Hernández, R., Bernal, S., Also-Rallo, E., Alías, L., Barceló, M., Hereu, M., Esquerda, J. E., & Tizzano, E. F. (2013). Synaptic defects in

type I spinal muscular atrophy in human development. *The Journal of Pathology*, *229*(1), 49-61. https://doi.org/10.1002/path.4080

Martynoga, B., Drechsel, D., & Guillemot, F. (2012). Molecular control of neurogenesis: a view from the mammalian cerebral cortex. *Cold Spring Harb Perspect Biol*, *4*(10). https://doi.org/10.1101/cshperspect.a008359

Masson, R., Brusa, C., Scoto, M., & Baranello, G. (2021). Brain, cognition, and language development in spinal muscular atrophy type 1: a scoping review. *Developmental Medicine & Child Neurology*, *63*(5), 527-536. https://doi.org/10.1111/dmcn.14798

Matera, A. G., & Wang, Z. (2014). A day in the life of the spliceosome. *Nature Reviews Molecular Cell Biology*, *15*(2), 108-121. https://doi.org/10.1038/nrm3742

Matesanz, S. E., Curry, C., Gross, B., Rubin, A. I., Linn, R., Yum, S. W., & Kichula, E. A. (2020). Clinical Course in a Patient With Spinal Muscular Atrophy Type 0 Treated With Nusinersen and Onasemnogene Abeparvovec. *J Child Neurol*, *35*(11), 717-723. https://doi.org/10.1177/0883073820928784

McCarthy, D. J., Chen, Y., & Smyth, G. K. (2012). Differential expression analysis of multifactor RNA-Seq experiments with respect to biological variation. *Nucleic Acids Research*, *40*(10), 4288-4297. https://doi.org/10.1093/nar/gks042

McGovern, V. L., Gavrilina, T. O., Beattie, C. E., & Burghes, A. H. M. (2008). Embryonic motor axon development in the severe SMA mouse. *Human Molecular Genetics*, *17*(18), 2900-2909. https://doi.org/10.1093/hmg/ddn189

McLean, Z. L., Gao, D., Correia, K., Roy, J. C. L., Shibata, S., Farnum, I. N., Valdepenas-Mellor, Z., Kovalenko, M., Rapuru, M., Morini, E., Ruliera, J., Gillis, T., Lucente, D., Kleinstiver, B. P., Lee, J.-M., Macdonald, M. E., Wheeler, V. C., Mouro Pinto, R., & Gusella, J. F. (2024). Splice modulators target PMS1 to reduce somatic expansion of the Huntington's disease-associated CAG repeat. *Nature Communications*, *15*(1). https://doi.org/10.1038/s41467-024-47485-0

McPheron, M. A., & Felker, M. V. (2024). Clinical perspectives: Treating spinal muscular atrophy. *Mol Ther*, *32*(8), 2489-2504. https://doi.org/10.1016/j.ymthe.2024.06.020

Mecklenburg, N., Kowalczyk, I., Witte, F., Gorne, J., Laier, A., Mamo, T. M., Gonschior, H., Lehmann, M., Richter, M., Sporbert, A., Purfurst, B., Hubner, N., & Hammes, A. (2021). Identification of disease-relevant modulators of the SHH pathway in the developing brain. *Development*, *148*(17). https://doi.org/10.1242/dev.199307

Melki, J., Abdelhak, S., Sheth, P., Bachelot, M. F., Burlet, P., Marcadet, A., Aicardi, J., Barois, A., Carriere, J. P., Fardeau, M., Fontan, D., Ponsot, G., Billette, T., Angelini, C., Barbosa, C., Ferriere, G., Lanzi, G., Ottolini, A., Babron, M. C., . . . Frezal, J. (1990). Gene for chronic proximal spinal muscular atrophies maps to chromosome 5q. *Nature*, *344*(6268), 767-768. https://doi.org/10.1038/344767a0

Mendell, J. R., Al-Zaidy, S., Shell, R., Arnold, W. D., Rodino-Klapac, L. R., Prior, T. W., Lowes, L., Alfano, L., Berry, K., Church, K., Kissel, J. T., Nagendran, S., L'Italien, J., Sproule, D. M., Wells, C., Cardenas, J. A., Heitzer, M. D., Kaspar, A., Corcoran, S., . . . Kaspar, B. K. (2017). Single-Dose Gene-Replacement Therapy for Spinal Muscular Atrophy. *New England Journal of Medicine*, *377*(18), 1713-1722. https://doi.org/10.1056/nejmoa1706198

Mendonça, R. H., Rocha, A. J., Lozano-Arango, A., Diaz, A. B., Castiglioni, C., Silva, A. M. S., Reed, U. C., Kulikowski, L., Paramonov, I., Cuscó, I., Tizzano, E. F., & Zanoteli, E. (2019). Severe brain involvement in 5q spinal muscular atrophy type 0. *Annals of Neurology*, *86*(3), 458-462. https://doi.org/10.1002/ana.25549

Mercuri, E., Darras, B. T., Chiriboga, C. A., Day, J. W., Campbell, C., Connolly, A. M., Iannaccone, S. T., Kirschner, J., Kuntz, N. L., Saito, K., Shieh, P. B., Tulinius, M., Mazzone, E. S., Montes, J., Bishop, K. M., Yang, Q., Foster, R., Gheuens, S., Bennett, C. F., & Farwell, W. (2018). Nusinersen versus Sham Control in Later-Onset Spinal Muscular Atrophy. *The New England journal of medicine.*, *378*(7), 625-635. https://doi.org/10.1056/NEJMoa1710504

Mercuri, E., Finkel, R., Montes, J., Mazzone, E. S., Sormani, M. P., Main, M., Ramsey, D., Mayhew, A., Glanzman, A. M., Dunaway, S., Salazar, R., Pasternak, A., Quigley, J., Pane, M., Pera, M. C., Scoto, M., Messina, S., Sframeli, M., Vita, G. L., . . . De Vivo, D. C. (2016). Patterns of disease progression in type 2 and 3 SMA: Implications for clinical trials. *Neuromuscul Disord*, *26*(2), 126-131. https://doi.org/10.1016/j.nmd.2015.10.006

Mercuri, E., Finkel, R. S., Muntoni, F., Wirth, B., Montes, J., Main, M., Mazzone, E. S., Vitale, M., Snyder, B., Quijano-Roy, S., Bertini, E., Davis, R. H., Meyer, O. H., Simonds, A. K., Schroth, M. K., Graham, R. J., Kirschner, J., Iannaccone, S. T., Crawford, T. O., . . . Szlagatys-Sidorkiewicz, A. (2018). Diagnosis and management of spinal muscular atrophy: Part 1: Recommendations for diagnosis, rehabilitation, orthopedic and nutritional care. *Neuromuscular Disorders*, *28*(2), 103-115. https://doi.org/10.1016/j.nmd.2017.11.005

Meyer, K., Ferraiuolo, L., Schmelzer, L., Braun, L., McGovern, V., Likhite, S., Michels, O., Govoni, A., Fitzgerald, J., Morales, P., Foust, K. D., Mendell, J. R., Burghes, A. H. M., & Kaspar, B. K. (2015). Improving

Single Injection CSF Delivery of AAV9-mediated Gene Therapy for SMA: A Dose–response Study in Mice and Nonhuman Primates. *Molecular Therapy*, *23*(3), 477-487. https://doi.org/https://doi.org/10.1038/mt.2014.210

Mill, P., Christensen, S. T., & Pedersen, L. B. (2023). Primary cilia as dynamic and diverse signalling hubs in development and disease. *Nature Reviews Genetics*, *24*(7), 421-441. https://doi.org/10.1038/s41576-023-00587-9

Miranda-Negrón, Y., & García-Arrarás, J. E. (2022). Radial glia and radial glia-like cells: Their role in neurogenesis and regeneration. *Frontiers in Neuroscience*, *16*. https://doi.org/10.3389/fnins.2022.1006037

Mirzadeh, Z., Han, Y.-G., Soriano-Navarro, M., García-Verdugo, J. M., & Alvarez-Buylla, A. (2010). Cilia Organize Ependymal Planar Polarity. *The Journal of Neuroscience*, *30*(7), 2600-2610. https://doi.org/10.1523/jneurosci.3744-09.2010

Monani, U. R. (2000). The human centromeric survival motor neuron gene (SMN2) rescues embryonic lethality in Smn-/- mice and results in a mouse with spinal muscular atrophy. *Human Molecular Genetics*, *9*(3), 333-339. https://doi.org/10.1093/hmg/9.3.333

Monani, U. R., Lorson, C. L., Parsons, D. W., Prior, T. W., Androphy, E. J., Burghes, A. H., & McPherson, J. D. (1999). A single nucleotide difference that alters splicing patterns distinguishes the SMA gene SMN1 from the copy gene SMN2. *Hum Mol Genet*, *8*(7), 1177-1183. https://doi.org/10.1093/hmg/8.7.1177

Montagrin, A., Saiote, C., & Schiller, D. (2018). The social hippocampus. *Hippocampus*, *28*(9), 672-679. https://doi.org/10.1002/hipo.22797

Montes, J., McDermott, M. P., Mirek, E., Mazzone, E. S., Main, M., Glanzman, A. M., Duong, T., Young, S. D., Salazar, R., Pasternak, A., Gee, R., De Sanctis, R., Coratti, G., Forcina, N., Fanelli, L., Ramsey, D., Milev, E., Civitello, M., Pane, M., . . . Mercuri, E. (2018). Ambulatory function in spinal muscular atrophy: Age-related patterns of progression. *PLoS One*, *13*(6), e0199657. https://doi.org/10.1371/journal.pone.0199657

Moreno-Mateos, M. A., Espina, Á. G., Torres, B., Del Estal, M. M. G., Romero-Franco, A., Ríos, R. M., & Pintor-Toro, J. A. (2011). PTTG1/securin modulates microtubule nucleation and cell migration. *Molecular Biology of the Cell*, *22*(22), 4302-4311. https://doi.org/10.1091/mbc.e10-10-0838

Morris, R. G. M., Garrud, P., Rawlins, J. N. P., & O'Keefe, J. (1982). Place navigation impaired in rats with hippocampal lesions. *Nature*, *297*(5868), 681-683. https://doi.org/10.1038/297681a0

Motyl, A. A. L., Faller, K. M. E., Groen, E. J. N., Kline, R. A., Eaton, S. L., Ledahawsky, L. M., Chaytow, H., Lamont, D. J., Wishart, T. M., Huang, Y. T., & Gillingwater, T. H. (2020). Pre-natal manifestation of systemic developmental abnormalities in spinal muscular atrophy. *Hum Mol Genet*, *29*(16), 2674-2683. https://doi.org/10.1093/hmg/ddaa146

Moultrie, F., Chiverton, L., Hatami, I., Lilien, C., & Servais, L. (2025). Pushing the boundaries: future directions in the management of spinal muscular atrophy. *Trends Mol Med*, *31*(4), 307-318. https://doi.org/10.1016/j.molmed.2024.12.006

Mugisha, N., Oliveira-Carneiro, A., Behlim, T., & Oskoui, M. (2023). Brain Magnetic Resonance Imaging (MRI) in Spinal Muscular Atrophy: A Scoping Review. *Journal of Neuromuscular Diseases*, *10*(4), 493-503. https://doi.org/10.3233/jnd-221567

Muller, O. F. (1786). *Animalcula infusoria fluvialia et marina, quae detexit, systematice descripsit et ad vivum delineari curavit Otho Fridericus Muller... sistit opus hoc posthumum quod... in lucem tradit vidua eius nobilissima, cura Othonis Fabricii*.

Munsat, T. L., & Davies, K. E. (1992). International SMA consortium meeting. (26-28 June 1992, Bonn, Germany). *Neuromuscul Disord*, *2*(5-6), 423-428. https://doi.org/10.1016/s0960-8966(06)80015-5

Munz, M., Bharioke, A., Kosche, G., Moreno-Juan, V., Brignall, A., Rodrigues, T. M., Graff-Meyer, A., Ulmer, T., Haeuselmann, S., Pavlinic, D., Ledergerber, N., Gross-Scherf, B., Rózsa, B., Krol, J., Picelli, S., Cowan, C. S., & Roska, B. (2023). Pyramidal neurons form active, transient, multilayered circuits perturbed by autism-associated mutations at the inception of neocortex. *Cell*, *186*(9), 1930-1949.e1931. https://doi.org/10.1016/j.cell.2023.03.025

Ngawa, M., Dal Farra, F., Marinescu, A.-D., & Servais, L. (2023). Longitudinal developmental profile of newborns and toddlers treated for spinal muscular atrophy. *Therapeutic Advances in Neurological Disorders*, *16*, 175628642311543. https://doi.org/10.1177/17562864231154335

Nigro, E., Grunebaum, E., Kamath, B., Licht, C., Malcolmson, C., Jeewa, A., Campbell, C., McMillan, H., Chakraborty, P., Tarnopolsky, M., & Gonorazky, H. (2023). Case report: A case of spinal muscular atrophy in a preterm infant: risks and benefits of treatment. *Frontiers in Neurology*, *14*. https://doi.org/10.3389/fneur.2023.1230889

O'Keefe, J., & Dostrovsky, J. (1971). The hippocampus as a spatial map. Preliminary evidence from unit activity in the freely-moving rat. *Brain Res*, *34*(1), 171-175. https://doi.org/10.1016/0006-8993(71)90358-1

O'Reilly, E., Stimpson, G., Rohwer, A., Milev, E., Wolfe, A., Baranello, G., Muntoni, F., & Scoto, M. (2025). Characteristics of Patients With Spinal Muscular Atrophy Who Have Switched Treatments: A Multi-Center Experience in the United Kingdom. *Muscle & Nerve*, *71*. https://doi.org/10.1002/mus.28383

O'Toole, J. F., Liu, Y., Davis, E. E., Westlake, C. J., Attanasio, M., Otto, E. A., Seelow, D., Nurnberg, G., Becker, C., Nuutinen, M., Kärppä, M., Ignatius, J., Uusimaa, J., Pakanen, S., Jaakkola, E., Van Den Heuvel, L. P., Fehrenbach, H., Wiggins, R., Goyal, M., . . . Hildebrandt, F. (2010). Individuals with mutations in XPNPEP3, which encodes a mitochondrial protein, develop a nephronophthisis-like nephropathy. *Journal of Clinical Investigation*, *120*(3), 791-802. https://doi.org/10.1172/jci40076

Oakley, B. R., Paolillo, V., & Zheng, Y. (2015). γ-Tubulin complexes in microtubule nucleation and beyond. *Molecular Biology of the Cell*, *26*(17), 2957-2962. https://doi.org/10.1091/mbc.e14-11-1514

Oechsel, K. F., & Cartwright, M. S. (2021). Combination therapy with onasemnogene and risdiplam in spinal muscular atrophy type 1. *Muscle & Nerve*, *64*(4), 487-490. https://doi.org/10.1002/mus.27375

Oskoui, M., Darras, B. T., & De Vivo, D. C. (2017). Chapter 1 - Spinal Muscular Atrophy: 125 Years Later and on the Verge of a Cure. In C. J. Sumner, S. Paushkin, & C.-P. Ko (Eds.), *Spinal Muscular Atrophy* (pp. 3-19). Academic Press. https://doi.org/https://doi.org/10.1016/B978-0-12-803685-3.00001-X

Oskoui, M., Levy, G., Garland, C. J., Gray, J. M., O'Hagen, J., De Vivo, D. C., & Kaufmann, P. (2007). The changing natural history of spinal muscular atrophy type 1. *Neurology*, *69*(20), 1931-1936. https://doi.org/10.1212/01.wnl.0000290830.40544.b9

Pagliardini, S., Giavazzi, A., Setola, V., Lizier, C., Di Luca, M., DeBiasi, S., & Battaglia, G. (2000). Subcellular localization and axonal transport of the survival motor neuron (SMN) protein in the developing rat spinal cord. *Hum Mol Genet*, *9*(1), 47-56. https://doi.org/10.1093/hmg/9.1.47

Parisi, M. A. (2009). Clinical and molecular features of Joubert syndrome and related disorders. *American Journal of Medical Genetics Part C: Seminars in Medical Genetics*, *151C*(4), 326-340. https://doi.org/10.1002/ajmg.c.30229

Park, S. M., Jang, H. J., & Lee, J. H. (2019). Roles of Primary Cilia in the Developing Brain. *Front Cell Neurosci*, *13*, 218. https://doi.org/10.3389/fncel.2019.00218

Park, S. M., Lim, J. S., Ramakrishina, S., Kim, S. H., Kim, W. K., Lee, J., Kang, H. C., Reiter, J. F., Kim, D. S., Kim, H. H., & Lee, J. H. (2018). Brain

Somatic Mutations in MTOR Disrupt Neuronal Ciliogenesis, Leading to Focal Cortical Dyslamination. *Neuron*, *99*(1), 83-97.e87. https://doi.org/10.1016/j.neuron.2018.05.039

Parker, C. C., Chen, H., Flagel, S. B., Geurts, A. M., Richards, J. B., Robinson, T. E., Solberg Woods, L. C., & Palmer, A. A. (2014). Rats are the smart choice: Rationale for a renewed focus on rats in behavioral genetics. *Neuropharmacology*, *76*, 250-258. https://doi.org/10.1016/j.neuropharm.2013.05.047

Parks, M., Court, S., Bowns, B., Cleary, S., Clokie, S., Hewitt, J., Williams, D., Cole, T., Macdonald, F., Griffiths, M., & Allen, S. (2017). Non-invasive prenatal diagnosis of spinal muscular atrophy by relative haplotype dosage. *European Journal of Human Genetics*, *25*(4), 416-422. https://doi.org/10.1038/ejhg.2016.195

Passini, M. A., Bu, J., Richards, A. M., Kinnecom, C., Sardi, S. P., Stanek, L. M., Hua, Y., Rigo, F., Matson, J., Hung, G., Kaye, E. M., Shihabuddin, L. S., Krainer, A. R., Bennett, C. F., & Cheng, S. H. (2011). Antisense oligonucleotides delivered to the mouse CNS ameliorate symptoms of severe spinal muscular atrophy [Article]. *Science Translational Medicine*, *3*(72), Article 72ra18. https://doi.org/10.1126/scitranslmed.3001777

Pellizzoni, L., Baccon, J., Charroux, B., & Dreyfuss, G. (2001). The survival of motor neurons (SMN) protein interacts with the snoRNP proteins fibrillarin and GAR1. *Current Biology*, *11*(14), 1079-1088. https://doi.org/10.1016/s0960-9822(01)00316-5

Pellizzoni, L., Kataoka, N., Charroux, B., & Dreyfuss, G. (1998). A Novel Function for SMN, the Spinal Muscular Atrophy Disease Gene Product, in Pre-mRNA Splicing. *Cell*, *95*(5), 615-624. https://doi.org/10.1016/s0092-8674(00)81632-3

Pera, M. C., Coratti, G., Pane, M., Masson, R., Sansone, V. A., D'Amico, A., Catteruccia, M., Agosto, C., Varone, A., Bruno, C., Messina, S., Ricci, F., Bruno, I., Procopio, E., Pini, A., Siliquini, S., Zanin, R., Albamonte, E., Berardinelli, A., . . . Briganti, E. (2024). Type I spinal muscular atrophy and disease modifying treatments: a nationwide study in children born since 2016. *eClinicalMedicine*, *78*, 102967. https://doi.org/10.1016/j.eclinm.2024.102967

Piepers, S., van den Berg, L. H., Brugman, F., Scheffer, H., Ruiterkamp-Versteeg, M., van Engelen, B. G., Faber, C. G., de Visser, M., van der Pol, W. L., & Wokke, J. H. (2008). A natural history study of late onset spinal muscular atrophy types 3b and 4. *J Neurol*, *255*(9), 1400-1404. https://doi.org/10.1007/s00415-008-0929-0

Poirier, A., Weetall, M., Heinig, K., Bucheli, F., Schoenlein, K., Alsenz, J., Bassett, S., Ullah, M., Senn, C., Ratni, H., Naryshkin, N., Paushkin, S., & Mueller, L. (2018). Risdiplam distributes and increases <scp>SMN</scp> protein in both the central nervous system and peripheral organs. *Pharmacology Research & Perspectives*, *6*(6), e00447. https://doi.org/10.1002/prp2.447

Polido, G. J., Barbosa, A. F., Morimoto, C. H., Caromano, F. A., Favero, F. M., Zanoteli, E., Reed, U. C., & Voos, M. C. (2017). Matching pairs difficulty in children with spinal muscular atrophy type I. *Neuromuscul Disord*, *27*(5), 419-427. https://doi.org/10.1016/j.nmd.2017.01.017

Prior, T. W., Krainer, A. R., Hua, Y., Swoboda, K. J., Snyder, P. C., Bridgeman, S. J., Burghes, A. H. M., & Kissel, J. T. (2009). A Positive Modifier of Spinal Muscular Atrophy in the SMN2 Gene. *The American Journal of Human Genetics*, *85*(3), 408-413. https://doi.org/10.1016/j.ajhg.2009.08.002

Prior, T. W., Snyder, P. J., Rink, B. D., Pearl, D. K., Pyatt, R. E., Mihal, D. C., Conlan, T., Schmalz, B., Montgomery, L., Ziegler, K., Noonan, C., Hashimoto, S., & Garner, S. (2010). Newborn and carrier screening for spinal muscular atrophy. *American Journal of Medical Genetics Part A*, *152A*(7), 1608-1616. https://doi.org/10.1002/ajmg.a.33474

Proud, C. M., Mercuri, E., Finkel, R. S., Kirschner, J., De Vivo, D. C., Muntoni, F., Saito, K., Tizzano, E. F., Desguerre, I., Quijano-Roy, S., Benguerba, K., Raju, D., Faulkner, E., & Servais, L. (2023). Combination disease-modifying treatment in spinal muscular atrophy: A proposed classification. *Annals of Clinical and Translational Neurology*, *10*(11), 2155-2160. https://doi.org/10.1002/acn3.51889

Qin, C., Bai, Y., Zeng, Z., Wang, L., Luo, Z., Wang, S., & Zou, S. (2018). The Cutting and Floating Method for Paraffin-embedded Tissue for Sectioning. *J Vis Exp*(139). https://doi.org/10.3791/58288

Qiu, C., Martin, B. K., Welsh, I. C., Daza, R. M., Le, T. M., Huang, X., Nichols, E. K., Taylor, M. L., Fulton, O., O'Day, D. R., Gomes, A. R., Ilcisin, S., Srivatsan, S., Deng, X., Disteche, C. M., Noble, W. S., Hamazaki, N., Moens, C. B., Kimelman, D., . . . Shendure, J. (2024). A single-cell time-lapse of mouse prenatal development from gastrula to birth. *Nature*, *626*(8001), 1084-1093. https://doi.org/10.1038/s41586-024-07069-w

Ramos, D. M., D'Ydewalle, C., Gabbeta, V., Dakka, A., Klein, S. K., Norris, D. A., Matson, J., Taylor, S. J., Zaworski, P. G., Prior, T. W., Snyder, P. J., Valdivia, D., Hatem, C. L., Waters, I., Gupte, N., Swoboda, K. J., Rigo, F., Bennett, C. F., Naryshkin, N., . . . Sumner, C. J. (2019). Age-dependent SMN expression in disease-relevant tissue and implications for SMA treatment. *Journal of Clinical Investigation*, *129*(11), 4817-4831. https://doi.org/10.1172/jci124120

Ramos-Vara, J. A., & Miller, M. A. (2014). When Tissue Antigens and Antibodies Get Along. *Veterinary Pathology*, *51*(1), 42-87. https://doi.org/10.1177/0300985813505879

Rao, Y. L., Ganaraja, B., Murlimanju, B. V., Joy, T., Krishnamurthy, A., & Agrawal, A. (2022). Hippocampus and its involvement in Alzheimer's disease: a review. *3 Biotech*, *12*(2). https://doi.org/10.1007/s13205-022-03123-4

Rashnonejad, A., Amini Chermahini, G., Gündüz, C., Onay, H., Aykut, A., Durmaz, B., Baka, M., Su, Q., Gao, G., & Özkınay, F. (2019). Fetal Gene Therapy Using a Single Injection of Recombinant AAV9 Rescued SMA Phenotype in Mice. *Molecular Therapy*, *27*(12), 2123-2133. https://doi.org/10.1016/j.ymthe.2019.08.017

Ratni, H., Ebeling, M., Baird, J., Bendels, S., Bylund, J., Chen, K. S., Denk, N., Feng, Z., Green, L., Guerard, M., Jablonski, P., Jacobsen, B., Khwaja, O., Kletzl, H., Ko, C. P., Kustermann, S., Marquet, A., Metzger, F., Mueller, B., . . . Mueller, L. (2018). Discovery of Risdiplam, a Selective Survival of Motor Neuron-2 (SMN2) Gene Splicing Modifier for the Treatment of Spinal Muscular Atrophy (SMA). *J Med Chem*, *61*(15), 6501-6517. https://doi.org/10.1021/acs.jmedchem.8b00741

Ratni, H., Scalco, R. S., & Stephan, A. H. (2021). Risdiplam, the First Approved Small Molecule Splicing Modifier Drug as a Blueprint for Future Transformative Medicines. *ACS Med Chem Lett*, *12*(6), 874-877. https://doi.org/10.1021/acsmedchemlett.0c00659

Reinhardt, V. P., Iosif, A. M., Libero, L., Heath, B., Rogers, S. J., Ferrer, E., Nordahl, C., Ghetti, S., Amaral, D., & Solomon, M. (2020). Understanding Hippocampal Development in Young Children With Autism Spectrum Disorder. *J Am Acad Child Adolesc Psychiatry*, *59*(9), 1069-1079. https://doi.org/10.1016/j.jaac.2019.08.008

Rhee, S., Kirschen, G. W., Gu, Y., & Ge, S. (2016). Depletion of primary cilia from mature dentate granule cells impairs hippocampus-dependent contextual memory. *Sci Rep*, *6*, 34370. https://doi.org/10.1038/srep34370

Richardson, L., Venkataraman, S., Stevenson, P., Yang, Y., Moss, J., Graham, L., Burton, N., Hill, B., Rao, J., Baldock, R. A., & Armit, C. (2014). EMAGE mouse embryo spatial gene expression database: 2014 update. *Nucleic Acids Res*, *42*(Database issue), D835-844. https://doi.org/10.1093/nar/gkt1155

Riessland, M., Ackermann, B., Förster, A., Jakubik, M., Hauke, J., Garbes, L., Fritzsche, I., Mende, Y., Blumcke, I., Hahnen, E., & Wirth, B. (2010). SAHA ameliorates the SMA phenotype in two mouse models for spinal

muscular atrophy. *Human Molecular Genetics*, *19*(8), 1492-1506. https://doi.org/10.1093/hmg/ddq023

Rigo, F., Chun, S. J., Norris, D. A., Hung, G., Lee, S., Matson, J., Fey, R. A., Gaus, H., Hua, Y., Grundy, J. S., Krainer, A. R., Henry, S. P., & Bennett, C. F. (2014). Pharmacology of a Central Nervous System Delivered 2′-O-Methoxyethyl–Modified Survival of Motor Neuron Splicing Oligonucleotide in Mice and Nonhuman Primates. *The Journal of Pharmacology and Experimental Therapeutics*, *350*(1), 46-55. https://doi.org/https://doi.org/10.1124/jpet.113.212407

Rijhsinghani, A., Yankowitz, J., Howser, D., & Williamson, R. (1997). SONOGRAPHIC AND MATERNAL SERUM SCREENING ABNORMALITIES IN FETUSES AFFECTED BY SPINAL MUSCULAR ATROPHY. *Prenatal Diagnosis*, *17*(2), 166-169. https://doi.org/10.1002/(sici)1097-0223(199702)17:2<166::aid-pd14>3.0.co;2-d

Ringers, C., Olstad, E. W., & Jurisch-Yaksi, N. (2020). The role of motile cilia in the development and physiology of the nervous system. *Philosophical Transactions of the Royal Society B: Biological Sciences*, *375*(1792), 20190156. https://doi.org/10.1098/rstb.2019.0156

Rivière, J., Lécuyer, R., & Hickmann, M. (2009). Early locomotion and the development of spatial language: Evidence from young children with motor impairments. *European Journal of Developmental Psychology*, *6*(5), 548-566. https://doi.org/10.1080/17405620701345712

Robinson, M. D., McCarthy, D. J., & Smyth, G. K. (2010). <tt>edgeR</tt>: a Bioconductor package for differential expression analysis of digital gene expression data. *Bioinformatics*, *26*(1), 139-140. https://doi.org/10.1093/bioinformatics/btp616

Roche, F. H.-L. (2022). *FDA approves Roche's Evrysdi for use in babies under two months with spinal muscular atrophy (SMA)*. https://www.roche.com/media/releases/med-cor-2022-05-31

Rochette, C., Gilbert, N., & Simard, L. (2001). SMN gene duplication and the emergence of the SMN2 gene occurred in distinct hominids: SMN2 is unique to Homo sapiens. *Human Genetics*, *108*(3), 255-266. https://doi.org/10.1007/s004390100473

Rubin, R. D., Watson, P. D., Duff, M. C., & Cohen, N. J. (2014). The role of the hippocampus in flexible cognition and social behavior. *Frontiers in Human Neuroscience*, *8*. https://doi.org/10.3389/fnhum.2014.00742

Ruggiu, M., McGovern, V. L., Lotti, F., Saieva, L., Li, D. K., Kariya, S., Monani, U. R., Burghes, A. H., & Pellizzoni, L. (2012). A role for SMN exon 7 splicing in the selective vulnerability of motor neurons in spinal muscular

atrophy. *Mol Cell Biol*, *32*(1), 126-138. https://doi.org/10.1128/MCB.06077-11

Sanchez, G., Dury, A. Y., Murray, L. M., Biondi, O., Tadesse, H., El Fatimy, R., Kothary, R., Charbonnier, F., Khandjian, E. W., & Cote, J. (2013). A novel function for the survival motoneuron protein as a translational regulator. *Hum Mol Genet*, *22*(4), 668-684. https://doi.org/10.1093/hmg/dds474

Schrank, B., Götz, R., Gunnersen, J. M., Ure, J. M., Toyka, K. V., Smith, A. G., & Sendtner, M. (1997). Inactivation of the survival motor neuron gene, a candidate gene for human spinal muscular atrophy, leads to massive cell death in early mouse embryos. *Proceedings of the National Academy of Sciences*, *94*(18), 9920-9925. https://doi.org/10.1073/pnas.94.18.9920

Schwartz, O., Vill, K., Pfaffenlehner, M., Behrens, M., Weiß, C., Johannsen, J., Friese, J., Hahn, A., Ziegler, A., Illsinger, S., Smitka, M., von Moers, A., Kölbel, H., Schreiber, G., Kaiser, N., Wilichowski, E., Flotats-Bastardas, M., Husain, R. A., Baumann, M., . . . group, S. s. (2024). Clinical Effectiveness of Newborn Screening for Spinal Muscular Atrophy: A Nonrandomized Controlled Trial. *JAMA Pediatrics*, *178*(6), 540-547. https://doi.org/10.1001/jamapediatrics.2024.0492

Scoto, M., Finkel, R. S., Mercuri, E., & Muntoni, F. (2017). Therapeutic approaches for spinal muscular atrophy (SMA). *Gene Therapy*, *24*(9), 514-519. https://doi.org/10.1038/gt.2017.45

Scoville, W. B., & Milner, B. (1957). LOSS OF RECENT MEMORY AFTER BILATERAL HIPPOCAMPAL LESIONS. *Journal of Neurology, Neurosurgery & Psychiatry*, *20*(1), 11-21. https://doi.org/10.1136/jnnp.20.1.11

Seliger, B., Al-Samadi, A., Yang, B., Salo, T., & Wickenhauser, C. (2022). In vitro models as tools for screening treatment options of head and neck cancer. *Frontiers in Medicine*, *9*. https://doi.org/10.3389/fmed.2022.971726

Sergott, R. C., Amorelli, G. M., Baranello, G., Barreau, E., Beres, S., Kane, S., Mercuri, E., Orazi, L., Santamaria, M., Tremolada, G., Santarsiero, D., Waskowska, A., Yashiro, S., Denk, N., Fürst-Recktenwald, S., Gerber, M., Gorni, K., Jaber, B., Jacobsen, B., . . . Marzoli, S. B. (2021). Risdiplam treatment has not led to retinal toxicity in patients with spinal muscular atrophy. *Annals of Clinical and Translational Neurology*, *8*(1), 54-65. https://doi.org/10.1002/acn3.51239

Serpieri, V., D'Abrusco, F., & Valente, E. M. (2025). The relevance of primary cilia in neurological disorders. *The Lancet Neurology*. https://doi.org/10.1016/s1474-4422(25)00226-1

Shababi, M., Habibi, J., Yang, H. T., Vale, S. M., Sewell, W. A., & Lorson, C. L. (2010). Cardiac defects contribute to the pathology of spinal muscular atrophy models. *Human Molecular Genetics*, *19*(20), 4059-4071. https://doi.org/10.1093/hmg/ddq329

Sharma, G., Paganin, M., Lauria, F., Perenthaler, E., & Viero, G. (2024). The SMN-ribosome interplay: a new opportunity for Spinal Muscular Atrophy therapies. *Biochemical Society Transactions*, *52*(1), 465-479. https://doi.org/10.1042/bst20231116

Sheng, L., Wan, B., Feng, P., Sun, J., Rigo, F., Bennett, C. F., Akerman, M., Krainer, A. R., & Hua, Y. (2018). Downregulation of Survivin contributes to cell-cycle arrest during postnatal cardiac development in a severe spinal muscular atrophy mouse model. *Human Molecular Genetics*, *27*(3), 486-498. https://doi.org/10.1093/hmg/ddx418

Shi, S.-R., Shi, Y., & Taylor, C. R. (2011). Antigen Retrieval Immunohistochemistry. *Journal of Histochemistry & Cytochemistry*, *59*(1), 13-32. https://doi.org/10.1369/jhc.2010.957191

Signoria, I., van der Pol, W. L., & Groen, E. J. N. (2023). Innovating spinal muscular atrophy models in the therapeutic era. *Dis Model Mech*, *16*(9). https://doi.org/10.1242/dmm.050352

Signoria, I., Zwartkruis, M. M., Geerlofs, L., Perenthaler, E., Faller, K. M. E., James, R., McHale-Owen, H., Green, J. W., Kortooms, J., Snellen, S. H., Asselman, F. L., Gillingwater, T. H., Viero, G., Wadman, R. I., van der Pol, W. L., & Groen, E. J. N. (2024). Patient-specific responses to SMN2 splice-modifying treatments in spinal muscular atrophy fibroblasts. *Mol Ther Methods Clin Dev*, *32*(4), 101379. https://doi.org/10.1016/j.omtm.2024.101379

Simon, C. M., Dai, Y., Van Alstyne, M., Koutsioumpa, C., Pagiazitis, J. G., Chalif, J. I., Wang, X., Rabinowitz, J. E., Henderson, C. E., Pellizzoni, L., & Mentis, G. Z. (2017). Converging Mechanisms of p53 Activation Drive Motor Neuron Degeneration in Spinal Muscular Atrophy. *Cell Reports*, *21*(13), 3767-3780. https://doi.org/10.1016/j.celrep.2017.12.003

Singh, N. K., Singh, N. N., Androphy, E. J., & Singh, R. N. (2006). Splicing of a Critical Exon of Human Survival Motor Neuron Is Regulated by a Unique Silencer Element Located in the Last Intron. *Molecular and Cellular Biology*, *26*(4), 1333-1346. https://doi.org/10.1128/mcb.26.4.1333-1346.2006

Sivaramakrishnan, M., McCarthy, K. D., Campagne, S., Huber, S., Meier, S., Augustin, A., Heckel, T., Meistermann, H., Hug, M. N., Birrer, P., Moursy, A., Khawaja, S., Schmucki, R., Berntenis, N., Giroud, N., Golling, S., Tzouros, M., Banfai, B., Duran-Pacheco, G., . . . Metzger, F. (2017).

Binding to SMN2 pre-mRNA-protein complex elicits specificity for small molecule splicing modifiers. *Nature Communications*, *8*(1). https://doi.org/10.1038/s41467-017-01559-4

Slavov, N., Semrau, S., Airoldi, E., Budnik, B., & Alexander. (2015). Differential Stoichiometry among Core Ribosomal Proteins. *Cell Reports*, *13*(5), 865-873. https://doi.org/10.1016/j.celrep.2015.09.056

Soler-Botija, C. (2002). Neuronal death is enhanced and begins during foetal development in type I spinal muscular atrophy spinal cord. *Brain*, *125*(7), 1624-1634. https://doi.org/10.1093/brain/awf155

Song, W., & Ke, X. (2025). Rehabilitation management for patients with spinal muscular atrophy: a review. *Orphanet Journal of Rare Diseases*, *20*(1). https://doi.org/10.1186/s13023-025-03888-w

Spassky, N., Merkle, F. T., Flames, N., Tramontin, A. D., García-Verdugo, J. M., & Alvarez-Buylla, A. (2005). Adult Ependymal Cells Are Postmitotic and Are Derived from Radial Glial Cells during Embryogenesis. *The Journal of Neuroscience*, *25*(1), 10-18. https://doi.org/10.1523/jneurosci.1108-04.2005

Squire, L. R. (2009). The Legacy of Patient H.M. for Neuroscience. *Neuron*, *61*(1), 6-9. https://doi.org/10.1016/j.neuron.2008.12.023

Sreng, L., Temime-Roussel, B., Wortham, H., & Mourre, C. (2016). Chemical Identification of “Maternal Signature Odors” in Rat. *Chemical Senses*, bjw124. https://doi.org/10.1093/chemse/bjw124

Steffens, P., Weiss, D., Perez, A., Appel, M., Weber, P., Weiss, C., Stoltenburg, C., Ehinger, U., von der Hagen, M., Schallner, J., Claussen, B., Lode, I., Hahn, A., Schuler, R., Russ, L., Ziegler, A., Denecke, J., & Johannsen, J. (2024). Cognitive function in SMA patients with 2 or 3 SMN2 copies treated with SMN-modifying or gene addition therapy during the first year of life. *Eur J Paediatr Neurol*, *51*, 17-23. https://doi.org/10.1016/j.ejpn.2024.05.002

Stiles, J., & Jernigan, T. L. (2010). The Basics of Brain Development. *Neuropsychology Review*, *20*(4), 327-348. https://doi.org/10.1007/s11065-010-9148-4

Stoner, R., Chow, M. L., Boyle, M. P., Sunkin, S. M., Mouton, P. R., Roy, S., Wynshaw-Boris, A., Colamarino, S. A., Lein, E. S., & Courchesne, E. (2014). Patches of Disorganization in the Neocortex of Children with Autism. *New England Journal of Medicine*, *370*(13), 1209-1219. https://doi.org/10.1056/nejmoa1307491

Strauss, K. A., Farrar, M. A., Muntoni, F., Saito, K., Mendell, J. R., Servais, L., McMillan, H. J., Finkel, R. S., Swoboda, K. J., Kwon, J. M., Zaidman, C.

M., Chiriboga, C. A., Iannaccone, S. T., Krueger, J. M., Parsons, J. A., Shieh, P. B., Kavanagh, S., Wigderson, M., Tauscher-Wisniewski, S., . . . Macek, T. A. (2022). Onasemnogene abeparvovec for presymptomatic infants with three copies of SMN2 at risk for spinal muscular atrophy: the Phase III SPR1NT trial. *Nature Medicine*, *28*(7), 1390-1397. https://doi.org/10.1038/s41591-022-01867-3

Sultana, O. F., Bandaru, M., Islam, M. A., & Reddy, P. H. (2024). Unraveling the complexity of human brain: Structure, function in healthy and disease states. *Ageing Research Reviews*, *100*, 102414. https://doi.org/https://doi.org/10.1016/j.arr.2024.102414

Sumner, C. J., & Crawford, T. O. (2022). Early treatment is a lifeline for infants with SMA. *Nat Med*, *28*(7), 1348-1349. https://doi.org/10.1038/s41591-022-01889-x

Tereshko, L., Turrigiano, G. G., & Sengupta, P. (2022). Primary cilia in the postnatal brain: Subcellular compartments for organizing neuromodulatory signaling. *Curr Opin Neurobiol*, *74*, 102533. https://doi.org/10.1016/j.conb.2022.102533

Thelen, M. P., Wirth, B., & Kye, M. J. (2020). Mitochondrial defects in the respiratory complex I contribute to impaired translational initiation via ROS and energy homeostasis in SMA motor neurons. *Acta Neuropathologica Communications*, *8*(1). https://doi.org/10.1186/s40478-020-01101-6

Thompson, J., & Bruce, A. (1893). *A case of progressive muscular atrophy in a child with a spinal lesion*.

Tizzano, E. F., Cabot, C., & Baiget, M. (1998). Cell-Specific Survival Motor Neuron Gene Expression during Human Development of the Central Nervous System. *The American Journal of Pathology*, *153*(2), 355-361. https://doi.org/10.1016/s0002-9440(10)65578-2

Tizzano, E. F., Lindner, G., Chilcott, E., Finkel, R. S., & Yáñez-Muñoz, R. J. (2025). In utero therapy for spinal muscular atrophy: closer to clinical translation. *Brain*. https://doi.org/10.1093/brain/awaf123

Tizzano, E. F., & Zafeiriou, D. (2018). Prenatal aspects in spinal muscular atrophy: From early detection to early presymptomatic intervention. *Eur J Paediatr Neurol*, *22*(6), 944-950. https://doi.org/10.1016/j.ejpn.2018.08.009

Tolman, E. C. (1948). Cognitive maps in rats and men. *Psychological Review*, *55*(4), 189-208. https://doi.org/10.1037/h0061626

Tomassoni-Ardori, F., Hong, Z., Fulgenzi, G., & Tessarollo, L. (2020). Generation of Functional Mouse Hippocampal Neurons. *BIO-PROTOCOL*, *10*(15). https://doi.org/10.21769/bioprotoc.3702

Tomuro, K., & Iwasaki, S. (2025). Advances in ribosome profiling technologies. *Biochemical Society Transactions*, *53*(03), 555-564. https://doi.org/10.1042/bst20253061

Tong, C. K., Han, Y.-G., Shah, J. K., Obernier, K., Guinto, C. D., & Alvarez-Buylla, A. (2014). Primary cilia are required in a unique subpopulation of neural progenitors. *Proceedings of the National Academy of Sciences*, *111*(34), 12438-12443. https://doi.org/10.1073/pnas.1321425111

Tosi, M., Cumbo, F., Catteruccia, M., Carlesi, A., Mizzoni, I., De Luca, G., Cherchi, C., Cutrera, R., Bertini, E., & D'Amico, A. (2023). Neurocognitive profile of a cohort of SMA type 1 pediatric patients and emotional aspects, resilience and coping strategies of their caregivers. *Eur J Paediatr Neurol*, *43*, 36-43. https://doi.org/10.1016/j.ejpn.2023.02.004

Trollmann, R., Johannsen, J., Vill, K., Köhler, C., Hahn, A., Illsinger, S., Pechmann, A., Hagen, M. V. D., & Müller-Felber, W. (2024). Postnatal management of preterm infants with spinal muscular atrophy: experience from German newborn screening. *Orphanet Journal of Rare Diseases*, *19*(1). https://doi.org/10.1186/s13023-024-03362-z

Tunster, S. J. (2017). Genetic sex determination of mice by simplex PCR. *Biology of Sex Differences*, *8*(1). https://doi.org/10.1186/s13293-017-0154-6

Urban, N., & Guillemot, F. (2014). Neurogenesis in the embryonic and adult brain: same regulators, different roles. *Front Cell Neurosci*, *8*, 396. https://doi.org/10.3389/fncel.2014.00396

Van Leewenhoeck, A. (1677). Observations, communicated to the publisher by Mr. Antony van Leewenhoeck, in a dutch letter of the 9th Octob. 1676. here English'd: concerning little animals by him observed in rain-well-sea- and snow water; as also in water wherein pepper had lain infus. *Philosophical Transactions of the Royal Society of London*, *12*(133), 821-831. https://doi.org/10.1098/rstl.1677.0003

Vidovic, M., Freigang, M., Aust, E., Linse, K., Petzold, D., & Günther, R. (2023). Cognitive performance of adult patients with SMA before and after treatment initiation with nusinersen. *BMC Neurology*, *23*(1). https://doi.org/10.1186/s12883-023-03261-z

von Gontard, A., Zerres, K., Backes, M., Laufersweiler-Plass, C., Wendland, C., Melchers, P., Lehmkuhl, G., & Rudnik-Schoneborn, S. (2002).

Intelligence and cognitive function in children and adolescents with spinal muscular atrophy. *Neuromuscul Disord*, *12*(2), 130-136. https://doi.org/10.1016/s0960-8966(01)00274-7

Wadman, R. I., Stam, M., Gijzen, M., Lemmink, H. H., Snoeck, I. N., Wijngaarde, C. A., Braun, K. P., Schoenmakers, M. A., van den Berg, L. H., Dooijes, D., & van der Pol, W. L. (2017). Association of motor milestones, SMN2 copy and outcome in spinal muscular atrophy types 0-4. *J Neurol Neurosurg Psychiatry*, *88*(4), 365-367. https://doi.org/10.1136/jnnp-2016-314292

Wang, C. H., Finkel, R. S., Bertini, E. S., Schroth, M., Simonds, A., Wong, B., Aloysius, A., Morrison, L., Main, M., Crawford, T. O., Trela, A., & null, n. (2007). Consensus Statement for Standard of Care in Spinal Muscular Atrophy. *Journal of Child Neurology*, *22*(8), 1027-1049. https://doi.org/10.1177/0883073807305788

Wang, L., & Dynlacht, B. D. (2018). The regulation of cilium assembly and disassembly in development and disease. *Development*, *145*(18), dev151407. https://doi.org/10.1242/dev.151407

Wang, L., Wen, X., Wang, Z., Lin, Z., Li, C., Zhou, H., Yu, H., Li, Y., Cheng, Y., Chen, Y., Lou, G., Pan, J., & Cao, M. (2022). Ciliary transition zone proteins coordinate ciliary protein composition and ectosome shedding. *Nature Communications*, *13*(1). https://doi.org/10.1038/s41467-022-31751-0

Waters, A. M., & Beales, P. L. (2011). Ciliopathies: an expanding disease spectrum. *Pediatric Nephrology*, *26*(7), 1039-1056. https://doi.org/10.1007/s00467-010-1731-7

Werdnig, G. (1891). Zwei frühinfantile hereditäre Fälle von progressiver Muskelatrophie unter dem Bilde der Dystrophie, aber anf neurotischer Grundlage [Article]. *Archiv für Psychiatrie und Nervenkrankheiten*, *22*(2), 437-480. https://doi.org/10.1007/BF01776636

Wexler, M. (2025). Spinal Muscular Atrophy treatment options.

White, T. A., Miller, S. L., Sutherland, A. E., Allison, B. J., & Camm, E. J. (2024). Perinatal compromise affects development, form, and function of the hippocampus part one; clinical studies. *Pediatric Research*, *95*(7), 1698-1708. https://doi.org/10.1038/s41390-024-03105-7

Wishart, T. M., Huang, J. P., Murray, L. M., Lamont, D. J., Mutsaers, C. A., Ross, J., Geldsetzer, P., Ansorge, O., Talbot, K., Parson, S. H., & Gillingwater, T. H. (2010). SMN deficiency disrupts brain development in a mouse model of severe spinal muscular atrophy. *Hum Mol Genet*, *19*(21), 4216-4228. https://doi.org/10.1093/hmg/ddq340

Xiao, L., Kang, S., Djordjevic, D., Gonorazky, H., Chiang, J., Ambreen, M., Nigro, E., Law, E., Weinstock, L., McCradden, M., & Amin, R. (2023). Understanding caregiver experiences with disease-modifying therapies for spinal muscular atrophy: a qualitative study. *Archives of Disease in Childhood*, *108*(11), 929-934. https://doi.org/10.1136/archdischild-2023-325762

Xu, B., Wei, C., Hu, X., Li, W., Huang, Z., Que, C., Qiu, J., Li, C., & Xiong, H. (2022). Scoliosis Orthopedic Surgery Combined With Nusinersen Intrathecal Injection Significantly Improved the Outcome of Spinal Muscular Atrophy Patient: A Case Report. *Front Neurol*, *13*, 869230. https://doi.org/10.3389/fneur.2022.869230

Yang, H., Yang, J., Xue, Y., Liao, L., Cai, Q., & Luo, R. (2023). *Cognitive impairment in children with 5q-associated spinal muscular atrophy type 1: two case reports and the review of the literature*. Research Square Platform LLC. https://dx.doi.org/10.21203/rs.3.rs-2880502/v1

Yeo, C. J. J., & Darras, B. T. (2020). Overturning the Paradigm of Spinal Muscular Atrophy as Just a Motor Neuron Disease. *Pediatr Neurol*, *109*, 12-19. https://doi.org/10.1016/j.pediatrneurol.2020.01.003

Yeo, C. J. J., Tizzano, E. F., & Darras, B. T. (2024). Challenges and opportunities in spinal muscular atrophy therapeutics. *Lancet Neurol*, *23*(2), 205-218. https://doi.org/10.1016/S1474-4422(23)00419-2

Youn, Y. H., & Han, Y. G. (2018). Primary Cilia in Brain Development and Diseases. *Am J Pathol*, *188*(1), 11-22. https://doi.org/10.1016/j.ajpath.2017.08.031

Zappa, G., Lomauro, A., Baranello, G., Cavallo, E., Corti, P., Mastella, C., & Costantino, M. A. (2021). Intellectual abilities, language comprehension, speech, and motor function in children with spinal muscular atrophy type 1. *Journal of Neurodevelopmental Disorders*, *13*(1). https://doi.org/10.1186/s11689-021-09355-4

Zerres, K., Rudnik-Schöneborn, S., Forrest, E., Lusakowska, A., Borkowska, J., & Hausmanowa-Petrusewicz, I. (1997). A collaborative study on the natural history of childhood and juvenile onset proximal spinal muscular atrophy (type II and III SMA): 569 patients. *J Neurol Sci*, *146*(1), 67-72. https://doi.org/10.1016/s0022-510x(96)00284-5

Zhai, D., Zhou, X., Xu, Z., Chen, X., Li, Y., Li, J., Zhou, T., & Xie, S. (2025). The role of primary cilia in physiological and pathological states of the central nervous system. *Journal of Genetics and Genomics*. https://doi.org/https://doi.org/10.1016/j.jgg.2025.11.011

Zhang, Q., Kim, N.-K., & Feigon, J. (2011). Architecture of human telomerase RNA. *Proceedings of the National Academy of Sciences*, *108*(51), 20325-20332. https://doi.org/10.1073/pnas.1100279108

Zhao, R., & Duncan, S. A. (2005). Embryonic development of the liver†. *Hepatology*, *41*(5), 956-967. https://doi.org/10.1002/hep.20691

Zhou, H., Janghra, N., Mitrpant, C., Dickinson, R. L., Anthony, K., Price, L., Eperon, I. C., Wilton, S. D., Morgan, J., & Muntoni, F. (2013). A Novel Morpholino Oligomer Targeting ISS-N1 Improves Rescue of Severe Spinal Muscular Atrophy Transgenic Mice. *Human Gene Therapy*, *24*(3), 331-342. https://doi.org/10.1089/hum.2012.211

Zhu, Y., Huang, R., Yu, L., Liu, Z., Liu, Y., Fan, W., Lin, G., Wang, Z., He, X., Xu, X., Ma, B., Chen, Y., Bai, Y., Li, J., Chen, B., Cheng, L., & Zhu, R. (2025). Engineered thoracic spinal cord organoids for transplantation after spinal cord injury. *Nature Biomedical Engineering*. https://doi.org/10.1038/s41551-025-01549-8

Zimmermann, K. W. (1898). Beiträge zur Kenntniss einiger drüsen und epithelien. *Archiv für mikroskopische Anatomie*, *52*(3), 552-706.